Author:
Basava-Reddi, Millie

Title:
Characterisation of the stable isotope composition of methane in UK groundwaters

Characterisation of the stable isotope composition of methane in UK groundwaters

Millie Basava-Reddi

Supervisors: Dr. Edward Hornibrook, Dr. Daren Gooddy, Dr. George Darling & Dr. Ian Parkinson

A dissertation submitted to the University of Bristol in accordance with the requirements for award of the degree of Doctor of Philosophy in the Faculty of Science

School of Earth Sciences

Date of Submission: 29th June 2018

Word Count: $\sim$ 36,000

Abstract

The primary aim was to use stable isotope analysis to characterise the origin and alteration of methane (CH_4) in UK groundwater. CH_4 is produced from a variety of processes, including archaeal metabolism in anaerobic environments, thermal breakdown of organic matter during burial, and abiogenic geological processes. The stable isotope composition depends initially on production pathway, composition of substrates, temperature and energetic conditions. Post-formation processes, such as transport or CH_4 oxidation, can continue to alter the stable isotope composition. Methane may enter groundwater from neighbouring formations, as well as be produced microbially in situ; alteration processes may further affect stable isotope composition. CH_4 in groundwater is often observed in low concentrations historically difficult to sample. A field sparging method was developed enabling stable isotope analysis with a lower limit of 0.5 – 1 µg L^{-1} for $\delta^{13}C(CH_4)$ and 2 – 3 µg L^{-1} for $\delta^{2}H(CH_4)$. Site investigation was carried out in three parts: 1. Sites within a syncline of the Lower Greensands aquifer where conditions change from confined to unconfined; 2. Sites within a shale gas development area in Lancashire; and 3. Sites within several aquifers in the UK to explore dominant geological and environmental controls on groundwater $\delta^{13}C(CH_4)$ and $\delta^{2}H(CH_4)$ values and the degree of variability. Local geology was observed to be an influencing factor on environmental conditions affecting methane production and oxidation processes. Redox conditions were observed to strongly influence the concentration of microbially produced CH_4 within groundwater in the UK. Strong correlations between CH_4 and both Eh and DO were recorded. A wide range of $\delta^{13}C(CH_4)$ and $\delta^{2}H(CH_4)$ values were measured ranging from -79 to -29 ‰ and -353 to +248 ‰, respectively. As CH_4 concentration decreases, both $\delta^{13}C(CH_4)$ and $\delta^{2}H(CH_4)$ values increase. A clear correlation of $\delta^{13}C(CH_4)$ and $\delta^{2}H(CH_4)$ values was observed as they increased proportionally to each other. These results indicate that in UK aquifers a kinetic isotope effect caused by post formational bacterial CH_4 oxidation is the dominant control on $\delta^{13}C(CH_4)$ and $\delta^{2}H(CH_4)$ values. Though CH_4 in UK aquifers is predominantly microbial, thermogenic CH_4 was also present in areas with known source rocks, such as the Coal Measures and evidence of mixing between sources was observed.

Author's Declaration

I declare that the work in this dissertation was carried out in accordance with the requirements of the University's Regulations and Code of Practice for Research Degree Programmes and that it has not been submitted for any other academic award. Except where indicated by specific reference in the text, the work is the candidate's own work. Work done in collaboration with, or with the assistance of, others, is indicated as such. Any views expressed in the dissertation are those of the author.

.....

Millie Basava-Reddi

29th June 2018

Acknowledgments

I would like to thank my supervisors; Ed Hornibrook, Daren Gooddy, George Darling and Ian Parkinson, for their guidance and encouragement throughout my project.

I would like to thank Paul Monaghan for his time, patience and ability to fix almost anything. I would also like to thank Charles Belanger and Donovan Hawley for both building essential field and lab equipment and for helpful advice on all things technical. Thank you also to Ian Bull for fixing the IRMS, without this, the project may not have been completed.

I would like to thank several people at the British Geological Survey (BGS) who have made this project possible, most especially Rachel Bell and Lindsay Holowka for organising fieldwork and being very helpful in all matters, and Debbie White, for training me and helping me with field equipment, as well as the invaluable help from Barry Townsend and Andy Butcher. I would like to thank Carol Arrowsmith from NIGL labs for training on the mass spectrometer, analysing samples and good advice.

Thank you to Kerry Klassen and Paul Middlestead a G.G. Hatch laboratories; for all of the work and the time taken to make it possible to analyse lower concentration samples, which was essential for this project.

Thank you to Greg Holland and Zheng Zhou at Lancaster University for welcoming me into their lab and allowing me use of the QCL, even though this method did not work out, it was a great opportunity to learn.

I would also like to thank the many people who allowed me access to sample their water supplies, and accompanied me on site; namely Jeff Hayes, Raphael Peraldi, Jenny Cass, Lindsay Northwood and Philip Onunkwo at Southeast Water; Keith Rafferty at SSE; Keith Simpson and the team at Horlicks; Simon Eyre, Ghislain Juvanon and John Johnson at Anglia Water; Mark Burton at South West Water (formerly Bournemouth Water); Sarah McLaughlin from SES Water; Sally Hughes, Simon Stockdale and Ben Scolari at Thames Water; Oliver

Grant at Newstead Farm; Richard Keates and Mark Botterill at Portsmouth Water; Rebekah Rice, Martin Berry and Natasha Clements at Bristol Water; Jim Hawker, Gareth Thomas, Gemma Harris at National Resources, Wales; Richard from Aberdare Golf Club; Bethany Atkinson, Kevin Freer, Kevin Ellwood and Stuart Watson at Yorkshire Water, Elaine Drinkall and everyone at Catshaw Farm; the Robinsons at Dean Slack Farm; Bob Holinski at Cirteq and Joe Leachy at the Great Yorkshire Showground.

I also thank my lab mates, Adam, Paul (again), Mari and Aoy, for good discussions, moral support and cups of tea.

This project was made possible by funding from the Natural Environment Research Council (NERC) and the BGS University Funding Initiative (BUFI).

Contents

List of Figures

List of Tables

Chapter 1

Introduction

1.1 Project aim and rationale

The primary aim of this project is to use stable isotope analysis to characterise the origin and alteration of methane (CH_4) in UK groundwater to establish baseline conditions against which future changes, if any, can be discerned and quantified. This investigation complements the CH_4 baseline survey conducted by the British Geological Survey (BGS), which has the remit of characterising major aquifers in the UK in areas where shale gas resources may be developed (Bell et al., 2017). The BGS baseline survey investigated water chemistry and CH_4 concentration across UK aquifers. This study is focused on characterisation of the stable carbon ($^{13}C/^{12}C$) and hydrogen ($^{2}H/^{1}H$) isotope compositions of CH_4 and $^{13}C/^{12}C$ ratios in dissolved inorganic carbon (DIC or ΣCO_2) and $^{2}H/^{1}H$ and $^{18}O/^{16}O$ ratios in H_2O.

1. Assess the range of stable isotope compositions of CH_4 within individual aquifers and across different UK aquifers in relation to geology and local conditions. **(O1)**

2. Extend the current scope of isotopic characterisation of CH_4 in UK groundwater through refinement of a pre-concentration method to improve the detection limit for $^{13}C/^{12}C$ analysis of dissolved CH_4 and enable the first characterisation of $^{2}H/^{1}H$ ratios in background levels of CH_4 in UK groundwater. **(O2)**

3. Evaluate the extent to which differences in CH_4 formation pathways and CH_4 oxidation contributes to variability in the stable isotope compositions of groundwater CH_4. **(O3)**

4. Establish the degree to which stable isotope characterisation of CH_4 in UK groundwater can be used reliably to detect influx of exogenous CH_4 into an aquifer based upon the limits and precision of field and laboratory techniques for CH_4 extraction and stable isotope analysis. **(O4)**

5. Assess the extent to which regional differences in the ^{2}H content of meteoric water influences $^{2}H/^{1}H$ ratios in dissolved CH_4. **(O5)**

1.2 Methane production

Methane is produced from a variety of processes (Schoell, 1988), including archaeal metabolism in anaerobic environments (microbial CH_4), thermal break-

down of organic matter during burial, such as in shale or coal (thermogenic CH_4), and abiogenic geological processes that do not involve organic matter.

Deep gas sources are generally considered to be formed from the thermogenic breakdown of organic matter, whereas shallower CH_4 sources are generally microbial; however, this is not always the case, as methanogens have been found at depth at many locations (Kotelnikova, 2002; Lollar et al., 2006; Suzuki et al., 2009).

1.2.1 Abiotic methane

Abiotic CH_4 is produced without involving any organic matter. This can involve high temperature magmatic processes or low temperature gas-water-rock interactions, which have been reviewed in detail by Etiope and Lollar (2013) and Kietäväinen and Purkamo (2015). High temperature reactions in the mantle include hydrolysis or hydrogenation of metal carbides (Lai, 2007), or reduction of carbonates with water (Beeskow et al., 2006), or later magmatic processes at lower temperatures, including re-speciation of C-O-H fluids (Potter and Konnerup-Madsen, 2003). Gas-water-rock reactions, include post-magmatic high temperature reactions, involving metal oxides, CO_2 and H_2O (Giggenbach, 1997), metamorphism of carbonate-graphite bearing rocks, iron-carbonate decomposition, carbonate methanation, uncatalyzed aqueous CO_2 reduction and lower temperature Fischer-Tropsch type (FTT) reactions, such as the Sabatier reaction, eq. 1.1, where H_2, produced by serpentinisation, reacts with CO_2, which can be from various sources (Etiope and Lollar, 2013). This reaction is supported by metal catalysts and can take place over a range of temperatures (25 - 500 °C).

$$CO_2 + 4H_2 \rightarrow CH_4 + 2H_2O \tag{1.1}$$

Methane produced by FTT reactions occurs at mid-ocean ridges (e.g. Konn et al., 2015), across onshore ultra-mafic deposits in many locations worldwide (e.g., Boschetti et al., 2013; Etiope et al., 2015), and in hyper-alkaline springs containing mature Mg-HCO_3 waters (Etiope et al., 2013). A recent study by Etiope et al. (2016) used ^{14}C to show that CH_4 in some hyperalkaline springs is much older than the dissolved inorganic carbon (DIC) from which it was previously thought to have formed, suggesting that the CH_4 is derived from an allochthonous source and follows an independent migration pathway. Similar analysis has not been carried out at other sites and it is not known whether this reaction pathway is common in other deposits.

1.2.2 Thermogenic methane

Thermogenic CH_4 is formed by the thermal breakdown of organic matter at temperatures > 150°C and elevated pressures, usually at depths greater than 1000 m. It is generally found in conjunction with its source rock - deposits of oil, coal and shale, and in association with other light hydrocarbons, which aid in the identification of thermogenic v.s. microbial gas (i.e., $C_1/(C_2 + C_3) < 100$; (Bernard et al., 1976). Thermogenic CH_4 also is old, typically containing very low levels of ^{14}C , which enables the radiocarbon (^{14}C) activity ratios to be used to determine whether a component of microbial CH_4 is present in gas (Slater et al., 2006). During thermal decomposition of organic matter ^{12}C-^{12}C and ^{1}H-^{1}H bonds are broken preferentially because ^{13}C-^{12}C and ^{2}H-^{1}H bonds are slightly stronger. Therefore, the CH_4 should be ^{13}C- and ^{2}H- poor relative to the initial organic material and other C_2+ hydrocarbon products become more ^{13}C- and ^{2}H-enriched with increasing carbon number (Fuex, 1977). Whether this pattern or the opposite is seen, can be used to distinguish between thermogenic and abiotic sources (Dai et al., 2004).

1.2.3 Microbial methane

Methane production by methanogenic archaea takes place under anoxic conditions; all methanogens are strict anaerobes belonging to the Euryarchaeota. They are all obligate CH_4-producers that acquire most of their energy from methanogenesis although there is an extreme genetic and metabolic diversity amongst the Euryarchaeota (Hedderich and Whitman, 2013). There are over 80 species of known methanogenic archaea, which exist in a wide variety of environments under a broad range of temperatures, salinity and pH conditions (Liu and Whitman, 2008).

Microbial communities where CH_4 is produced are complex, consisting of hydrolytic, fermentative, acetogenic and methanogenic organisms (Bryant, 1979; Whiticar et al., 1986). There are three main stages involved during CH_4 production: (i) first fermentative bacteria hydrolyse materials such as lipids, proteins and polysaccharides, then ferment most products excreting acetate and other fatty acids, (ii) hydrogen-producing acetogenic bacteria produce H_2 and acetate from the end products of the first stage, and (iii) methanogens catabolise the end products, mainly acetate, CO_2 and H_2, produced by the first two groups of microorganisms.

There are three metabolic pathways by which CH_4 is produced; hydrogenotrophic methanogenesis (Eq. 1.2), where CO_2 is reduced to CH_4, acetoclastic methano-

genesis (Eq. 1.3), with acetate as the carbon source and methyl group reduction, e.g. methanol reduction (Eq. 1.4). In freshwater environments, methyl group reduction has been found to be rare (Conrad and Claus, 2005), and typically is excluded from studies.

$$CO_2 + 4H_2 \rightarrow CH_4 + 2H_2O \tag{1.2}$$

$$CH_3COOH \rightarrow CO_2 + CH_4 \tag{1.3}$$

$$4CH_3OH \rightarrow H_2O + CO_2 + 3CH_4 \tag{1.4}$$

Most methanogens are hydrogenotrophs that utilise the CO_2 reduction pathway (Eq. 1.2). Fewer are methylotrophic (Eq. 1.4) and only two known genera are able to employ the acetoclastic methanogenesis pathway (Eq. 1.3) and only one of these two microorganisms is a dedicated acetate utiliser (Liu and Whitman, 2008). These numbers, however, are not indicative of the amount of CH_4 produced from each pathway. Methane is commonly produced via acetoclastic methanogenesis in freshwater environments even though only a small proportion of methanogens utilise the pathway and some methanogens can utilise multiple pathways depending on substrate availability (Londry et al., 2008).

Methane production may occur via more than one pathway in anaerobic environments and the predominant pathway in an environment will depend mainly on substrate availability and the microbial community. Higher availability of labile organic matter will generally result in dominance of acetoclastic methanogenesis (Hornibrook et al., 1997; Sugimoto and Wada, 1993); however, if the supply of acetate is limited then hydrogenotrophic methanogenesis may become the dominant methanogenic pathway. Therefore, in the presence of older, recalcitrant organic matter, hydrogenotrophic methanogenesis is more likely to occur compared to younger sediments, where acetoclastic methanogenesis is more common (Conrad, 2005). This association of pathways with different supplies and quality of organic matter has been confirmed using ^{14}C approaches (Chanton et al., 1995; Nakagawa et al., 2002).

Competition for labile organic matter can also affect CH_4 production pathways because high concentrations of sulphate will generally enable sulphate-reducing bacteria to outcompete methanogens for labile substrates such as acetate. This led to an assumption by Whiticar et al. (1986) in developing an isotope proxy model for methanogenesis that the dominant CH_4 production pathway is CO_2 reduction in high sulphate marine environments. In contrast, anoxic freshwa-

ter environments, which typically contain low concentrations of sulphate, such as wetlands, typically produce CH_4 via the acetoclastic methanogenesis pathway (Whiticar et al., 1986). This is not always the case as acetoclastic methanogenesis dominates in marine environments if there is an excess of organic matter (e.g., Carr et al., 2018) and hydrogenotrophic methanogenesis may dominate in freshwater if there is a lack of labile organic matter (e.g., Hornibrook et al., 1997) and often methanogenesis in freshwater is a combination of acetoclastic and hydrogenotrophic methanogenesis (Conrad, 2005).

1.3 Stable isotope notation

Stable isotope data are presented in the standard delta notation:

$$\delta[‰] = \frac{R_{sample}}{R_{standard}} - 1 \tag{1.5}$$

Where R is the ratio of the heavy to light isotope for the sample and standard, e.g. $^{13}C/^{12}C$ for carbon and $^{2}H/^{1}H$ for hydrogen (Coplen, 2011). Fractionation factors are used to report the extent to which isotope-substituted molecules have been partitioned on a mass selective basis through physical, chemical and/or biological processes and are represented as α, which is defined as:

$$\alpha_{A-B} = \frac{R_A}{R_B} \tag{1.6}$$

or

$$\alpha_{A-B} = \frac{\delta X_A + 1000}{\delta X_B + 1000} \tag{1.7}$$

Where R is the ratio of the heavy to light isotope in materials A and B, respectively and δX is the stable isotope composition of materials A and B expressed in the standard delta notation.

The enrichment factor (ε) is another way to describe stable isotope partitioning and is defined as:

$$\epsilon = 1000(1 - \alpha) \tag{1.8}$$

Where α is a fractionation factor as described in Eq. 1.6 and Eq. 1.7

1.4 Stable isotopes and methane production

The stable isotope composition of CH_4 is governed strongly by formation pathway, though it is important also to fully characterise the range of physical and biological processes involved in CH_4 cycling because a range of factors can affect $^{13}C/^{12}C$ and $^{2}H/^{1}H$ ratios in CH_4, including the isotopic composition of substrates (Burke, 1993; Waldron et al., 1999), transport processes such as diffusion (Schloemer and Krooss, 2004; Zhang and Krooss, 2001), bacterial or anaerobic archaeal oxidation, and mixing with other CH_4 sources (Martini et al., 1998; Osborn and McIntosh, 2010). It is also possible for the dominant methanogenic pathway to change temporally and spatially in an environment, depending on substrate availability (e.g., Gehring et al., 2015; Hershey et al., 2014) and other environmental factors such as temperature (Fey et al., 2004); and higher formation temperatures, will result in more ^{13}C- and ^{2}H-enriched CH_4 because of limited mass discrimination between light and heavy isotopes.

Thermogenic CH_4 typically will have different isotopic compositions depending on the initial organic material as well as the maturity of the gas (Golding et al., 2013; Molofsky et al., 2013) and in areas of CH_4 extraction, the isotopic composition can change over time (Kirk et al., 2012). Methane produced by microorganisms contains less ^{13}C than CH_4 generated by thermogenic or abiotic process because of significant kinetic isotope effects associated with microbial metabolism (Whiticar, 1999). Consequently, microbial CH_4 has the most negative $\delta^{13}C(CH_4)$ and $\delta^{2}H(CH_4)$ values (i.e., lowest content of ^{13}C and ^{2}H). The kinetic isotope effects are due to microorganisms preferentially utilising lighter isotopes in their metabolic processes as a result of bond strength for ^{12}C being weaker (i.e., more reactive). In contrast, the isotope composition of abiotic CH_4 is dependent on the isotopic composition of the precursor compounds and temperature, which yields $\delta^{13}C(CH_4)$ values that are more positive than both microbial and thermogenic CH_4 (Etiope and Lollar, 2013; Schoell, 1988).

The microbial production pathway is important for both $\delta^{13}C(CH_4)$ and $\delta^{2}H(CH_4)$ values, though there are still variations within each production pathway. The relative difference in $\delta^{13}C$ values for CH_4 and coexisting CO_2 is typically ~ 60 ‰ in environments dominated by the CO_2 reduction pathway (Whiticar, 1999; Whiticar et al., 1986) yielding $\delta^{13}C(CH_4)$ values of -95 to -55 ‰ compared $\sim$ -55 to -40 ‰ for CH_4 produced by acetoclastic methanogenesis. Expression of stable C isotope fractionation can vary within a single environment as the dominant methanogenic pathway changes with depth in response to the availability and quality of organic matter or temperature (Hornibrook et al., 2000).

Methane produced via hydrogenotrophic methanogenesis likely has all four

hydrogen atoms sourced from water (Daniels et al., 1980), whereas CH_4 produced via acetoclastic methanogenesis likely has three hydrogen atoms derived from the methyl group in acetate and a fourth from water (Whiticar, 1999; Whiticar et al., 1986). However hydrogen isotope exchange between acetate and water can take place within the final step of the acetoclastic methanogenesis pathway (de Graaf et al., 1996), increasing the effects of $\delta^2H(H_2O)$ on $\delta^2H(CH_4)$; evidence of this has been seen in laboratory experiments (Waldron et al., 1998) and within freshwater environments (Waldron et al., 1999). It has also been hypothesised that H isotope exchange catalised by hydrogenase enzymes within hydrogenotrophic methanogen populations may take place post CH_4 formation (Okumura et al., 2016).

Stable isotope fractionation will be dependent on growth rate (e.g. Balabane et al., 1987; Botz et al., 1996; Valentine et al., 2004), methanogen species (e.g. Conrad et al., 2012; Games et al., 1978) temperature (Botz et al., 1996) and energetic conditions during production (Okumura et al., 2016; Penning et al., 2005; Valentine et al., 2004), which can affect steps within the production pathway. Increased H_2 in the system will affect $\delta^{13}C(CH_4)$ of CH_4 produced by hydrogenotrophic methanogenesis (Valentine et al., 2004) by changing the enzymatic reaction in step 4 of 7 in the production pathway. In high H_2 conditions, where H_2 can act as an electron donor, the reaction is highly reversible and a low fractionation factor is seen, whereas low H_2 conditions result in a reaction with a lower reversibility and a higher fractionation factor; these results can be seen across a range of laboratory experiments (Table 1) and is particularly significant as high H_2 pressures have often been used, especially in the earlier experiments (e.g. Botz et al., 1996; Fuchs et al., 1979; Games et al., 1978); in some later experiments a coculture including syntrophic H_2 producing bacteria has been used in order to maintain a low P_{H_2}, more representative of environmental conditions (e.g. Hattori et al., 2012; Penning et al., 2005; Valentine et al., 2004; Yoshioka et al., 2008). A relationship between P_{H_2} and $\delta^{13}C(CH_4)$ has been observed in experiments using a range of substrates and syntrophic bacteria to produce H_2 and CO_2; and across all experiments, a relationship between the Gibbs free energy and carbon isotope fractionation in hydrogenotrophic methanogenesis was observed (Penning et al., 2005).

$\delta^2H(CH_4)$ may also be affected by H_2 in the system, early experiments indicated decreased $\delta^2H(CH_4)$ with increased P_{H_2} (Balabane et al., 1987), leading to the proposal that hydrogenase aided equilibration of H_2 and H_2O under high P_{H_2} conditions causing increased H fractionation in CH_4 (Burke, 1993). This relationship was observed in some experiments (Hattori et al., 2012), but not in others (Yoshioka et al., 2008), and could sometimes be attributed to catabolic rate

(Valentine et al., 2004). Further work (Kawagucci et al., 2014; Okumura et al., 2016) indicated that a H_2 effect on $\delta^2H(CH_4)$ is dependent on the methanogenic growth rate in addition to P_{H_2}. With a high catabolic rate, H_2 consumption is as fast as trans-membrane H_2O transport and equilibration of H_2 and H_2O is able to take place and therefore $\delta^2H(H_2O)$ will affect $\delta^2H(CH_4)$ via isotopic equilibration with H_2O.

Incubation experiments (Table 1.1 and references within) provide a summary of published experiments conducted to determine stable isotope fractionation factors for methanogenesis based upon different substrates and a range of experimental conditions, such as temperature and P_{H_2}. Hydrogenotrophic methanogenesis has a large range of fractionation factors, the lower end of which shares a significant area of overlap with acetoclastic methanogenesis and it may be difficult to determine the production pathway if considering only $\delta^{13}C(CH_4)$ and $\delta^{13}C(CO_2)$. Therefore the environmental conditions, including substrate availability and energetic conditions also need to be considered.

The relative contribution of hydrogenotrophic and acetogenic methanogenesis can be estimated by measuring the isotope composition of the methyl group in acetate, the $\delta^{13}C$ values of CH_4 and CO_2 and by using α values for each methanogenic pathway determined from incubation experiments (Conrad, 2005). The incubation experiments used to determine α values have been conducted with only one type of methanogenesis operating, which is typically achieved using selective inhibitors, such as methyl fluoride (CH_3F) to eliminate acetogenic methanogenesis (Frenzel and Bosse, 1996; Janssen and Frenzel, 1997). Conrad (2005) reported the mass balance equations necessary to determine stable carbon isotope fraction for methanogenesis via each pathway:

$$F_{mc} = \frac{\delta CH_4 - \delta_{ma}}{\delta_{mc} - \delta_{ma}} \tag{1.9}$$

where F_{mc} is the fraction of CH_4 produced by the hydrogenotrophic pathway, δ_{ma} is the isotope composition of CH_4 produced from acetogenic methanogenesis, and δ_{mc} is the isotope composition of CH_4 produced from hydrogenotrophic methanogenesis. The methanol pathway typically is not included in mass balance estimates of methanogenic metabolism because it is regarded as an uncommon pathway for CH_4 production in natural environments; however, it does exhibit a large stable C isotope fractionation (Table 1.1). Recently it was suggested that methanol-based methanogenesis may be more common in anoxic natural environments than previously thought (Penger et al., 2012).

In environments where labile organic matter is degraded anaerobically, producing CH_4 as a terminal end product of decay, it is generally expected, based

upon reducing equivalents in polysaccharides that form cellulose, that a maximum of 1/3 of CH_4 is produced by hydrogenotrophic methanogenesis and 2/3 by acetate fermentation (Conrad, 1999). Four H_2 molecules are produced for every acetate molecule in the breakdown of polysaccharides although it is possible that the H_2 may be consumed by other microorganisms, such as sulphate reducing bacteria, which could shift the relative proportion of CH_4 formation to acetogenic methanogenesis. The ratio also may be altered if other acetate sinks or additional H_2 sources exist, or measurements are conducted under non-steady state conditions. Consequently, net fractionation factors for methanogenesis and stable isotope composition for CH_4 can exhibit variability spatially and temporally within individual environments (Conrad et al., 2009) or between similar sites (Conrad et al., 2011). If precise α values for methanogenesis are required for a site, then typically it is necessary to conduct incubation experiments specific to the conditions and substrate sources for the environment inoculated with material collected in situ.

Table 1.1 Fractionation factors (α_C and α_H values) for methanogenesis from incubation experiments

Process	Methanogen/ Sample	pH_2 (Pa)	T (°)	α_C	α_H	Reference
Hydrogenotrophic	*Methanosarcina barkeri*	8x10^4	40	1.045		Games et al. (1978)
methanogenesis	*Methanobacterium* strain MoH	8x10^4	40	1.061		Games et al. (1978)
	M. thermoautotrophicum	2.4x10^5	65	1.025		Games et al. (1978)
	M. barkeri strain MS	8x10^4	36	1.049		Krzycki et al. (1987)
	M. thermoautotrophicum	8x10^4	65	1.034		Fuchs et al. (1979)
	M. thermoautotrophicum	8x10^5	65	1.039		Fuchs et al. (1979)
	M. fromicicum	2.4x10^5	34	1.048	1.67	Balabane et al. (1987)
	Methanobacterium strain ivanov	8x10^4	37	1.034		Belyaev et al. (1983)
	Methanobacterium strain ivanov	8x10^4	46	1.032		Belyaev et al. (1983)
	Methanococcus vanielii	8x10^4	35	1.067		Botz et al. (1996)
	M. thermolithotrophicus	8x10^4	45	1.064		Botz et al. (1996)
	M. thermolithotrophicus	8x10^4	55	1.062		Botz et al. (1996)
	M. thermolithotrophicus	8x10^4	65	1.059		Botz et al. (1996)
	M. igneus	8x10^4	85	1.056		Botz et al. (1996)
	Methanothermobacter marburgensis	3.1x10^2	65	1.064		Valentine et al. (2004)
	Methanothermobacter marburgensis	8x10^4	65	1.031		Valentine et al. (2004)
	Methanothermobacter marburgensis	7x10^4	65		1.42	Valentine et al. (2004)
	Methanothermobacter thermautotrophicus	6x10^1	55	1.074	1.51	Okumura et al (2016)
	Methanobacterium sp.	1x10^1	25	1.079	1.54	Okumura et al (2016)
	Methanothermococcus okinawensis	2.1x10^5	60	1.038		Okumura et al (2016)
	Methanobacterium sp.	2.2x10^5	30	1.046	1.47	Okumura et al (2016)
	Methanothermobacter thermoautotrophicus	2.4x10^5	55		1.32	Yoshioka et al (2008)

Table 1.1 continued

Process	Methanogen/ Sample	pH_2 (Pa)	T (°)	α_C	α_H	Reference
	Methanothermobacter thermoautotrophicus	$2.4x10^5$	65		1.34	Yoshioka et al (2008)
	Methanothermobacter thermoautotrophicus	low	55		1.38	Yoshioka et al (2008)
	Methanothermobacter marburgensis	$8x10^4$	65	1.036		Penning et al (2005)
	Methanothermobacter marburgensis	$5x10^3$	65	1.063		Penning et al (2005)
	Methanosarcina barkeri	$8x10^4$	37	1.043		Londry et al (2008)
	Methanosarcina barkeri	5x103	37	1.056		Londry et al (2008)
	Rice soil	$5x10^2$	30	1.05		Chidthaisong et al. (2002)
	Rice roots	$5x10^2$	30	1.057		Chidthaisong et al. (2002)
	Rice soil	$8x10^4$	30		1.56	Chidthaisong et al. (2002)
	Rice roots	$8x10^4$	30		1.76	Chidthaisong et al. (2002)
	Groundwater	low	55	1.068	1.41	Hattori et al (2012)
	Groundwater	low	65	1.067	1.38	Hattori et al (2012)
	Groundwater	$2.5x10^5$	55	1.022	1.55	Hattori et al (2012)
	Groundwater	$2.5x10^5$	65	1.022	1.52	Hattori et al (2012)
	Lake sediments		10	1.043 - 1.097		Conrad et al (2009)
	Soil - Vercelli		25	1.045 - 1.060		Conrad et al (2012)
	Soil - Fuyang		25	1.050 - 1.060		Conrad et al (2012)
	Soil - Suwan		25	1.040 - 1.055		Conrad et al (2012)
	Rice soil		30	1.045	1.46	Sugimoto & Wada (1993, 1995)
	Buck Hollow bog		25	1.069		Avery et al (1999)
	Kings Lake bog		18	1.073		Lansdown et al (1992)

Table 1.1 continued

Process	Methanogen/ Sample	pH_2 (Pa)	T (°)	α_C	α_H	Reference
	Rice soil -Texas		30	1.060		Tyler et al (1997)
	Rice soil - Italy		24	1.060		Fey et al (2004)
	Rice soil - Italy		25	1.070		Fey et al (2004)
	Rice soil - Italy		50	1.073		Fey et al (2004)
	Tropical lake sediment			1.057 - 1.085		Conrad et al (2011)
	Swamp soil - Florida (oligotrophic)			1.073		Holmes et al (2014)
	Swamp soil - Florida (transition)			1.074		Holmes et al (2014)
	Swamp soil - Florida (eutrophic)			1.081		Holmes et al (2014)
Methanol dependent methanogenesis	*M. barkeri* strain MS		37	1.079		Krzycki et al. (1987)
	Methanosarcina barkeri		37	1.059		Londry et al (2008)
	Methanosarcina acetivorans		37	1.072		Penger et al (2012)
	Methanosarcina barkeri		37	1.074		Penger et al (2012)
	Methanolobus zinderi		37	1.083		Penger et al (2012)
	Marine sediments		30	1.081		Rosenfeld and Silverman (1959)
	Marine sediments		23	1.094		Rosenfeld and Silverman (1959)
	Lake sediment - hyperalkaline		20	1.074		Oremland et al. (1982)
Acetoclastic methanogenesis	*M. barkeri* strain MS		37	1.021		Krzycki et al. (1987)
	M. barkeri strain 227		37	1.021		Gelwicks et al. (1994)
	Methanosaeta thermophila strain		61	1.007		Valentine et al. (2004)

Table 1.1 continued

Process	Methanogen/ Sample	pH_2 (Pa)	T (°)	α_C	α_H	Reference
	Methanosarcina barkeri		37	1.024		Londry et al (2008)
	Methanosaeta concilii		37	1.009		Penning et al (2006)
	Methanosarcina acetivorans		37	1.024		Conrad (2009)
	Methanosarcina barkeri		30	1.027		Conrad (2009)
	Marine sediments and sludge		30	1.019		Heyer et al. (1976)
	Lake sediments - Cape Lookout Bight		26	1.034		Blair and Carter (1992)
	Rice soil				2.29	Sugimoto and Wada (1995)

1.4.1 Mixing of sources

It is possible for CH_4 originating from two or more sources to mix together within an aquifer and the resulting CH_4 will have a stable isotope composition between these two end members, A and B. This will be governed by simple mass balance:

$$\delta_{sample} = f.\delta_A + (1 - f).\delta_B \tag{1.10}$$

If there is more than one component, this will become more complex and another component may need to be considered, such as Cl.

1.4.2 Clumped isotopes

Multiple substituted isotopologues (or 'clumped isotopes' in which molecules contain more than one rare isotope e.g., $^{13}C^2H^1H_3$ or $^{12}C^2H_2{}^1H_2$) can be used to determine CH_4 formation temperatures on the basis that the rarer isotopes are distributed stochastically at higher temperatures. Though this possibility is well known, it is only relatively recently that it has been possible to measure clumped isotopes as a result of advances in mass spectrometry and laser spectroscopy techniques (Eiler et al., 2013; Ono et al., 2014). The approach thus far has been used successfully to study formation temperatures for thermogenic CH_4, which is produced at higher temperatures than microbial CH_4. The method is however, unsuitable for use as a temperature proxy for microbial sources because unless CH_4 generation rates are low (Stolper et al., 2014a, 2014b), internal equilibrium will not be attained in the CH_4 molecule (Stolper et al., 2015).

1.5 Methane oxidation

Methane can be oxidised aerobically or anaerobically by microorganisms. Aerobic oxidation by methanotrophic bacteria occurs in the presence of oxygen (eq. 1.11). In anoxic environments, CH_4 can be oxidized in the presence of sulphate (eq. 1.12) (Hoehler et al., 1994) or nitrite (eq. 1.13) (Raghoebarsing et al., 2006) or other species, such as Mn or Fe, that are able to act as electron acceptors. Aerobic CH_4 oxidation will always occur preferentially if O_2 is present. If O_2 is introduced into anaerobic environments, aerobic methanotrophy will take place, with anaerobic methanotrophy re-occurring after O_2 depletion (Case et al., 2017).

$$CH_4 + O_2 \rightarrow CO_2 + H_2O \tag{1.11}$$

$$CH_4 + SO_4^{2-} \rightarrow HCO_3^- + HS^- + H_2O \quad (1.12)$$

$$3CH_4 + 8HNO_2 \rightarrow 3CO_2 + 4N_2 + 10H_2O \quad (1.13)$$

Aerobic CH_4 oxidation is carried out by methanotrophic bacteria in the presence of O_2. Hanson and Hanson (1996) detail the process, which can involve a wide range of over 100 different bacteria, which can be separated into three classes based on the pathway used to metabolise CH_4: type I, II and X, which are all alpha- or gamma-Proteobacteria. The first step of the process is the oxidation of CH_4 to methanol by methane monooxygenase (MMO) enzymes, which are either soluble (sMMO) or particulate (pMMO). The methanol is then oxidised to formaldehyde by a periplasmic methanol dehydrogenase (MDH), which is then oxidised to CO_2 via formate.

Methanotrophs generally grow at moderate pH and temperatures (pH 5-8, 20-35 °C; Anthony, 1982) although can also exist in more extreme environments, including under pH 1 conditions (Semrau et al., 2008). Methanotrophy commonly occurs in freshwater environments where there is a constant supply of O_2, such as lakes (Murase et al., 2003; Samad and Bertilsson, 2017), rivers (Dzyuban, 2011; Shelley et al., 2014), estuaries (Abril et al., 2007; de Angelis and Scranton, 1993) and wetlands (King, 1990; Segers, 1998); as well as landfills (Liptay et al., 1998; Whalen et al., 1990) and contaminated land (Amos et al., 2012; Revesz et al., 1995).

Sulphate dependent anoxic methane oxidation (S-DAMO) was first suggested when declining CH_4 and sulphate concentrations were observed in anoxic marine sediments (Barnes and Goldberg, 1976; Reeburgh, 1976). Anaerobic methanotrophic archaea (ANME) act in conjunction with sulphate reducing bacteria (SRB) to simultaneously oxidise CH_4 and reduce SO_4^{2-}, by a form of 'reverse methanogenesis' whereby a methanogenic substrate is produced and transferred between species. Experiments have excluded several common substrates, including acetate, formate, methanol, CO and H_2 (Meulepas et al., 2010). Other potential substrates could be methyl sulphides (Moran et al., 2008) or zero-valent sulphur (Milucka et al., 2012), which would be produced by archaea and transferred to the SRB. ANME also have been reported to possess methanogenic capabilities (Bertram et al., 2013), suggesting that both methanogenesis and methanotrophy can occur together in anaerobic sediments.

S-DAMO has been observed primarily in marine sediments where ANME and SRB are ubiquitous (e.g. Borowski, 2004). It is the dominant CH_4 oxidation pro-

cess and involves consumption of large amounts of sulphate. Methane oxidation coupled to sulphate reduction is intensified in areas with a strong CH_4 supply, such as above gas hydrates (Borowski, 2004; Çağatay et al., 2001).

Nitrite dependent anoxic oxidation of methane (N-DAMO) is a more recently discovered CH_4 oxidation process (Raghoebarsing et al., 2006). *Methylomirabilis oxyfera* has been identified as the bacterium which carries out this process (Rasigraf et al., 2012). Oxygen is produced intracellularly and used for the activation of CH_4 by a phylogenetically distinct pMMO, which then follows the pathway of aerobic CH_4 oxidation. N-DAMO can be a dominant oxidation process in ecosystems containing high nitrate and nitrite concentrations. It has been observed in freshwater environments, such as nutrient-contaminated rivers (Ding et al., 2015; Long et al., 2017) and wetlands (Shen et al., 2015a) but also in marine environments (He et al., 2015; Shen et al., 2015b). It can also be utilised in wastewater treatment plants (Bhattacharjee et al., 2016; Xu et al., 2017) in order to reduce CH_4 emissions.

Metal anoxic oxidation of methane (metal-AOM) is an even more recently discovered process, whereby CH_4 oxidation can be linked to reduction of Mn, Fe (Ettwig et al., 2016; Fu et al., 2016; Scheller et al., 2016) and Cr (Lu et al., 2016). Several strains of ANME-2 have been shown to be capable of metal-AOM, which were previously thought to be solely nitrite-dependent microorganisms. The exact mechanism of metal-AOM remains unclear but is thought to follow a 'reverse methanogenesis' pathway similar to S-DAMO and not the intracellular oxygen production pathway of N-DAMO because metal oxides cannot be transported into cells (He et al., 2018). Metal-AOM has been observed in rivers (Beal et al., 2009), lakes (Crowe et al., 2011), coastal sediments (Egger et al., 2015) and hydrothermal systems (Wankel et al., 2012).

1.6 Stable isotopes and methane oxidation

Laboratory incubation experiments in methanotrophy (Table 1.2) and field observations (Feisthauer et al., 2012; Ward et al., 1996; Williams et al., 1999) have attempted to quantify the magnitude of stable carbon and hydrogen isotope fractionation that occurs during bacterial CH_4 oxidation. Coleman et al (1981) showed that the change in $\delta^2H(CH_4)$ values is 8 to 14 times greater than the change in $\delta^{13}C(CH_4)$, which may be useful for differentiating between thermogenic CH_4 and microbial CH_4 that has been altered. Several other studies have reported a relationship between the magnitude of values and temperature (Chanton et al., 2008; Mahieu et al., 2006; Nihous, 2010).

Rates of CH_4 oxidation typically increase with increasing O_2 concentration in freshwater environments (e.g. Happell et al., 1994; Murase et al., 2003). Recent studies of methanotrophy in rivers (Sawakuchi et al., 2016) and lakes (Cadieux et al., 2016) have reported particularly large fractions of CH_4 oxidation leading to highly positive $\delta^{13}C(CH_4)$ and $\delta^{2}H(CH_4)$ values. Cadieux et al. (2016) showed a linear correlation between $\delta^{13}C(CH_4)$ and $\delta^{2}H(CH_4)$ values in freshwater lakes, which is consistent with a common CH_4 source consumed to varying degrees by methanotrophic activity. Moreover, $\delta^{13}C$ and $\delta^{2}H$ values of CH_4 typically decrease with depth in the water column of lakes because bacterial oxidation of CH_4 occurs at shallower and more oxygenated depths (Jedrysek, 2005). A similar pattern is present in the water columns of rivers and estuaries; however, it is commonly more complicated because of turbulent flow. Bacterial oxidation of CH_4 in water has been reported to increase with increasing concentration of suspended particles, often associated with turbulence, because the sediments commonly contain populations of active methanotrophs (de Angelis and Scranton, 1993).

Table 1.2 Fractionation factors (α_C and α_H values) for methanotrophy from incubation experiments

Sample	T (°C)	α_C	α_H	Reference
Culture A (from drip tray)	26	1.025	1.325	Coleman (1981)
Culture B (from water sample in gassy well)	11.5	1.013	1.103	Coleman (1981)
Culture B (from water sample in gassy well)	26	1.024	1.297	Coleman (1981)
Landfill soil, Nashua, New England	25	1.022		Liptay et al (1998)
Forest soil, New Hampshire, 8-13 cm	22	1.016		Tyler et al (1994)
Forest soil, New Hampshire, 4-8 cm	22	1.014		Tyler et al (1994)
Forest soil, New Hampshire, 8-13 cm	-	1.024		Tyler et al (1994)
Forest soil, New Hampshire, 4-8 cm	-	1.021		Tyler et al (1994)
Forest soils (in-situ), May 90	-	1.029		Tyler et al (1994)
Forest soils (in-situ), Aug 90	-	1.025		Tyler et al (1994)
Forest soils (in-situ), Oct 90	-	1.017		Tyler et al (1994)
Forest soils (in-situ), Nov 90	-	1.021		Tyler et al (1994)
Forest soils (in-situ), Jul 91	23	1.0313 to 1.0052		Barker and Fritz (1981)
Forest soils (in-situ), Sep 91	25	1.010		Teh et al (2006)
Stream sediment	25	1.013		Teh et al (2006)
Tropical soil[a], 1600 ppm CH_4 21 ppm O_2	25	1.013		Teh et al (2006)
Tropical soil[a], 3800 ppm CH_4 21 ppm O_2	25	1.023		Teh et al (2006)
Tropical soil[a], 1600 ppm CH_4 3 ppm O_2	25	1.019		Teh et al (2006)
Tropical soil[a], 1600 ppm CH_4 5 ppm O_2	25	1.018		Teh et al (2006)
Tropical soil[a], 1600 ppm CH_4 10 ppm O_2	25	1.012		Teh et al (2006)
Tropical soil[a], 1600 ppm CH_4 21 ppm O_2	25	1.013		Teh et al (2006)
Landfill soil, Iowa	23.7	1.033		Chanton et al (2008)

Table 1.2 continued

Sample	T (°C)	α_C	α_H	Reference
Landfill soil, Kentucky	24.6	1.026		Chanton et al (2008)
Landfill soil, Illinois	25.6	1.024		Chanton et al (2008)
Landfill soil, Illinois	23.9	1.048		Chanton et al (2008)
Landfill soil, Florida (10-20 cm)	6	1.030		Chanton et al (2008)
Landfill soil, Florida (10-20 cm)	15	1.029		Chanton et al (2008)
Landfill soil, Florida (10-20 cm)	25	1.028		Chanton et al (2008)
Landfill soil, Florida (10-20 cm)	33	1.030		Chanton et al (2008)
Landfill soil, Florida (10-20 cm)	43	1.031		Chanton et al (2008)
Landfill soil, Florida (20-30 cm)	6	1.039		Chanton et al (2008)
Landfill soil, Florida (20-30 cm)	15	1.030		Chanton et al (2008)
Landfill soil, Florida (20-30 cm)	25	1.029		Chanton et al (2008)
Landfill soil, Florida (20-30 cm)	33	1.026		Chanton et al (2008)
Landfill soil, Florida (20-30 cm)	43	1.029		Chanton et al (2008)
Landfill soil, Fiborna	25	1.017		Borjesson et al (2007)
Landfill soil, Heljestorp	25	1.019		Borjesson et al (2007)
Landfill soil, Hoegbytorp	25	1.016		Borjesson et al (2007)
Landfill soil, Sundsvall	25	1.015		Borjesson et al (2007)
Landfill soil, Hagby	25	1.017		Borjesson et al (2007)
Landfill soil, Visby	25	1.015		Borjesson et al (2007)
Landfill clay 1, Leon, Florida	8	1.032		Chanton and Liptay (2000)
Landfill clay 2, Leon, Florida	8	1.049		Chanton and Liptay (2000)
Landfill mulch 1, Leon, Florida	8	1.035		Chanton and Liptay (2000)

Table 1.2 continued

Sample	T (°C)	α_C	α_H	Reference
Landfill mulch 2, Leon, Florida	8	1.039		Chanton and Liptay (2000)
Landfill clay 1, Leon, Florida	12	1.034		Chanton and Liptay (2000)
Landfill clay 2, Leon, Florida	12	1.034		Chanton and Liptay (2000)
Landfill mulch 1, Leon, Florida	12	1.035		Chanton and Liptay (2000)
Landfill mulch 2, Leon, Florida	12	1.038		Chanton and Liptay (2000)
Landfill clay 1, Leon, Florida	24	1.030		Chanton and Liptay (2000)
Landfill clay 2, Leon, Florida	24	1.031		Chanton and Liptay (2000)
Landfill mulch 1, Leon, Florida	24	1.033		Chanton and Liptay (2000)
Landfill mulch 2, Leon, Florida	24	1.031		Chanton and Liptay (2000)
Landfill clay 1, Leon, Florida	35	1.028		Chanton and Liptay (2000)
Landfill clay 2, Leon, Florida	35	1.028		Chanton and Liptay (2000)
Landfill mulch 1, Leon, Florida	35	1.026		Chanton and Liptay (2000)
Landfill mulch 2, Leon, Florida	35	1.025		Chanton and Liptay (2000)

[a] Tropical soil incubated under different mixing ratios of CH_4 and O_2 to vary methanotrophy rates

1.6.1 Open and closed systems

When modelling stable isotope compositions of CH_4 in relation to methanotrophy, it is necessary to consider the degree to which an environment is either an open or closed system. A closed system (eq. 1.14) assumes no transport of CH_4 into or out of the system, and consumption of the CH_4 is modelled via a form of Rayleigh distillation (Coleman et al., 1981; Mahieu et al., 2006):

$$logf = \frac{log(\delta A + 1000) - log(\delta E + 1000)}{\alpha - 1} \tag{1.14}$$

where f is the fraction of CH_4 remaining, δA is the stable isotope composition of unaltered CH_4, δE is the stable isotope composition of CH_4 that has been subjected to methanotrophy, and α is the fractionation factor associated with bacteria oxidation of CH_4.

In an open system (eq. 1.15), influx and outflux of CH_4 may occur by mass transport, including via diffusion, which also may impart a further stable isotope fractionation (Happell et al., 1994):

$$F_{ox} = \frac{\delta E - \delta A}{1000(\alpha - \alpha_{trans})} \tag{1.15}$$

Where F_{ox} is the fraction of CH_4 oxidised, α_{trans} is the fractionation factor associated with CH_4 transport, and δA, δE and α are the same as defined for eq. 1.14.

Transport of CH_4 in an open system by mass transport yields $\alpha_{trans} = 1$ (no fractionation); however, a component of CH_4 transport via diffusion can produce a stable C isotope fractionation up to a theoretical maximum of 1.014 (De Visscher et al., 2004).

The open system model is used in instances where there is ongoing CH_4 production and emission, and assumed mass transport of the CH_4, such as within landfill sites (Liptay et al., 1998), or in soils overlying a CH_4 source (Teh et al., 2006; Tyler et al., 1994). Sawakuchi et al. (2016) considered both open and closed system models when attempting to calculate the fraction of CH_4 oxidised in rivers, which for highly oxidised areas, resulted in the fraction of CH_4 oxidised being greater than 1 for an open scenario indicating a closed system; however, CH_4 flux measurements indicate an open system. Similar considerations will need to be made when investigating CH_4 oxidation in groundwater, depending on whether the aquifer is open or closed, and whether CH_4 is transported from deeper, more anoxic parts of the aquifer or produced in-situ.

1.7 Methane in groundwater

The majority of dissolved carbon within groundwater is likely to be dissolved inorganic carbon (DIC), which consists of dissolved CO_2 (H_2CO_3), HCO_3^- and CO_3^{2-}, the exact proportions of which will depend on pH (Clark and Fritz, 1997); the source of DIC is a combination of soil CO_2 and dissolved carbonate. There may also be a proportion of dissolved organic carbon (DOC), the amount of which will be determined by the influx of organic matter. Carbon for CH_4 production may originate within these pools and CO_2 formed by CH_4 oxidation will add back into them. Exogenous CH_4 may also enter the system and may be of a thermogenic (e.g., Osborn et al., 2011) or abiotic source (e.g., Boschetti et al., 2013). Contamination of an aquifer may add to the dissolved carbon pool by the degradation of organic matter sourced within the contaminating fluid, the final stage of which may be CH_4 production (Baker et al., 2012; Revesz et al., 1995). This in turn is likely to increase the rate of CH_4 oxidation, assuming that there are available electron acceptors for this to occur.

Methane is commonly present in UK groundwaters though generally at low concentrations (Darling and Gooddy, 2006). The majority of UK groundwaters studied to date have low concentrations of CH_4 (e.g., 80 % < 10 µg L^{-1}) with only a few locations exhibiting elevated concentrations (e.g., 4 % > 100 µg L^{-1}) and none with concentrations higher than the US government suggested risk action level (e.g., 10,000 µg L^{-1}) (Bell et al., 2017).

The number of studies investigating CH_4 in groundwater has increased in recent years because of a desire to establish baseline conditions prior to shale gas exploration and development for the purpose of future assessment of potential contamination of groundwater sites. Consequently, more studies have been conducted in areas where thermogenic gas may be present, which historically was less common in groundwater CH_4 studies.

Work characterising groundwater CH_4 prior to shale gas development has taken place in a number of locations worldwide (e.g., McIntosh et al., 2014; McPhillips et al., 2014; Moritz et al., 2015; Schloemer et al., 2016) and in the UK via a baseline survey conducted by the British Geological Survey (BGS) (Bell et al., 2017), which involved compiling existing BGS and UK Environment Agency (EA) groundwater CH_4 data and supplementing these with new analyses from selected boreholes. Such studies have yielded a broad scope of baseline CH_4 concentrations in groundwater, which depend on the specific geological and hydrogeological history of an area. Most investigations have reported the presence of microbial CH_4 produced within the shallow groundwater aquifers being investigated (Down et al., 2015; Huang et al., 2017; Schloemer et al., 2016). Several

have additionally identified one or more thermogenic sources of CH_4 migrating from deeper in the basin and mixing with shallower microbial sources (Bordeleau et al., 2015, 2018; Eymold et al., 2018; Humez et al., 2016; Lavoie et al., 2016) and some aquifers contain primarily thermogenic CH_4 (Nicot et al., 2017a).

Elevated concentrations of CH_4 in groundwater have been associated with geochemical indicators associated with conditions favourable for CH_4 production, such as reducing conditions, low sulphate and nitrate concentrations (LeDoux et al., 2016), and Na-rich vs. Ca-poor waters (Bordeleau et al., 2015; Humez et al., 2016; McPhillips et al., 2014; Moritz et al., 2015). Geological structures such as faults can also facilitate migration of CH_4 from depth into shallow groundwater (Grasby et al., 2016; Kreuzer et al., 2018; Li et al., 2016; Moritz et al., 2015; Nicot et al., 2017b) and wells located in lowland areas typically are more CH_4-rich compared to upland areas because the interface between deeper CH_4-bearing saline water and shallow fresh water is closer to the surface in the former (Molofsky et al., 2013). Sites commonly show a combination of these factors (Molofsky et al., 2016), for example, Na-rich groundwater in valleys are more likely to contain a higher concentration of CH_4 (Christian et al., 2016).

Elevated CH_4 concentrations in groundwater close to shale gas wells have been reported (Hammond, 2016; Jackson et al., 2013; Osborn et al., 2011); however, the extent of well contamination with CH_4 has been debated with subsequent studies in the same areas with larger datasets not finding a significant relationship (Siegel et al., 2015), and others suggesting the primary reason for the presence of CH_4 to be topography-related (Molofsky et al., 2013); i.e., the interface between deep methane bearing waters and shallower waters are closer to the surface in lowland areas. A correlation between the amount of CH_4 in groundwater and the presence of uncased gas wells that intersect faults at depths has been reported by Li et al. (2016).

Most of these studies involve groundwater containing a high CH_4 concentration, commonly from a thermogenic source, that has mixed with a background microbial source. Few studies have investigated areas where dissolved CH_4 is present solely at a low-level background concentration and fewer studies still have investigated the stable isotope composition of CH_4 in groundwater at all but the highest concentration sites, in particular, to measure $\delta^2H(CH_4)$ values. The lack of such isotope data makes it uncertain whether the low levels of CH_4 present are the result of limited methanogenesis or highly efficient methanotrophy that has left only a small CH_4 residual in groundwater.

1.8 Study objectives and approach

The aims stated at the start of this chapter were conducted by sampling a selection of boreholes from a range of UK aquifers that exhibit a breadth of CH_4 concentration in different geological contexts. In addition to stable C and H isotope analysis of CH_4, this study also quantifies the concentration of H_2, the $\delta^{13}C$ value of dissolved inorganic carbon (DIC), and the $\delta^{18}O$ and $\delta^{2}H$ values of water, parameters necessary to evaluate the isotope systematics of CH_4 cycling in groundwater, which were not measured as part of the broader BGS CH_4 baseline survey. This project had access to geochemical data and physical parameters measured as part of the BGS baseline study. The project began with a comprehensive compilation and review of stable isotope data reported to date for CH_4 in UK groundwater and natural and human sources that might contribute CH_4 to groundwater (Chapter 2).

Previous characterisation of the stable isotope compositions of dissolved CH_4 in groundwater ($\delta^{13}C(CH_4)$ and $\delta^{2}H(CH_4)$ values) was conducted primarily in aquifers that contain high concentrations of CH_4. There is a particular dearth of $\delta^{2}H(CH_4)$ data for aquifers that contain low to moderate concentrations of CH_4. Consequently, this study included a significant investment of time in developing a method to extract and concentrate low levels of dissolved CH_4 in a quantity sufficient to conduct both $\delta^{13}C(CH_4)$ and $\delta^{2}H(CH_4)$ analyses (Chapter 4). The new approach enabled baseline characterisation of the stable C and H isotope compositions of CH_4 at concentrations as low as 2 - 3 µg L^{-1} for a broad range of UK aquifers.

A selection of boreholes within the Lower Greensand aquifer in the Hampshire and Surrey area was used to investigate CH_4 formation and oxidation within a single major aquifer (Chapter 5). The Lower Greensand aquifer is situated within a syncline providing samples from a range of depths possessing different hydrochemical properties and open and closed conditions. The investigation has provided new insights into the potential variability of stable isotope compositions of CH_4 arising from a range of environmental conditions within a single aquifer.

Groundwater CH_4 was investigated in the shallow and non-continuous Middle Sands aquifer and the deeper Sherwood Sandstone aquifer in Lancashire (Chapter 6), a region where shale gas exploration is planned. A major N-S striking fault crosses the study area dividing the boreholes sampled into Middle Sands to the west and Sherwood Sandstone to the east. The study provided an opportunity to investigate the prospect of existing fluid migration along a major fault and to examine the feasibility of accurately characterising baseline stable isotope compositions of CH_4 in groundwater from a geologically complex area prior to shale

gas development.

Finally, a broad selection of boreholes from major UK aquifers was sampled for CH_4 to explore dominant geological and environmental controls on groundwater $\delta^{13}C(CH_4)$ and $\delta^2H(CH_4)$ values and to establish the degree of variability in the stable isotope composition of CH_4 in UK aquifers (Chapter 7). The boreholes sampled for stable isotope analysis of CH_4 are a subset of the sites investigated as part of the BGS CH_4 baseline survey. The geographic range of the UK-wide borehole study provided an opportunity to investigate relationships between $\delta^2H(CH_4)$ and the δ^2H values of meteoric water.

Hypotheses explored within these studies include:

1. Methane in UK aquifers primarily has a microbial origin and is produced in-situ. **(H1)**

2. Despite the majority of CH_4 having a microbial origin, $\delta^{13}C(CH_4)$ and $\delta^2H(CH_4)$ values and the amount of CH_4 will exhibit high degrees of variability governed by a breadth of environmental conditions. **(H2)**

3. A subset of aquifers will be impacted locally by allochthonous CH_4 sources such as coalfields, landfills, etc. **(H3)**

4. Values of $\delta^2H(CH_4)$ will be linked the deuterium content of local meteoric water. **(H4)**

5. The amount of CH_4 in aquifers impacted by bacterial oxidation, will relate to the degree to which an aquifer is open, the Eh and P_{O_2} of the aquifer, and be reflected in an increase and correlation between $\delta^{13}C(CH_4)$ and $\delta^2H(CH_4)$ values. **(H5)**

Chapter 2

Stable isotope tracing of autochthonous and allochthonous sources of groundwater CH_4 in the United Kingdom

Summary

Methane (CH_4) concentration and $\delta^{13}C$ and δ^2H values have been compiled for UK aquifers and groundwater globally. Stable isotope data also are compiled for allochthonous sources of CH_4 that are capable of contaminating groundwater.

Paired $\delta^{13}C(CH_4)$ and $\delta^2H(CH_4)$ data are scarce for aquifers in the UK and globally but available data suggest that most CH_4 present in aquifers is microbial and alteration by methanotrophic bacteria is common. The $\delta^{13}C$ and δ^2H values of allochthonous CH_4 that may contaminate aquifers are similar worldwide because there are relatively few biochemical pathways and substrates used by Archaea to produce CH_4. Under similar conditions, biogenic processes that degrade organic matter generate CH_4 that has $\delta^{13}C$ and δ^2H values that fall within relatively narrow ranges.

Allochthonous sources such as coal formations may contribute CH_4 directly to groundwater; however, sources such as landfills may leak both CH_4 and labile carbon that may serve as a substrate for methanogenesis with aquifers.

Future baseline characterisation of groundwater CH_4 should include $\delta^2H(CH_4)$ in addition to more readily available measurements of $\delta^{13}C(CH_4)$ and C_{2+} components to ensure less ambiguity in distinguishing thermogenic CH_4 from archaeal CH_4 altered by bacterial methanotrophy. Inclusion of clumped isotopologue measurements that provide information about CH_4 formation temperature will further refine the ability to distinguish ingress of deep thermal CH_4 and in situ alteration of microbial CH_4.

2.1 Introduction

There is increasing interest worldwide in the development and extraction of shale gas and other unconventional gas sources. The shale gas industry in the United Kingdom is in its infancy compared to the United States of America where it has been growing rapidly since the early 2000s. Although the geology and regulatory regimes differ in these two countries, experience and knowledge gained from activities in the USA could help to inform decision-making in the UK (Hays et al., 2015). In the UK, resource estimates (gas-in-place) for the Bowland Shale are 822 to 2281 trillion cubic feet (tfc) (Andrews, 2013) and a further 49.4 to 134.6 tcf in the Midland Valley of Scotland (Monaghan, 2014). Andrews (2014) reported that the Weald basin while not containing significant natural gas may possess a shale oil resource of 300 to 1100 million tonnes.

There has been central government support for shale gas exploration and development in the UK (Vaughan, 2015; Watt, 2014). The Independent Task Force on shale gas recommends that natural gas is a necessary part of the UK's energy mix both in the short- and medium-term, and that it is not feasible to create a renewable energy industry that can meet all UK energy needs in the short-term (Task Force on Shale Gas, 2015). However, the Scottish government recently backed a ban on shale gas development (BBC, 2017a) and a moratorium on development has existed in Wales since 2015 (Flint, 2017), reflecting significant opposition to shale gas extraction both nationally and at a local level (BBC, 2018, 2017b). Public support for shale gas exploration and mining appears to have shifted recently. It was increasing prior to August 2013 and then began to wane, with a recent survey in 2016 showing for the first time that a majority of people do not support shale gas development (O'Hara et al., 2016, 2013).

Unplanned seismic activity from an early test well in 2011 in Lancashire led to a temporary moratorium on UK shale gas exploration with a subsequent investigation confirming that the seismic events resulted from hydraulic fracturing (Green et al., 2012). A Royal Society report (Royal Society, 2012) highlighted this incident and other environmental concerns, including management and potential contamination of water resources, well integrity issues, monitoring of potential leaks and implementing best practice for risk management. The report led to the UK Department for Energy and Climate Change (DECC) making additions to the process for onshore drilling approval specifically for shale gas wells, which now require an early stage high-level environmental risk assessment (ERA), requiring detailed plans for monitoring operations, including the use of the seismic traffic light system, and development and implementation of a communications strategy aimed at the public and stakeholders (DECC, 2015).

Several exploration licences were granted in the 2015 licencing round (OGA, 2018) and there are multiple exploration programs at different stages underway in the UK, mainly in Lancashire, Yorkshire and in the Weald basin. To date, planning permission has been granted for drilling and hydraulic fracturing at two UK sites. Permission to drill at Preston New Road, Lancashire was granted in October 2016, and drilling of horizontal wells by Cuadrilla is scheduled for completion in 2018. In Kirby Misperton, Yorkshire, planning permission was granted to drill in May 2016 (Third Energy, 2018); however, subsequent financial issues halted operations in early 2018 (Helm, 2018).

Part of the opposition to shale gas development is due to environmental and safety concerns, including potential groundwater contamination. Claims of groundwater contamination after shale gas exploration in the United States have occurred in a number of locations (Begos, 2014; Legere, 2013). The US Environmental Protection Agency have also confirmed specific instances of contamination, though there is no evidence for systemic impacts on drinking water (US EPA, 2015).

Investigations to characterise groundwater methane (CH_4) prior to shale gas development have been conducted at a number of locations worldwide, including parts of Canada, The USA, Germany, China and the UK (Bell et al., 2017; Bordeleau et al., 2018; Huang et al., 2017; Humez et al., 2016; McIntosh et al., 2014; McPhillips et al., 2014; Moritz et al., 2015; Schloemer et al., 2016). However, in the USA where the majority of shale gas mining presently occurs there have been relatively few baseline studies, although there have been recent attempts to provide such information belatedly (Down et al., 2015; McPhillips et al., 2014; Rhodes and Horton, 2015). In some areas of suspected contamination, there has been disagreement whether CH_4 in groundwater is due to shale gas activities or natural gas migration. Several studies of the same region show multiple interpretations from similar datasets (Jackson et al., 2013; Molofsky et al., 2013; Osborn et al., 2011; Siegel et al., 2015) because it is difficult to determine the source of CH_4 in areas that contain multiple thermogenic and microbial sources, which commonly migrate and mix.

To characterise local sources of groundwater CH_4, baseline studies should quantify stable carbon ($^{13}C/^{12}C$) and hydrogen ($^{2}H/^{1}H$) isotope compositions of CH_4. Methane produced from thermal breakdown of shale or coal at depth has a different isotopic composition to CH_4 produced via microbial processes in the subsurface or in surface sources, (e.g., wetlands or landfill sites) that may subsequently migrate into aquifers.

In the UK a significant proportion of drinking water comes from groundwater

abstraction (DEFRA, 2013) and there is concern that exploration and development of shale gas and other unconventional gas resources could impact water quality, including the introduction of CH_4 into aquifers. Though CH_4 is not, strictly speaking, a contaminant as there are no health implication, it is still important to monitor, especially because, if CH_4 from the shale gas formation enters the system, so may chemicals from within fracking fluids. The ability to distinguish ingress of CH_4 relies in part on characterisation of aquifers prior to drilling activity. Such a characterisation ideally will include an assessment of $\delta^{13}C(CH_4)$ and $\delta^{2}H(CH_4)$ values in addition to baseline CH_4 concentration.

The aim of this review is to collate data from studies to date that have measured $\delta^{13}C(CH_4)$ and $\delta^{2}H(CH_4)$ values in UK groundwater and sources that might contribute CH_4 to groundwater. The review encompasses both deep and shallow aquifers and CH_4 sources and attempts to evaluate the predominant origin of CH_4 in the various sources based upon a well-established stable isotope proxy model (Whiticar et al., 1986; Whiticar, 1999).

2.2 Data Compilation

Figure 2.1 shows locations in the UK where CH_4 in groundwater has been studied or where sources of CH_4 exist that might impact groundwater. Information in the figure includes both specific locations (e.g., boreholes, landfills, etc.) and generalized areas that commonly contain elevated concentrations of CH_4 (e.g., shale and coal formations, wetland-rich regions, etc.). Table 2.1 contains borehole and well data from UK groundwater sites reporting concentration and stable isotope data for CH_4 and other solutes relevant to methanogenesis or methanotrophy. Figure 2.2 shows paired $\delta^{13}C$ and $\delta^{2}H$ values for UK groundwater sites and potential sources that may contribute CH_4 to groundwater. Stable hydrogen isotope values are one of the least available data types for CH_4 from any source but are required for effective assessment of the origin and alteration of CH_4 (Whiticar, 1999).

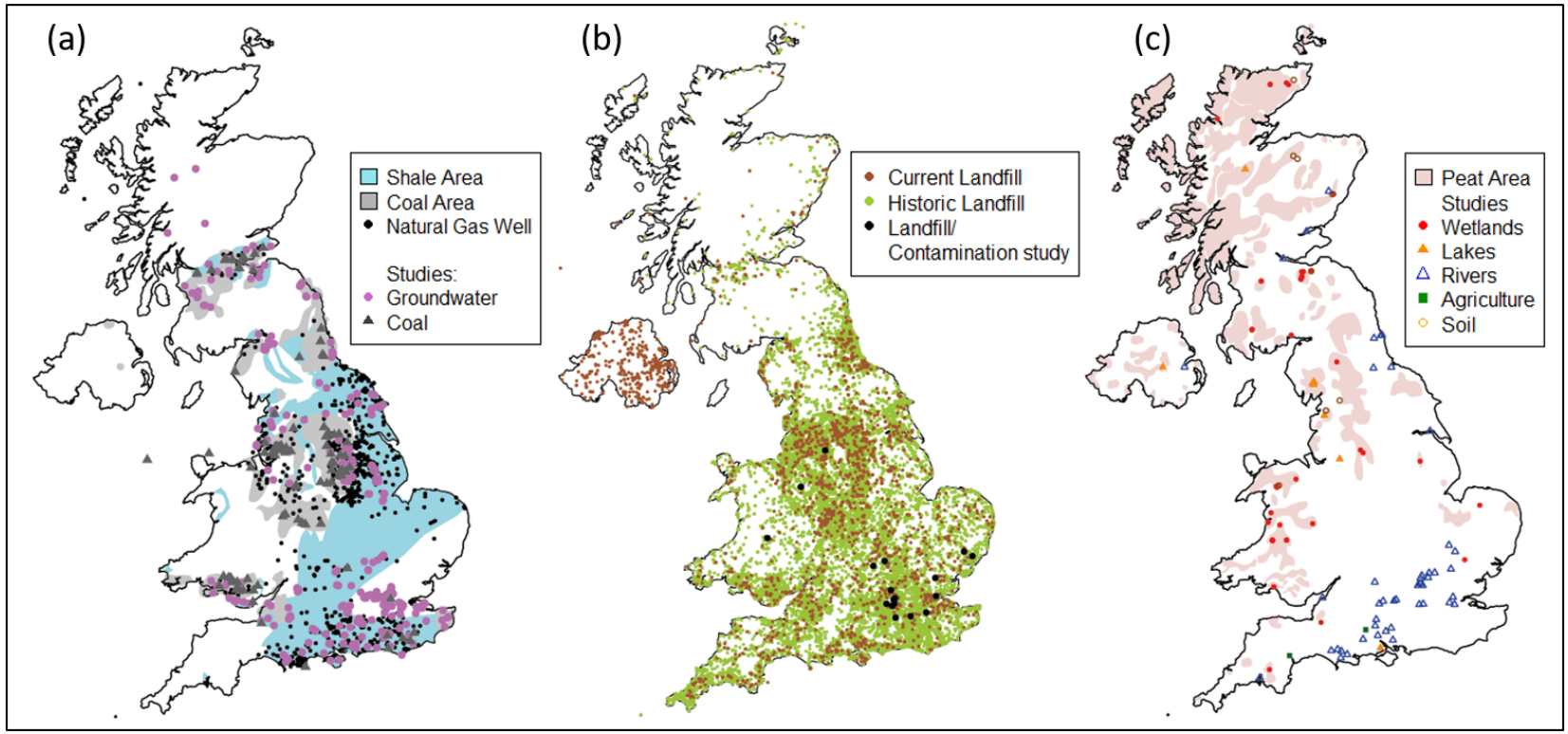

Figure 2.1 Groundwater methane (CH_4) and potential sources of CH_4 input to groundwater in the United Kingdom: (a) shale and coal bearing areas (approximated using data from DECC (2012) and Appleton (2011), respectively), onshore natural gas wells (DECC, 2012), groundwater CH_4 (Bell et al., 2017; Gooddy and Darling, 2006; Bath et al., 1988; Dochartaigh et al., 2011; Abesser et al., 2005; Bishop and Lloyd, 1990; Cuadrilla, 2014; BGS, 2015), site specific coal CH_4 occurrences (Appleton et al., 2005; Potter and Longstaffe, 2007; Györe et al., 2018; Zazzeri et al., 2016); (b) current and historic landfill locations (Environment Agency, England and Wales; Scottish Environment Protection Agency, Scotland; Department of the Environment, Northern Ireland); site specific landfill data (Riddick et al., 2018; Zazzeri et al., 2015; Nwachukwu and Anonye, 2012; Williams et al., 2010; Lowry et al., 2001; Ward et al., 1996), and contaminated land sites (Baker et al., 2012); (c) peatland areas (JNCC, 2011), specific wetland sites (Billett and Harvey, 2013; Dinsmore et al., 2013; Trimmer et al., 2009, 2010; Hornibrook et al., 2009; Parkes et al., 2012; Clymo and Bryant, 2008; Waldron et al., 1999; Charman et al., 1999; Freeman et al., 2002; Gray et al., 2013; Green and Baird, 2013; Levy et al., 2012; Hornibrook and Bowes, 2007; Green et al., 2017; Pangala et al., 2015; Comas et al., 2013; Garnett et al., 2011), periodically wet soil (McNamara et al., 2006; Sgourdis and Ullah, 2017; Drewer et al., 2017), rivers (Hope et al., 2001; Sanders et al., 2007; Trimmer et al., 2009; Shelley et al., 2014; Garnett et al., 2013; Webster et al., 2010; Viggi et al., 2017; Harley et al., 2015; Upstill-Goddard and Barnes, 2016; Upstill-Goddard et al., 2000; Middelburg et al., 2002; Barth et al., 2003), lakes (Deines and Grey, 2006; Banning et al., 2005; Kelly et al., 2004; Grey et al., 2001; Spooner et al., 1994), and agricultural sources (Gooddy et al., 2000; Nazaries et al., 2013).

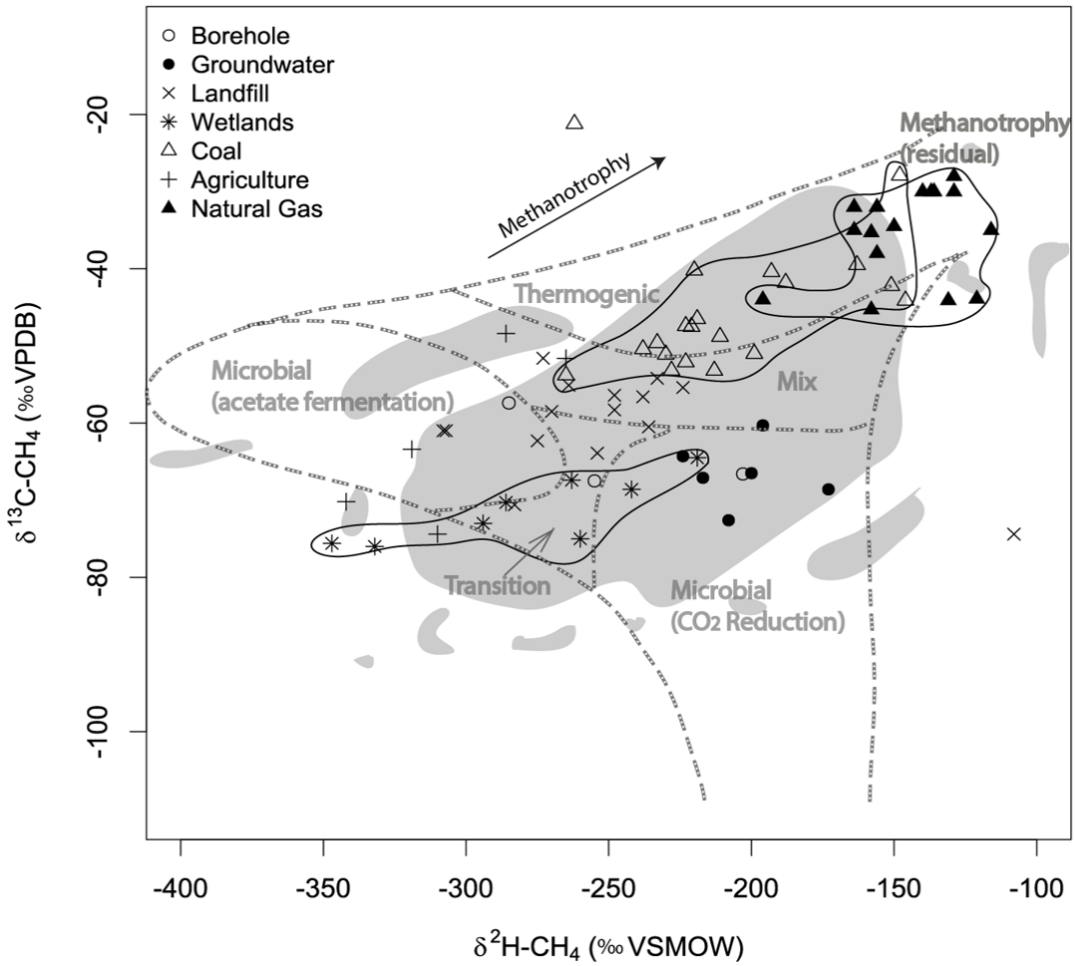

Figure 2.2 $\delta^{13}C$ and $\delta^{2}H$ values for CH_4 from UK groundwater and sources that potentially contribute CH_4 to groundwater. The grey areas in the background are stable isotope ranges from global groundwater data presented in Table 2.2. The data were compiled from Hitchman et al. (1989), Bath et al. (1988), Waldron et al. (1999), Clymo and Bryant (2008), Lokhurst et al. (1997) and Györe et al. (2018). Methane origin classification outlines are adapted from Whiticar et al. (1986).

2.2.1 Methane in UK Groundwater

The UK meets its water demands from both groundwater and surface water, with groundwater abstraction more prevalent in the south east of England (DEFRA, 2013). Methane is common in UK groundwater; however, generally it is present in low quantities with only a few locations exhibiting elevated concentrations of CH_4 (80 % $<$ 10 µg L^{-1} and only 4 % $>$ 100 µg L^{-1}; (Bell et al., 2017; Darling and Gooddy, 2006). Gooddy and Darling (2005) estimate that groundwater contributes a maximum of 0.05 % of total UK CH_4 emissions to the atmosphere.

A recent UK-wide baseline study conducted by Bell et al (2017) reports large variations in CH_4 concentration across 343 sites and multiple aquifers. $\delta^{13}C(CH_4)$

values also were reported for a small subset of sites. High CH_4 concentration sites typically exhibited more positive $\delta^{13}C(CH_4)$ values, suggesting a thermogenic origin. The majority of sites contained CH_4 considered to have a microbial origin subjected to varying amounts of methanotrophy, which exhibits ^{13}C and ^{2}H enrichment (Bell et al., 2017). High concentrations of CH_4 in groundwater at the Wyresdale tunnel in Lancashire appear to be microbial in origin based upon $\delta^{13}C(CH_4)$ and $\delta^{2}H(CH_4)$ values reported by Bath et al. (1988) (Fig. 2.2 and Table 2.1).

There are likely local sources of thermogenic CH_4 in coal and shale areas but the majority of CH_4 in UK aquifers appears to have a microbial autochthonous origin. However, the paucity of UK groundwater CH_4 data precludes a conclusive assessment of the extent to which allochthonous CH_4 sources have impacted aquifers locally. Contamination of groundwater by landfill gas and other anthropogenic sources has been observed in the UK and elsewhere, in particular, in shallow aquifers (e.g., Thornton et al., 2001; Williams et al., 2010; Baker et al., 2012).

Publically available stable isotope and concentration data for CH_4 in groundwater globally are presented in Table 2.2. The amount of data per nation reflects in part the extent to which natural gas and shale gas resources have been developed in each country. The ranges of $\delta^{13}C(CH_4)$ and $\delta^{2}H(CH_4)$ values from Table 2.2 are plotted in the background of Figure 2.2 to provide context for the UK data. The stable isotope compositions of CH_4 from UK groundwater, albeit available for only a limited number of sites, are similar to values observed in groundwater elsewhere in the world. Microbial methanogenesis is the most common source of CH_4 in aquifers globally. The CH_4 is frequently enriched in both ^{13}C and ^{2}H in individual aquifers most likely as a result of methanotrophy although mixing with thermogenic gas cannot be excluded as a possible cause of increases in $\delta^{13}C(CH_4)$ and $\delta^{2}H(CH_4)$ values. However, thermogenic gas commonly contains C_{2+} hydrocarbons (i.e., ethane, propane, butane, etc.), which provides a means to attribute ^{13}C and ^{2}H enrichment to mixing with deep CH_4 sources. In the absence of C_{2+} components (or C_{2+} data) a positive shift in $\delta^{13}C(CH_4)$ and $\delta^{2}H(CH_4)$ is reasonably attributed to in situ methanotrophy. Regardless, the range of $\delta^{13}C(CH_4)$ and $\delta^{2}H(CH_4)$ values in aquifers (Tables 2.1 and 2.2) highlights the importance of including stable isotope measurements as part of any comprehensive baseline characterisation of CH_4 in aquifers prior to shale gas exploration and development. Inclusion of such data helps to eliminate the possibility that naturally occurring ^{13}C- and ^{2}H-enrichment in groundwater CH_4 due to methanotrophy might be mistakenly attributed to ingress of thermogenic

CH_4.

Table 2.1 Concentration and stable isotope data for UK sources of methane.

Site	Easting	Northing	CH_4 ($\mu g\ L^{-1}$)	CH_4 (%)	CO_2 ($mg\ L^{-1}$)	CO_2 (%)	HCO_3 ($mg\ L^{-1}$)	$\delta^{13}C(CH_4)$ (‰)	$\delta^{2}H(CH_4)$ (‰)	$\delta^{13}C(DIC)$ (‰)	$\delta^{13}C(CO_2)$ (‰)	$\delta^{2}H(H_2O)$ (‰)	$\delta^{18}O(H_2O)$ (‰)	Ref
Groundwater														
WT 509	353	459	2714		434		378	-60.3	-196	-12.8		-42	-6.3	a, b
WT 4343	355	455	16001		0.24		583	-64.3	-224	-8.1		-40	-6.4	a, b
WT 4980	355	455	3000		5.1		411	-66.5	-200	-13.8		-39	-6.4	a, b
WT 5090	355	455	13001		60		417	-67.1	-217	-11.6		-41	-6.3	a, b
WT 5340	355	455	15001		13		451	-72.6	-208	-10.3		-41	-6.2	a, b
WT 5787	355	454	2429		271		410	-68.6	-173	-15.6		-40	-6.5	a, b
LL5	507	371	1700					-71.8		-1.5				b
LL6	507	370	2300					-72.6		-2.1				b
Southampton	442	112	5540					-45.8		-15.5				b
Balcombe	531	129	11000					-52						c
OK	474	136	6.9					-69.2						d
BN	484	146	4.1					-32.3						d
TL	488	144	2.3					-55.2						d
TG	488	148	6.5					-57.7						d
BH	486	149	7.8					-51.2						d
TM	488	149	10					-50.9						d
SHP	495	182	9.7					-58.2						d
HL	497	180	5.8					-49.9						d
MH	494	142	2.5					-29.3						d
WG-1	563	143	6.1					-66.4						d
WG-4	553	137	30.3					-59.3						d
HT-1	432	97	12.7					-79.8						d
CM-2	279	203	649.2					-34.1						d
MS-7	331	432	15.4					-45						d
Coal														
Notts1	463	367		33		1		-47.5	-221					e
Notts2	463	367		56		1.4		-53.2	-228					e
Notts3	463	367		22		0.5		-21.2	-262					e
Notts4	463	367		40		5.9		-42.2	-151		-42			e

Table 2.1 continued

Site	Easting	Northing	CH_4 ($\mu g\ L^{-1}$)	CH_4 (%)	CO_2 ($mg\ L^{-1}$)	CO_2 (%)	HCO_3 ($mg\ L^{-1}$)	$\delta^{13}C(CH_4)$ (‰)	$\delta^{2}H(CH_4)$ (‰)	$\delta^{13}C(DIC)$ (‰)	$\delta^{13}C(CO_2)$ (‰)	$\delta^{2}H(H_2O)$ (‰)	$\delta^{18}O(H_2O)$ (‰)	Ref
Barnsley	406	391		4.8				-44.1	-146					e
WL1	366	404		21.2		0.9		-53.8	-265					e
WL2	366	404		15.3		5.4		-53.2	-213		-38.1			e
WL3	366	404		8.5		3.6		-51	-199		-54			e
WL4	366	404						-52.1	-223		-46.4			e
Nant Helen	285	211						-27.9	-148		-3.1			f
Airth-1	229	685						-40.2	-220					g
Airth-2	229	685						-39.5	-163					g
Airth-6	288	685						-43.5						g
Airth-8	288	685						-41.8	-188					g
Airth-10	289	685						-40.4	-193					g
Old Mill Lane	455	362						-50.4	-238					g
Prince of Wales	445	423						-49.6	-233		-24.5			g
Warsop-1	455	368						-51.1	-230		-7.9			g
Crown Farm	457	362						-48.8	-211		-11.2			g
Bevercotes-1	470	374						-46.5	-219					g
Newmarket Lane	436	426						-47.4	-223		-13.8			g
Kellingley	452	424						-46.5						h
Maltby	455	392						-45.4						h
Hatfield	465	411						-48.8						h
Thoresbury	463	367						-51.2						h
Daw Mill	426	290						-51.4						h
Cwmllynfell	273	213						-41.2						h
Abercrave	281	211						-41.4						h
Aberpergwm	287	206						-33.3						h
Unity	288	204						-30.9						h
Natural gas														
N Sea (Carb)	612	462		80-95		0-5		-44 to -33	-146 to -137					i
N Sea (Rotliegend)	612	462		70-90		0-2		-38 to -28	-164 to -116					i
Southern Basin 1	612	462		94				-34.5	-150					e

Table 2.1 continued

Site	Easting	Northing	CH_4 ($\mu g\ L^{-1}$)	CH_4 (%)	CO_2 ($mg\ L^{-1}$)	CO_2 (%)	HCO_3 ($mg\ L^{-1}$)	$\delta^{13}C(CH_4)$ (‰)	$\delta^{2}H(CH_4)$ (‰)	$\delta^{13}C(DIC)$ (‰)	$\delta^{13}C(CO_2)$ (‰)	$\delta^{2}H(H_2O)$ (‰)	$\delta^{18}O(H_2O)$ (‰)	Ref
Southern Basin 2	612	462						-44.1	-131					e
Southern Basin 3	612	462		84.6				-43.9	-121					e
Southern Basin 4	612	462		87.4				-45.3	-158					e
Southern Basin 5	612	462		88.4				-35.3	-158					e
Egham	500	171						-33.9						j
Causeway	497	172						-33.8						j
Wetlands														
River mud				10				-75.6	-347		-16.2			e
Lake mud				5				-70.3	-286		-8.5			e
borehole1				39		19		-64.5	-219		-23.9			e
borehole2				12		17		-67.4	-263		-28.5			e
peat				19.5		0.9		-68.6	-242		-7.8			e
Ellergower Moss	248	579	32000		748			-60	-294		10	-37.7		k, l
Tor Royal	259	72						-67.3						m
Crymlyn Bog A	269	195						-51.9						n
Crymlyn Bog B	269	195						-53.1						n
Gors Lywd A	269	264						-57.2						n
Gors Lywd B	269	264						-57.2						n
Blaen Fign A	291	264						-70.2						n
Blaen Fign B	291	264						-64.8						n
Cors Caron A	269	264						-78.1						n
Cors Caron B	269	264						-78.6						n
LMA	264	651						-70.6						o
LMB	264	651						-66.1						o
Lake														
Esthwaite	336	495						-70						p
River														
Langlands Moss	264	651						-60						q

Table 2.1 continued

Site	Easting	Northing	CH_4 ($\mu g\ L^{-1}$)	CH_4 (%)	CO_2 ($mg\ L^{-1}$)	CO_2 (%)	HCO_3 ($mg\ L^{-1}$)	$\delta^{13}C(CH_4)$ (‰)	$\delta^{2}H(CH_4)$ (‰)	$\delta^{13}C(DIC)$ (‰)	$\delta^{13}C(CO_2)$ (‰)	$\delta^{2}H(H_2O)$ (‰)	$\delta^{18}O(H_2O)$ (‰)	Ref
Soil														
Gisburn	375	471						-55						r
Res exc 1				9.4		0.2		-67.5	-255					e
Res exc2								-66.6	-203					e
Deep bore								-57.4	-285		-6.8			e
Agriculture														
Abattoir waste				67		27		-70.2	-342		10.6			e
Brewery waste				75		17.7		-48.4	-286		-2.5			e
Dairy waste				61		39		-63.4	-319		0.5			e
Sewage				62		38		-51.6	-265		2.8			e
Poultry				60		39		-74.4	-310		14.4			e
Landfill														
Domestic 2				28		43		-61	-307		5.3			d
Domestic 3				63		36		-58.3	-248		10.8			e
Domestic lqd				57.4		28.9		-55.4	-224		0.7			e
Domestic com				57		23.5		-61	-308		-2.3			e
Dom inc				57		16		-56.6	-238		10.5			e
Dom industrial				50		20		-62.3	-275		12			e
Dom chem1a				46.5		29		-60.5	-236		10.3			e
Dom chem1b				44		31.5		-56.4	-248		6.7			e
Ind dom				35		28		-58.5	-270		2.1			e
Ind com				21.8		8.6		-54.2	-233		-7.7			e
Brogborough1	370	182		40		60		-55.1	-264		6.9			e
Brogborough2	370	182		28		71		-63.9	-254		12.8			e
Brogborough5	370	182		53		46.5		-51.6	-273		7.4			e
Brogborough6	370	182		13		80		-74.4	-108		-12.6			e
Foxhall	624	244		62.7		37.3		-70.6	-283		3.8			s,t
Sherwood sands	357	342	8000					-55						u

Table 2.1 continued

Site	Easting	Northing	CH_4 ($\mu g\ L^{-1}$)	CH_4 (%)	CO_2 ($mg\ L^{-1}$)	CO_2 (%)	HCO_3 ($mg\ L^{-1}$)	$\delta^{13}C(CH_4)$ (‰)	$\delta^{2}H(CH_4)$ (‰)	$\delta^{13}C(DIC)$ (‰)	$\delta^{13}C(CO_2)$ (‰)	$\delta^{2}H(H_2O)$ (‰)	$\delta^{18}O(H_2O)$ (‰)	Ref
Colnbrook	502	175						-52.6						v
Ascot	491	169						-51.7						v
Trumps farm	500	166						-51.4						v
Norlands	503	169						-50.8						v
Albury	505	148						-59.7						w
Bletchley	486	232						-58.8						w
Calvert	469	225						-58.5						w
Colnbrook	504	177						-60.2						w
Greatness	554	157						-57.4						w
Mucking	569	182						-56.1						w
Redhill	529	151						-59.6						w
Roxwell	567	209						-55.2						w
Wapsey's Wd	497	189						-57.3						w

WT – Wyresdale tunnel, Dom – domestic, Ind – industrial; [a]Bath et al (1988), [b]Gooddy & Darling (2006), [c]Perry et al. (2014), [d]Bell et al (2017), [e]Hitchman et al (1989), [f]Potter & Longstaffe (2007), [g]Györe et al (2018), [h]Zazzeri et al (2016), [i]Lokhorst et al (1997), [j]Lowry et al (2001), [k]Clymo & Bryant (2008), [l]Waldron et al (1999), [m]Charman et al (1999), [n]Hornibrook & Bowes (2007), [o]Garnett et al (2011), [p]Deines & Grey (2006), [q]Garnett et al (2013), [r]McNamara et al (2006), [s]Ward et al (1996), [t]Williams et al (1999), [u]Baker et al (2012), [v]Zazzeri et al (2015).

2.2.2 Allochthonous CH_4 Sources

2.2.2.1 Coal Gas

The association of CH_4 with coal has led to underground explosions since the early days of coal mining (Humphrey, 1960). All deep coal mining in the UK has been abandoned but there remains interest in the CH_4 resources contained in the formations both for the purposes of reducing explosive hazards, which includes leakage and migration in groundwater, and potential exploitation of the gas as an energy resource (Jones et al., 2005).

In the 1990s, the British Geological Survey (BGS) mapped areas that may be affected by emission or leakage of CH_4 (and CO_2) from coal deposits and coal mining operations (Appleton et al., 1995). The compilation did not include groundwater CH_4 concentration data but did provide a comprehensive record of locations where CH_4 emissions related to coal and other natural gas have been recorded, which are shown in Figure 2.1 and listed in Table 2.1. Subsequently, CH_4 has been detected in the Millstone Grit aquifer (Abesser et al., 2005), which may have migrated from a deep thermogenic source. O'Dochartaigh et al. (2011) reported the possible presence of coal-associated CH_4 in the Midland Basin, Scotland on the basis of a low C_1/C_2 ratio in the gas. Stable isotope analysis of the CH_4 was not conducted. More recently, fugitive CH_4 emissions have been monitored near abandoned UK oil and gas wells (Boothroyd et al., 2016) and 30 % of the sites exhibited local CH_4 levels that were significantly higher than CH_4 concentrations at nearby control sites. Where stable isotope data are available for UK sites, the compositions are typical for coal-associated CH_4 that has a thermogenic origin with $\delta^{13}C(CH_4)$ values ranging from -30 to -52 ‰ and $\delta^{2}H(CH_4)$ values from -163 to -238 ‰ (Table 2.1; $\delta^{13}C$ values from atmospheric CH_4, (Zazzeri et al., 2015, 2016); $\delta^{13}C(CH_4)$ and $\delta^{2}H(CH_4)$ values from gas well samples, (Györe et al., 2018)).

2.2.2.2 Wetlands

Methane production and emission from wetlands have been well studied since the 1990s because of their importance in global greenhouse gas budgets (Aselmann and Crutzen, 1989; Bartlett and Harriss, 1993). Peatlands in the UK, hold significant stores of carbon and generate significant quantities of CH_4 that may enter groundwater if the wetland is situated in a recharge area such as cool moist uplands. However, the majority of wetland investigations have focused on quantifying CH_4 in peat soil or flux to the atmosphere or streams (Billett and Harvey, 2013; Clymo and Bryant, 2008; Dinsmore et al., 2013, 2010; Garnett et

al., 2013; Hope et al., 2001; Hornibrook et al., 2009; Parkin et al., 2007; Quay et al., 1999). The foci of such studies commonly are seasonal and daily variability in CH_4 production or flux (Bonnett et al., 2006; Gallagher et al., 1994), effects on CH_4 production and emission of vegetation (Gray et al., 2013; Green and Baird, 2013; Levy et al., 2012; McNamara et al., 2008; Pangala et al., 2015), water table levels (Daulat and Clymo, 1998; Hughes et al., 1999; Levy et al., 2012), temperature (Beckmann et al., 2004; Hargreaves and Fowler, 1998; van Winden et al., 2012), drought (Freeman et al., 2002), burning (Worrall et al., 2011), and peatland restoration (Cooper et al., 2014; Green et al., 2018).

The $\delta^{13}C$ value of CH_4 has been characterised in a variety of UK peatlands (Charman et al., 1999; Clymo and Bryant, 2008; Garnett et al., 2013; Hitchman et al., 1989) and ranges from -80 to -60 ‰. Only two studies to date (Hitchman et al., 1989; Waldron et al., 1999b) have reported δ^2H values for CH_4 in UK wetlands (range -330 to -240 ‰). Waldron et al. (1999b) identified two isotopically distinct CH_4 reservoirs in the subsurface of Ellergower Moss, a peatland that possesses an unusually deep accumulation of peat extending to ∼6 m depth. Below a depth of 2 to 2.5 m, the CH_4 stores were static with little gas movement or change in composition in contrast to a more dynamic CH_4 pool at depths <2.5 m (Waldron et al., 1999b). The stability of the lower gas reservoir suggests that connection or loss to groundwater may be minimal. The isotopic composition of CH_4 in UK peatlands suggests archaeal production primarily from the acetate fermentation pathway; however, an inverse relationship between $\delta^{13}C$ (-68 ‰) and δ^2H (-240 ‰) values reported by Hitchman et al. (1989) at an unspecified wetland suggest a predominance of CO_2/H_2 methanogenesis. The low pH of pore water in ombrotrophic peatlands can limit acetate dissociation resulting in the production of CH_4 that has highly negative $\delta^{13}C$ values as a result of methanogenesis occurring predominately via the CO_2 -reduction pathway (Bowes and Hornibrook, 2006; Duddleston et al., n.d.; Hines et al., 2008, 2001; Hornibrook et al., 2009; Hornibrook and Bowes, 2007).

2.2.2.3 Agriculture

Agriculture is a major global source of greenhouse gases with agricultural land accounting for 40 % of global anthropogenic CH_4 emissions (IPCC, 2013) and 53 % of UK CH_4 emissions in 2015 (DEFRA, 2017). Not all agricultural CH_4 is emitted directly to the atmosphere and a portion may enter the subsurface and groundwater systems. Boon et al. (2014) investigated the potential effects of grazing animals on grasslands, showing that CH_4 enters the subsurface. Other studies have detected CH_4 in groundwater that can be directly attributed to

agriculture (Gooddy et al., 2000, Jahangir et al., 2012). Drewer et al. (2017) investigated the effects of ploughing on greenhouse gas fluxes, concluding that the practice resulted in significant N_2O emissions but variable and inconclusive effects on CH_4 emissions.

Gooddy et al. (2000) investigated the impacts of farm waste stores on groundwater quality, reporting that two out of eight sites contributed CH_4 to groundwater (location information not reported). At one site, the concentration of dissolved CH_4 attained levels similar to quantities that occur in landfill sites. However, the effect was not continuous and measurements showed that the concentration could decrease significantly without direct remediation. Modelling at the sites (Gooddy et al., 2001) and further geochemical analyses (Gooddy et al., 2002) showed that the CH_4 plume produced by storage of agricultural water was a significant risk to groundwater contamination at one site.

Jahangir et al. (2012) investigated four agricultural catchments in Ireland, which all showed the presence of groundwater CH_4. The occurrence of CH_4 in aquifers as a result of agricultural activity was episodic but indirect emissions from groundwater were concluded to be an important part of farm and national scale greenhouse gas budgets.

2.2.2.4 Landfill and Contaminated Land

Landfills generate significant quantities of CH_4 due to the presence of large amounts of organic matter, anaerobic conditions, and a stable, elevated core temperature. Landfills are estimated to account for $\sim$ 37 % of CH_4 emissions in the UK (DEFRA, 2014). The substantial quantities of CH_4 produced in landfills can be collected and used for energy production, or vented and flared to avoid hazardous accumulation of CH_4 (Aitkenhead and Williams, 1986). Methane levels in closed landfill sites typically require monitoring to ensure that dangerous conditions do not develop (Nwachukwu and Anonye, 2013). Methane that is not captured or flared can escape to the atmosphere or diffuse slowly through a soil cover and be partially or completely oxidized by methanotrophic bacteria. Failure of landfill liners can result in leakage of leachate and CH_4 to groundwater (Mitchell et al., 1990).

Landfill CH_4 has a microbial origin and associated stable isotope composition similar to natural systems, that can be altered by methanotrophy during transport. Methane plume dissipation and oxidation can be modelled (Williams et al., 1999) to estimate the extent of gas migration and infer CH_4 oxidation rates. Methane from landfills in the US and continental Europe tends to have $\delta^{13}C(CH_4)$ values in the range -60 to -50 ‰ and $\delta^{2}H(CH_4)$ values of -330 to -270

‰ (Bergamaschi et al., 1998; Liptay et al., 1998). Stable isotope analysis of CH_4 from UK landfills yields similar values (Table 2.1; Hitchman et al., 1989; Lowry et al., 2001). The stable isotope composition of landfill CH_4 is indicative of methanogenesis via acetate fermentation, which is consistent with the high concentration of volatile fatty acids commonly present in landfill leachate (Kjeldsen et al., 2002). However, as with natural systems, acetate fermentation cannot account for all CH_4 produced in landfill and CO_2/H_2 methanogenesis typically also contributes to CH_4 formation (Bogner et al., 1996).

Some contaminated land studies include CH_4 as a documented contaminant (Baker et al., 2012; Thornton et al., 2001; Williams et al., 2010) although most do not specify CH_4 but instead quantify total organic carbon (TOC) and/or chemical oxygen demand (COD) (Robinson, 1987; Robinson and Grantham, 1988; Thornton et al., 2000). TOC includes all organic carbon and is useful as a potential proxy for subsequent production of CH_4 in aquifers impacted by landfill leachate. In UK landfill studies that have measured CH_4 levels in leachate, the highest concentration reported was 22,400 µg L^{-1}at Nantmel tip, mid-Wales (Williams et al., 2010); however, the site is unusual in that a constructed wetland also overlies the tip. The amount of CH_4 in landfill contaminated sites and aquifers will decrease with time due to decline in CH_4 production rates as organic substrates are depleted and via natural attenuation of migrating CH_4 by methanotrophic bacteria (Thornton et al., 2001).

2.2.2.5 Lakes

Lakes are increasingly recognized as an important source of CH_4 emissions to the atmosphere (Tranvik et al., 2009). In the UK, the majority of studies that have investigated CH_4 in lakes have done so in the context of food web investigations (Spooner et al., 1994; Grey et al., 2001; Kelly et al., 2004; Banning et al., 2005; Deines and Grey, 2006). Stable carbon isotopes can be used to evaluate the extent to which CH_4 contributes carbon and energy to lake foodwebs via methanotrophic bacteria as an initial food source. Methane is formed at depth in either anoxic sediment or lower portions of stratified anoxic water columns in lakes and subsequently migrates to the oxic/anoxic interface where it is consumed by methanotrophic bacteria. The location of the oxic/anoxic interface will depend on the mixing regime of the lake, which also will influence which organisms are able to feed on the CH_4-oxidising bacteria (Grey et al., 2001). Kelly et al. (2004) investigated chironomid populations and their stable isotope compositions in five UK lakes (and one in Germany) and reported that the extreme ^{13}C-depletion observed could not be explained by different feeding modes

but rather resulted from ingestion of ^{13}C-poor methanotrophic bacteria biomass. Studies at Esthwaite water, determined larval biomass, larval and CH_4 stable isotope compositions, and potential rates of CH_4 production from sediments underlying different water column depths (Deines et al., 2009; Deines and Grey, 2006). Methane production rates increased with depth and larvae became more ^{13}C-depleted. Jones and Grey (2011) also suggested that lower than expected $\delta^{13}C$ values of chironomid larvae in Loch Ness are due to consumption of a ^{13}C-depleted food source, which is likely to be methantrophic bacterial biomass. The majority of UK lake studies do not report CH_4 concentration or stable isotope data but such data are commonly available for freshwater lakes globally.

2.2.2.6 Rivers

Rivers and streams are a globally significant source of CH_4 with annual emissions estimated to be approximately one third of freshwater wetlands and lakes (Stanley et al., 2016). Methane can be transported via streams from high concentration production areas, such as upland mires (Hope et al., 2004, 2001). In peatland areas, CH_4 and CO_2 flux from streams are generally indicative of fluxes across the whole catchment (Dawson et al., 2004, 2002; Hope et al., 2004).

Chalk rivers in southern England are reported to receive CH_4 saturated groundwater as well as having their own methanogenic microbial communities within river sediments (Sanders et al., 2007). Methanogenesis occurs in the river Lambourn in oxygen-depleted silty sands in the river bed while overlying gravels, with oxygen-enriched pore waters and CH_4 concentrations lower than surface waters, host methanotrophic communities (Trimmer et al., 2010). Such methanotrophic communities are a significant contributor to local food webs (Trimmer et al., 2009).

Carbon fixation due to methanotrophy has been reported in 32 chalk streams, and in 15 of those streams, the amount is comparable to carbon fixation via photosynthesis (Shelley et al., 2014). Differences exist across streams but the carbon conversion efficiency is relatively constant at $\sim$ 50 % (Trimmer et al., 2015). Though photosynthesis is the dominant process, methanotrophy may also be a significant contributor of carbon and energy to the riverine food web as it can provide new carbon at the light-limited river surface and deeper in the dark riverbed. The proportion of carbon fixation due to photosynthesis is greater in lighter areas, not only due to greater photosynthesis, but also due to light actively inhibiting methanotrophy as demonstrated by testing the CH_4 oxidation potential of shaded versus unshaded sediments (Shelley et al., 2017).

Estuaries exhibit a general pattern of decreasing CH_4 abundance with in-

creasing salinity, then an increase of CH_4 levels before decreasing again offshore, which suggests a source of CH_4 from tidal mud flats (Middelburg et al., 2002; Upstill-Goddard et al., 2000; Upstill-Goddard and Barnes, 2016). There may also be a seasonal variation to CH_4 cycling in estuaries with one study in the Tay estuary reporting substantially higher concentrations of CH_4 during summer months (Harley et al., 2015).

Although it is possible for CH_4 to enter groundwater via streams and pipes, it is more likely that CH_4 will be lost from groundwater via upwelling in streams and rivers.

2.3 Global Overview

$\delta^{13}C(CH_4)$ and $\delta^2H(CH_4)$ values for CH_4 in groundwater and allochthonous sources of CH_4 in the UK (Table 2.1) and worldwide (Table 2.2) exhibit considerable overlap in ranges as illustrated in Figure 2.2. A further summary of the ranges and means is provided in Table 2.3 for comparison.

There is a dearth of stable isotope data for CH_4 in UK groundwater, in particular, $\delta^2H(CH_4)$ values generally and both $\delta^{13}C(CH_4)$ and $\delta^2H(CH_4)$ values for aquifers that contain low concentrations of CH_4. The pattern of availability likely stems from challenges in measuring the stable isotope composition of dissolved CH_4 at trace levels and the tendency for investigations to focus studies on locations where groundwater already contains higher concentrations of CH_4 due to unusual natural conditions or human impacts on aquifers. The only other compilation to date of stable isotope data for UK CH_4 sources was completed by Hitchman et al. (1989) for the purposing of improving the ability to identify CH_4 sources based on stable isotope composition. However, the report by Hitchman et al. (1989) does not disclose the locations of study sites, which limits the ability to compare and evaluate processes controlling the stable isotope composition of CH_4 and to monitor future changes in CH_4 amount and stable isotope composition.

This study demonstrates that considerable variability exists in $\delta^{13}C(CH_4)$ and $\delta^2H(CH_4)$ values between UK locations but that the ranges and means of stable isotope compositions are very similar to other sources globally. Paired measurements of $\delta^{13}C(CH_4)$ and $\delta^2H(CH_4)$ values are necessary to identify sources and to help ascertain whether CH_4 has a microbial or thermogenic origin; however, even with both $\delta^{13}C(CH_4)$ and $\delta^2H(CH_4)$ values available there may be still be ambiguity between thermogenic CH_4 and residual microbial CH_4 that has been altered by methanotrophy. Additional supporting data could include C_{2+} content and if possible, CH_4 isotopologue measurements, which can provide information

about the temperature of CH_4 formation (Stolper et al., 2014). $\delta^{13}C(CO_2)$ values also can help to distinguish a microbial CH_4 residual because of ^{12}C -enrichment as a result of preferential oxidation of $^{12}CH_4$.

In general, in the absence of allochthonous CH_4 sources most UK groundwater appears to have a microbial origin (Table 2.1 and Figure 2.2) similar to aquifers worldwide (Table 2.2). However, based upon the limited data available, there appears to be considerable variability between aquifers, which necessitates detailed baseline characterisation of CH_4 in any groundwater system that might be impacted by human activities and allochthonous sources. The concentration of CH_4 is low in most pristine aquifers (Bell et al., 2017), which will require the use of pre-concentration techniques to acquire sufficient CH_4 for $\delta^{13}C(CH_4)$ and $\delta^2H(CH_4)$ analysis. Relatively few laboratories have the capacity to measure δ^2H values of CH_4 at low concentrations and analyses can be costly. In contrast, analysis of $\delta^{13}C(CH_4)$ is becoming increasingly routine because of the availability of laser spectroscopy instrumentation.

Finally, there have been few long-term studies that have investigated the stability of $\delta^{13}C(CH_4)$ and $\delta^2H(CH_4)$ values with time in aquifers. It is unlikely that stable isotope compositions will exhibit much variability in deep groundwater; however, shallow aquifers are more likely to be impacted by surficial processes and human activities. Baseline data collection for the latter sites may need to extend over a period of time to capture changes driven by natural or anthropogenic processes and to ascertain the timeframe in which perturbations may dissipate with time.

Table 2.2 Concentration and stable isotope compositions of dissolved CH_4 in groundwater from global sites

Country	Location	Formation	Depth (m)	CH_4 (µg L^{-1})	$\delta^{13}C(CH_4)$ (‰)	$\delta^{2}H(CH_4)$ (‰)	Ref
Australia	SE Queensland	Condamine alluvium	Up to 130	10 - 535	-78 to -49	-315 to -186	a
Canada	Southern Ontario	Alliston aq		15000 to 56000	-89 to -71	-281 to -240	b
	Southern Ontario	Bedrock		24000 to 74000	- 69 to -89	-280 to -228	b
	SW Ontario	ob (kettle point)	20 to 37		-75 to -57	-301 to -265	c
	SW Ontario	kettle point	19 to 73		-67 to -58	-299 to -264	c
	SW Ontario	ob (Hamilton grp)	32 to 57		-87 to -73	-314 to -285	c
	SW Ontario	Hamilton Grp	16 to 92		-90 to -63	-312 to -263	c
	SW Ontario	Marcellus	86		-80	-310	c
	SW Ontario	Ob (Dundee)	72		-66	-298	c
	SW Ontario	Amherstburg	16		-76	-265	c
	SW Ontario	Georgian Bay	93		-78	-282	c
	S Alberta	shallow gw	9 to 130		-72.1 ± 6.8	-297 ± 17	d
	Alberta			Up to 42900	-86 to -47	-437 to -202	e
	Nova Scotia	Carb & Trias basins		14 to 6000	-63 to -49	-215 to -69	f
	St Lawrence Lowlands, Quebec	gw above Utica shl		Up to 40000	-63 to -50	-250 to -170	g
	Alberta	Horseshoe canyon Fm			av -68.5	av -302	h
	James Bay lowlands, Ontario	Seds abv kimberlites		Up to 10000	-82 to -62	-289 to -254	i
	Ardley coal zone, Alberta			22100 to 36200	-51 to -46	-278 to -268	j
	Elk Valley, British Columbia			39000	-58	-288	k
	Alberta	Milk River aq			-77 to -70	-320 to -161	l
China	Qaidam basin	quaternary seds			-71 to -64	-800 to -700*	m
Denmark	Rømø	sandy aq (Holocene)			-80 to -50	-320 to -300	n
Israel	Dead sea Transform	Hula basin	1500	704	-48	-66	o
	Dead sea Transform	Kinnerot basin		720	-28	-74	o
	Dead sea Transform	dead sea alluvial aq		1312	-41	-128	o
	Dead sea Transform	sedom salt flat		4224	-80	-171	o
Netherlands	Boxtel	Banisveld landfill			-72.6	-241	p
Taiwan	Chianan/ Ilan	confined aq			-65.3	-211.8	q
USA	Illinois	glacial deposits	20 to 200		-85 to -72	-241 to -194	r
	Illinois	Palaeozoic seds	20 to 200		-84 to -72	-265 to -214	r
	East central Texas	Yegua aq		5600 to 15000	-71 to -61	-183 to -177	s

Table 2.2 continued

Country	Location	Formation	Depth (m)	CH_4 ($\mu g\ L^{-1}$)	$\delta^{13}C(CH_4)$ (‰)	$\delta^{2}H(CH_4)$ (‰)	Ref
	East central Texas	Cook Mountain aq		15680	-64	-182	s
	East central Texas	Sparta aq		15440 to 27700	-67 to -53	-186 to -165	s
	East central Texas	Queen City aq		1229	-58	-185	s
	East central Texas	Reklaw aq		1346	-65	-192	s
	Wisconsin	Till and Loess	2 to 30	up to 43000	-81 to -64	-240 to -194	t
	NE Pensylvania	Catskill	36 to 190	26800	-40 to -30	-230 to -170	u
	NE Pensylvania	Lockhaven	36 to 190	50400	-50 to -30	-230 to -160	u
	Upstate NY	Genessee (active)	36 to 190	300	-34	-170	u
	Upstate NY	Genessee (non-active)	36 to 190	1500	-75 to -45	-260 to -160	u
	NE Pensylvania (Tioga)	shallow gw			-75 to -35	-266 to -106	v
	Dimock, NE Pensylvania	shallow gw			-46 to -30	-280 to -170	w
	North central WV	Conemaugh/Monongahela	13.7 to 19.4	> 100	-69 to -42	-224 to -99	x
	NE PA	Catskill and Lockhaven	Up to 305	Up to 120000	-67 to -34	-261 to -163	y
	NY state	aq above Marcellus shl		Up to 28700	-52 to -49	-270 to -250	z
	Williston Basin	gw above Bakken Fm		1 to 23600	-91.7 to -70	-308 to -183	a'
	Northern Colorado	aq above oil/gas field		Up to 37100	-82 to -69	-290 to -240	b'
	East -central Illinois	Mohomet aquifer		Up to 64000	-86 to -70	-240 to -140	c'
	Piceance Basin, Colorado	Rio Blanco county			-73.8 to -35	-297 to -161	d'
	Piceance Basin, Colorado	Garfield county			-66 to -42	-192 to -146	d'
	Washington	Columbia River Basalts			-88 to -35	-265 to -134	e'
	North Carolina	Deep River Triassic basin		240 to 280	-69.5 to -61	-155 to -140	f'
	Arkansas	aq above shale field	30 to 40	800 to 4300	-69.9 to -42.3	-180 to -122	g'
	Colarado	Denver-Julesberg basin		up to 30000	-88 .1to -39.6	-276 to -213	h'

* Data not used in Figure 2; Aq – aquifer, Fm formation, gw – groundwater, Carb – Carboniferous, Trias – Triassic, shl – shale, sed – sediment; [a]Owen et al (2016), [b]Aravena et al (1995), [c]McIntosh et al (2014), [d]Cheung et al (2010), [e]Humez et al (2016), [f]Kennedy and Drage (2015), [g]Bordeleau et al (2015), [h]Mayer et al (2015), [i]Sader et al (2013), [j]Harrison et al (2006), [k]Aravena et al (2003), [l]Drimmie et al (1991), [m]Shuai et al (2013), [n]Hansen et al (2001), [o]Avrahamov et al (2015), [p]van Breukelen et al (2003), [q]Liu et al (2009), [r]Coleman et al (1988), [s]Grossman et al (1989), [t]Simpkins and Parkin (1993), [u]Osborn et al (2011), [v]Revesz et al (2010), [w]Molofsky et al (2013), [x]Sharma et al (2013), [y]Baldassare (2014), [z]Christian et al (2016), [a']McMahon et al (2015), [b']Li and

Carlson (2014), [c']Hackley et al (2010), [d']McMahon et al (2013), [e']Johnson et al (1993), [f']Down et al (2015), [g']Warner et al (2013), [h']Sherwood et al (2016)

Table 2.3 Ranges of isotopic compositions of UK CH_4 sources compared to global mean values

Source	$\delta^{13}C(CH_4)$ (‰)		$\delta^{2}H(CH_4)$ (‰)	
	UK	Global mean	UK	Global mean
Wetlands	-76 to -64	-60*	-347 to -242	-320*
Landfills	-62 to -50	-50*	-330 to -270	-310*
Natural Gas (thermogenic)	-45.3 to -28	-43*	-164 to -116	-185*
Coal Mining	-53 to -21	-36*	-265 to -146	-140*
Agriculture	-74 to -48	-60*	-342 to -265	-300*
		Global Range		Global Range
Groundwater	-79.8 to -29.3	-92 to -28	- 224 to -173	-800 to -66

* Quay et al (1999). All ranges are from Tables 2.1 and 2.2

2.4 Conclusions

The concentrations and $\delta^{13}C$ and $\delta^{2}H$ values of CH_4 in UK groundwater appear to be similar to amounts and isotope compositions of CH_4 in aquifers elsewhere in the world. However, the amount of data available for the UK is small and $\delta^{2}H(CH_4)$ is lacking for many locations. Most CH_4 present in aquifers has an archaeal origin and enrichment in ^{13}C and ^{2}H is common due to bacterial methanotrophy.

The stable isotope compositions of allochthonous CH_4 sources that may impact aquifers also are similar in the UK and elsewhere because the microbial substrates and biochemical pathways for CH_4 are small in number and governed by conditions that are common to the different locations. Thermogenesis of organic matter also tends to produce CH_4 having $\delta^{13}C$ and $\delta^{2}H$ values that lie within relatively narrow ranges. Shallow and surficial sources of CH_4 readily impact the amount and stable isotope composition of CH_4 in shallow aquifers.

Chapter 3

Methodology

3.1 Introduction

Groundwater samples were collected and analysed from multiple boreholes. Field measurements were conducted, including measurements of pH, specific electrical conductivity (SEC), dissolved oxygen (DO), oxidation-reduction potential (ORP) and total alkalinity. Discrete water samples were collected and subsequently analysed for CH_4 concentration, H_2 concentration, $\delta^{13}C(CH_4)$, $\delta^{13}C(DIC)$, $\delta^{2}H(H_2O)$ and $\delta^{18}O(H_2O)$ values. An onsite water sparging technique was used to extract and collect dissolved CH_4 for subsequent analysis of $\delta^{2}H(CH_4)$. The latter approach involved significant equipment and methodological development and is presented separately in Chapter 4 because it will be submitted for peer-review and possible publication as a new research method article.

3.2 Field measurements

Some boreholes at field sites had a sample tap, which could be connected via tubing to the field equipment. Other sites were observation boreholes where a pump needed to be used. In the latter case a 3-stage 12 V caravan pump with integrated tubing was used, which was connected to field equipment. Field measurements of pH, SEC, DO, ORP were carried out using standard British Geological Survey equipment and methods. The pH, DO and ORP probes were placed in a flow cell to minimise atmospheric contamination and water flowed through until readings stabilised. A Y-tubing connector was used to allow water to flow through the flow cell and to the SEC probe simultaneously.

Dissolved oxygen (DO) was measured using an InLab® 605 probe connected to a Mettler Toledo SG6 SevenGo Pro Dissolved Oxygen meter that had an accuracy of ± 0.2 mg L^{-1}. Prior to use it was calibrated in water-saturated air.

Oxygen reduction potential (ORP) was measured using a VWR 2812-ORP probe and Mettler Toledo SG8 SevenGo Pro pH/ Ion meter that had an accuracy of 0.1 mV. The meter was calibrated with Zobells solution. The ORP measurements were converted to Eh by correcting for the electrode potential of the reference electrode with an additional temperature correction. Groundwater pH was measured using a Jenway probe connected to a Mettler Toledo SG8 SevenGo Pro pH/Ion meter that had an accuracy of ± 0.002. The meter was calibrated using pH 4 and 7 buffer solutions.

Specific electrical conductivity (SEC) was measured using a Mettler Toledo SevenGo SG3 conductivity meter and probe that had an accuracy of $\pm 0.5\%$. The probe was calibrated using a 1413 µS cm^{-1} standard solution and checked with

a µS cm^{-1} standard solution. To convert SEC to total dissolved solids (TDS), an ion-dependent conversion factor can be used, for NaCl, a the factor is 0.5; however, because the factor varies slightly depending on the composition, it was decided to use the raw number for analyses. The SEC probe also contains a temperature sensor that has a measurement accuracy of 0.2 °C.

Alkalinity was measured by placing 100 ml of groundwater in a conical flask with 6 drops of Bromocresol green indicator solution. A Hach digital titrator was used to dispense 1.6 N sulphuric acid. The output reading was given in $CaCO_3$ mg L^{-1} and buffering was assumed to be completely due to HCO_3^- and CO_3^{2-}. Total DIC was calculated by summing HCO_3^-, CO_3^{2-} and H_2CO_3, which are assumed to be in equilibrium and can thus be calculated (Eqs. 3.1, 3.2, 3.3 and 3.4).

For sites where both total alkalinity and $\delta^{13}C(DIC)$ have been obtained, it was also be possible to calculate $\delta^{13}C(CO_2)$ assuming isotopic equilibrium, due to low reaction times (Eqs. 3.9, 3.10 and 3.11, (Deines et al., 1974; Mook et al., 1974; Vogel et al., 1970)). Equilibrium constants are temperature dependent (Clark and Fritz, 1997) and can also be corrected (Eqs 3.5, 3.6, 3.7 and 3.8).

$$2TA - [HCO_3^-] + 2[CO_3^{2-}] + [OH^-] \tag{3.1}$$

$$K_1 = \frac{[H^+][CO_3^-]}{[HCO_3^-]} \tag{3.2}$$

$$K_2 = \frac{[H^+][HCO_3^-]}{[H_2CO_3]} \tag{3.3}$$

$$K_{CO_2} = \frac{[H_2CO_3]}{pCO_2} \tag{3.4}$$

$$pK_{CO_2} = -(7 \times 10^{-5})T^2 + 0.016T + 1.11 \tag{3.5}$$

$$pK_1 = (1.1 \times 10^{-4})T^2 + 0.012T + 6.58 \tag{3.6}$$

$$pK_2 = (9 \times 10^{-5})T^2 + 0.0137T + 10.62 \tag{3.7}$$

$$pK_1CaCO_3 = (6 \times 10^{-5})T^2 + 0.0025T + 8.38 \tag{3.8}$$

$$10^3 ln\alpha^{13}C_{CO_{2(aq)}-CO_{2(g)}} = -373(10^3T^{-1}) + 0.19 \tag{3.9}$$

$$10^3 ln\alpha^{13}C_{HCO_3-CO_{2(g)}} = 9.552(10^3 T^{-1}) - 21.10 \quad (3.10)$$

$$10^3 ln\alpha^{13}C_{CO_3-CO_{2(g)}} = 0.87(10^6 T^{-2}) - 3.4 \quad (3.11)$$

3.3 CH_4 concentration

For each site, four samples for analysis of CH_4 concentration were collected in 100 ml Wheaton^{TM} vials (120 ml total volume: 100 ml water and 20 ml of headspace). Each Wheaton vial was sealed with a 20 mm Bellco^{TM} septum stopper and 20 mm aluminium crimp seal. The vials were evacuated to 10^{-3} bar using an Edwards RV5 vacuum pump. Each vial was weighed before and after sample collection to determine by mass the amount of water collected.

At the field site a 6-mm tube was connected to the groundwater supply. Water was collected in a 60 ml syringe with an attached 2-way Luer^{TM} stopcock. The syringe was flushed 2 to 3 times and then 60 ml of water was collected. A 1.1 mm x 50 mm needle was then attached to the stopcock. 10 ml of water was used to flush the needle and the remaining 50 ml was injected into a 100 ml pre-evacuated Wheaton^{TM} vial. This process was then repeated to give a total volume of 100 ml water. The vials were kept inverted in an ice box with ice packs/ ice until taken to the laboratory for inverted storage at 4°C until analysis.

Each vial was over-pressured by 1 atmosphere by injecting 40 ml of He into the 20 ml of headspace. The vials were then shaken for 10 minutes using a SF-1 Stuart Scientific Flask shaker to move dissolved CH_4 into the headspace and allowed to warm and equilibrate at room temperature. The headspace pressure was noted and then the sample was analysed on a Carlo Erba^{TM} HRGC 5300 gas chromatograph (GC) including a gas-sampling valve (1 cm^3 sample loop), Porapak^{TM} QS packed column (3 mm x 4 m) and flame ionization detector (FID). The flow rate of the carrier gas (N_2) was 35 ml min^{-1}, and flow rates of FID support gases were 30 ml min^{-1} (H_2) and 400 ml min^{-1} (zero air). Samples were injected through a 1 cm^3 magnesium perchlorate packed cartridge to remove H_2O. Relative precision of gas analysis in air samples, based on replicate injections of actual samples as well as BOC Specialty Gases alpha-gravimetric standards, was typically better than $\pm 2\%$.

The first sample was analysed using a ramped run, where the oven was set to 37°C for 12 minutes, then the temperature was ramped to 180°C, at a rate of 10°C min^{-1}, for 40 minutes, to check for the presence of higher hydrocarbons. If there were no higher hydrocarbons, then subsequent analyses were run at 37°C.

Headspace CH_4 concentration was calibrated against BOC standards containing 1.6 ppm, 50 ppm or 5000 ppm CH_4 as appropriate for sample concentration. A Scott Speciality calibration gas containing 1.5% n-butane, 6.1% ethane, 0.298% n-hexane, 1.51% iso-butane, 0.300% iso-pentane, 19.9% methane, 0.298 n-pentane and 3.00% propane was used to calibrate concentrations of higher hydrocarbons; however, no higher hydrocarbons were observed at any groundwater study sites.

The dissolved concentration of CH_4 was determined by first calculating the amount of CH_4 stripped into the headspace using the partial pressure of CH_4 (ppm) determined by gas chromatography and the ideal gas law:

$$PV = nRT \tag{3.12}$$

where: P is pressure of the headspace (atm), V is volume of the headspace (L), n is moles of CH_4 (to be determined), R is the gas constant (0.082 L atm K^{-1} mol-1), and T is the ambient temperature (K)

The small amount (<5%) of total CH_4 that was not stripped into the headspace was accounted for by applying an empirical correction factor to the amount of CH_4 (μmol) in the headspace. The number of micromoles of CH_4 (headspace + residual) and the volume (L) of water in the sample vial were then used to determine the dissolve CH_4 concentration (Eq. 3.13)

$$CH_4(\mu gL^{-1}) = \frac{\Sigma CH_4(\mu mol)}{\Sigma H_2O(L)} \tag{3.13}$$

3.4 H_2 Concentration

Four 100 ml Wheaton vials were used to collect water for analysis of H_2. The vials were prepared, filled and stored according to the same protocol used to collect water samples for measurement of CH_4 concentration.

Prior to analysis, vials were over-pressured by 1 atmosphere by injecting 40 ml of N_2 into the 20 ml of headspace. Each vial then was shaken for 10 minutes on a flask shaker. The headspace pressure in the vial was measured and recorded. The concentration of H_2 in the headspace was then measured using a Peak Performer 1 (PP1) reduction gas analyser (RGA). Gas samples were introduced into the RGA via a 1 cm^3 sample loop. Molecular H_2 was separated from other gases on a molecular sieve 5A packed column heated to 105°C prior to flowing into a bed of HgO heated to 265°C where the H_2 was oxidised, releasing Hg gas. An ultraviolet (254 nm) absorption photometer was used to quantify the Hg gas. The instrument was calibrated using a 5 ppm H_2 Scott Speciality gas alpha-gravimetric standard. The precision of the analysis was ±2% and the lower detection limit for H_2 was

~5 parts per billion (ppb).

The dissolved concentration of H_2 was determined in a similar way to CH_4. The correction factor for remnant H_2 was determined experimentally for two different boreholes. At each site, three 40 ml samples were collected in 60 ml syringes and 16 ml N_2 was added to mimic the sample:headspace ratio. The sample was shaken for 10 minutes and then the H_2 concentration was determined using the RGA. The stripping process was repeated on each sample until H_2 was below detection the detection limit of the RGA. An average of 29 % H_2 remained dissolved in samples, which is comparable with the expected theoretical value of 23 % (Lovley et al., 1994; Wilhelm et al., 1977).

3.5 $\delta^{13}C(CH_4)$ Analysis

Four samples of approximately 3 L of water were collected from each borehole in gas and water tight foil polymer bags. The bags were constructed of MarvelSeal 360®, which is composed of 5 layers: 0.6 mm biaxially oriented nylon, 1.4 mm polyethylene, 0.0003 mm aluminium foil, 1.2 mm polyethylene and 1.5 mm linear low-density polyethylene. The material was cut to form bags having dimensions of 40 x 24 cm that were fitted with a valve 10 cm from one end of the bag. The bags were sealed at ~180°C using a Sontex Star® 91 MkV heat sealer. Valve fittings were either nylon fittings connected to a 6 or 4 mm ball valve or Halkey Roberts® barbed on/off valves that were superglued in an open position and heat sealed to 6 mm tubing connected to a Luer Lok® 2-way stopcock.

The aluminium foil polymer ('Al-foil') bags were flushed with N_2 and evacuated before use. The bags could be reused after rinsing with an antimicrobial solution (benzalkonium chloride and de-ionised (DI) water), which had been sparged with O_2 free N_2 to remove dissolved CH_4. The sterilized bags were then evacuated and 30 ml of a 10 % wt solution of benzalkonium chloride was added prior to filling with groundwater. Addition of the antimicrobial solution was the equivalent of 100 mg L^{-1} benzalkonium chloride, which has been determined to remove 98 % of bacterial isolates from organic foods (Fernández-Fuentes et al., 2012).

Methane was extracted from groundwater samples using a purpose-built processing line (Fig. 3.2), which contained a sealed vessel for sparging the water with 'ultra zero air'. The sparging gas contained <1 part per billion CH_4 and was prepared by repeatedly cycling air through CuO held at 875°C. The sparging vessel was constructed of polyvinyl chloride (PVC) lid and base plates (Fig. 3.1) fitted with valves for entry and draining of water, and inflow and outflow

of gases. A lightly greased neoprene o-ring was placed between the PVC lid and base and an acrylic tube (133 mm diameter x 5 mm thick walls) that formed the upright portion of the vessel. Pressure was applied to seal the o-rings via $^1/_4''$ threaded steel rods and wing nuts and a PVC ring placed mid-vessel for stability. Two connections on the top of the vessel used $^1/_4''$ Swagelok fittings connected by steel tubing to 2-way valves. The inlet connection at the base of the jar was a 6-mm pneumatic fitting that allowed attachment of 6-mm tubing and a 2-way stopcock to allow connection of Al-foil sample bags. Two lengths of acrylic tube (345 or 790 mm) having an inner diameter of 190 mm were used to create small and large volume vessels to accommodate different sized water samples. Larger volume samples were required for low CH_4 concentration boreholes to acquire sufficient CH_4 for stable isotope analysis.

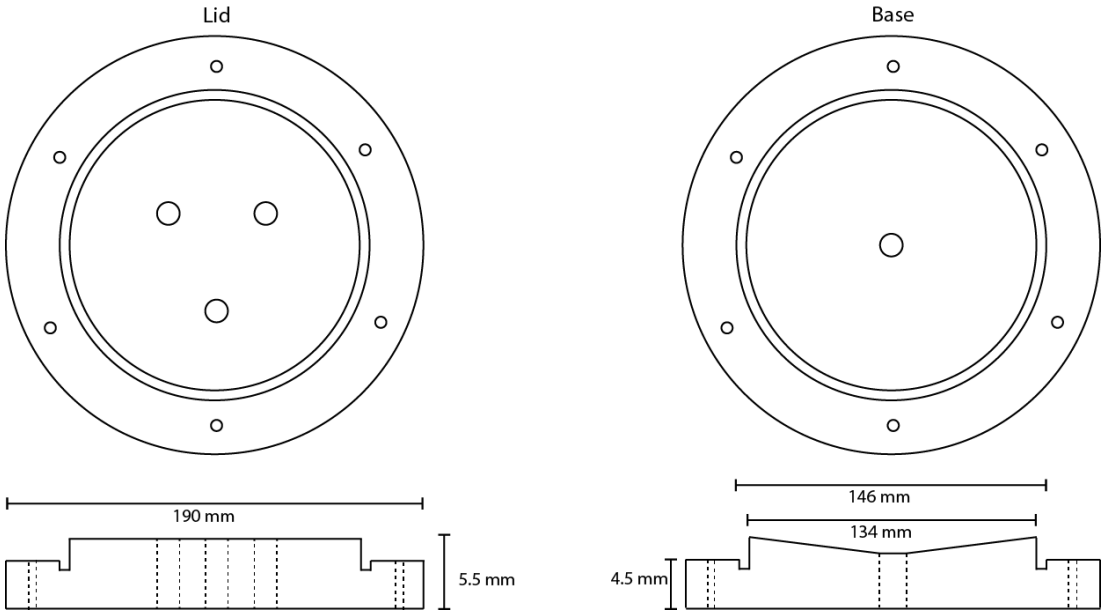

Figure 3.1 Polyvinyl chloride (PVC) lid and base of field sparging jar. The six outer holes hold $^1/_4''$ threaded steel rods used to compress a neoprene o-ring contained in the circular trough against the top and bottom edges of the Perspex^{TM} (acrylic) tube that forms the walls of the vessel. The o-ring is lightly coated in silicon grease. The holes in the lid and base are $^1/_4''$ NPT to hold valves and Swagelok^{TM} fittings.

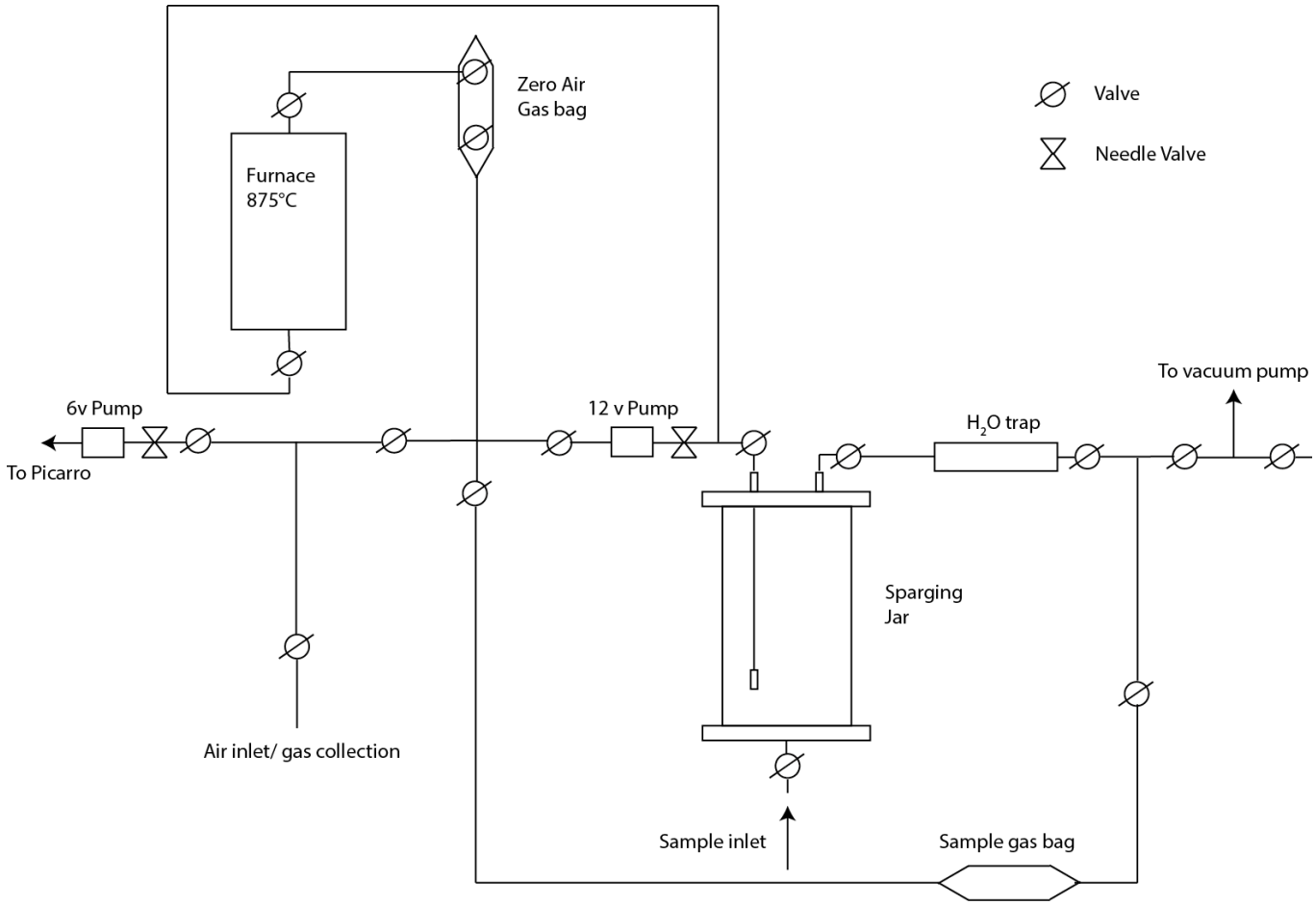

Figure 3.2 Sparging line for extraction of CH_4 from water for analysis of $\delta^{13}C(CH_4)$. Ultra zero air (<1 ppb CH_4) is produced by circulating zero air repeatedly through CuO pellets at 875°C. The sparging jar is evacuated to 10^{-3} bar prior to filling with water. A portion of the ultra-zero air is transferred to the 'sample gas bag' and then cycled through the sample jar via a stainless steel sparging frit to facilitate stripping of dissolved CH_4 from the water sample. The extracted CH_4 in air is then transferred to 100 ml evacuated Wheaton^{TM} vials for analysis by gas chromatography combustion isotope ratio mass spectrometry (GC-C-IRMS). The zero air and sample gas bags are constructed of MarvelSeal 360^{TM} polymer-coated aluminium foil.

PreCon® processing of extracted samples in preparation for $\delta^{13}C$ analysis by isotope ratio mass spectrometry required a gas sample containing minimal H_2O and approximately atmospheric levels of CO_2 (∼400 ppm). During gas extraction, the sparging gas was circulated through silica gel beads to remove H_2O. Prior to initiating sparging, 5 ml of 20 % NaOH solution was added to the vessel to raise the water pH to 12, causing dissolved inorganic carbon to form CO_3^{2-} and remain in solution during CH_4 extraction.

The detailed protocol for creating ultra zero air and using it to extract CH_4 from groundwater in the sparging jar involves first evacuating the line to 10^{-3} bar and then filling the zero air reservoir with room air. The room air is circulated through a quartz tube packed with CuO pellets heated to 875°C. The furnace consisted of a Thermcraft® vertical split tube furnace (460 mm length) fitted with a ceramic heating element (inner diameter 20 mm and outer diameter 42 mm). The heated air exited the top of the quartz tube, which was wrapped in copper tubing connected to a Laudine RE104 Ecoline cooler set to 12°C that circulated water through the tubing. The zero air was circulated through the furnace for ∼20 minutes using a 12 V diaphragm pump, which was connected to a needle valve to control the flow. For the CH_4-scrubbing part of the process the needle valve was kept fully open. The CH_4 content of the ultra zero air was measured with a G112-i Picarro® Cavity Ringdown Spectrometer. The air was transfered to the Picarro® using a 6 V pump and needle valve to control the flow to 100 ml min^{-1}. The Picarro® analyser requires ∼30 ml min^{-1}, which it extracts via a tee-branch from the 100 ml min^{-1} flow venting to room. If the ultra zero air contained <1 ppb CH_4 then the sparging process could begin. The sparging line was closed to the vacuum pump and the sparging jar isolated from the line, allowing the NaOH solution and sample water to be introduced into the jar. The needle valve was then used to control the flow of ultra zero air from the zero air reservoir bag through the sparging frit into the sparging jar. Once pressure equilibrated and bubbling was nearly halted, the vessel opened to the gas collection bag, and the pump used to fill the gas collection bag. Whe this was filled to ∼1 L, the pump was switched off and the airflow between the jar and the zero air closed immediately to avoid any backfflow. The ultra zero air was then circulated via pump through the sparging jar, silica filter and collection bag. The water was sparged for 10 minutes. Air flow was halted intermittently to allow dissipation of foam, which formed in the headspace of the vessel due to the benzalkonium chloride preservative. Gas from the collection bag was then transferred to pre-evacuated Wheaton vials fitted with Bellco stoppers. The remaining gas was pumped to the Picarro analyser to measure the concentration

of CH_4 in the extracted gas. If the mixing ratio of CH_4 was >20ppm then a $\delta^{13}C(CH_4)$ value could also be measured by cavity ringdown spectrometry.

A modified trace gas pre-concentrator (PreCon®) was used (Fisher et al., 2006) to remove CO_2 and H_2O and then quantitatively convert CH_4 to CO_2 at 780°C using palladium powder on quartz wool. This was attached to Thermo-Electron XP continuous flow isotope ratio mass spectrometer for the analysis of $\delta^{13}C$.

Standard delta (δ) notation is used and given in permil (‰) relative to Vienna Pee Dee Belemnite (VPDB). The ISO series (B, L, T and H) of $\delta^{13}C(CH_4)$ standards (Isometric Instruments, Victoria, BC Canada) were used to confirm accurate analysis. Replicate analysis of a 2 ppmv CH_4 alpha-gravimetric standard (BOC Ltd) was used to determine an analytical precision ($\pm$0.1‰).

The ideal CH_4 concentration for PreCon® processing is 2 – 10 ppm in a 100 ml vial. If the CH_4 concentration was higher or lower then a different size of Wheaton vials had to be used. Picarro analysis of CH_4 in extracted gas at the end of each sparging run was important for managing vial selection for gas storage and PreCon® processing. Additionally, extracted gas containing 100 to 500 ppm CH_4 had to be diluted with ultra zero air to enable analysis via the PreCon®. For samples exceeding 500 ppm, the GasBench® interface was used. CH_4 was separated in a 0.32 mm x 30 m PLOT Q capillary column prior to quantitative combustion to CO_2 at 950°C using a consistent flow (0.2 ml min^{-1}) of a high purity blend of 1 % O_2 in He, in a ceramic reactor containing Pt and Cu wires.

3.6 Data Processing and Rejection

All stable isotope analyses that had a mass 44 voltage of <1 V were rejected due to poor accuracy of the IRMS. In instances where stable isotope measurements were inconsistent across replicate samples from a single site, data were rejected if the magnitude of voltage from IRMS analysis did not match the CH_4 concentration of samples analysed independently by gas chromatography. The inconsistencies of voltage versus dissolved gas concentration provided a check that errors had not occurred during transfer of samples from the extraction line to the vial (this would usually include a shift of $\delta^{13}C(CH_4)$ towards atmospheric values $\sim$ -47 ‰) or if any issues arose with the PreCon®, such as a blocked or partially blocked needle.

3.7 δ^{13}C(DIC) Analysis

For each site, four samples of 6 ml of groundwater were collected in pre-evacuated 12 ml Exetainers®. At the borehole head a 6-mm tube was connected to the tap through an airtight connection. A bubble-free sample of groundwater was collected into 10 ml syringe connected to a 2-way luer stopcock. The syringe was flushed with groundwater 2 – 3 times before 7 ml was collected. A 0.5 mm x 16 mm needle was then fitted to the syringe and the needle was flushed with 1 ml of groundwater. The remaining 6 ml was injected into the Exetainer®. The Exetainers® were then stored inverted on ice in a cooler in the field and then at 4°C in the laboratory.

Prior to IRMS analysis, each sample was acidified with pure orthophosphoric acid such that vitually all DIC was converted to CO_2, which accumulated in the vial headspace and could be analysed by IRMS. Mass balance calculations were used to determine the volume of acid required to shift the pH consistently to <2:

$$M_{acid}V_{acid} + M_{sample}V_{sample} = M_{target}(V_{acid} + V_{sample}) \tag{3.14}$$

Where V = volume and M = molarity of acid ($[H^+]$ or 10^{-pH}). To achieve a pH = 4, 0.0015 ml would be required and for pH 2, 0.15 ml was required. Thus, 0.5 ml was used for all samples to ensure a pH <2 and complete conversion of DIC to CO_2 (g). For most samples, the concentration of CO_2 exceeded the maximum detection limit of the IRMS and samples had to be diluted by ∼50 % with He.

The δ^{13}C values of CO_2 were measured by Gas Chromatography Combustion Isotope Ratio Mass Spectrometry (GC-C-IRMS) using a Thermoelectron XP mass spectrometer. For samples collected during 2015 to 2017 δ^{13}C values of DIC were analysed by commercial laboratory Iso Analytical Laboratories because of problems with the GasBench unit in the University of Bristol lab. A similar approach involving addition of phosphoric acid to samples was used followed by IRMS analysis of the liberated CO_2 gas on a Europa Scientific 20-20 IRMS. The reference gas used to determine the δ^{13}C value of the CO_2 was IA-CO_2 -7 (δ^{13}C = -38.48 ‰ vs. V-PDB). IA-CO_2 -7 is traceable to NBS-18 (δ^{13}C value of –5.01 ‰ vs. V-PDB), which is distributed as an isotope reference standard by the International Atomic Energy Agency, Vienna. Samples of IA-CO_2 -7 were analysed as check samples along with blind replicate samples for quality control.

3.8 $\delta^2H(H_2O)$ and $\delta^{18}O(H_2O)$ Analysis

Groundwater was collected in 30 ml Nalgene bottles for analysis of $\delta^2H(H_2O)$ and $\delta^{18}O(H_2O)$ values. The bottles were rinsed 2 – 3 times and over filled before sealing to ensure that air bubbles or a headspace were absent during storage. A duplicate water sample was collected from every tenth borehole.

The water samples were analysed the BGS NERC Isotope Geosciences Laboratory (NIGL) in Keyworth via stable isotope ratio mass spectrometry. Oxygen isotope ($\delta^{18}O$) measurements were conducted using the headspace CO_2 equilibration method and an Isoprime 100 mass spectrometer equipped with an Aquaprep device. Deuterium isotope (δ^2H) measurements were performed via an online Cr reduction method using a EuroPyrOH-3110 system coupled to a Micromass Isoprime mass spectrometer. The stable isotope measurements were calibrated against BGS in-house standards that were calibrated against the international standards VSMOW2 and VSLAP2. Analytical errors were typically ± 0.05 ‰ for $\delta^{18}O(H_2O)$ and ± 1.0 ‰ for $\delta^2H(H_2O)$.

3.9 $\delta^2H(CH_4)$ Analysis

The amount of CH_4 required for δ^2H analysis is approximately one order of magnitude greater than what is needed for $\delta^{13}C$ analysis. The more significant challenge is that the equivalent of a PreCon® device does not exist for focusing and converting CH_4 to H_2 for $^2H/^1H$ analysis. Groundwater CH_4 typically is present at low concentrations (<10 µg L^{-1}), which necessitates an additional pre-concentration step to acquire sufficient CH_4 for stable isotope analysis. A field device and technique were developed for that purpose in this study based upon the laboratory sparging method used to process groundwater samples for $\delta^{13}C$ analysis. The equipment and method are described in full in Chapter 4. The time invested in development of the method was considerable. The approaches attempted before the final technique was adopted are described briefly:

1. An offline vacuum extraction line was constructed at the University of Bristol to purify CH_4 (remove H_2, H_2O and CO_2), combust CH_4 and focus the H_2O produced on metallic zinc, which was then reacted at 450°C to convert H_2O to H_2 for δ^2H analysis at BGS NIGL in Keyworth. Consistent (i.e., precise) results were achieved but accuracy issues could not be resolved. The problem was thought to be caused by degassing of aluminium vacuum fittings, which can corrode to form aluminium hydroxides. There were insufficient resources and time to construct a new extraction line constructed

from high grade stainless steel or glass so the approach was abandoned. There also were issues with the quantity of groundwater that had to be treated with preservative, transported and stored for laboratory processing.

2. An approach was investigated based upon adapting a new dual laser quantum cascade laser system at Lancaster University that was designed to measure 'clumped' isotopologues of CH_4 (e.g., $^{13}C^2H^1H_3$); however, the instrument required 1 cm^3 of purified CH_4, which presented analytical challenges, both analytical and financial, that were comparable to, or greater than, the offline CH_4 processing approach that had been abandoned. There also were issues about the QCL wavelengths, which were optimized for $^{13}C^2H^1H_3$ and not $\delta^2H(CH_4)$ analysis.

The final approach was developed collaboratively with the G.G. Hatch Stable Isotope Laboratory, University of Ottawa, Canada. The Ottawa laboratory had a GC-pyrolysis-IRMS method already in place for $\delta^2H(CH_4)$ analysis at higher CH_4 concentrations. They optimized the method, lowering the threshold for analysis to ~25 ppm and in concert an approach was developed at the University of Bristol to field sparge large volumes of water to pre-concentrate groundwater CH_4 to the required concentration. The extracted gas samples were stored and shipped at ~2 to 3 bar pressures in gas tight tubes.

In the laboratory, gas samples collected in the field (method described in Chapter 4) that contained at least 25 ppm CH_4 were transferred to Isotech IsoTubes®. The IsoTubes were pre-evacuated to 10^{-3} bar via a septum valve using an Edwards vacuum pump. The sample was pumped from the sample gas bag into the IsoTube® using a 12 V diaphragm pump. IsoTubes® were over-pressured to 15 to 25 psi above ambient pressure. Two IsoTubes® were filled for each discrete gas sample bag. The samples were shipped to the G.G. Hatch Stable Isotope Laboratory, University of Ottawa, Canada for δ^2H analysis. The CH_4 was separated using a PoraBOND Q column (0.53 mm) and cryo-focussed in a sample loop at liquid N_2 temperatures, followed by continuous flow gas chromatography – pyrolysis - isotope ratio mass spectrometry (GC-py-IRMS). The analysis was conducted using a Thermo-Fisher GC-Isolink, with molecular sieve 5A PLOT column (0.32 mm x 30 m) at a helium gas flow rate of 1.0 ml min^{-1}. The GC oven was set to 35°C for 7 minutes, ramped at 25°C min^{-1} to 200°C and held for 2 minutes. The GC was connected to a Delta V IRMS via a Conflo IV interface. Pyrolysis at 1420°C was used to produce H_2 from CH_4. Samples were calibrated to international CH_4 isotope standards NGS1 and NGS2.

3.10 Gibbs Free Energy

The energetics of CO_2/H_2 methanogenesis in aquifers were calculated for the reaction in Eq. 3.15 using Eq. 3.16:

$$4H_2 + HCO_3^- + H^+ \rightarrow 3H_2O + CH_4 \tag{3.15}$$

$$\Delta G = \Delta G^\circ + RTlnQ \tag{3.16}$$

Where ΔG is the change in Gibbs free energy (J mol^{-1}) of the reaction under in situ conditions, ΔG ° is the change in Gibbs free energy under standard conditions (-175.4 kJ mol^{-1}), R is the universal gas constant (J mol^{-1}), T is temperature (K), and Q is the reaction quotient defined in Eq. 3.15.

$$Q = \frac{[CH_4][H_2O]^3}{[H_2]^4[HCO_3^-][H^+]} \tag{3.17}$$

For calculation of Q, the activity of H_2O is unity, and in situ measurements of the other parameters were in units of mol L^{-1} (HCO_3^-), activity (H^+) and bar (CH_4 and H_2). Concentration (mol L^{-1}) measurements of CH_4 and H_2 were converted to bar using Henry's Law. The Henry's Law constants were temperature corrected to in situ conditions using National Institute of Standards and Technology (NIST) empirical equations to ensure that partial pressures of CH_4 and H_2 represented conditions that existed in the aquifers.

Chapter 4

A method for extraction and pre-concentration of trace levels of dissolved CH_4 for $\delta^{13}C$ and $\delta^{2}H$ analysis

Summary

Shale gas development has the potential to cause methane (CH_4) contamination of aquifers, which poses potential hazards in areas where human infrastructure exists or water is abstracted for industry or domestic use. Stable isotopes provide an effective means to characterise baseline CH_4 in groundwater and assess the cause of any future changes in the CH_4 content of aquifers; however, the concentration of CH_4 in aquifers typically is below thresholds that allow for routine extraction and analysis of $\delta^{13}C$ and δ^2H values. The size of water sample that must be collected to obtain sufficient CH_4 for $\delta^{13}C$ and δ^2H analyses commonly is challenging to transport and store without CH_4 loss or alteration. This study developed a new sparging method to enable efficient extraction of CH_4 from large volumes of groundwater in the field. Ultra-high purity (UHP) air initially containing <1 part per billion CH_4 is circulated through a fine frit in a sealed vessel containing ∼3 litres of water. New groundwater flows continuously through the vessel. Methane stripped from water via a finely dispersed bubble stream gradually accumulates in the vessel headspace and an external air reservoir. The method can be used to obtain approximately 3 to 4 litres of air containing 25 to 35 ppm CH_4 in one hour from water containing ∼2 µg CH_4 L^{-1}. Trial data demonstrate that $\delta^{13}C$ and δ^2H values of CH_4 are invariant with time while CH_4 concentration increases continuously in the UHP gas reservoir. The new approach should help to increase availability of baseline $\delta^{13}C$ and δ^2H data for groundwater CH_4 and lower the routine concentration threshold to a level that is common in pristine aquifers containing low levels of CH_4 produced by natural microbial methanogenesis. The method also is suitable for other applications where low concentrations of CH_4 are present, such as investigations in rivers and lakes.

4.1 Introduction

The stable isotope composition of carbon and hydrogen in CH_4 can be used to distinguish different CH_4 formation processes and to understand post formation processes, such as CH_4 oxidation (Whiticar et al., 1986, Whiticar, 1999). Methane is produced from a variety of processes (Schoell, 1988), including Archaeal methanogenesis in anaerobic environments (microbial CH_4), thermal breakdown of organic matter at depth, such as in shale or coal gas (thermogenic CH_4) and abiogenic processes that do not involve organic matter (abiotic or geogenic CH_4). During microbial methanogenesis, kinetic isotope effects occur whereby ^{12}C and ^{1}H are preferentially incorporated into CH_4 to different degrees, depending on the production pathway. The result is more negative $\delta^{13}C(CH_4)$ and $\delta^{2}H(CH_4)$ values for microbially produced CH_4 relative to thermogenic and abiotic CH_4. Subsequently, methanotrophic (CH_4 oxidizing) bacteria preferentially consume CH_4 bearing ^{12}C and ^{1}H, which can result in a CH_4 residual having more positive $\delta^{13}C(CH_4)$ and $\delta^{2}H(CH_4)$ values.

Analysis of $\delta^{13}C(CH_4)$ and $\delta^{2}H(CH_4)$ can be conducted by isotope ratio mass spectrometry, whereby CH_4 is combusted to CO_2 to determine $^{13}C/^{12}C$ ratios (Fisher et al., 2006) and to H_2 for $^{2}H/^{1}H$ analysis, either via pyrolysis (Bock et al., 2014; Brass and Röckmann, 2010) or combustion to H_2O and subsequent reduction to H_2 (Coleman et al., 1982). Alternatively, laser absorption techniques can be used to directly analyse the absolute amounts of $^{12}C^{1}H_4$, $^{13}C^{1}H_4$ and $^{12}C^{2}H^{1}H_3$ to determine $\delta^{13}C(CH_4)$ and $\delta^{2}H(CH_4)$ values (Bergamaschi et al., 1994; Eyer et al., 2016; Tsuji et al., 2010). In all cases, low CH_4 concentration samples need to be pre-concentrated and potentially purified to remove contaminants prior to analysis. Additionally, analysis of $\delta^{2}H(CH_4)$ values generally requires larger quantities of CH_4 and typically analysis has been limited to groundwater containing higher concentrations of CH_4.

Dissolved CH_4 generally occurs in groundwater in relatively low concentrations, commonly in the range 1 to 20 µg CH_4 L^{-1} (Darling and Gooddy, 2006). The concentration of CH_4 typically is even lower at <1 µg L^{-1} although can be much higher in areas where subsurface sources are venting CH_4 into bottom waters (Lamontagne et al., 1973).

Current methods for sampling groundwater to analyse dissolved CH_4 and its isotopic composition usually involve collection of water in airtight containers followed by processing and extraction of the CH_4 in a laboratory (Holt et al., 1995; Jahangir et al., 2012; Liotta and Martelli, 2012) or by equilibrating the CH_4-bearing water with high purity gas (usually N_2) in a headspace (Thornton et al., 2001; Walsh and McLaughlan, 1999) with the gas being analyzed subsequently.

More recently, continuous pumping methods have been used to allow analysis of lower CH_4 concentration waters (Dean et al, 2017; Sparrow and Kessler, 2017).

Hydrogen (H_2) derived from 2 µL of water (in turn derived from CH_4) is the ideal quantity for δ^2H analysis by conventional dual-inlet, dynamic gas-source isotope ratio mass spectrometry (Horita and Kendall, 2004). Groundwater containing 2 µg CH_4 L^{-1} would require a sample of approximately 450 litres of water to be processed, an amount that is not easily stored and transported when replicates, the need to store the water in a gas tight vessel and the need to keep the water cold (<4°C), are factored into the sampling protocol.

4.2 Background

Measurement of low concentration analytes dissolved in water is not a new problem and methods have been developed to overcome transportation and storage issues. There are two main on-site approaches: (i) large quantities of water are filtered to extract select organic compounds or contaminants, and (ii) water is processed through a collection system that includes a gas or liquid phase that extracts and concentrates the analyte of interest.

The first set of methods is used most commonly to study contaminated freshwater sites or to measure dissolved organic carbon (DOC) and still involves an initial collection of large quantities of water, which is then filtered through resin, chromatography columns or liquid solvents, depending on the analyte of interest (Thurman and Malcolm, 1981; Pearson et al., 1996; Swackhamer et al., 1998; Datta et al., 2004).

The second set of methods is most relevant to the method developed in this study. A commonly used approach is to employ finely dispersed bubbles to strip volatile compounds from water. The adapted method was developed originally to analyse dissolved H_2 in groundwater (Lovley et al., 1994) and has been subsequently refined and optimised (Alter and Steiof, 2005; Chapelle et al., 1997; Dorgerloh et al., 2010; Heimann et al., 2003; Lovley et al., 1994; McInnes and Kampbell, 2000). Groundwater is pumped through a gas-sampling bulb, which is flushed thoroughly with sample water before introduction of H_2-free N_2 to form a headspace in the bulb. Water flows continually through the bulb, equilibrating with the gas phase. The gas phase is then sampled once the H_2 concentration has stabilised. This method also has been applied successfully to CH_4 collection for concentration analysis, eliminating the need for transport of groundwater (Baker et al., 2012; Thornton et al., 2001); however, it does not pre-concentrate CH_4 to levels typically that are sufficient for stable isotope analysis of CH_4.

Another approach involves flowing water through a gas-tight sampling tube that contains a length of silicone tubing through which dissolved gases diffuse and accumulate (Jacinthe and Groffman, 2001). The concentrated gas can then be extracted from a sampling port at the top of the sampler. This method has been used successfully to measure dissolved N_2O and CO_2 in groundwater (Jacinthe and Groffman, 2001).

Dissolved gas also can be sampled by pumping-induced ebullition (Browne, 2004) whereby buoyancy is used to trap bubbles within a collection tower. Ebullition occurs when the sum of the partial pressures of the volatile species exceed ambient hydrostatic pressure. The gases are exsolved from water by pumping through a narrow 'restrictor' tube into the collection chamber. This approach is effective for stripping dissolved gas but the small diameter of tubing needed to force ebullition may also greatly restrict the flow rate of water and consequently, the volume of water that can be processed.

More recent methods have enabled extraction of low concentrations of CH_4 from very large quantities of water (Dean et al., 2017; Sparrow and Kessler, 2017). One approach involves a collapsible gas-tight vessel containing hydrophobic, gas-permeable membrane tubing (Dean et al, 2017). Water containing gas flows through the tubing and equilibrates with the headspace in the collapsible vessle, which can contain either CH_4-free air or N_2. The method has been used successfully for collection and analysis of $\delta^{14}C(CH_4)$ and $\delta^{13}C(CH_4)$. The equilibration vessel and flowing water can be left unattended for 24 hours or longer to allow CH_4 to concentrate.

Sparrow and Kessler (2017) present a method designed to analyse $\delta^{14}C(CH_4)$ and $\delta^{13}C(CH_4)$ and $\delta^{2}H(CH_4)$ from seawater containing 2 nM CH_4 (0.03 µg CH_4 L^{-1}). The method involves pumping seawater via a flow meter and filter system through two gas extractors that operate in parallel. The gas extractors contain hydrophobic, gas permeable membranes that extract all dissolved gases from the water flowing through them. The gas is collected in reuseable 400 L reservoir bags via a vacuum pump, passing through a water vapour trap and gas flow meter. Once the reservoir bag is filled, the gas is compressed into a 1.7 L gas cylinder. The process involves pumping 20,000 to 40,000 L of water to extract 300 to 400 L of gas over a 2 to 3 hours period, or 4 to 5 hours including pre- and post-collection procedures. The extracted gas is processed onshore via a vacuum line for analysis of $\delta^{14}C(CH_4)$ and $\delta^{13}C(CH_4)$ and $\delta^{2}H(CH_4)$.

The method reported here is designed for extraction of CH_4 from groundwater containing as little as 2 µg CH_4 L^{-1}. The ideal sampling outcome is ∼4 L gas containing ≥30 ppm CH_4 collected in 1 hour or less. Groundwater containing

lower concentrations of dissolved CH_4 also can be sampled by increasing the sparging time and processing larger volumes of water.

4.3 Method Description

4.3.1 Materials

The size and other specifications of the lid and base of the field sparging vessel are shown in Figure 4.1 . The sparging vessel and full gas extraction and collection system are shown in Figure 4.2. The lid and base are constructed of grey polyvinyl chloride (PVC). The upright portion of the vessel is a clear acrylic tube that has an inner diameter of 190 mm and length 345 mm. Lightly greased neoprene o-rings (5 mm thickness and 133 mm diameter) fitted in the lid and base seal against the ends of the acrylic tube. The o-rings are pressed against the tube via $1/4''$ threaded steel rods, an intermediate PVC stabilizing ring, and $1/4''$ wing nuts that thread through the lid and base. Openings in the lid connected to the gas bag and overflow tubes (Fig. 4.2) via $1/4''$ Swagelok fittings and 3-way valves. The water inflow, outflow and overflow tubes are composed of polyurethane. The overflow tubes have a $1/4''$ outer diameter (OD), the inflow tube $1/2''$ OD, and outflow tube $1''$ OD.

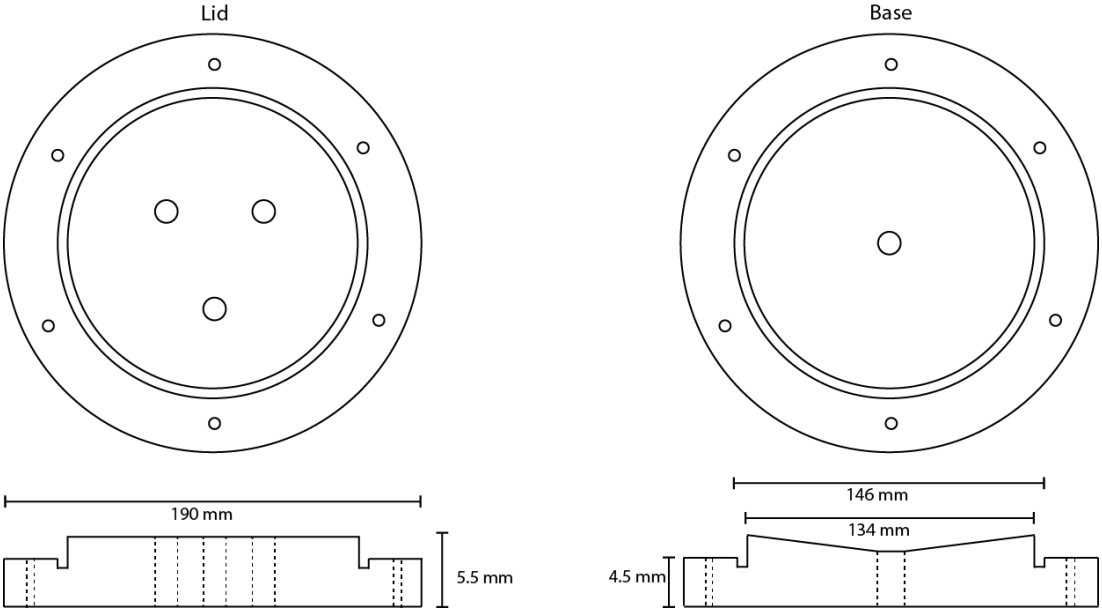

Figure 4.1 Polyvinyl chloride (PVC) lid and base of field sparging jar. The six outer holes hold $1/4''$ threaded steel rods used to compress a neoprene o-ring contained in the circular trough against the top and bottom edges of the Perspex^{TM} (acrylic) tube that forms the walls of the vessel. The o-ring is lightly coated in silicon grease. The holes in the lid and base are $1/4''$ NPT to hold valves and Swagelok^{TM} fittings.

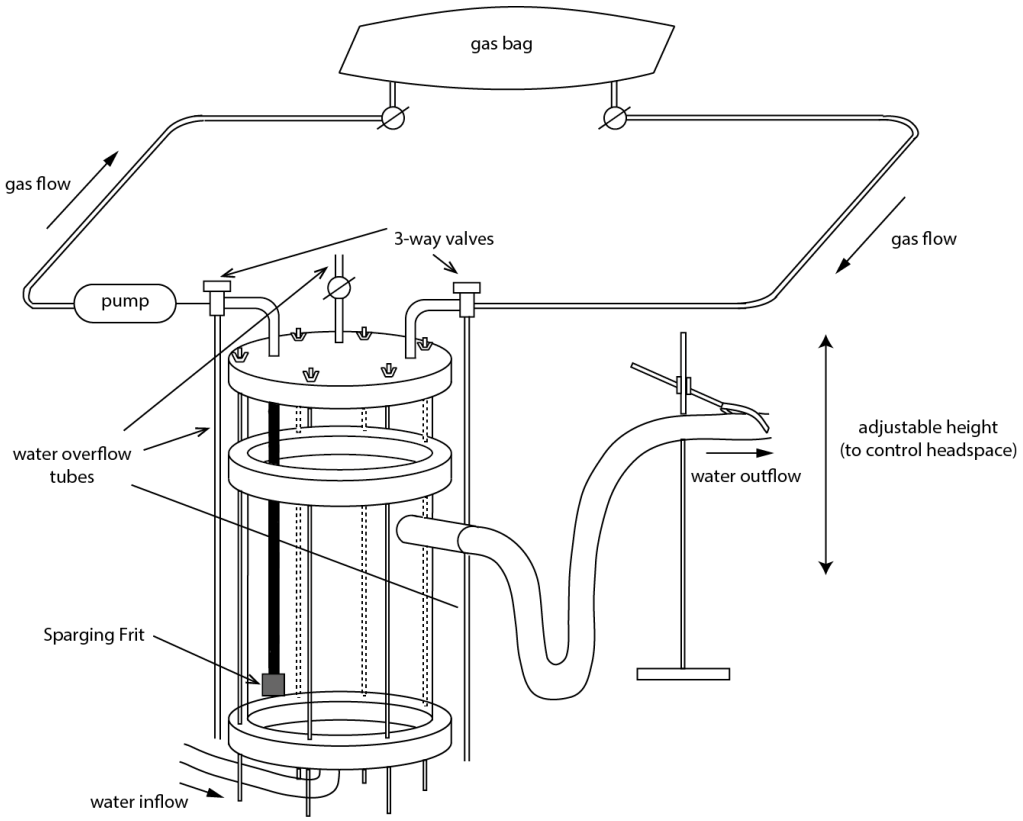

Figure 4.2 Field sparging system for extraction and collection of dissolved CH_4 for analysis of $\delta^2H(CH_4)$ analysis. Water flows into the vessel (4 L) from the base and exits via the outflow pipe. The water-level in the vessel is maintained fully above the outlet to prevent loss of headspace gas. The 'ultra zero air' that initially contains <1 part per billion CH_4 is pumped through the water via the sparging frit and collected in the gas bag

The gas reservoir bag is constructed from Marvelseal® 360 polymer-coated foil, which is composed of 5 layers: 0.6 mm biaxially oriented nylon, 1.4 mm polyethylene, 0.0003 mm aluminium foil, 1.2 mm polyethylene and 1.5 mm linear low-density polyethylene. The dimensions of the bag are 300 by 420 mm and it has a volume of ∼4 to 5 litres. It has two valve openings to allow air flow through the bag and extraction line circuit. The bag is filled with 'ultra zero air' (<1 part per billion CH_4), which is produced in the laboratory by circulating air through CuO pellets heated to 875°C. The concentration of CH_4 in the ultra-zero air is measured by cavity ringdown spectroscopy before transfer to Al polymer-coated bags for use in the field.

4.3.2 Field deployment

The inflow tube of the sparging vessel is connected with gas tight fittings to the groundwater supply, through a tap if available, or a pump in a borehole. Water is allowed to fill the vessel and flow freely from the overflow tubes. The

water outflow tube fitted in the side of the acrylic tube initially is set at a height greater than the jar to prevent air from entering the vessel. Once the jar has been flushed, the valves in the lid are closed to direct all flow to the side outlet. Flow rate through the vessel is then measured by timing the capture of 1 litre of water in a graduated cylinder. A flow rate of ∼5 L min^{-1} was determined to be optimal for extraction of CH_4 from groundwater containing µg CH_4 L^{-1}. The flow of water was stopped momentarily and a headspace was created in the vessel by pumping ultra-zero air from the gas reservoir. Once the desired headspace was achieved, the ultra-zero air was circulated through the sparging frit, vessel headspace and gas bag. Water flow into the vessel was resumed and the height of the water outlet tube was adjusted to maintain a constant headspace in the vessel that did not permit entry of ambient air. The approximate concentration of CH_4 in groundwater at each site was known from prior sampling visits. The sparging time was determined on that basis. For example, groundwater estimated to contain ∼8 µg CH_4 L^{-1} was processed at a flow rate of 5 L min^{-1} for approximately 15 to 20 minutes. For a site containing ∼2 µg CH_4 L^{-1}, the same flow of water was sparged for ∼1 hour.

When a sufficient volume of water had been sparged, the air circulation pump was switched off. The lack of air flow allows the water-level to rise in the vessel, displacing most of the headspace containing CH_4 back into the gas reservoir bag. The gas bag was isolated and water flow to the vessel was stopped. The gas sample was disconnected from the sparging line for transport to the laboratory.

4.3.3 Validation

The method was tested at a groundwater borehole at Wallingford, Oxfordshire, UK that was known to contain ∼3.5 µg CH_4 L^{-1}. Groundwater flowing through the vessel at 4.5 L min^{-1} was sparged continuously for 2 hours, stopping only to sub-sample gas from the gas reservoir at 10, 20, 30, 60 and 120-minutes after the onset of sparging. Samples were collected for both analysis of CH_4 concentration and analysis of $\delta^{13}C(CH_4)$ values. The sample collected at 120-minues was also analysed for $\delta^2H(CH_4)$. A second sample was analyzed for $\delta^2H(CH_4)$ from a separate 40-minute deployment of the sparging vessel.

Samples for analysis of CH_4 concentration were collected in gas-tight plastic syringes fitted with 2-way Luer Lok® stopcocks. The gas samples were analysed the following day using a Carlo Erba HRGC 5300 gas chromatograph (GC) equipped with a Porapak® QS packed column (3 mm x 4 m), flame ionization detector (FID) and gas-sampling valve (1 cm^3 sample loop). A N_2 carrier gas (35 mL min^{-1}) was used as well as, and FID support gases: H_2 (30 mL min^{-1})

and zero air (400 mL min^{-1}). Gas samples were injected through a 1 cm^3 magnesium perchlorate packed cartridge to remove H_2O. Based on replicate injections of BOC Specialty Gases alpha-gravimetric standards and actual samples, the relative precision of gas analysis in air samples was determined to be typically better than ±2 ‰.

Samples for analysis of $\delta^{13}C(CH_4)$ were extracted into a gas-tight plastic syringe fitted with a 2-way Luer Lok® stopcock and then immediately injected through a CO_2 filter filled with Decarbite® into a crimp-sealed 125-ml Wheaton vial. The $\delta^{13}C$ value of CH_4 in each vial was analysed using a modified trace gas pre-concentrator (PreCon®) (Fisher et al., 2006) to remove CO_2 and H_2O and then quantitatively convert CH_4 to CO_2 at 780°C using palladium powder on quartz wool. This was attached to ThermoElectron XP continuous flow isotope ratio mass spectrometer for the analysis of $\delta^{13}C$.

Samples for $\delta^2H(CH_4)$ analysis were transferred from the foil polymer bags into Isotech IsoTubes®, which had been pre-evacuated to 10^{-3} bar. The gas sample was pumped from the foil polymer bag to the IsoTube® using a 12 V diaphragm pump to an overpressure of 15 to 25 psig. IsoTubes® were filled for each sample, which were subsequently analysed at the G.G. Hatch Stable Isotope Laboratory, University of Ottawa, Canada. Briefly, the method employed for $\delta^2H(CH_4)$ analysis involved injection of gas via a sample loop onto a Porabond Q capillary column followed by cryo-focussing of separated CH_4 on a Porabond Q column (Molesieve 5A plot, 0.32 mm x 30 m). Pyrolysis of CH_4 at 1420°C yielded H_2 which analysed using a ThermoElectron Delta V isotope ratio mass spectrometry. The $\delta^2H(CH_4)$ values were calibrated to international CH_4 isotope standards NGS1 and NGS2.

The concentration of CH_4 in the gas reservoir increased linearly during the first sparging trial from 8 ppm at 10 minutes to 90 ppm at 120 minutes (Table 4.1; Fig. 4.3). The $\delta^{13}C$ value of extracted CH_4 was relatively constant from 20 minutes onward. The first sample collected at 10 minutes had a $\delta^{13}C(CH_4)$ value that was 0.8 ‰ higher than subsequent measurements. The ^{13}C -enrichment may have resulted from air contamination ($\sim$ -47 ‰) during subsequent placement of sample into the Wheaton vial for testing; however, there is no evidence from field observations to suggest that air entered the vessel during the sparging trial. The two $\delta^2H(CH_4)$ collected at 120-minutes in trial 1 and at 40-minutes in trial 2 differ by 1 ‰, which is well within the analytical error typically associated with $\delta^2H(CH_4)$ analysis.

The CH_4 concentration data show the potential for extraction and accumulation of CH_4 to any desired ppm quantity through longer sparging times and

Table 4.1 Sparging test results from Wallingford, UK borehole.

Test	Time (min)	CH_4 (ppm)	$\delta^{13}C(CH_4)$ (‰)	$\delta^2H(CH_4)$ (‰)
Trial 1[a]	10	8	-58.2	
	20	16	-59.0	
	30	24	-59.2	
	60	43	-59.1	
	120	90	-58.9	-311
Trial 2[b]	40	32		-310

[a]Sparge trial 1 involved stopping the water and gas flows at intervals to collect samples.
[b]Sparge trial 2 was continuous for 40 minutes.

processing of greater volumes of water (Table 4.1; Fig. 4.3). The $\delta^{13}C$ values demonstrate the lack of stable isotope fractionation during a trial lasting two hours. The δ^2H values demonstrate consistency in analysed values between independent runs.

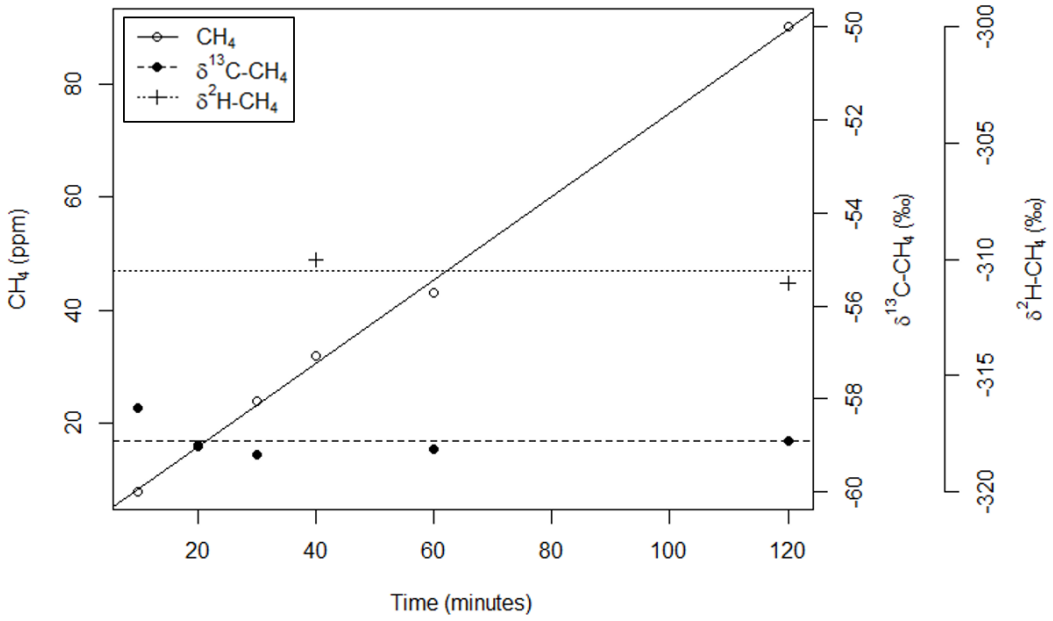

Figure 4.3 Sparging test results from the Wallingford borehole site. Gas samples collected at 10, 20, 30, 60 and 120 minute after sparging began showing a steady increase in CH_4 concentration and a stable $\delta^{13}C(CH_4)$ value from 20 minutes onwards. The $\delta^2H(CH_4)$ values were measured from two different sparging trials: one sample from 120-minutes at the end of trial 1 and a second sample from a separate 40-minute sparging trial.

This method was designed and tested for extracting and concentrating low levels of CH_4 from groundwater; however, it is equally well suited for investigations of any natural or human-impacted aquatic environment that contain trace levels of CH_4. For example, the sparging vessel and protocol could be used for

collecting CH_4 from streams draining peatland or the water column of lakes.

4.4 Conclusions

A sparging vessel and protocol were developed for field extraction and concentration of trace levels of CH_4 from groundwater for $\delta^{13}C$ and $\delta^{2}H$ analysis. The method was tested successfully on a borehole site containing 3.5 µg CH_4 L^{-1}. The concentration of CH_4 increased linearly with time in the headspace of the sparging vessel, which suggests it should be possible to collect an adequate quantity of CH_4 for stable isotope analysis from lower CH_4 concentration groundwater by increasing the duration of sparging and volume of water processed. No fractionation of stable C isotopes was observed during the 120-minute trial. The approach also yielded reproducible $\delta^{2}H(CH_4)$ values from independent deployments of the sparging device. The technique was developed for groundwater investigations of CH_4; however, it could potentially be used for studies in any aqueous environment where stable isotope analysis of trace concentrations of CH_4 are of interest.

Chapter 5

Methane in the Lower Greensand aquifer, southeast England

Summary

Methane production and consumption processes are related to variations of environmental conditions which can vary across an aquifer within a single structure. The stable isotope composition of CH_4 is dependent on the rates of methanogenesis and methanotrophy, which in turn are dependent on temperature, pH and redox conditions, which can be affected by depth, geology and geochemistry, and whether conditions are confined or unconfined. Dissolved CH_4, $\delta^{13}C(CH_4)$ and $\delta^{2}H(CH_4)$ were measured from boreholes within the Lower Greensand (LGS) aquifer across the synclinal structure in the western London Basin, allowing for a range of conditions to be considered. In the deep confined aquifer, low DO and Eh and relatively high CH_4 was recorded; there was a narrow range of CH_4 isotope compositions, $\delta^{13}C(CH_4)$ (-57.6 to -48.2 ‰) and $\delta^{2}H(CH_4)$ (-183 to -93 ‰) and a relationship of C and H stable isotope fractionation with temperature was observed. In the shallow unconfined aquifer varying Eh, CH_4 and DO were measured, in addition to a wide range of isotope compositions, $\delta^{13}C(CH_4)$ (-29.3 to -69.5 ‰) and $\delta^{2}H(CH_4)$ (-136 to +114 ‰). For this wide range of C- and H- stable isotope fractionation, there was no observed relationship to temperature. The narrow variability of CH_4 stable isotope composition within the deeper aquifer is potentially due to variation of C- and H- fractionation with temperature during methanogenesis, however, there may also be a component of post-production CH_4 oxidation. The wide variability of isotope composition observed across the shallow aquifer, is likely due to differing rates of methanotrophy. The findings highlight the importance of characterisation of geochemical conditions, CH_4 concentration and stable isotope compositions in aquifers prior to shale gas exploration or development if the baseline data are to be used effectively to assess future changes in the geochemistry or gas content of the groundwater system.

5.1 Introduction

The Lower Greensand (LGS) aquifer has been well studied (e.g. Casey, 1961; Hopson et al., 2008; Middlemiss, 1975; Morgan-Jones, 1985; Shand et al., 2003, 2007) and therefore the geology, structure and hydrology are broadly understood; a large reason for this is its use as a major aquifer in the south of England. This area was chosen for study to test the effects of changing conditions, such as transition from unconfined to confined conditions, depth and temperature to stable isotope composition of CH_4 ($\delta^{13}C(CH_4)$ and $\delta^2H(CH_4)$) within a single aquifer. This study contributed to project objectives O1, O2, O3 and O5 as described in Chapter 1 and allowed testing of hypotheses H1, H2, H4 and H5.

The area of interest within the LGS aquifer is situated in the synclinal basin to the west of London, whose limbs have a southern outcrop area in Hampshire and Surrey and a northern outcrop area in Bedfordshire (Fig. 5.1). The Hythe Formation sites were only sampled in the shallow, unconfined section of the aquifer because the deeper sites are not drilled deep enough to reach the Hythe Formation and instead terminate within the Folkestone Formation (Fig. 5.2). The possible exception to this are the wells classified as undifferentiated because the sub-formations are not defined. To the north the LGS is undifferentiated and known as the Woburn Sands, and is thought to have been deposited contemporaneously with the Sandgate and Folkestone Formations.

In total, 12 sites were sampled in the LGS. The sites were chosen to cover the full depth range across the aquifer, including confined and unconfined sections, to investigate variability across the aquifer. Some sites were visited twice, to attempt to gain a full suite of analyses, though at some sites, this was not possible for logistical reasons, and not all analyses could be carried out for each site, particularly $\delta^2H(CH_4)$, because the ability to analyse this parameter depends on the CH_4 concentration at the site.

Sites were analysed for CH_4 concentration, H_2 concentration, $\delta^{13}C(CH_4)$, $\delta^2H(CH_4)$, $\delta^{13}C(DIC)$, $\delta^2H(H_2O)$ and $\delta^{18}O(H_2O)$ and field measurements were conducted for pH, specific electrical conductance (SEC), dissolved oxygen (DO), oxidation-reduction potential (ORP) and total alkalinity. Full details of analysis methods are provided in Chapter 3.

5.2 Background

The Lower Greensand (LGS) is situated in south east England where it outcrops on the Isle of Wight, around the Weald, and to the SW and NW of London

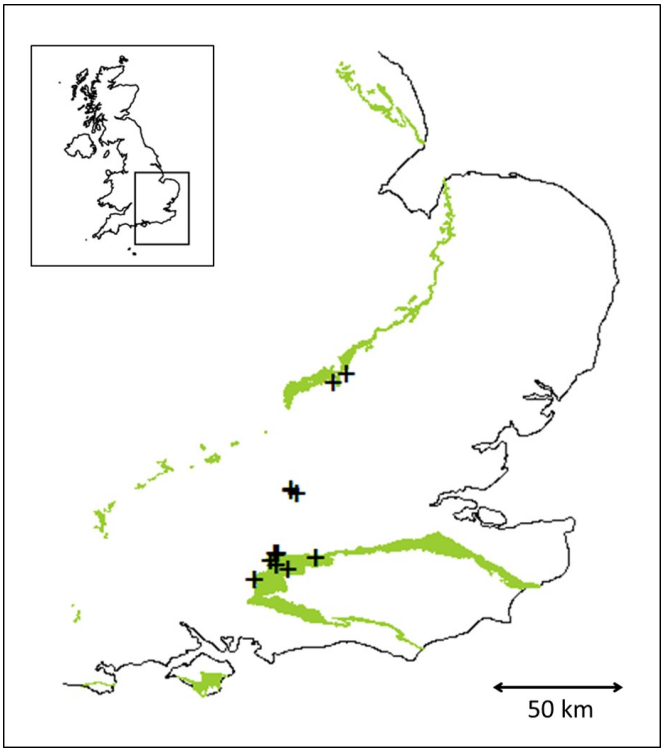

Figure 5.1 Map of study area showing outcrop of Lower Greensands (green) and study sites locations (crosses). Borehole study sites are located within a syncline whose limbs have a southern outcrop area in Hampshire and Surrey and a northern outcrop area in Bedfordshire.

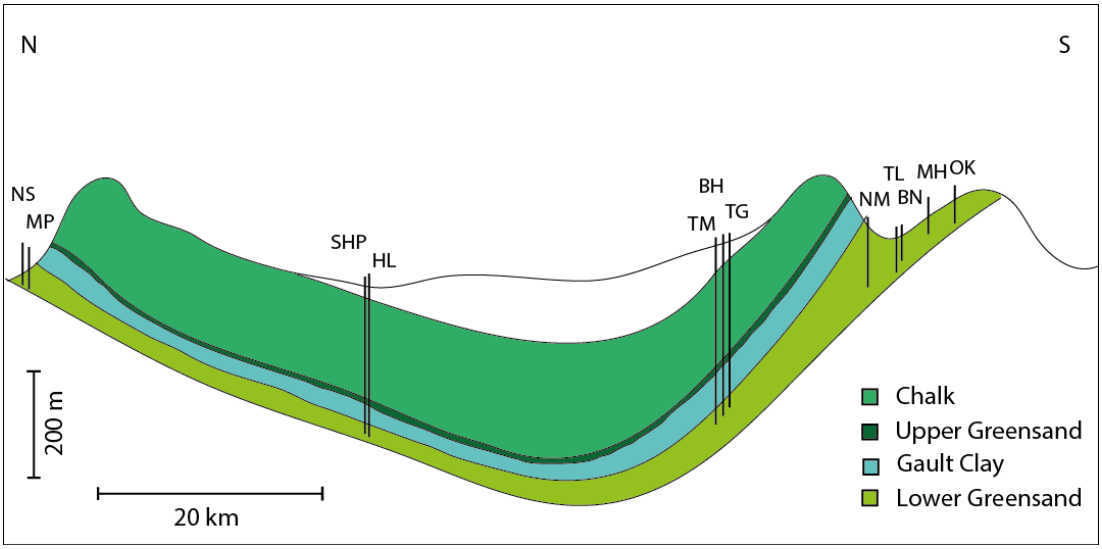

Figure 5.2 Schematic cross-section of Lower Greensand syncline (image adapted from Morgan-Jones, 1985). Vertical lines are the approximate location of boreholes sampled in this study. Formations within the Lower Greensand are not shown separately. Southern study sites (codes provided in Table 1) OK, MH, BM, TL and NM are within the Hythe Formation, TM, BH and TG are within the Folkestone Formation, SHP and HL are within the undifferentiated section, and NS and MP are within the Woburn Sands.

(Fig. 5.1). Post-depositional tectonic activity has resulted in generally E–W fold structures. The LGS, while outcropping over a comparatively small area, is a major aquifer where abstraction has taken place for over 100 years, providing potable water to the southeast of England. It has been studied in detail over the years, with work carried out between 1875 and 1975 summarised by Middlemiss (1975) and detailed, up to date lithological descriptions reported in Hopson et al. (2008). The hydrogeology and hydrochemistry of the LGS has been investigated previously in multiple studies, including as part of groundwater baseline study in UK aquifers (Shand et al., 2003, 2007). For the present study, British Geological Survey (BGS) baseline data were made available for the composition of major and minor ions for sites visited.

The LGS was deposited during the Aptian to Albian stages of the lower Cretaceous and has been dated meticulously using ammonites, allowing detailed stratigraphic correlation of field sections (Casey, 1961). It lies unconformably on Jurassic rocks, with a large range in thickness, the maximum being observed on the Isle of Wight at 245 m. The lower contact is sharp with signs that the deposition of the LGS was preceded by gentle folding and erosion of the Jurassic Wealden beds, whereas the upper contact is more gradational, changing from sandy to clay-rich sediment (Casey, 1961). The LGS can be sub-divided from oldest to youngest into the Atherfield, Hythe, Sandgate and Folkestone Formations. The Hythe and Folkestone Formations (colloquially 'Beds') are the two main aquifer units, though discrimination between the two is only useful in the southern sections, which is the main outcrop area. In the confined central section of the syncline and the northern outcrop area, they can be considered a single aquifer unit.

The Atherfield Formation (colloquially 'Clay') was deposited following the rapid ingress of the sea between the London Platform and Brittany (Middlemiss, 1975). It has an approximate thickness of 18 m and consists of a yellowish brown to pale grey sandy mudstone, with intermittent phosphate pebble beds containing vertebrate bone, gritty sandstone or very shelly, sandy mudstone, and with glauconite at its base (Hopson et al., 2008). This was followed by an influx of sandy sediment and the deposition of the Hythe Beds, with the source rock thought to be partly from the erosion of Jurassic rocks on the uplifted London Platform (Middlemiss, 1975). The Hythe Beds consist of a thickness range of 18 to 100 m and consists of fine to medium grained, sparsely glauconitic sands, sandstones and silts. It may be locally pebbly, with calcareous or siliceous cement in the beds or lenses (Hopson et al., 2008). The sands are more calcareous to the east, which is thought to be due to erosion from limestones on the London platform.

At the end of the period of deposition of the Hythe Beds, there was a period of tectonic activity, during which there was some erosion of sediments. This is seen in the tectonic disturbance in the Hog's Back area in Surrey which resulted in stripping of sediments north of Guildford (Middlemiss, 1975). Following on from this was another transgression resulting in the deposition of the Sandgate Beds. The Sandgate Beds have a thickness range of 50 – 100 m and consist of fine sands, silts and silty clays, and are commonly glauconitic with some sands limonitic or calcareous (Hopson et al., 2008). The Folkestone Beds were deposited in a shallower setting and have a thickness range of 0.5 – 80 m, consisting of medium- and coarse-grained, well-sorted cross-bedded sands and weakly cemented sandstones that in some areas contain calcareous sandstones (Hopson et al., 2008).

The LGS is thought to have accumulated across two basins separated by the London Platform. In the northern basin, the sea never fully regressed (Casey, 1961) and in Bedfordshire and Cambridgeshire the formation is known as the Woburn Sands, which were deposited contemporaneously to the Sandgate and Folkestone Beds, lying unconformably on Jurassic shales. Erosion during the lower Cretaceous created a gently undulating topography, which was flooded by a marine transgression in the Aptian – the so-called 'Bedfordshire Straits'. Isopach maps of the LGS suggest that the Woburn Sands were deposited in a shallow palaeo-valley about 50 km wide and up to 50 m deep (Bristow, 1995). Distinct lithological units or brown sands, silver sands, silty beds and red sands are identified, but lateral variation within the sands is such that they do not form mappable units (Shephard-Thorn, 1994).

Hydraulic properties of the LGS have been determined from pumping test data (Allen et al., 1997). Transmissivity values range from 33 to 3400 m^2 d^{-1}, with the mean and median both 270 m^2d^{-1}. Storage coefficient estimates range from 10^{-5} to 0.08, with a mean and median of $6x10^{-4}$. Hydraulic conductivity data varied from 10^{-4} to 10 m d^{-1}, with a mean of 0.46 m d^{-1} and a median of 0.53 m d^{-1}. The porosity ranged from 6 to 41 %, with a median and mean of 29.5 and 28 %, respectively (Allen et al., 1997). Piezometric contours from the Hythe and Folkestone Beds rarely coincide, indicating that the two aquifers are hydraulically separate, with the Sandgate Beds acting as an aquiclude. Groundwater flow in the Hythe Beds is mostly intergranular where the sands are poorly cemented and by fracture flow where consolidated. In the Folkestone aquifer, the sands are more uniform and the flow is predominantly intergranular (Morgan-Jones, 1985).

Abstraction is mostly within the unconfined southern part of the aquifer, where there is a large recharge area and a relatively high recharge rate (Allen et al., 1997). However, there has also been significant abstraction in the confined

area around Slough since the 1930s (Mather et al., 1973). Though the LGS in the Slough area has been abstracted for over a century, it is still artesian and does not appear over-exploited, which was a potential concern previously (Mather et al., 1973). It has since been suggested that downward flow from the Chalk could be partly responsible for recharge of the aquifer and the low HCO_3 concentrations compared to the Chalk explained by infiltration through the Gault Clay (Egerton, 1994). Radioisotope analysis of ^{14}C-DIC (Mather et al., 1973) indicate older water (29 ka) in the confined parts of the aquifer, suggesting that storage is high. Minor elements Sr, Li and F, good indicators of residence time, also increase towards the confined section of the aquifer (Shand et al., 2003). Comparison of stable isotope composition of water with ^{14}C-DIC, give a bimodal distribution (Darling et al., 1997), which indicates that the older groundwater was recharged at cooler temperatures, likely during the most recent glacial period. Whereas, the second grouping in the shallower, unconfined section is recharged with modern rainwater.

The rocks of the LGS are generally depleted in soluble mineral species, though there is slightly higher carbonate content in the eastern part of the aquifer, which is thought to be due to calcareous bands (Morgan-Jones, 1985). The Hythe Beds are richer in clay minerals (5 – 10 %) compared to the Folkestone ($\sim$ 2 %). The clay minerals in the Hythe consist of mainly mica and smectite, with little to no kaolinite, in the predominantly quartz sands, there is abundant glauconite and magnetite and impersistent nodules and bands of chert in some areas. The Folkestone clay minerals are mainly kaolinite and mica in association with various mixed layers; in the also predominantly quartz sands, glauconite is less abundant and magnetite and pyrite were only detected in samples taken from depth. Localised ironstone bands were formed by re-precipitation of iron (Morgan-Jones, 1985).

The groundwater is dominantly of the Ca-HCO_3 type, with a trend towards Na-HCO_3 in the more confined Folkestone Beds (Shand et al., 2003). The Hythe Beds are generally low in Mg, Na and K. Bicarbonate is present in small quantities in the unconfined aquifer, likely due to calcite dissolution, and in larger quantities in the deeper confined section (Morgan-Jones, 1985). Groundwater within the Folkestone Beds contains a larger range of Ca concentrations, although this along with bicarbonate is low in the deeper and shallow sections, with some higher values in the eastern part of the aquifer, are likely due to local variations in mineralogy. Na and K are naturally low, except for areas affected by human activity (Morgan-Jones, 1985). In the deeper aquifer, increased Na and Cl concentrations are likely due to mixing with older more saline water (Morgan-Jones, 1985). Shand et al (2003) investigated variations along the groundwater flow

path and observed that temperature and SEC increase and Eh and DO decrease. The concentration of Ca continuously increases in the Hythe Beds whereas the Folkestone Beds retain a low Ca. The confined Folkestone Beds contain higher Na, Cl and K concentrations, whereas the confined Hythe Beds possess the lowest concentrations of these elements. Where the aquifers become confined, there is a decrease in NO_3 and an increase in Fe.

Methane concentrations in the LGS were previously measured by Darling and Gooddy (2006) and reported to range from <0.05 to 22 µg L^{-1} .

5.3 Results

Results are summarised in Tables 5.1 and 5.2.

5.3.1 Geochemistry and redox conditions

Piper plots using BGS data from 2013 are presented in Figure 5.3 and are broadly similar to results from Morgan-Jones (1985) and Shand et al. (2003). The sites within the unconfined section (Hythe Formation and Woburn Sands) of the aquifer contain Ca-HCO_3 type waters, while sites in the more confined sections (Folkestone Formation and undifferentiated sections) of the aquifer contain Na-HCO_3 type waters. Concentration of Na increases with depth and there is a general decrease in Ca (Fig. 5.4h and Fig. 5.4i). Deeper sites also contain a slightly higher concentration of Cl (Fig. 5.3).

The groundwater temperature follows a geothermal gradient of 26.5°C/km (Fig. 5.4a) exhibiting no major temperature anomalies with the exception of two boreholes in the Woburn Sands that are 1-2°C warmer than expected.

Redox conditions in the LGS are partially dependent on aquifer depth (Fig. 5.4). Eh decreases with depth and a stronger relationship between Eh and depth is evident at the deeper sites (>300 m), whereas the shallower sites (<200 m) exhibit a greater degree of variability. At depths <200 m, there are a large range of values of DO, Mn, Fe, H_2 and CH_4, and there is little correlation between these variables and depth. In the deep boreholes (>300 m), Eh, DO, Mn, Fe and H_2 decrease with depth and CH_4 increases with depth. There is a clear negative correlation between Eh and CH_4 (Fig. 5.5) with CH_4 increasing with decreasing Eh.

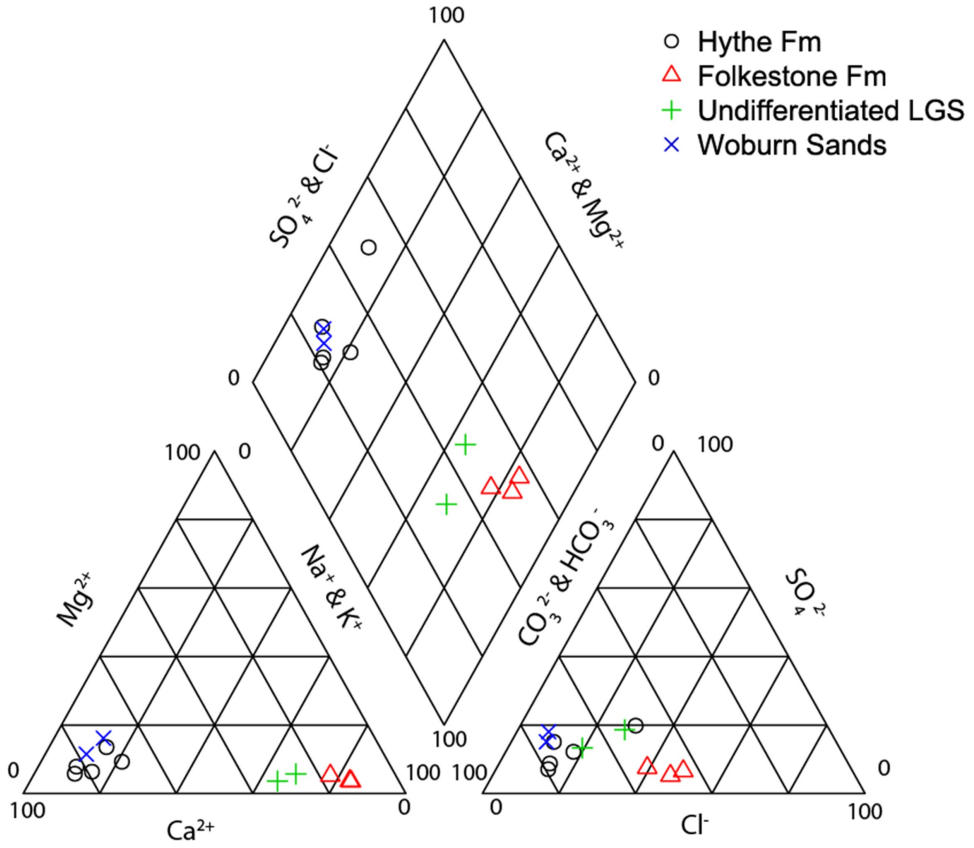

Figure 5.3 Piper plot of water geochemistry sampled from the Lower Greensand sites. Shallow sites in the unconfined part of the aquifer (Hythe Formation and Woburn sands) contain predominantly Ca-type waters whereas the deeper sites in the more unconfined part of the aquifer (Folkestone Formation and undifferentiated sections) contain predominantly Na-.

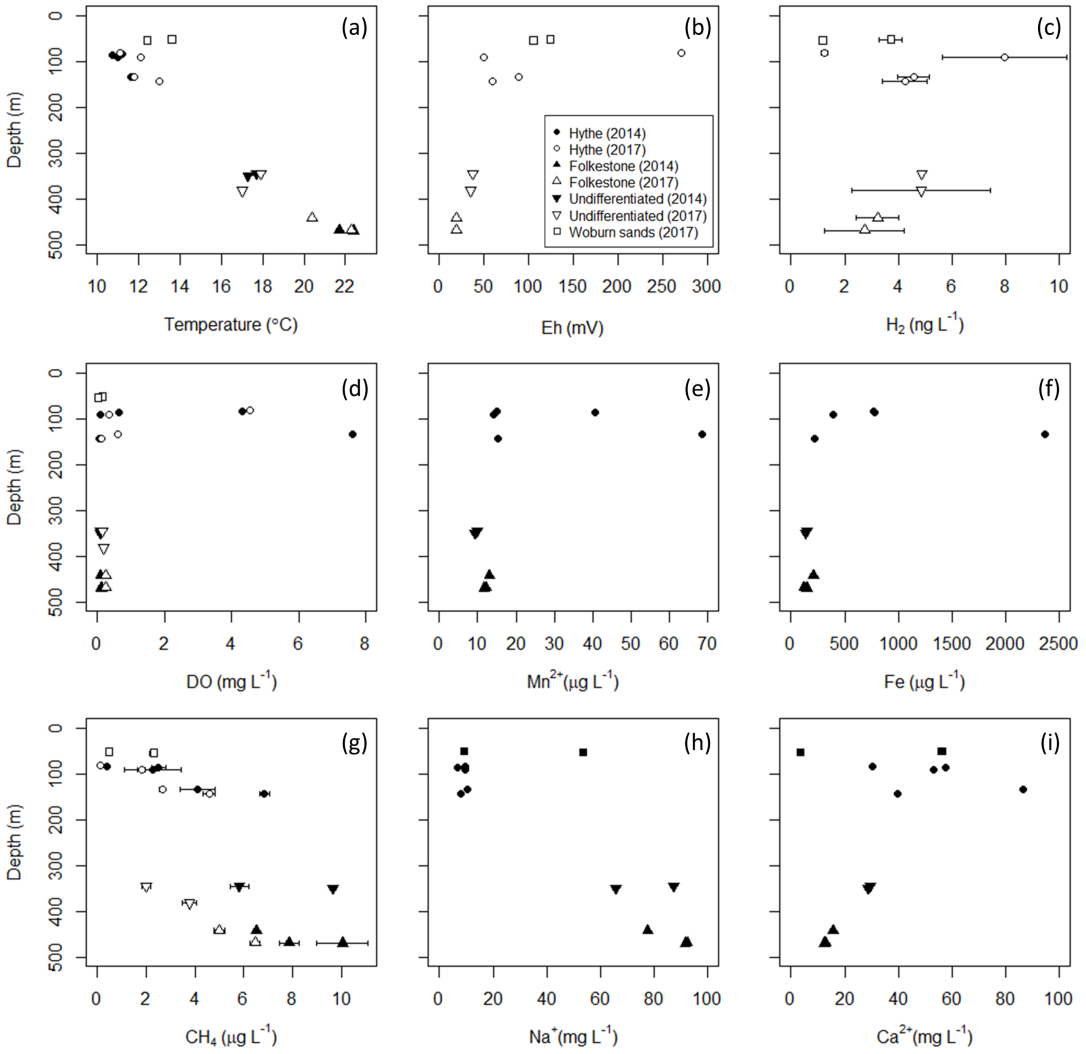

Figure 5.4 Variation of geochemistry, redox conditions and methane with depth in Lower Greensand study sites. Plots are depth versus (a) temperature, (b) Eh, (c) H_2, (d) O_2, (e) Mn, (f) Fe, (g) CH_4, (h) Na, and (i) Ca. Cation and anion data were provided by the British Geological survey from site sampled in 2013 (panels e, f, h and i). Temperature increases evenly along a geothermal gradient and conditions become more reducing with depth as demonstrated by decreasing Eh, DO, Mn, Fe and increasing CH_4 and H_2. Increasing Na and decreasing Ca with depth indicates the change from predominantly Ca-HCO_3 waters to predominantly Na-HCO_3 waters.

Table 5.1 Lower Greensands borehole site details and geochemical data[a]

Site	Sub Formation	E	N	Depth (m)	Ca^{2+} (mg L^{-1})	Mg^{2+} (mg L^{-1})	Na^{+} (mg L^{-1})	K^{+} (mg L^{-1})	Cl^{-} (mg L^{-1})	SO_4^{2-} (mg L^{-1})	NO_3- (mg L^{-1})	Mn (µg L^{-1})	Fe (µg L^{-1})	Cr (µg L^{-1})	DOC (mg L^{-1})
OK	Hythe	476	135	135	39.7	4.56	7.8	2.98	12.1	8.52	0.435	15.2	222	<0.05	-
BN	Hythe	484	145	109	86.6	5.02	10.6	2.55	20.1	36.9	0.025	68.6	2370	<0.05	0.78
TL	Hythe	487	143	52	53.0	2.60	9.7	2.88	14.7	13.2	0.035	14.1	390	<0.05	0.48
NM	Hythe	507	147	78	30.5	2.47	9.6	1.77	19.1	17.8	21.1	15	768	0.08	0.24
MH	Hythe	493	141	80	57.8	2.43	6.7	2.89	21.0	18.7	0.139	40.5	783	0.57	0.9
MP	Woburn sands	514	236	73	56.4	7.80	9.4	4.00	12.5	27.8	<0.1	-	-	-	-
NS	Woburn sands	521	241	56	103.7	9.30	14.3	3.60	18.3	53.9	<0.1	-	-	-	-
TG	Folkestone	487	148	74	15.6	2.92	77.7	6.06	58.8	15.3	<0.02	13.1	208	<0.05	0.44
BH	Folkestone	486	149	72	12.8	2.25	92.4	5.82	85.4	15.5	<0.02	12.2	123	<0.05	0
TM	Folkestone	488	149	72	12.4	2.14	91.6	5.85	86.3	13.2	<0.02	11.7	148	<0.05	0.44
SHP	undifferentiated	494	181	34	28.8	2.00	65.8	2.62	73.5	66.6	0.288	9.3	134	<0.05	0.43
HL	undifferentiated	497	180	28	29.6	3.99	87.2	4.43	39.0	36.2	0.222	9.9	147	1.14	0.88

[a]Unpublished geochemical data provided by British Geological Survey from field campaigns in 2013.

Table 5.2 Lower Greensand data

Site	Sample date	T (°C)	pH	SEC (µS cm^{-1})	DO (mg L^{-1})	Eh (mV)	HCO_3^- (mg L^{-1})	H_2 (µg L^{-1})	CH_4 (µg L^{-1})	$\delta^{13}C$ (CH_4) (‰)	δ^2H (CH_4) (‰)	Range (‰)	$\delta^{13}C$ (DIC) (‰)	Range (‰)	δ^2H (H_2O) (‰)	$\delta^{18}O$ (H_2O) (‰)
OK	22/07/2014	13.0	8.05	260	0.07		-	-	6.9 ±0.21	-69.5 ±1.04	-		-16.3	-16.3 to -16.2	-	-
	21/08/2017	13.0	7.86	249	0.13	59	120	4.2 ±0.83	4.6 ±0.26	-61.7 ±2.69	-38	-39 to -38	-15.3	-	-39.1	-6.0
BN	22/07/2014	11.6	7.10	491	7.61		245[a]	-	4.1 ±0.73	-32.3 ±0.10	-		-12.6	-12.9 to -12.4	-	-
	09/08/2017	11.8	7.38	484	0.61	89	229	4.6 ±0.60	2.7 ±0.10	-34.3 ±1.54	114	109 to 121	-11.5	-	-44.9	-6.8
TL	23/07/2014	11.0	7.52	324	0.10		149[a]	-	2.3 ±1.15	-55.2 ±0.09	-		-12.0	-12.2 to -11.9	-	-
	09/08/2017	12.1	7.72	302	0.35	50	149[a]	8.0 ±2.32	1.8 ±0.16	-55.0 ±0.89	-136	-140 to -130	-11.2	-	-45.5	-6.9
NM	14/10/2014	11.2	5.25	237	4.30		71[b]	-	0.4 ±0.06	-33.0 ±0.54	-		-14.9	-15.1 to -14.7	-	-
	20/09/2017	11.1	6.77	343	4.53	270	130	1.3 ±0.12	0.1 ±0.01	-	-		-13.1	-13.1 to -12.9	-46.2	-7.0
MH	22/10/2014	10.7	6.76	303	0.64		60[b]	-	2.5 ±0.29	-29.3 ±0.16	-		-12.8	-	-46.4	-7.0
MP	17/07/2017	13.6	7.02	338	0.15	124	177	3.7 ±0.43	0.5 ±0.03	-61.8 ±2.38	-		-13.2	-13.3 to -13.1	-49.4	-7.3
NS	17/07/2017	12.4	7.19	598	0.02	105	279	1.2 ±0.02	2.3 ±0.15	-50.8 ±1.39	-103	-103 to -102	-12.2	-	-49.1	-7.3
TG	23/07/2014	20.4	7.87	464	0.10		172[a]	-	6.5 ±0.03	-57.6 ±0.72	-		-16.0	-16.1 to -15.9	-	-
	05/10/2017	20.4	7.79	463	0.25	19	136	3.2 ±0.79	5.0 ±0.22	-53.5 ±3.14	-118	-119 to -117	-15.3	-15.3 to -15.2	-51.6	-7.7
BH	24/07/2014	21.7	7.91	544	0.13		162[b]	-	7.8 ±0.41	-49.8 ±3.09	-		-16.0	-16.2 to -15.9	-	-
	05/10/2017	22.3	7.91	543	0.25	19	131	2.7 ±1.48	6.5 ±0.20	-54.3 ±0.45	-91	-94 to -89	-15.5	-15.5 to -15.4	-50.3	-7.5
TM	24/07/2014	22.4	7.87	451	0.13		154[a]	-	10.0 ±1.06	-50.9 ±0.10	-		-16.2	-16.4 to -15.7	-49.2	-7.4
SHP	25/07/2014	17.3	7.89	673	0.08		226[b]	-	9.7 ±0.14	-58.4 ±0.54	-		-11.1	-11.3 to -10.9	-	-
	24/05/2017	17.0	7.92	738	0.19	35	241	4.8 ±2.57	3.8 ±0.29	-56.7 ±1.43	-183	-183 to -182	-10.4	-	-54.3	-8.0
HL	25/07/2014	17.7	7.82	549	0.08		244[b]	4.9 ±1.22	5.8 ±0.38	-50.0 ±0.52	-		-11.7	-11.7 to -11.6	-	-
	25/07/2017	17.9	7.88	560	0.16	37	230	-	2.0 ±0.19	-48.2 ±1.62	-150	-159 to -145	-11.1	-11.2 to -11.1	-55.5	-8.2

[a]HCO_3^- concentration data collected during British Geological Survey field campaigns in 2011.

[b]HCO_3^- concentration data collected during British Geological Survey field campaigns in 2013.

Table 5.3 Calculated values of dissolved inorganic carbon (DIC) concentration and $\delta^{13}C(CO_2)$.

					Calculated values			
Site	Sample date	HCO_3^- (mg L^{-1})	pH	$\delta^{13}C$(DIC) (‰)	DIC (mg L^{-1})	$CO_{2\ aq}$ (mg L^{-1})	$CO_{2\ g}$ (‰)	$\delta^{13}C(CO_2)$ (‰)
OK	22/07/2014	-	8.05	-16.3	-	-	-	-
	21/08/2017	120	7.86	-15.3	125	4.7	0.01	-24.2
BN	22/07/2014	245[a]	7.10	-12.6	302	56.5	0.05	-20.0
	09/08/2017	229	7.38	-11.5	256	27.5	0.07	-19.8
TL	23/07/2014	149[a]	7.52	-12.0	163	13.3	0.06	-20.7
	09/08/2017	149[a]	7.72	-11.2	158	8.2	0.03	-20.0
NM	14/10/2014	71[b]	5.25	-14.9	1245	1174	0.77	-14.4
	20/09/2017	130	6.77	-13.1	195	64.8	1.38	-19.0
MH	22/10/2014	60[b]	6.76	-12.8	90	30.7	0.21	-18.8
MP	17/07/2017	177	7.02	-13.2	224	47.0	0.10	-20.2
NS	17/07/2017	279	7.19	-12.2	330	51.3	0.18	-20.0
TG	23/07/2014	172[a]	7.87	-16.0	178	5.7	0.00	-24.1
	05/10/2017	136	7.79	-15.3	142	5.4	0.01	-23.3
BH	24/07/2014	162[b]	7.91	-16.0	167	4.7	0.00	-24.0
	05/10/2017	131	7.91	-15.5	135	3.8	0.00	-23.4
TM	24/07/2014	154[a]	7.87	-16.2	159	4.9	0.00	-24.1
SHP	25/07/2014	226[b]	7.89	-11.1	234	7.5	0.01	-19.6
	24/05/2017	241	7.92	-10.4	249	7.5	0.01	-18.9
HL	25/07/2014	244[b]	7.82	-11.7	254	9.5	0.01	-20.0
	25/07/2017	230	7.88	-11.1	239	7.8	0.01	-19.5

[a]BGS field campaign 2011. [b]BGS Field campaign 2013.

5.3.2 Methane isotope variability

With decreasing Eh, CH_4 concentration increases (Fig. 5.5a) while $\delta^{13}C(CH_4)$ and $\delta^2H(CH_4)$ values generally decrease (Fig. 5.5b and c) with the exception of the MP borehole in the Woburn Sands where there is high Eh, low CH_4 concentration but very negative $\delta^{13}C(CH_4)$. For shallow sites (<200 m), there are wide ranges in both $\delta^{13}C(CH_4)$ and $\delta^2H(CH_4)$ values of -69.5 to -29.3 ‰ and -136 to +114 ‰, respectively. In deeper sites (>300 m), there is a much narrower range of $\delta^{13}C(CH_4)$ and $\delta^2H(CH_4)$ values; -57.6 to -48.2 ‰ and -150 to -91 ‰, respectively (Fig. 5.6a and b). Where DO concentrations are higher (Fig. 5.6e and f), $\delta^{13}C(CH_4)$ values are more positive whereas lower concentrations of DO generally are associated with more negative and more variable $\delta^{13}C(CH_4)$ values. The $\delta^{13}C(CH_4)$ and $\delta^2H(CH_4)$ values also vary widely with respect to CH_4 concentration (Fig. 5.6c and d) with the largest ranges of isotope composition occurring typically at the lowest concentration sites.

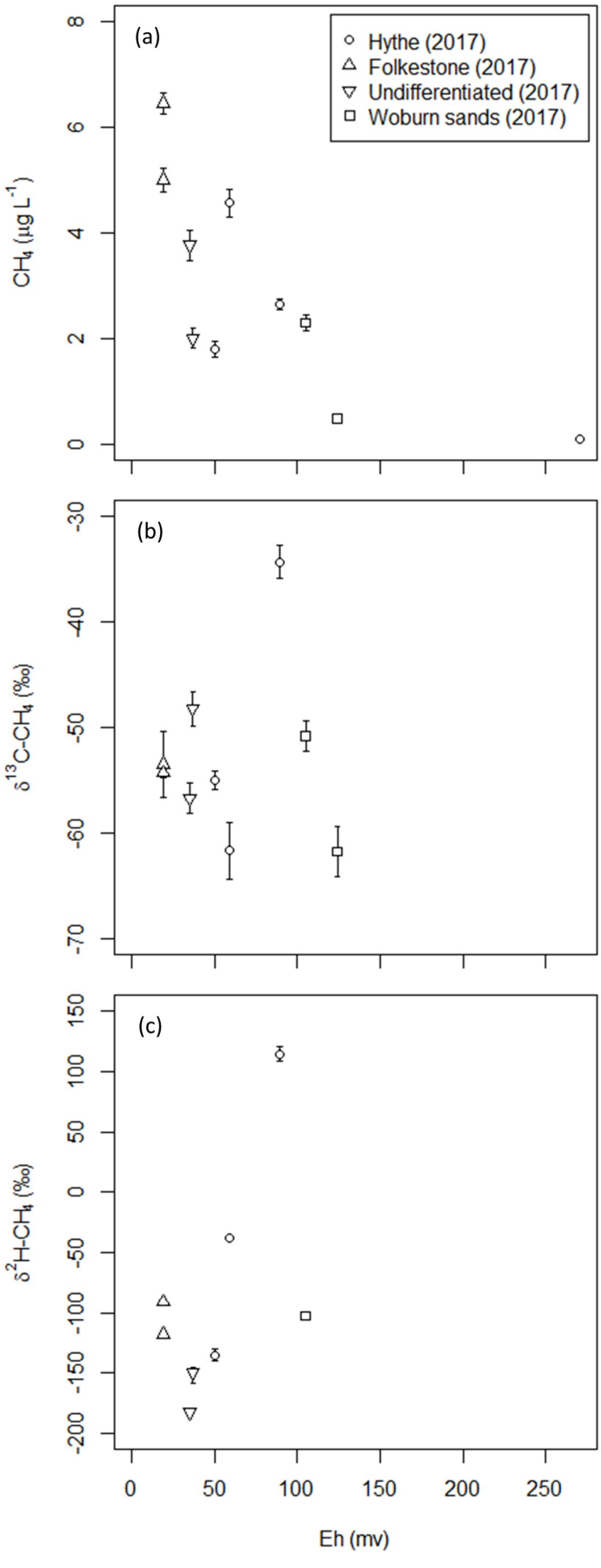

Figure 5.5 Relationships between (a) Eh and CH_4 concentration, (b) Eh and $\delta^{13}C(CH_4)$ values, and (c) Eh and $\delta^{2}H(CH_4)$ values. The concentration of CH_4 increases with decreasing Eh. A correlation with $\delta^{13}C(CH_4)$ is less clear. $\delta^{2}H(CH_4)$ values appear to increase with increasing Eh.

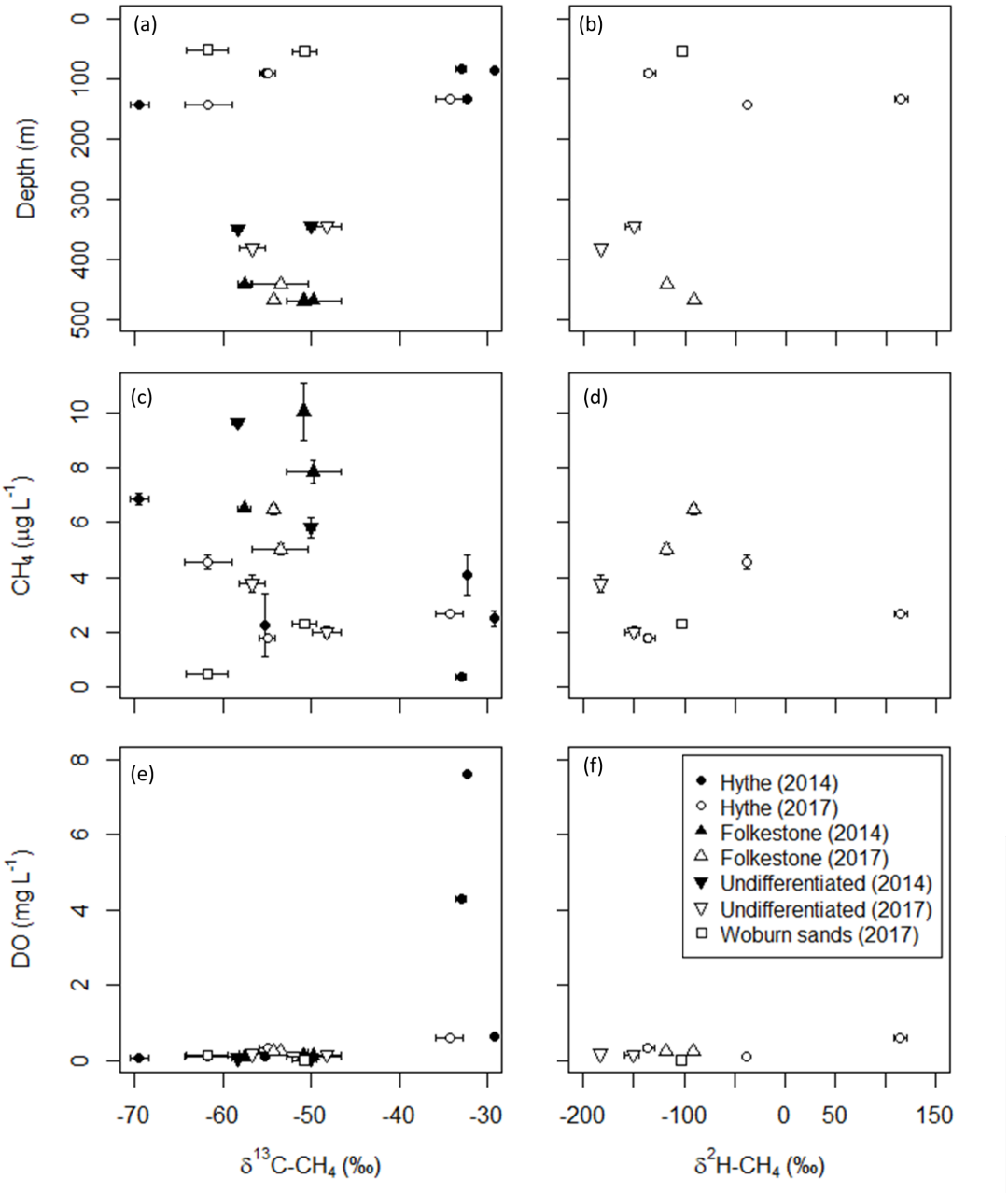

Figure 5.6 Plots show (a) depth vs $\delta^{13}C(CH_4)$; (b) depth vs $\delta^{2}H(CH_4)$; (c) CH_4 vs $\delta^{13}C(CH_4)$; (d) CH_4 vs $\delta^{2}H(CH_4)$; (e) dissolved O_2 (DO) vs $\delta^{13}C(CH_4)$; and (f) DO vs $\delta^{2}H(CH_4)$. Deep boreholes (>300 m) have narrow ranges of both $\delta^{13}C(CH_4)$ and $\delta^{2}H(CH_4)$ values whereas shallow sites (<200 m) exhibit a wide range of both $\delta^{13}C(CH_4)$ and $\delta^{2}H(CH_4)$ values. Low CH_4 concentration and high DO correlate with more negative $\delta^{13}C(CH_4)$ values.

5.3.3 Relationships between stable isotope compositions

The LGS $\delta^{18}O(H_2O)$ and $\delta^{2}H(H_2O)$ values plot closely to the global meteoric water line (Craig, 1961) (Fig. 5.7a). The differences in values between the deep

and shallow basin (Fig. 5.7b and c) are likely due to mixing with older, more ^{18}O and ^{2}H -depleted water at depth that entered the aquifer during cooler climatic times early in the Holocene. There is a positive correlation of $\delta^{13}C(CH_4)$ with $\delta^{2}H(CH_4)$ (Fig. 5.8a), though the correlation increases if considering only the shallow sites in the Hythe Beds and the Woburn Sands, whereas the deeper sites in the Folkestone Beds and the undifferentiated LGS form a tighter cluster. There is a positive correlation between $\delta^{2}H(CH_4)$ and $\delta^{2}H(H_2O)$ values (Fig. 5.8b), particularly in the deeper sites. Sites in the undifferentiated section, plot much closer the theoretical values for CH_4 formed via the CO_2 reduction methanogenic pathway (Whiticar et al., 1986). There is no clear relationship between $\delta^{13}C(CH_4)$ and $\delta^{13}C(DIC)$ values or $\delta^{13}C(CH_4)$ and $\delta^{13}C(CO_2)$ values (Fig. 5.6c and d), even when considering deep or shallow sites separately. In all cases it should be noted that the concentration of CO_2 is 3 to 5 orders of magnitude greater than that of CH_4, depending on the site.

The Gibbs free energy available for hydrogenotrophic methanogenesis in the LGS was calculated from the activity of reactant and products ($[HCO_3^-]$, $p[CH_4]$ and $p[H_2]$; (Conrad et al., 1986)) and compared to the apparent $\alpha_{CO_2\text{-}CH_4}$ values (Fig. 5.11) and a relationship between ΔG and $\alpha_{CO_2\text{-}CH_4}$ previously identified by Penning et al. (2005). All sites exhibited a smaller fractionation than predicted by the relationship from Penning et al. (2005).

5.3.4 Relationships between temperature and $\Delta^{2}H_{CH_4\text{-}H_2O}$ and $\Delta^{13}C_{CH_4\text{-}CO_2}$

Positive correlations exist between both $\Delta^{2}H_{CH_4\text{-}H_2O}$ and $\Delta^{13}C_{CH_4\text{-}CO_2}$ values and temperature for sites at depths >300 m (Fig. 5.10), indicating decreased fractionation during microbial methanogenesis for H and C isotopes with increasing temperature. There is a decrease in H and C fractionation with increasing temperature in the deeper Folkestone and undifferentiated sites but no correlation with temperature in the shallower sites (<200 m depth) in the Hythe Beds and the Woburn Sands, which also exhibit a much larger range of $\Delta^{2}H_{CH_4\text{-}H_2O}$ and $\Delta^{13}C_{CH_4\text{-}CO_2}$ values.

5.3.5 Oxidation models

The proportion of CH_4 that has been oxidised at each site can be determined if the initial stable isotope composition is known, as well as the C-isotope fractionation factor, and whether the system is open or closed. If the system is open then fractionation due to transport should also be considered (Eqs. 1.14 and 1.15 in

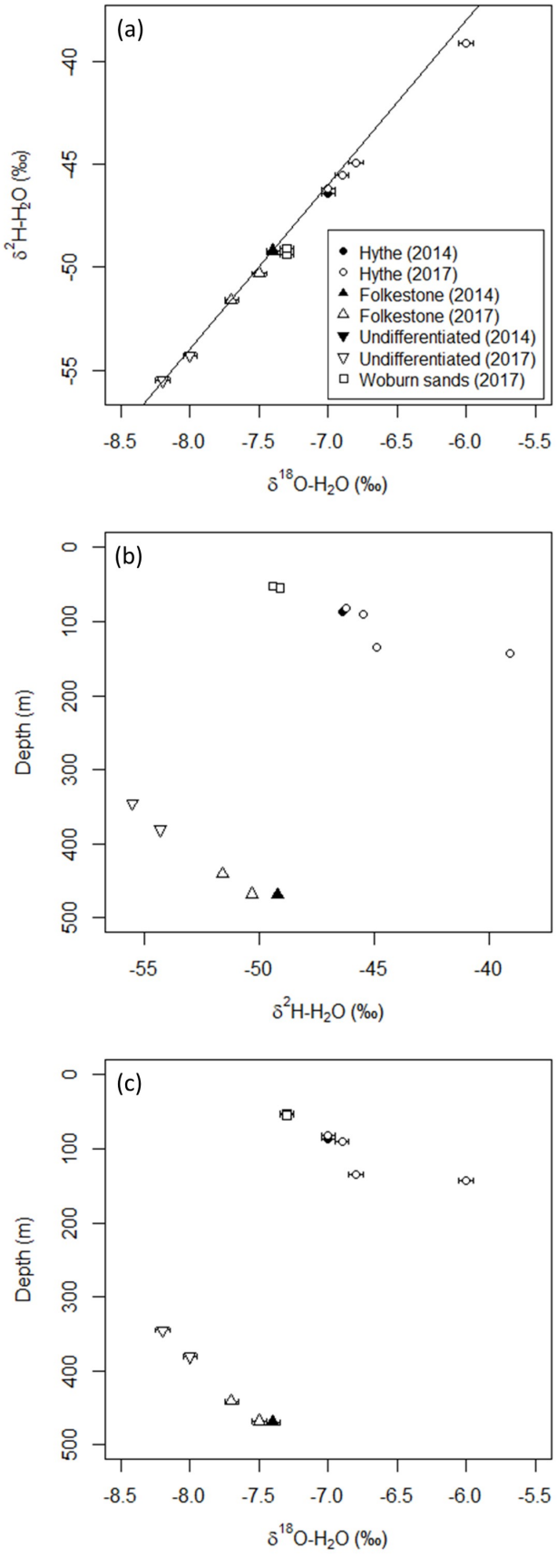

Figure 5.7 (a) $\delta^2H(H_2O)$ vs $\delta^{18}O(H_2O)$ from Lower Greensands boreholes and the global meteoric water line (solid line; Craig, 1961); and variation with depth of (b) $\delta^2H(H_2O)$, and (c) $\delta^{18}O(H_2O)$. Water from deeper boreholes has more negative $\delta^{18}O(H_2O)$ and $\delta^2H(H_2O)$ values, consistent with an older recharge age during periods when surface temperature was lower.

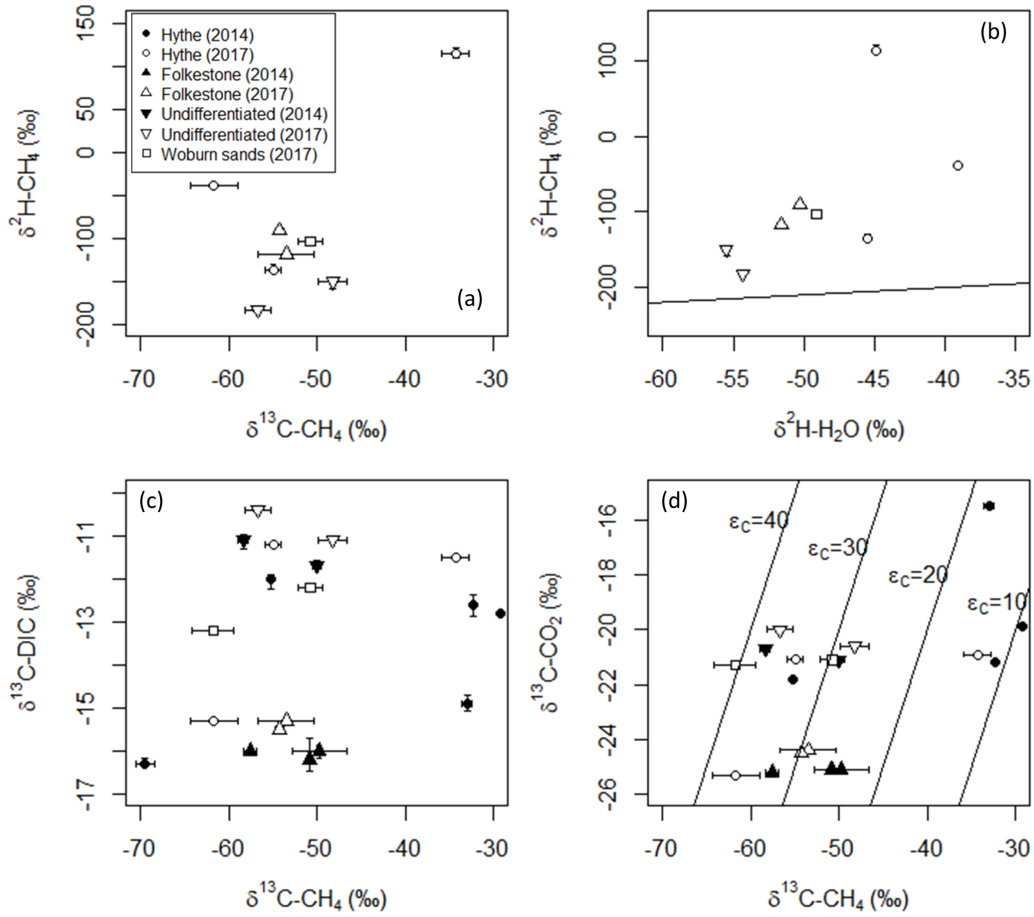

Figure 5.8 Relationships between the stable isotope compositions of CH_4 , DIC and $\delta^2H(H_2O)$ presented as (a) $\delta^2H(CH_4)$ versus $\delta^{13}C(CH_4)$ values; (b) $\delta^2H(CH_4)$ versus $\delta^2H(H_2O)$ values with the solid line representing the theoretical composition of CH_4 produced by CO_2 /H_2 methanogenesis (Whiticar et al., 1986); (c) $\delta^{13}C(DIC)$ versus $\delta^{13}C(CH_4)$ values; and (d) $\delta^{13}C(CO_2)$ versus $\delta^{13}C(CH_4)$ values with lines representing constant 13C fractionation. There is a positive correlation between $\delta^2H(CH_4)$ and $\delta^{13}C(CH_4)$ (panel a), in particular, for shallow wells and a positive correlation between $\delta^2H(CH_4)$ and $\delta^2H(H_2O)$ values. No clear relationship exists between $\delta^{13}C(DIC)$ (or $\delta^{13}C(CO_2)$) and $\delta^{13}C(CH_4)$ values (panel d).

Chapter 1). Carbon enrichment factors (ε_C) for CH_4 oxidation are typically ~22 ‰ but can range from 10 to 40 ‰ (Barker and Fritz, 1981; Chanton et al., 2008; Coleman et al., 1981; Liptay et al., 1998; Teh et al., 2006; Tyler et al., 1994). Enrichment factors for hydrogen (ε_H) are generally ~8 to 13 times greater than ε_C, ranging from 100 to 325 ‰ (Coleman et al., 1981).

To determine an approximate fraction of CH_4 that has been oxidised (Fox), $\delta^{13}C(CH_4)$ from the OK site sampled in 2014 was used as an initial value. This site was selected due to the value of $\delta^{13}C(CH_4)$ (-69.5 ‰), which is lower than all other visited sites, as well as lower compared to the second visit to the same

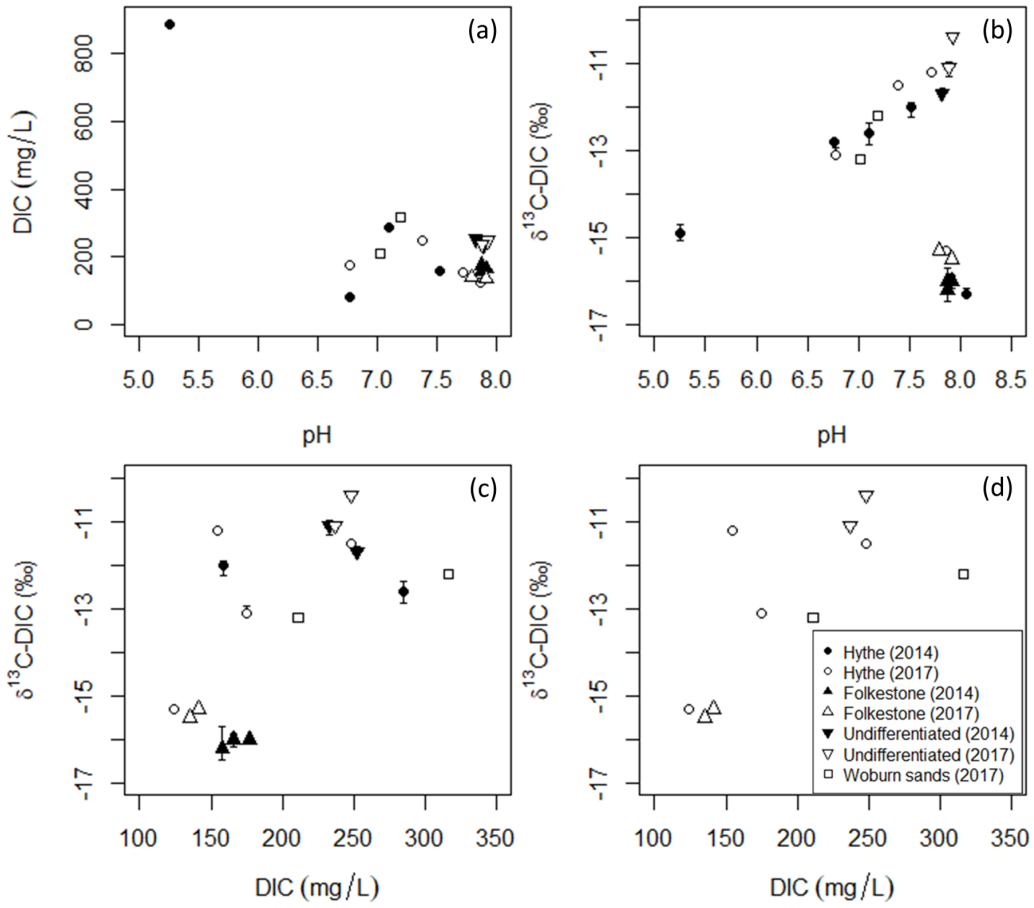

Figure 5.9 Relationships between pH, DIC and $\delta^{13}C$(DIC) values: (a) DIC versus pH, (b) $\delta^{13}C$(DIC) values versus pH, and (c) and (d) showing $\delta^{13}C$(DIC) versus DIC with (c) containing additional data points calculated using BGS legacy HCO_3^- concentration data, which are omitted in (d) (details in Table 5.3). The BGS data also are included in panel (a). There is a positive correlation between $\delta^{13}C$(DIC) values and DIC, indicating a possible dependence on carbonate mineral dissolution. The range of observed $\delta^{13}C$(DIC) values is consistent with formation of DIC from carbonate rock dissolution.

site in 2017 (-61.7 ‰) and is therefore most likely closest to a 'pristine' value, i.e. isotopic composition of CH_4 produced in situ and unaffected by post-prodcution processes, such as oxidation or transportation. While some oxidation may have taken place, the low $\delta^{13}C(CH_4)$ indicates that this is likely minimal. Fractionation factors due to CH_4 oxidation (α_{ox}) of 1.022, 1.010 and 1.040 were used as the expected value and possible range as reported in the literature (Chanton et al., 2008; Coleman et al., 1981; Tyler et al., 1994). Both open and closed system scenarios were modelled. For the open system three α_{ox} values of 1.022, 1.010 and 1.040 were used with an assumed α_{trans} of 1. A fourth model also was used with

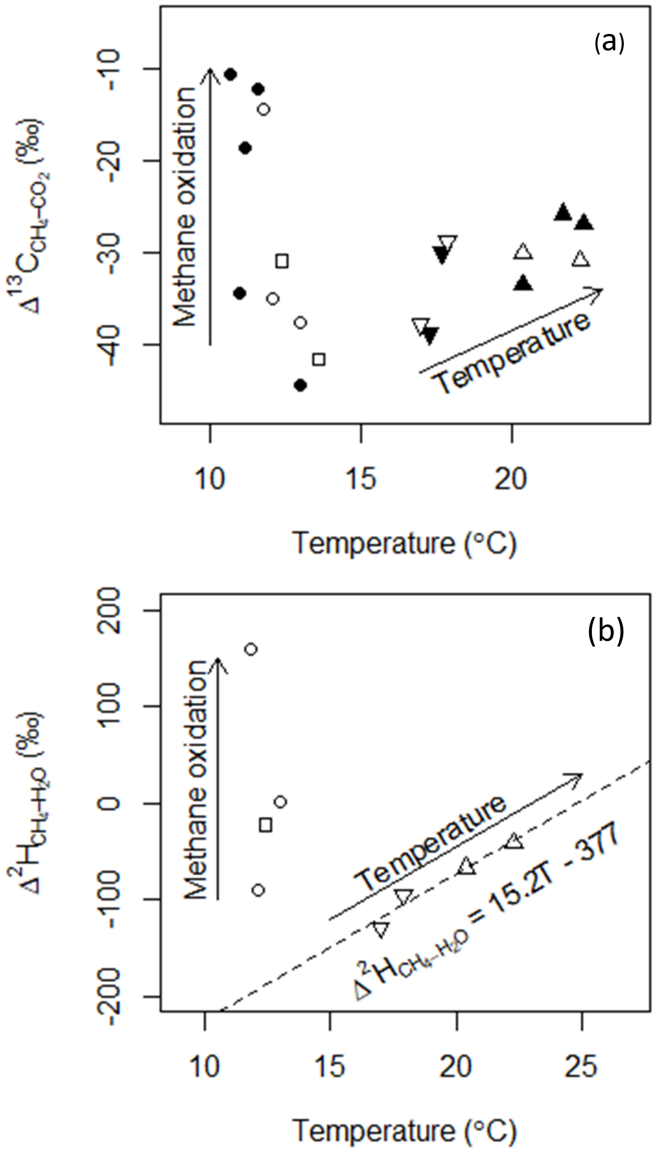

Figure 5.10 Relationship between temperature and stable carbon and hydrogen isotope fractionation. (a) $\Delta^{13}C_{CH_4\text{-}CO_2}$ versus temperature, and (b) $\Delta^2H_{CH_4\text{-}H_2O}$ versus temperature. The deeper sites (Folkestone and Undifferentiated) exhibit a positive correlation between both $\Delta^{13}C_{CH_4\text{-}CO_2}$ and $\Delta^2H_{CH_4\text{-}H_2O}$ with temperature. The shallower sites show a large range of $\Delta^{13}C_{CH_4\text{-}CO_2}$ and $\Delta^2H_{CH_4\text{-}H_2O}$ values over a small range of temperature and no correlation, suggesting that CH_4 oxidation processes strongly impact the stable isotope compositions of CH_4 within the open part of the aquifer (<200 m). Less altered CH_4 at depth (>300 m) appears to retain evidence of a temperature dependence imparted by microbial methanogenesis.

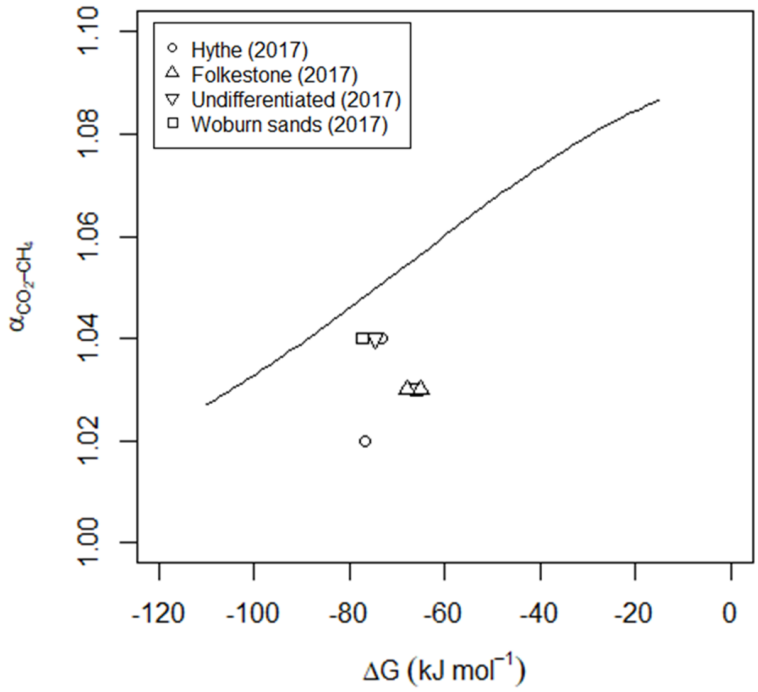

Figure 5.11 Apparent $\alpha_{CO_2\text{-}CH_4}$ and Gibbs free energy (ΔG). The solid line is the relationship between $\alpha_{CO_2\text{-}CH_4}$ and Δ G predicted for hydrogenotrophic methanogenesis according to Penning et al. (2005). All sites plot below the theoretical line suggesting that a portion of CH_4 has been oxidized by bacterial methanotrophy or it contains a component of CH_4 from the acetoclastic methanogenic pathway.

α_{ox} of 1.022 and an α_{trans} of 1.014, the theoretical maximum value (De Visscher et al., 2004), in order to explore the potential effect of isotope fractionation due to diffusion of CH_4 through the aquifer (Table 5.4 and Fig. 5.12). Fewer $\delta^2H(CH_4)$ data were available, and it was only possible to carry out modelling for one site, for which the range of α_{ox} values used were 1.1, 1.2 and 1.3, similar to those reported in the literature (Coleman et al., 1981).

Table 5.4 Estimated fraction of CH_4 oxidised at sites in the Hythe Formation.

	^{13}C-CH_4						^{2}H-CH_4				
Site	δA (‰)	δE (‰)	α_{ox}	α_{trans}	F_{ox} closed	F_{ox} open	δA (‰)	δE (‰)	α_{ox}	F_{ox} closed	F_{ox} open
OK - 2014	-69.5	-69.5	1.022	1	0	0					
OK - 2017	-69.5	-61.7	1.022	1	0.32	0.35					
	-69.5	-61.7	1.01	1	0.57	0.78					
	-69.5	-61.7	1.04	1	0.19	0.2					
	-69.5	-61.7	1.022	1.014	-	0.97					
BN - 2014	-69.5	-32.3	1.022	1	0.83	1.69	-38	114	1.1	0.77	1.52
	-69.5	-32.3	1.01	1	0.98	3.72	-38	114	1.2	0.52	0.76
	-69.5	-32.3	1.04	1	0.62	0.93	-38	114	1.3	0.39	0.51
	-69.5	-32.3	1.022	1.014	-	4.65					
BN - 2017	-69.5	-34.3	1.022	1	0.82	1.6					
	-69.5	-34.3	1.01	1	0.98	3.52					
	-69.5	-34.3	1.04	1	0.6	0.88					

Table 5.4 continued

Site	^{13}C-CH_4 δA (‰)	δE (‰)	α_{ox}	α_{trans}	F_{ox} closed	F_{ox} open	^{2}H-CH_4 δA (‰)	δE (‰)	α_{ox}	F_{ox} closed	F_{ox} open
	-69.5	-34.3	1.022	1.014	-	4.4					
TL - 2014	-69.5	-55.2	1.022	1	0.5	0.65					
	-69.5	-55.2	1.01	1	0.78	1.43					
	-69.5	-55.2	1.04	1	0.32	0.36					
	-69.5	-55.2	1.022	1.014	-	1.79					
TL - 2017	-69.5	-55	1.022	1	0.5	0.66					
	-69.5	-55	1.01	1	0.79	1.45					
	-69.5	-55	1.04	1	0.32	0.36					
	-69.5	-55	1.022	1.014	-	1.81					
NM - 2014	-69.5	-33	1.022	1	0.83	1.66					
	-69.5	-33	1.01	1	0.98	3.65					
	-69.5	-33	1.04	1	0.62	0.91					
	-69.5	-33	1.022	1.014	-	4.56					
MH - 2014	-69.5	-29.3	1.022	1	0.85	1.83					
	-69.5	-29.3	1.01	1	0.99	4.02					
	-69.5	-29.3	1.04	1	0.65	1.01					
	-69.5	-29.3	1.022	1.014	-	5.03					

δA = initial $\delta^{13}C(CH_4)$.
δE = final $\delta^{13}C(CH_4)$.
α_{ox} = fractionation factor for CH_4 oxidation.
α_{trans} = fractionation factor for CH_4 transport.
F_{ox} – fraction of CH_4 oxidised.

5.4 Discussion

5.4.1 Relations between CH_4 and groundwater geochemistry

Methane production rates are typically greater under anoxic reducing conditions (Schimel et al., 1993), in areas with high substrate availability (Bergman et al., 1998). Substrates for methanogenesis are formed from C within the available DIC and DOC pools; DIC is relatively high across the aquifer, with the majority as HCO_3^- and a proportion of CO_2 (Table 5.3). Reducing conditions exist mainly in the deeper parts of the aquifer, i.e. at sites within the Folkestone and undifferentiated LGS. The deeper and more confined section of the aquifer is geochemically distinct from the shallower, unconfined parts. The waters are older and the $\delta^{18}O(H_2O)$ and $\delta^{2}H(H_2O)$ values are more negative, which is indicative of meteoric water recharged under cooler conditions, likely during the last glacial period as previously postulated by Darling et al. (1997). Ion exchange between Na and Ca has had time to take place (Figs 5.3, 5.4g and 5.4h), and there is a transition from Ca-HCO_3 type waters to Na-HCO_3 type waters with depth.

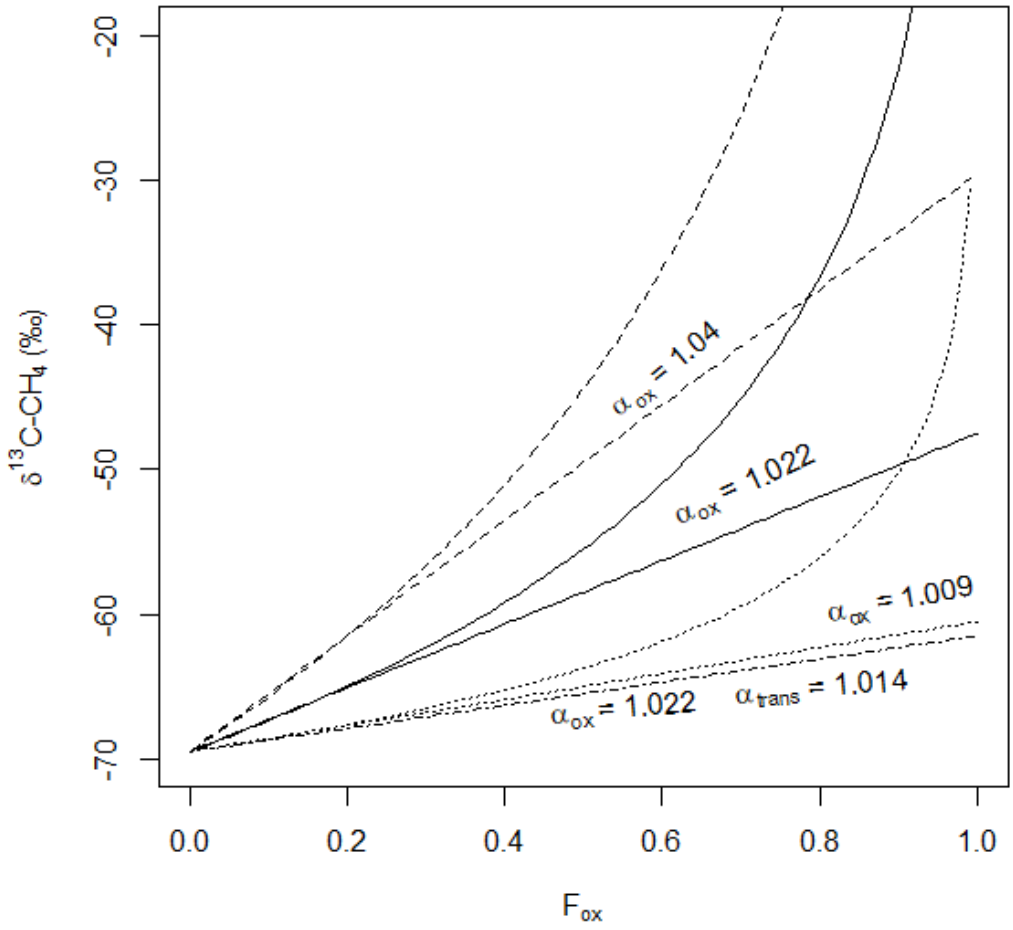

Figure 5.12 Methane oxidation models show $\delta^{13}C$ compositional pathways for CH_4 residuals associated with different fractionation factors for methanotrophy (solid line, $\alpha_{ox} = 1.022$; dashed line, $\alpha_{ox} = 1.04$; dotted line, $\alpha_{ox} = 1.009$; dot-dash line, $\alpha_{ox} = 1.022$ and $\alpha_{trans} = 1.014$). Straight and curved lines represent open and closed system models, respectively.

There is also a slight increase in Cl, which could be due to some mixing with deeper saline waters, which is consistent with previous studies (Morgan-Jones, 1985; Shand et al., 2003). Therefore, deeper waters with low Eh, low DO and other redox dependent species, such as Fe and Mn, decreasing Ca and increasing Na, coincide with CH_4 production or at least CH_4 preservation.

In the shallower part of the aquifer, CH_4 concentration is much more variable likely due to a large Eh range and combination of CH_4 production and oxidation. Sites with high DO correlate with low CH_4, though sites with low DO concentration host a range of CH_4 concentrations. Overall, Eh appears to be a better predictor of CH_4 concentration than DO (Fig. 5). As depth increases,

conditions become more reducing, leading to a decrease in DO and an increase in CH_4 production. Higher concentrations of DO generally coincide with lower concentrations of CH_4, however with low concentrations of DO, again a range of CH_4 can occur similar to conditions at shallower depths in the aquifer.

5.4.2 Formation processes in the aquifer

5.4.2.1 Origins of dissolved inorganic carbon

Dissolved inorganic carbon (DIC) can originate from respiration of organic matter in soil in recharge areas or within the aquifer, and from carbonate dissolution in the aquifer. The LGS is a sandstone aquifer, which is known to contain a calcareous cement (Hopson et al., 2008). Soil CO_2 generally has a $\delta^{13}C$ of $\sim$ -26 ‰ whereas marine-derived carbonate generally has a $\delta^{13}C$ $\sim$0 ‰, though this can vary by a few per mil depending on the conditions of formation (Clark and Fritz, 1997). Stoichiometric dissolution of rock carbonate by soil CO_2 would produce a DIC value of $\sim$13 ‰; however, this value can be modified under open-system conditions by re-equilibration with soil CO_2 to give more negative $\delta^{13}C$ values, or under closed-system conditions by dissolution-reprecipitation to yield more positive $\delta^{13}C$ values. In the LGS $\delta^{13}C$(DIC) values increase with increasing DIC concentration, with the range of $\delta^{13}C$(DIC) values of -16.3 to -10.4 ‰ consistent with a transition from unconfined to confined conditions in the aquifer (Fig. 5.9).

5.4.2.2 Methane formation

Methane can be formed by acetogenic or hydrogenotrophic methanogenesis depending on methanogen population and substrate availability (Conrad, 2005). While there is some dissolved organic carbon (DOC) within the aquifer (Table 5.1), there is no correlation with CH_4 or stable isotope composition of CH_4. The DOC is likely indicative of an older carbon source, not an influx of labile organic matter, which would enable acetogenic methanogenesis. $\Delta^{13}C_{CH_4\text{-}CO_2}$ values for more reducing sites (lower Eh) where CH_4 oxidation is likely to be minimal (Figs. 5.6d and 5.8a) correspond to enrichment factors (ε_C) ranging from -25.8 to -41.6 ‰. The ε_C for hydrogenotrophic methanogenesis range from -25 ‰ (Games et al., 1978) to -80 ‰ (Holmes et al., 2014) though typically has a value of approximately -70 ‰ (Conrad et al., 2011). The highest values often occur under higher H_2 availability and therefore increased energetic conditions and higher pathway reversibility (Valentine et al., 2004). The ^{13}C fractionation can then be related to energetic conditions and ΔG (Penning et al., 2005) and for the energy available in this system, an $\varepsilon_C \sim$ -50 ‰ would be expected, which

is close to the largest fractionations observed in the LGS (Fig. 11). Enrichment factors for acetoclastic methanogenesis range from -7 to -35 ‰, but generally lie between -10 and -20 ‰ (Goevert and Conrad, 2009; Krzycki et al., 1987; Londry et al., 2008; Penning et al., 2006; Valentine et al., 2004). There also appears to be a relationship between $\delta^2H(CH_4)$ and $\delta^2H(H_2O)$, especially for the deeper sites, which plot fairly close to theoretical values for CH_4 production by hydrogenotrophic methanogenesis (Fig. 5.6b) (Whiticar et al., 1986). Theoretical values for acetoclastic methanogenesis plot too far below the scale of the graph and are not shown.

The apparent lack of labile organic matter indicates hydrogenotrophic methanogenesis to be the more likely microbial pathway for CH_4 formation. However, enrichment factors for LGS sites with a presumed low amount of CH_4 oxidation (sites with low Eh and relatively high CH_4) fall within the lower range, i.e. small fractionation, for hydrogenotrophic methanogenesis, and potentially for some sites on the higher end for acetoclastic methanogenesis.

The possibilities are that there is a combination of hydrogenotrophic and acetoclastic methanogenesis, and that the DOC measured contains an element of labile organic matter. Hydrogenotrophic methanogenesis may be more favourable than would appear due to the presence of a H_2 gradient, i.e. methanogenesis takes place within microsites, where methanogens exist with syntrophic H_2-producing bacteria and so the H_2 concentration measured is not representative of the actual H_2 availability for methanogenesis. Alternately, there may have been a greater amount of CH_4 oxidation within some sites in the confined section of the aquifer.

There is no clear relationship between $\delta^{13}C(CO_2)$ and $\delta^{13}C(CH_4)$ values (Fig. 5.8d) for either shallow or deep sites, which would be expected; however, when considering the fractionation between $\delta^{13}C(CO_2)$ and $\delta^{13}C(CH_4)$, a correlation with temperature is observed, which is also present for $\delta^2H(CH_4)$ and $\delta^2H(H_2O)$ values (Fig. 5.10). For sites within the low temperature range (shallow and unconfined sites), there is a very large range in both $\Delta^2H_{CH_4\text{-}H_2O}$ and $\Delta^{13}C_{CH_4\text{-}CO_2}$ values, which is consistent with varying amounts of CH_4 oxidation. The temperature correlation observed may also be partly or predominantly due to bacterial CH_4 oxidation; however, it is also a possibility that it reflects differences in isotopic fractionation during CH_4 formation. For ^2H fractionation, the correlation is stronger and a linear regression yields the relationship of $\Delta^2H_{CH_4\text{-}H_2O} = 15.2T - 377$.

5.4.2.3 Methane oxidation

The shallow unconfined aquifer has a large range of $\delta^{13}C(CH_4)$ and $\delta^{2}H(CH_4)$ values, for which there is a positive correlation (Fig. 5.8a). The relationship is even stronger when considering only the shallow sites within the unconfined sections of the Woburn Sands and Hythe Beds. It is most likely due to CH_4 oxidation occurring post-formation whereby $\delta^{13}C(CH_4)$ and $\delta^{2}H(CH_4)$ values increase concurrently as a result of preferential consumption of ^{12}C and ^{1}H -bearing CH_4 by methanotrophic bacteria.

The largest fractionations for C and H occur at sites with the highest DO. As DO decreases, the strength of the correlation diminishes, i.e., there is either high DO and high fractionation, or low DO and low to medium but variable amounts of fractionation. The trend is likely due to $\delta^{13}C(CH_4)$ and $\delta^{2}H(CH_4)$ values being determined by the balance of the rate of CH_4 production (or CH_4 influx via transportation from the deeper aquifer) and the rate of CH_4 oxidation. It is also clear when considering C and H fractionations versus temperature (Fig. 10) where there is a large range of $\delta^{13}C(CH_4)$ and $\delta^{2}H(CH_4)$ values within the shallower sites at lower temperatures.

When considering carbon fractionation in relation to Gibbs free energy (Fig. 5.11), all sites exhibit a lower apparent $\alpha_{CO_2\text{-}CH_4}$ than might be expected. Though the ΔG-α relationship (Penning et al., 2005) was recorded under specific lab conditions with all known reactions accounted for, it is not unreasonable to assume that a similar relationship might be found in methanogenic environments where similar reactions are expected to occur. That the sites all plot below the curve suggests that there is either another exogenous source of CH_4 (or CO_2) or that the $\delta^{13}C(CH_4)$ values have been altered post-formation e.g., by bacterial methane oxidation.

An open system model (Eq. 1.15 in Chapter 1) assumes an ongoing supply of CH_4 and a corresponding outward flux, whereas a closed system assumes a pool of CH_4 which is either oxidised or retained within the system. Open system models (Eqs. 1.14 in Chapter 1) commonly are used to model CH_4 oxidation in soil and landfill sites, where mass transport by advection is assumed and therefore fractionation via transport can be ignored (e.g., Liptay et al., 1998; Tyler et al., 1994); however in a groundwater system a portion of CH_4 transport via diffusion in addition to mass transport is more likely. An open system would also imply a CH_4 flux at the surface, though this has not been measured. The ranges of isotope composition are also an indication that the system is generally closed – smaller fractionations typically are observed in open systems because there is a constant influx of 'pristine' CH_4 and an outflux of oxidised CH_4 (Liptay et al.,

1998; Tyler et al., 1994).

For the sites with the most positive $\delta^{13}C(CH_4)$ values, an open system model gives a fraction oxidised greater than 1, indicating that the system is likely, not open. For sites with the highest $\delta^{13}C(CH_4)$ values, a closed system model, yields a range of 65 – 95 % CH_4 oxidation and even sites with relatively low $\delta^{13}C(CH_4)$ values of -55.2 ‰ and -55.0 ‰ the range is 32 – 79 % CH_4 oxidation, or 36 – 100 % for an open system model. The site used for the $\delta^{13}C(CH_4)$ of 'pristine' CH_4 was revisited during the 2017 campaign where an increased $\delta^{13}C(CH_4)$ value was measured alongside a reduced CH_4 concentration from 6.9 to 4.6 µg L^{-1}. The reduction of 33 % coincides with the fraction of CH_4 oxidised for both closed and open systems of 0.32 and 0.34, respectively, indicating that an assumed fractionation factor of 1.022 is likely reasonable. It should also be noted that it is not known if the value of 69.5 ‰ used as the 'pristine' $\delta^{13}C(CH_4)$ in situ value (i.e. unaffected by post-formation processes) is accurate because it is possible partial oxidisation has taken place. It is also not known if every site produces the same initial $\delta^{13}C(CH_4)$ values.

5.5 Conclusions

Sampling across the LGS aquifer in the western London Basin has highlighted differences in CH_4 production and oxidation processes, which are location and depth dependent. The deeper, confined part of the aquifer, in which boreholes are into the stratigraphically higher Folkestone Beds and undifferentiated sections, contain more reducing conditions and are of Na-HCO_3 water type. Measured values and concentrations of Eh, DO, Mn, Fe are low and CH_4 concentration is relatively high. The ranges of $\delta^{13}C(CH_4)$ and $\delta^{2}H(CH_4)$ values are relatively narrow, with the difference potentially due to decreased fractionation with increasing temperature but also possibly due to post formation bacterial CH_4 oxidation. The shallower less-confined section of the aquifer consists of sites screened in the Hythe Beds in the south and the Woburn Sands in the north. Sites are generally of Ca-HCO_3 water type, typical of fresh waters, but other geochemical factors are much more variable. Conditions across the shallow sites range from highly reducing to highly oxidising with large ranges of Eh and DO values. There are variable CH_4 concentrations and very large ranges of both $\delta^{13}C(CH_4)$ and $\delta^{2}H(CH_4)$ values, which are controlled by differing rates of CH_4 oxidation. The findings highlight the importance of both local and broad scale characterisation of geochemical conditions and CH_4 concentration and stable isotope compositions in aquifers prior to shale gas exploration or development if the baseline data are

to be used effectively to assess future changes in the geochemistry or gas content of the groundwater system.

Chapter 6

Groundwater methane in the Lancashire area

Summary

This study area was selected due to its location in an area of shale gas exploration, where further development and exploitation are scheduled in 2018. Therefore, understanding the processes of CH_4 production and consumption processes within the area before exploration will be useful in case of future detection of potential exogenous sources of CH_4. The area of study in the Fylde of Lancashire consists of two aquifers, the Sherwood Sandstone, principal aquifer, exploited to the east of the study area and the Middle Sands secondary aquifer, exploited to the west of the area. Due to the fault system, the Sherwood Sandstone is confined to the west and water is not abstracted in that area. The Middle Sands aquifer is laterally discontinuous, adding to the complexity of the area. This investigation was conducted concurrently with a larger British Geological Survey (BGS) study, which is characterizing baseline water chemistry in the area, enabling several visits to the area to enable assessment of temporal variation of CH_4 and $\delta^{13}C(CH_4)$ in boreholes as well as establish an overall characterisation of CH_4 stable isotope compositions. Variation across the Middle Sands aquifer indicates mixing of reducing and oxidizing waters originating, respectively, near the fault system and the Middle Sands aquifer. Sites for which both $\delta^{13}C(CH_4)$ and $\delta^{2}H(CH_4)$ values were collected exhibit a clear correlation indicating varying levels of bacterial CH_4 oxidation across sites. Temporal variations in CH_4 and $\delta^{13}C(CH_4)$ for most sites were not significant, but where observed, they generally took place in concert, i.e., an increase in $\delta^{13}C(CH_4)$ accompanied a decrease in CH_4, indicating a change in the comparative rates of methanotrophy and methanogenesis. The Woodsfold fault system appears to significantly impact redox conditions and groundwater chemistry in the aquifers, which in turn affects CH_4 production and oxidation processes. Oxidation models indicate that CH_4 concentration may be controlled by both CH_4 oxidation rate and transport of CH_4 within, and potentially out, of the aquifer.

6.1 Introduction

The area in Lancashire was selected for investigation due to ongoing exploration for shale gas development. The boreholes are located in the Fylde of Lancashire (Fig. 6.1) and sites are in both the principal aquifer of the Sherwood Sandstone and a local secondary aquifer, the Middle Sands, which is situated within glacial deposits that cover the area.

Eight sites in the area have been investigated by Cuadrilla for potential shale gas development (Cuadrilla, 2018). One site at Elswick was first hydraulically fractured in 1993 and is now nearing the end of its productive life. Two other sites were considered potentially productive (Roseacre and Preston New Road) and planning permission to drill was requested for both. Permission was granted to hydraulically fracture at the Preston new road site in October 2017 and horizontal wells are expected to be completed in 2018 (Cuadrilla, 2018).

The shale gas source rock in the area is the Bowland shale situated at approximately 1500 m depth and overlain consecutively by the Millstone Grit, Collyhurst Sandstone, Manchester Marl, Sherwood Sandstone and Mercia Mudstone (Fig. 6.2a). To the east of the Woodsfold fault, the sequence is eroded to within the Sherwood Sandstone. The whole area is covered in superficial glacial deposits, within which the Middle Sands aquifer is located (Fig. 6.2b). The Middle Sands aquifer is not laterally consistent over the entire area, varying in thicknesses and content of local lenses of clay, the exact locations of which are not known. Five boreholes in the study area are located within the Sherwood Sandstone aquifer and a further ten boreholes within the Middle Sands aquifer. All the Sherwood Sandstone sites are located east of the Woodsfold fault where the aquifer is known to be unconfined.

The British Geological Survey (BGS) have conducted quarterly measurements of ground and surface water in this area since February 2015 to develop a baseline characterisation of water quality before new shale gas development (BGS, 2018). Fieldwork for this project was conducted concurrently with BGS sampling, which allowed for usage of BGS geochemical data from August 2016 in this study as well as field data for temperature, pH, SEC, DO, Eh and total alkalinity. Sampling was conducted in the area during February, May and November 2015 and May 2017. It was not possible to visit all boreholes in the area during each trip due to logistical issues. During the 2015 visits, samples were taken for the analysis of CH_4 concentration, $\delta^{13}C(CH_4)$ and $\delta^{13}C(DIC)$ and water isotopes (once for each site). During the 2017 visit sites also were sampled for H_2 concentration and $\delta^{2}H(CH_4)$.

Characterisation of baseline CH_4 in the Lancashire aquifer system was con-

ducted to address project objectives O1, O2, O3 and O5 described in Chapter 1. The data will also contribute towards evaluation of objective O4. Boreholes in the Lancashire area provide an opportunity to test project hypotheses H1, H2, H4 and H5

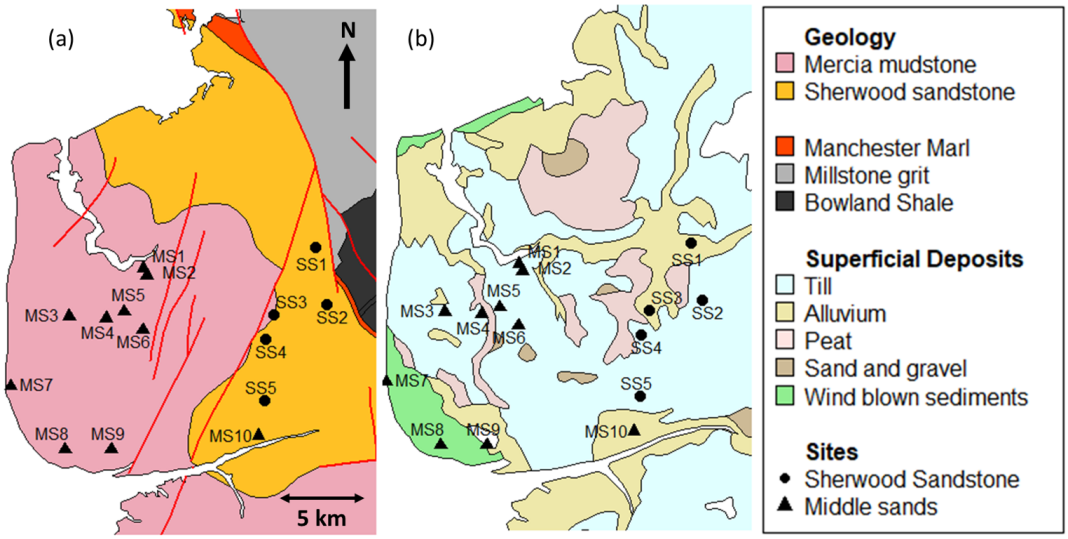

Figure 6.1 Fylde geology and study site locations: (a) bedrock geology, and (b) superficial deposits. Superficial deposits cover the entire area with no exposure of underlying geology. Middle Sands boreholes (filled triangles) are situated within the glacial deposits that cover the area and are positioned between the Upper and Lower Boulder Clay (till) deposits, consisting of sands and gravel. The Sherwood Sandstone borehole are all located within the unconfined aquifer to the east of the Woodsfold fault.

6.2 Background

The Fylde region is covered in a thick layer of glacial drift. Details of underlying geology are mainly from borehole and seismic data (Wilson and Evans, 1990). The Sherwood Sandstone and Mercia Mudstones were deposited during the Triassic at the eastern edge of the Irish Sea basin (Jackson, 1995). The thickness of sandstones varies between 200 and 750 m and was deposited in aeolian and fluvial settings with brief marine transgressions recorded in the sequence (Jackson, 1995). Bedrock geology is detailed in Wilson and Evans (1990) and further information on the Irish Sea basin geology is described by Jackson (1995). The lithostratigraphy of the Sherwood Sandstone were updated in Ambrose et al. (2014). The lower boundary is defined as disconformable on the Cumbrian Coast Group (Permian) in Lancashire and Cumbria and in other areas it rests unconformably on rocks ranging from Precambrian to Carboniferous in age. The upper boundary is defined as gradational into the Tarporley Siltstone Formation of the Mercia

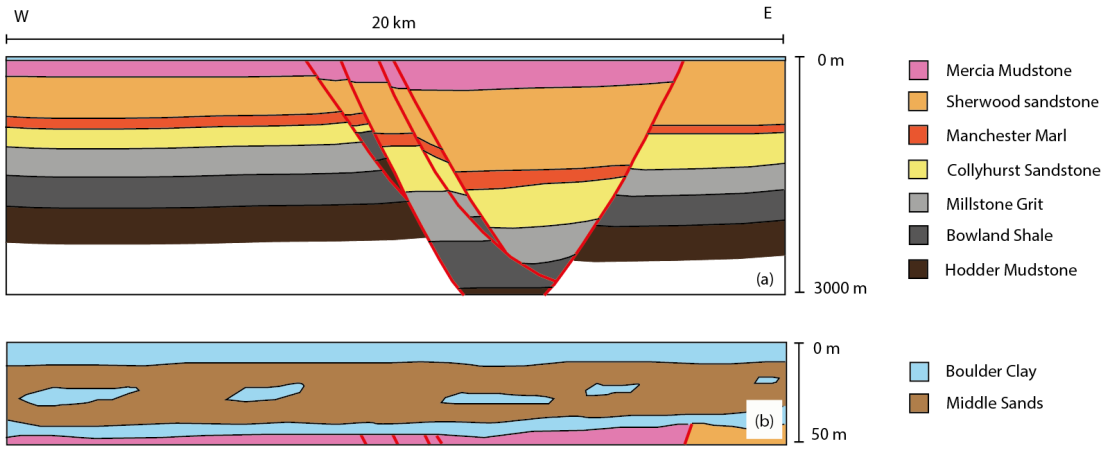

Figure 6.2 Simplified schematic cross-sections across the Fylde: (a) geological cross-section adapted from Cuadrilla (2014), and (b) drift deposit cross-section based on Cuadrilla (2014) and partial cross-sections from Wilson and Evans (1990). The Middle Sands aquifer contains multiple clay lenses and is not laterally continuous. The clay content generally increasing towards the north and consequently the schematic section in panel (b) does not show actual locations of clay lenses. The MS boreholes are located within the superficial deposits. All are situated in deposits overlying Mercia Mudstone with the exception borehole MS-10 in the east, which is located in superficial deposits overlying the unconfined section of the Sherwood Sandstone aquifer. All SS boreholes sites are located in the eastern unconfined section of the Sherwood Sandstone.

Mudstone group, where mudstone and siltstone become dominant over sandstone. The sandstone consists almost entirely of fine to medium grained sands and more rarely coarse-grained sands, dominantly reddish brown, but locally grey near the top (Wilson and Evans, 1990). The sequence can be divided into three members: (i) the lowest member is a fine- to medium-grained sandstone containing a few, thin coarse layers, largely of aeolian origin, with temporary fluvial conditions; (ii) the middle member contains a higher proportion of mudstones, as thin beds and pebbles, and is dominantly fluvial; and (iii) the upper member is a fine- to coarse-grained sandstone with common cross-bedding, some probable adhesion ripples, and a mudstone bed containing desiccation cracks (Wilson and Evans, 1990).

Mercia Mudstone overlies the Sherwood Sandstone west of the Woodsfold fault. The Mercia Mudstone Group consists of a series of mudstone layers, ranging from large structureless units to thinly laminated muds interspersed with salt layers of varying thickness, some of which have been exploited economically. There are four facies within the mudstones: (i) loessic (wind-blown dust) sediments, (ii) interlaminated mudstones containing gypsum veins deposited in shallow waters that periodically dried out, (iii) halite crystals in a red mudstone likely derived from saline groundwater, and (iv) bedded salt hosting thin partings of mudstone deposited in shallow water, occasionally drying out and reforming

at the same site (Wilson and Evans, 1990). The entire area is overlain by a thick blanket of glacial sediment, which is described in detail by Wilson and Evans (1990). The glacial deposits consist of the Lower Boulder Clay, the Middle Sands and the Upper Boulder Clay. The Lower Boulder Clay is generally very hard, highly compacted and consolidated, and rich in erratics of a Cumbrian provenance. It varies in thickness with the thickest sections located in troughs and valleys of the underlying bedrock surface. The Middle Sands have a variable grain size, ranging from fine sand to gravel with local lenses of silt, clay and stony clay, which is probably till. The thickness is variable (up to 40 m) and generally thickest where the whole drift sequence is thickest. The Upper Boulder Clay is a brown silty clay containing abundant erratic pebbles and cobbles, with thin layers locally, mostly within the basal 1 m. It is generally draped evenly over the irregular upper surface of the Middle Sands. The glacial deposits are thought to be from a single glacial event, with the Lower Boulder Clay representing lodgement tills laid down at the base of the ice sheet. The Middle Sands were transported from the north west and are generally thought to be deposited by fluvio-glacial streams or tunnel valley deposits under the glacial sheet. In the southern half of the Fylde, the Middle Sands are more continuous than would be expected from fluvial deposits, suggesting that the ice sheet may have floated on melt water with sand gradually washed underneath it. The Upper Boulder Clay is thought to be englacial material deposited as the glacier melted and retreated.

The Middle Sands aquifer generally is more continuous in the southern versus northern parts of the Fylde. In the northwest, the Middle Sands typically are absent with the space occupied mostly by drumlins of till, some with cores of sand. The northeast is covered largely by sheets of till and was host to glacial lakes marked by extensive flats (Wilson and Evans, 1990).

Both the Sherwood Sandstone and Middle Sands aquifers are exploited for groundwater. In the area west of the Woodfold fault (downthrow of up to 600 m) the Mercia Mudstone acts as a confining layer to the Sherwood Sandstone and that section of the aquifer is not exploited commercially. To the east of the fault, the aquifer generally is unconfined and exploited due to the high quality of the groundwater, which is used to supply the local area with mains water. Flow within the aquifer is a combination of intergranular flow and fracture flow (Worthington, 1977). The importance of fracture flow is supported by the presence of several abstraction wells along main fault zones (Environment Agency, 1997). The Sherwood Sandstone thickens westward but active groundwater flow is probably restricted to the upper 200 m (Environment Agency, 1997) and a portion of the aquifer having a mean permeability of 0.2 m d^{-1}. Recharge of the aquifer

is thought to be controlled by the glacial sands within the drift deposit based upon flow paths established using bicarbonate concentration (Sage and Lloyd, 1978). Low bicarbonate zones correlate well with glacial sand distribution and the locations where the sands merge with present day river courses.

The Middle Sands aquifer is exploited locally for private drinking water, golf courses and farms. The total drift sequence can be up to 60 m in thickness and the Middle Sands up to 40 m thick. The sequence is thinnest in the central part of the Fylde at less than 15 m.

6.3 Results

6.3.1 Geochemistry and redox conditions

Groundwater in the area consists mainly of Ca-HCO_3 type water (Fig. 6.3, Table 6.1) with the exception of borehole MS-9 in the Middle Sands aquifer, which contains Na-Cl type water and an overall different geochemistry, including a much higher SEC compared with all other sites. The concentrations of dissolved CH_4, O_2 (DO) and H_2 vary with Eh (Fig. 6.4). Stronger reducing conditions (decreasing Eh) correspond with a decrease in DO and an increase in CH_4 and H_2 concentrations. Redox conditions vary across the area with strong reducing conditions in the east, near the fault system, accompanied by low DO and higher H_2 concentration (Fig. 6.5). Corresponding changes in CH_4 concentration are less clear because of anomalously high CH_4 concentrations at borehole MS-8.

There is a general temperature increase in groundwater toward the west and a slight increase in both Na and Cl ions (Fig. 6.5d, g and h). Water isotopes, $\delta^2H(H_2O)$ and $\delta^{18}O(H_2O)$, plot along a local meteoric line (Fig. 6.6), covering a relatively small range of values, and do not appear to vary laterally across the area (Fig. 6.5i and j).

6.3.2 Methane concentration and stable isotope compositions

An increase in CH_4 concentration corresponds with decreasing $\delta^{13}C(CH_4)$ and $\delta^2H(CH_4)$ values (Fig. 6.7e and f, also Table 6.2). The $\delta^{13}C(CH_4)$ and $\delta^2H(CH_4)$ values correlate with redox conditions (Fig. 6.7a and b). Generally, increasing DO correlates positively with increasing $\delta^{13}C(CH_4)$ and $\delta^2H(CH_4)$ values (Fig. 6.7c and d) and for most sites SO_4^{2-} concentration also increases with increasing $\delta^{13}C(CH_4)$ and $\delta^2H(CH_4)$ values.

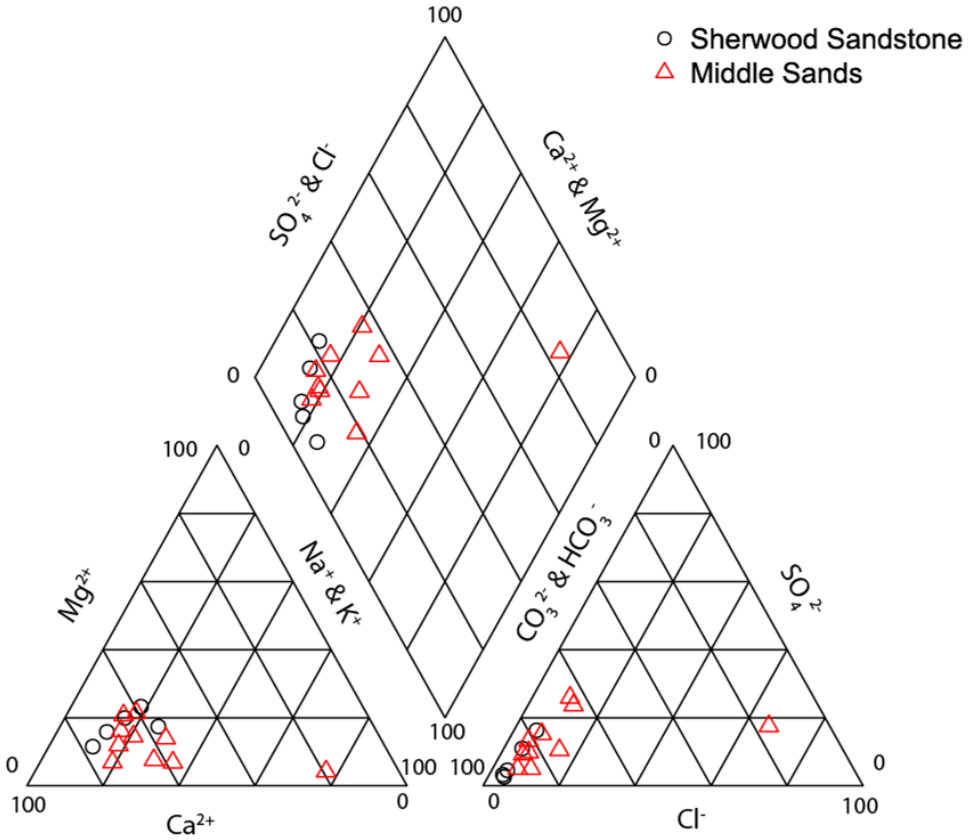

Figure 6.3 Piper diagram for Lancashire borehole sites. The majority of sites contain Ca-HCO_3-type waters. Sherwood Sandstone sites showing a tighter cluster and Middle Sands site MS-9 has Na-Cl-type water. Ca-HCO_3-type waters are common fresh water whereas Na-Cl-type water typically occurs in deeper mature aquifers and can indicate mixing with deeper sources.

The exception to this pattern is borehole MS-9, where SO_4^{2-} concentration correlates with $\delta^{13}C(CH_4)$ and $\delta^2H(CH_4)$ values but not DO. MS-9 hosts the most positive $\delta^2H(CH_4)$ value of +248 ‰, a low DO concentration of 0.03 mg $L^{-1}$and an unusually high SO_4^{2-} concentration of 330 mg L^{-1}(Fig. 6.7h).

There is a weak correlation between $\delta^{13}C(CH_4)$ and $\delta^{13}C(CO_2)$ values (Fig. 6.8a), and $\delta^2H(CH_4)$ and $\delta^2H(H_2O)$ values (Fig. 6.8b). The relationship between $\alpha_{CO_2\text{-}CH_4}$ and ΔG is consistent with the expected trend for hydrogenotrophic methanogenesis (Fig. 6.10).

There is a strong positive correlation between $\delta^{13}C(CH_4)$ and $\delta^2H(CH_4)$ values (Figs. 6.8c and d). Least squares linear regression analysis of the Sherwood Sandstone borehole data yields a slope of 10.1. Similar analysis for the Middle Sands sites produces a slope of 11.7. The magnitudes of stable C and H isotope fractionation do not appear to correlate with temperature (Figs. 6.9a and b).

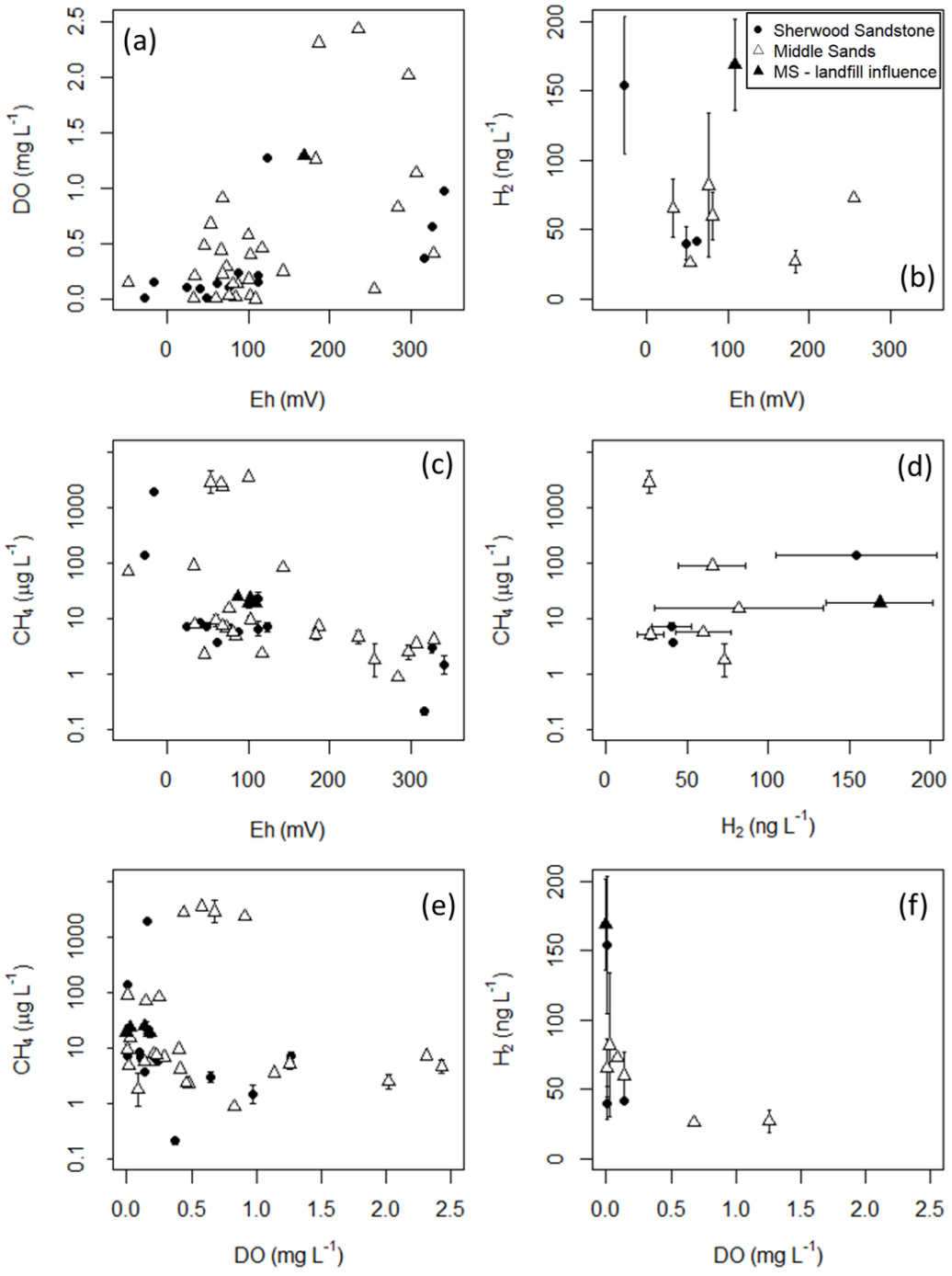

Figure 6.4 Redox conditions and relationship with dissolved CH_4, H_2 and O_2 (DO): (a) DO versus Eh, (b) H_2 versus Eh, (c) CH_4 verses H_2, (d) CH_4 versus Eh, (e) CH_4 versus DO, and (f) H_2 versus DO. Increasing Eh indicates less reducing conditions. Where higher DO, lower H_2 and lower CH_4 concentrations are present correlations exist between DO, H_2 and CH_4.

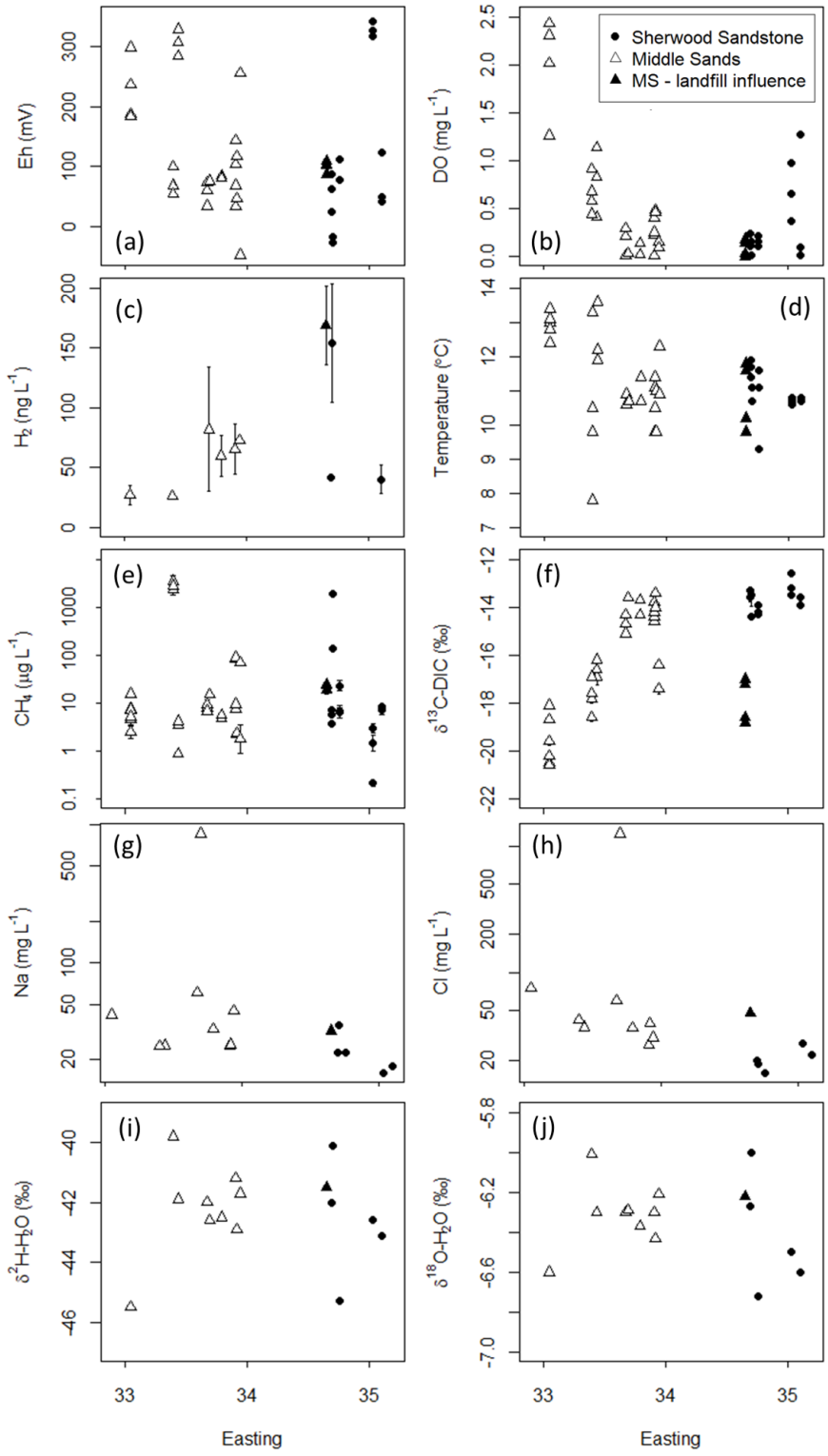

Figure 6.5 Lateral variations in geochemical parameters extending from west to east across the Lancashire study area: (a) Eh, (b) DO, (c) H_2 concentration, (d) temperature, (e) CH_4 concentration, (f) $\delta^{13}C(DIC)$ values, (g) Na concentration, (h) Cl concentration, (i) $\delta^{2}H(H_2O)$ values, and (j) $\delta^{18}O(H_2O)$ values. The Middle Sand boreholes with the exception of MS-10 are situated to the west of the fault system and the Sherwood Sandstone boreholes are located to the east. Generally, conditions are less reducing furthest from the fault to the west. Changes in $\delta^{13}C(DIC)$, Na and Cl suggest that there may be some mixing across the aquifer system. The similarity of water stable isotope compositions (panels (i) and (j)) suggests that water does not differ significantly in its recharge age.

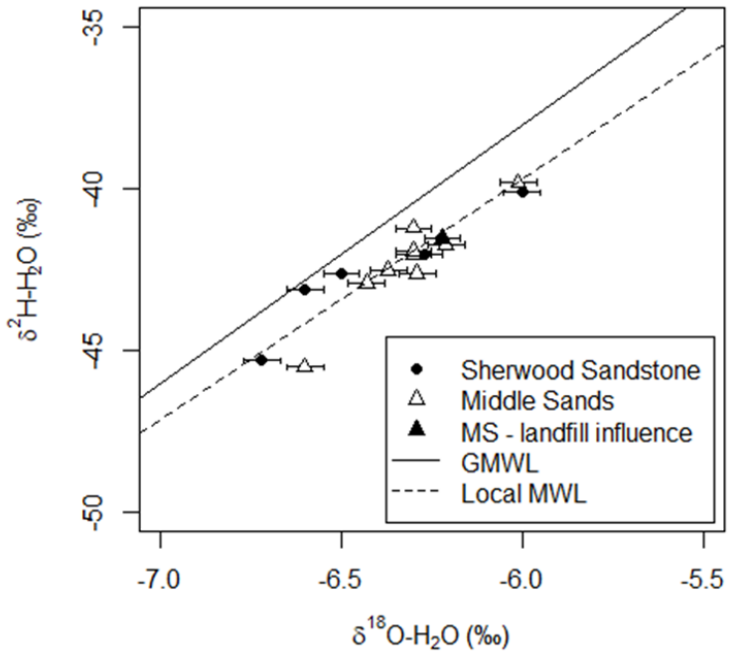

Figure 6.6 $\delta^2H(H_2O)$ and $\delta^{18}O(H_2O)$ values from Lancashire borehole sites, gobal meteoric water line (solid line; Craig, 1961), and local UK meteoric water line (Darling and Talbot, 2003). The isotope composition of water from the borehole sites deviates little from the UK local meteoric water line and the sites fall within a small range of values.

Table 6.1 Lancashire study site details and geochemical data[a].

Site	Formation	Depth (m)	Ca^{2+} (mg L^{-1})	Mg^{2+} (mg L^{-1})	Na^{+} (mg L^{-1})	K^{+} (mg L^{-1})	Cl^{-} (mg L^{-1})	SO_4^{2-} (mg L^{-1})	Mn (µg L^{-1})
SS-1	Sherwood Sandstone	100	119	17.8	15.9	1.99	27.1	74.4	103
SS-2	Sherwood Sandstone	50	105	23.4	17.7	1.7	22.1	49.8	322
SS-3	Sherwood Sandstone	107	79	31.4	22.2	2.62	15.9	14.3	91
SS-4	Sherwood Sandstone	30	116	35.6	35.1	17.8	18.9	11.7	408
SS-5	Sherwood Sandstone	152	99	30.7	22.2	2.13	20.2	22.3	63
MS-1	Middle Sands	30	111	26.7	25.7	1.82	39.4	76.6	188
MS-2	Middle Sands	20	89	10.5	45.1	8.41	30.3	74.9	346
MS-3	Middle Sands	30	116	37.4	25.1	2.07	36.7	50.9	17
MS-4	Middle Sands	39	124	30.7	60.9	4.12	59.4	155	162
MS-5	Middle Sands	15	109	24.5	33.1	1.82	36.3	71.7	262
MS-6	Middle Sands	39	91	32.2	25.0	2.23	26.7	41.9	544
MS-7	Middle Sands	15	103	12.4	42.1	6.41	74.8	52.8	99
MS-8	Middle Sands	5	116	10.8	25.0	4.85	41.7	20.8	861
MS-9	Middle Sands	30	217	48.0	861	5.39	1257	332	281
MS-10	Middle Sands	5	168	28.6	32.3	11.3	47.3	36.2	1043

[a]Geochemistry data provided by British Geological Survey from campaigns conducted in 2016.

Table 6.2 Summary of data for Lancashire sites[a].

Site	Sample date	T (°C)	pH	SEC (µS cm^{-1})	Eh (mV)	DO (mg L^{-1})	HCO_3^- (mg L^{-1})	H_2 (µg L^{-1})	CH_4 (µg L^{-1})	$\delta^{13}C$ (CH_4) (‰)	$\delta^{2}H$ (CH_4) (‰)	Range (‰)	$\delta^{13}C$ (DIC) (‰)	Range (‰)	$\delta^{2}H$ (H_2O) (‰)	$\delta^{18}O$ (H_2O) (‰)
SS-1	03/02/2015	10.6	7.10	770	326	0.65	355	-	3.0 ±0.68	-35.5 ±2.15	-		-13.5	-13.6 to -13.4	-	-
	07/05/2015	10.7	7.07	749	341	0.97	339	-	1.5 ±0.56	-32.4 ±3.89	-		-13.2	-13.5 to -13.1	-	-
	17/11/2015	10.8	7.09	772	317	0.37	379	-	0.2 ±0.03	-29.7 ±2.49	-		-12.6	-	-42.6	-6.5
SS-2	13/05/2015	10.7	7.31	723	41	0.1	383	-	8.5 ±0.83	-34.9 ±4.14	-		-13.9	-14.0 to -13.9	-	-
	18/11/2015	10.8	7.29	725	124	1.27	-	-	7.1 ±1.24	-34.1 ±2.29	-		-13.6	-13.6 to -13.6	-	-
	10/05/2017	10.8	7.26	719	49	0.01	304	40 ±12	7.3 ±1.09	-38.0 ±1.74	-66	-67 to -64	-13.6	-13.6 to -13.5	-43.1	-6.6
SS-3	11/02/2015	9.3	7.26	692	77	0.11	410	-	6.8 ±1.08	-56.1 ±4.22	-		-14.2	-14.3 to -14.2	-	-
	06/05/2015	11.1	7.24	690	112	0.22	395	-	6.6 ±1.88	-64.9 ±1.17	-		-14.3	-14.3 to -14.2	-	-
	10/11/2015	11.6	7.29	699	112	0.15	416	-	23 ±5.66	-96.3 ±3.21	-		-13.9	-	-45.3	-6.7
SS-4	02/02/2015	10.7	6.95	981	-17	0.16	-	-	1862	-73.1 ±0.87	-		-13.5	-14.0 to -13.5	-	-
	09/05/2017	11.1	7.01	973	-27	0.01	416	154 ±49	137 ±15.7	-68.0 ±4.59	-278	-279 to -277	-14.4	-	-40.1	-6.0
SS-5	14/05/2015	11.4	7.19	765	24	0.11	447	-	7.2 ±0.59	-39.7 ±2.16	-		-13.6	-13.8 to -13.5	-	-
	11/11/2015	11.9	7.24	765	87	0.24	433	-	5.92 ±0.37	-40.2 ±3.19	-		-13.3	-	-	-
	10/05/2017	11.7	7.20	747	62	0.14	283	42 ±0.5	3.7 ±0.15	-37.2 ±1.18	119	118 to 121	-13.3	-	-42.0	-6.3
MS-1	11/05/2015	9.8	7.21	843	46	0.48	387	-	2.3 ±0.14	-38.7 ±4.33	-		-14.0	-14.1 to -13.9	-	-
	09/11/2015	11.0	7.14	841	117	0.46	403	-	2.3 ±0.17	-39.1 ±3.28	-		-13.4	-13.5 to -13.3	-42.9	-6.4
MS-2	09/11/2015	12.3	7.19	886	-48	0.15	460	-	68.7	-70.8 ±3.83	-		-17.4	-17.6 to -17.2	-	-
	11/05/2017	10.9	7.16	883	256	0.09	282	73 ±2.3	1.8 ±1.22	-46.0 ±3.91	-		-16.4	-16.5 to -16.4	-41.7	-6.2
MS-3	06/02/2015	12.2	7.09	918	307	1.14	428	-	3.5 ±0.13	-27.9 ±1.80	-		-16.9	-17.2 to -16.8	-	-
	15/05/2015	11.9	7.12	906	329	0.41	446	-	4.1 ±0.36	-24.1 ±0.65	-		-16.6	-16.6 to -16.5	-	-
	10/11/2015	13.6	7.11	927	284	0.83	454	-	0.9 ±0.09	-	-		-16.2	-16.2 to -16.1	-41.9	-6.3
MS-4	04/02/2015	10.6	7.38	1083	34	0.21	383	-	7.9 ±0.07	-43.9 ±0.75	-		-15.1	-15.1 to -15.0	-	-
	06/05/2015	10.9	7.29	1072	60	0.01	396	-	9.1 ±2.07	-45.9 ±0.59	-		-14.7	-14.9 to -14.6	-	-
	12/11/2015	10.9	7.42	1074	73	0.29	410	-	6.8 ±0.39	-	-		-14.3	-	-42.0	-6.3
MS-5	13/05/2015	10.7	7.22	800	84	0.02	378	-	4.8 ±0.23	-45.6 ±0.91	-		-14.3	-14.7 to -14.3	-	-
	11/05/2017	11.4	7.17	819	81	0.14	195	60 ±17	5.7 ±0.49	-43.9 ±2.12	52	50 to 54	-13.7	-13.8 to -13.7	-42.5	-6.4
MS-6	05/02/2015	9.8	7.22	799	68	0.23	383	-	7.4 ±0.29	-63.0 ±2.49	-		-14.6	-14.7 to 14.5	-	-
	06/05/2015	10.5	6.81	794	103	0.40	407	-	9.6 ±1.31	-57.2 ±9.34	-		-14.4	-14.2 to -14.3	-	-
	12/11/2015	11.1	7.40	782	143	0.25	417	-	81.5 ±12.1	-79.6 ±8.50	-		-14.2	-	-	-
	11/05/2017	11.4	7.33	779	33	0.01	381	65 ±21	89.7 ±10.5	-81.5 ±1.67	-353	-354 to -351	-13.8	-13.9 to -13.8	-41.2	-6.3

Table 6.2 continued

Site	Sample date	T (°C)	pH	SEC (µS cm^{-1})	Eh (mV)	DO (mg L^{-1})	HCO_3^- (mg L^{-1})	H_2 (µg L^{-1})	CH_4 (µg L^{-1})	$\delta^{13}C$ (CH_4) (‰)	$\delta^{2}H$ (CH_4) (‰)	Range (‰)	$\delta^{13}C$ (DIC) (‰)	Range (‰)	$\delta^{2}H$ (H_2O) (‰)	$\delta^{18}O$ (H_2O) (‰)
MS-7	27/10/2014	13.4	7.20	802	-	-	329	-	15.4 ±2.07	-45.0 ±0.41	-		-18.1	-	-	-
	12/01/2015	13.0	7.11	870	-	-	-	-	7.6 ±0.46	-47.0 ±0.66	-		-19.6	-19.7 to -19.5	-	-
	03/02/2015	12.4	7.09	959	187	2.31	317	-	7.3 ±0.07	-53.0 ±0.77	-		-20.5	-20.7 to -20.4	-	-
	07/05/2015	12.8	7.09	893	236	2.43	316	-	4.7 ±1.31	-47.9 ±1.15	-		-20.2	-20.3 to -20.2	-	-
	17/11/2015	13.1	6.69	988	298	2.02	376	-	2.5 ±0.73	-43.9 ±1.46	-		-20.6	-	-	-
	08/05/2017	13.4	7.12	823	183	1.26	-	28 ±8.1	5.3 ±1.07	-44.2 ±0.27	77	-75 to 78	-18.7	-	-45.5	-6.6
MS-8	10/02/2015	9.8	7.17	756	68	0.91	351	-	2320 ±321	-69.5 ±0.70	-		-18.6	-18.8 to -18.5	-	-
	08/05/2015	7.8	7.20	722	100	0.58	340	-	3449 ±156	-73.0 ±0.77	-		-17.8	-18.0 to -17.2	-	-
	18/11/2015	13.3	7.21	633	67	0.44	-	-	2710 ±126	-	-		-17.6	-	-	-
	09/05/2017	10.5	7.07	717	54	0.68	266	26 ±1.9	2826 ±1270	-72.2 ±0.33	-227	-227 to -226	-16.9	-	-39.8	-6.0
MS-9	09/05/2017	10.7	7.23	2170	76	0.03	303	82 ±52	15.1 ±0.52	-32.3 ±0.41	248	247 to 249	-13.6	-	-42.6	-6.3
MS-10	11/02/2015	9.8	7.04	1180	87	0.14	635	-	25.3 ±1.42	-54.5 ±0.44	-		-18.8	-18.9 to -18.8	-	-
	14/05/2015	10.2	7.01	1134	103	0.03	631	-	23.4 ±3.13	-52.7 ±2.18	-		-18.6	-18.8 to -18.5	-	-
	11/11/2015	11.6	7.04	1109	101	0.18	625	-	19.2 ±3.59	-54.6 ±0.25	-		-17.2	-	-	-
	10/05/2017	11.8	6.99	1124	109	0.00	452	169 ±33	19.3 ±2.79	-56.4 ±0.35	-202	-202 to -201	-17.0	-	-41.5	-6.2

[a]Field measurements of DO, SEC, pH, temperature and alkalinity titrations were collected by the BGS and are used with permission.

Table 6.3 Summary of calculated values of DIC concentration and $\delta^{13}C(CO_2)$ values.

				Calculated values				
Site	Sample date	HCO_3^- (mg L^{-1})	pH	$\delta^{13}C$(DIC) (‰)	DIC (mg L^{-1})	$CO_{2(aq)}$ (mg L^{-1})	$CO_{2(g)}$ (mg L^{-1})	$\delta^{13}C(CO_2)$ (‰)
SS-1	03/02/2015	355	7.10	-13.5	412	57	0.23	-21.0
	07/05/2015	339	7.07	-13.2	398	59	0.24	-20.7
	17/11/2015	379	7.09	-12.6	442	62	0.26	-20.1
SS-2	13/05/2015	383	7.31	-13.9	421	38	0.28	-22.1
	18/11/2015	-	7.29	-13.6	-	-	-	-
	10/05/2017	304	7.26	-13.6	339	34	0.25	-21.6
SS-3	11/02/2015	410	7.26	-14.2	456	46	0.17	-22.4
	06/05/2015	395	7.24	-14.3	441	46	0.18	-22.2
	10/11/2015	416	7.29	-13.9	459	43	0.17	-21.9
SS-4	02/02/2015	-	6.95	-13.5	-	-	-	-
	09/05/2017	416	7.01	-14.4	499	82	0.93	-21.5
SS-5	14/05/2015	447	7.19	-13.6	506	59	0.16	-21.4
	11/11/2015	433	7.24	-13.3	483	50	0.14	-21.2
	10/05/2017	283	7.20	-13.3	320	36	0.10	-21.1
MS-1	11/05/2015	387	7.21	-14.0	435	48	0.53	-22.0
	09/11/2015	403	7.14	-13.4	462	59	0.66	-21.1
MS-2	09/11/2015	460	7.19	-17.4	520	60	0.91	-25.1
	11/05/2017	282	7.16	-16.4	322	40	0.59	-24.1
MS-3	06/02/2015	428	7.09	-16.9	498	70	0.80	-24.3
	15/05/2015	446	7.12	-16.6	515	69	0.78	-24.1
	10/11/2015	454	7.11	-16.2	526	71	0.82	-23.5
MS-4	04/02/2015	383	7.38	-15.1	416	32	0.29	-23.5
	06/05/2015	396	7.29	-14.7	438	41	0.37	-22.8
	12/11/2015	410	7.42	-14.3	442	32	0.29	-22.8
MS-5	13/05/2015	378	7.22	-14.3	424	46	0.82	-22.3
	11/05/2017	195	7.17	-13.7	222	27	0.48	-21.5
MS-6	05/02/2015	383	7.22	-14.6	430	47	0.42	-22.6
	06/05/2015	407	6.81	-14.4	534	128	1.15	-20.6
	12/11/2015	417	7.40	-14.2	451	34	0.31	-22.5
	11/05/2017	381	7.33	-13.8	418	36	0.33	-22.0
MS-7	27/10/2014	329	7.20	-18.1	371	42	0.77	-25.8
	12/01/2015	-	7.11	-19.6	-	-	-	-
	03/02/2015	317	7.09	-20.5	369	52	0.95	-27.9
	07/05/2015	316	7.09	-20.2	368	52	0.95	-27.6
	17/11/2015	376	6.69	-20.6	532	156	2.85	-26.1
	08/05/2017	-	7.12	-18.7	-	-	-	-
MS-8	10/02/2015	351	7.17	-18.6	400	48	1.40	-26.4
	08/05/2015	340	7.20	-17.8	384	43	1.24	-25.9
	18/11/2015	-	7.21	-17.6	-	-	-	-
	09/05/2017	266	7.07	-16.9	312	46	1.35	-24.3
MS-9	09/05/2017	303	7.23	-13.6	339	36	0.40	-21.6
MS-10	11/02/2015	635	7.04	-18.8	753	117	3.42	-26.2
	14/05/2015	631	7.01	-18.6	757	125	3.66	-25.8
	11/11/2015	625	7.04	-17.2	741	116	3.43	-24.5
	10/05/2017	452	6.99	-17.0	546	94	2.79	-24.0

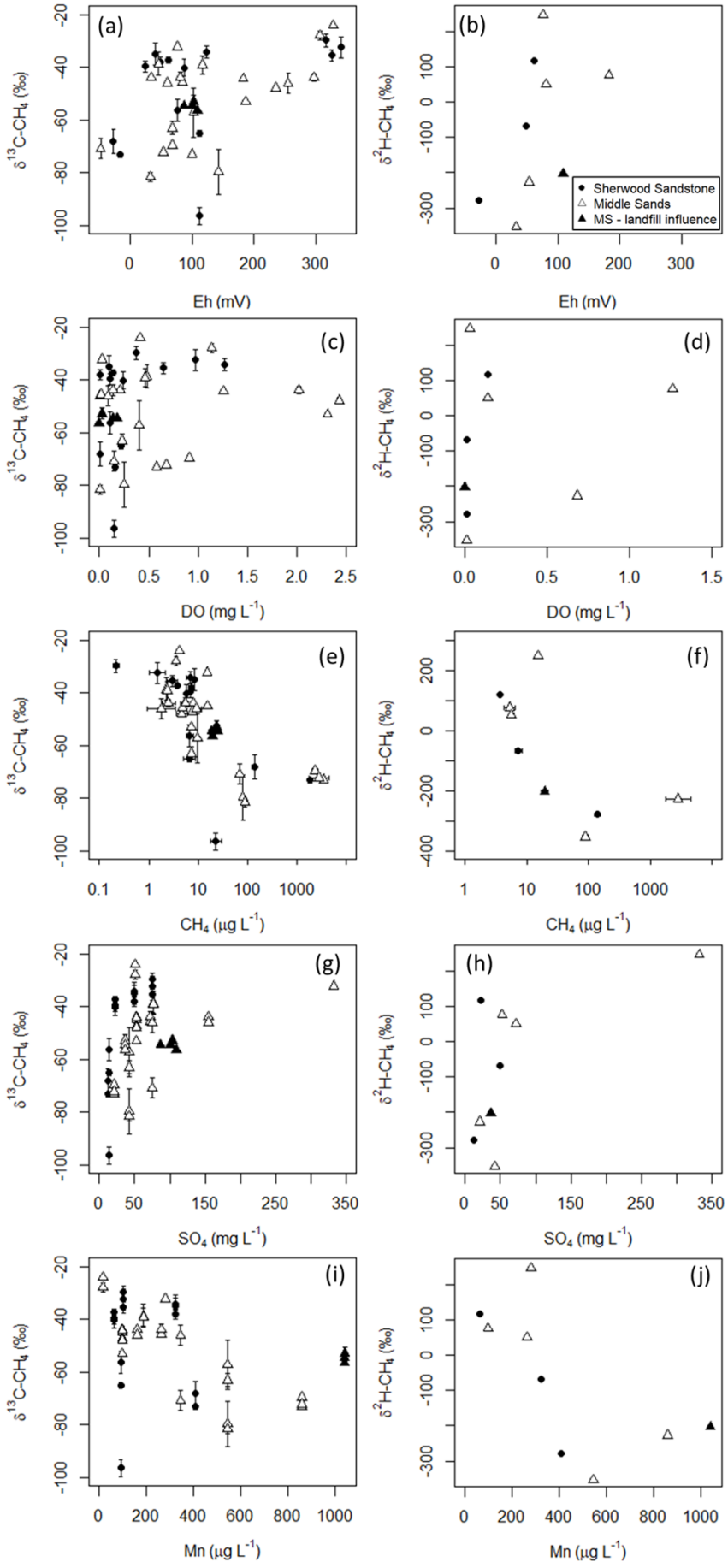

Figure 6.7 Relationship between CH_4 stable isotope composition and geochemical indicators of redox conditions in the aquifer: (a) $\delta^{13}C(CH_4)$ and (b) $\delta^{2}H(CH_4)$ variations with Eh, (c) $\delta^{13}C(CH_4)$ and (d) $\delta^{2}H(CH_4)$ variations with DO, (e) $\delta^{13}C(CH_4)$ and (f) $\delta^{2}H(CH_4)$ variations with CH_4 concentration, (g) $\delta^{13}C(CH_4)$ and (h) $\delta^{2}H(CH_4)$ variations with SO_4^{2-} concentration, (i) $\delta^{13}C(CH_4)$ and (j) $\delta^{2}H(CH_4)$ variations with Mn concentration. The CH_4 isotope compositions generally vary with changing redox conditions. As conditions become more oxidising $\delta^{13}C(CH_4)$ and $\delta^{2}H(CH_4)$ values generally increase i.e., become more ^{13}C- and ^{2}H-enriched likely due to methane oxidation processes.

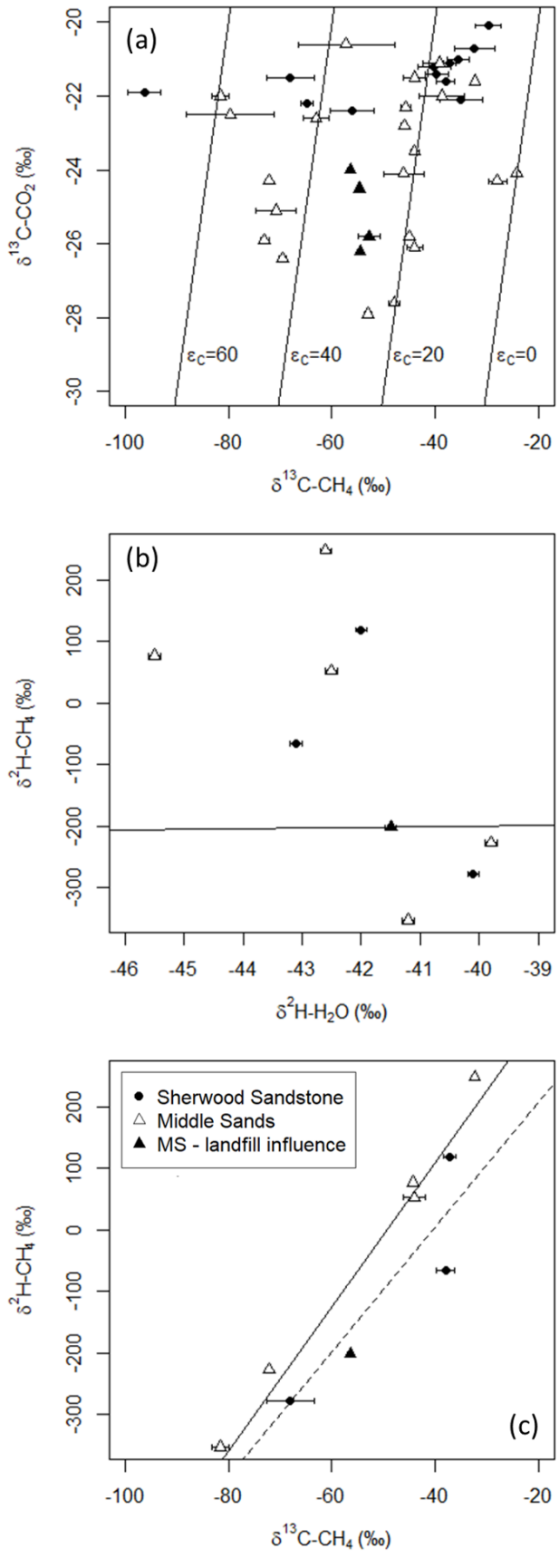

Figure 6.8 Relationships of between stable isotope compositions of CH_4, DIC and H_2O: (a) $\delta^{13}C(CO_2)$ versus $\delta^{13}C(CH_4)$ values with lines representing constant fractionation factors; (b) $\delta^2H(CH_4)$ versus $\delta^2H(H_2O)$ values with line representing theoretical fractionation for hydrogenotrophic methanogenesis (Whiticar et al., 1986); (c) $\delta^2H(CH_4)$ versus $\delta^{13}C(CH_4)$ values with regression of data from the Middle Sands (solid line) and Sherwood Sandstone (dashed line) boreholes. No clear relationships exist between $\delta^{13}C(CO_2)$ and $\delta^{13}C(CH_4)$ or $\delta^2H(CH_4)$ and $\delta^2H(H_2O)$ values, which can be interpreted in the context of CH_4 formation processes. Strong correlations exist between $\delta^2H(CH_4)$ and $\delta^{13}C(CH_4)$ values which indicates an influence of bacterial CH_4 oxidation, resulting in ^{13}C- and ^2H- enrichment of residual CH_4, masking the original stable isotope compositions impacted by formation processes.

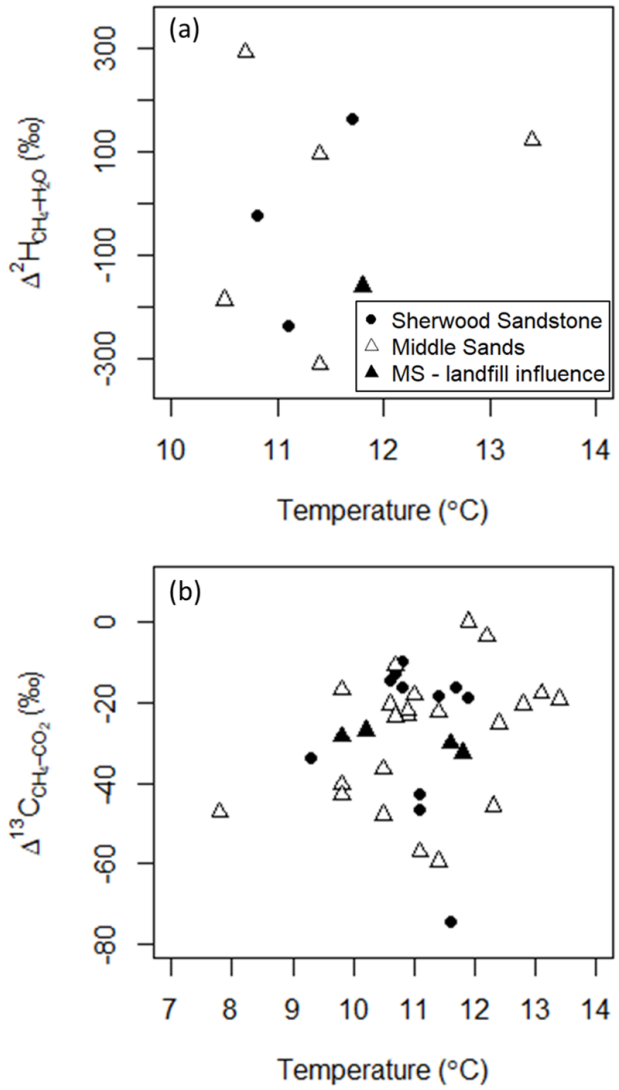

Figure 6.9 Relationship of isotope fractionation with temperature: (a) $\Delta^{13}C_{CH_4\text{-}CO_2}$ versus temperature, and (b) $\Delta^2H_{CH_4\text{-}H_2O}$ versus temperature. The correlation is poor for both $\Delta^2H_{CH_4\text{-}H_2O}$ and $\Delta^{13}C_{CH_4\text{-}CO_2}$ with temperature, which could indicate either masking of formation processes by post formation processes, small temperature range across sites, or temperatures insufficiently variable to affect fractionation processes.

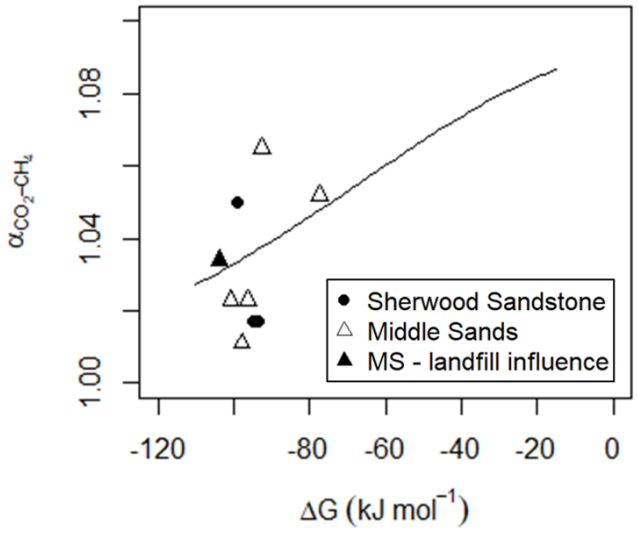

Figure 6.10 Apparent $\alpha_{CO_2\text{-}CH_4}$ and Gibbs free energy (ΔG). The solid line is a relationship between $\alpha_{CO_2\text{-}CH_4}$ and ΔG for hydrogenotrophic methanogenesis reported by Penning et al. (2005).

6.3.3 Temporal variation

For most sites, there was insignificant change in CH_4 concentration or $\delta^{13}C(CH_4)$ values across the time period of sampling (Figs. 6.11 and 6.12). However, for the sites where a change does occur, there is a change in both CH_4 concentration and $\delta^{13}C(CH_4)$ values. In the Sherwood Sandstone boreholes, changes across site visits were recorded for SS-1 and SS-3. At SS-3, which is located on the Woodsfold fault, there was an increase in CH_4 (6.59 to 23.0 µg L^{-1}) between May and November 2015 (Fig. 6.11a) and a corresponding decrease in $\delta^{13}C(CH_4)$ values (-64.9 to -96.3 ‰); Fig. 6.11c). There did not appear to be a significant change in redox conditions, with low Eh and DO (Table 6.2) maintained. For SS-1, there is high Eh and low CH_4 concentration. The concentration of CH_4 decreases with time 2.98 to 1.48 to 0.22 µg L^{-1}) and there is a corresponding increase in $\delta^{13}C(CH_4)$ values (-35.5 to -32.4 to -29.7 ‰). There is also a small increase in $\delta^{13}C(DIC)$ values with time (Fig. 6.11d).

In the Middle Sands boreholes, changes across site visits were recorded for MS-6 and MS-7 (Fig. 6.12). For MS-6, there is a large difference between the first two and last two visits where a 10-fold increase occurs in CH_4 concentration (7.39 and 9.58 µg L^{-1} to 81.5 and 89.7 µg L^{-1}) and $\delta^{13}C(CH_4)$ decreases from (-63.0 and -57.2 ‰ to -79.6 and -81.5 ‰). A gradual decrease also occurs in DO between the 2nd and 4th visit, Eh greatly decreases, pH declines slightly and there is an increase in HCO_3^- concentration. At MS-7, where there were an additional two visits prior to the start of general sampling (Table 6.2), there is a decrease in CH_4 concentration with time (15.4, 7.63, 7.32, 4.69, 2.53 µg L^{-1}), except for the final visit, where there is a slight increase to 5.29 µg L^{-1}. There is an initial decrease in $\delta^{13}C(CH_4)$ values over the first three visits (-45.0, -47.0, -53.0 ‰) followed by an increase over the next three sampling visits (-47.9, -43.9, -44.2 ‰). The $\delta^{13}C(DIC)$ values also decreased over the first three visits, then stabilized before the last visit when it increased again (-18.1, -19.6, -20.5, -20.2, -20.6, -18.7 ‰). For all sites in the Middle Sands there is a slight increase in $\delta^{13}C(DIC)$ values with time.

6.3.4 Methane oxidation

Open and closed system Rayleigh distillation models (Eqs. 1.13 and 1.14 in Chapter 1) were used to estimate the proportion of CH_4 oxidised (F_{ox}) in groundwater (Table 6.4 and Fig 6.13). Fractionation factors (α_{ox}) were employed based upon values reported in the literature for aerobic methanotrophy (Chanton et al., 2008; Coleman et al., 1981; Tyler et al., 1994). A mid-range value of 1.022 was used

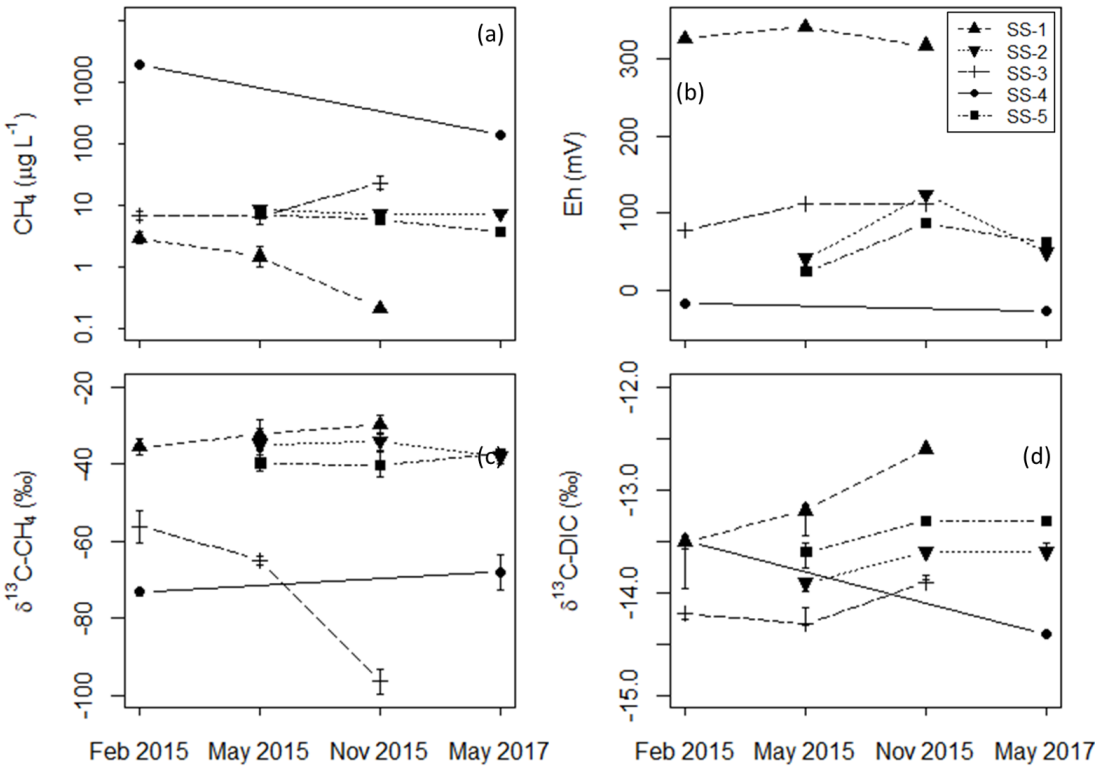

Figure 6.11 Temporal variation of select data for Sherwood sandstone sites: (a) CH_4 concentration, (b) Eh, (c) $\delta^{13}C(CH_4)$ values, (d) $\delta^{13}C(DIC)$ values. Sites SS-2 and SS-5 exhibit little variation with time. SS-3 had a decreasing CH_4 concentration and corresponding increase in $\delta^{13}C(CH_4)$ values with time. Sites SS-1 and SS-4 both showed an increasing CH_4 concentration between site visits and a corresponding decrease in $\delta^{13}C(CH_4)$ values, which may indicate changes in CH_4 production or oxidation rates.

with high and low values of 1.04 and 1.01. For the open system model, an additional scenario was tested using α_{ox} of 1.022 (mid-range value) and a fractionation associated with transport (α_{trans}) of 1.014, which is the theoretical maximum value for CH_4 transport (De Visscher et al., 2004). The α_{ox} values used to model H fractionation were 1.100, 1.200 and 1.300 for high, middle and low oxidation scenarios (Coleman et al., 1981).

Boreholes exhibiting a decrease in CH_4 concentration and an increase in $\delta^{13}C(CH_4)$ values with time were modelled and compared with the estimated fraction of CH_4 lost over the same time interval (Table 6.4). For borehole sites sampled in 2017, models were run assuming initial stable isotope compositions based on stable isotope analysis of CH_4 sites MS-6 and SS-3 for the Middle Sands and Sherwood Sandstone aquifer, respectively (Fig. 6.13 and Table 6.5). Borehole SS-3 was not revisited in 2017 so only modelling of $\delta^{13}C(CH_4)$ values was possible for the Sherwood Sandstone sites. For Middle Sands sites, initial $\delta^{13}C(CH_4)$ and $\delta^{2}H(CH_4)$ values were calculated from $\delta^{13}C(CO_2)$ and $\delta^{2}H(H_2O)$ values us-

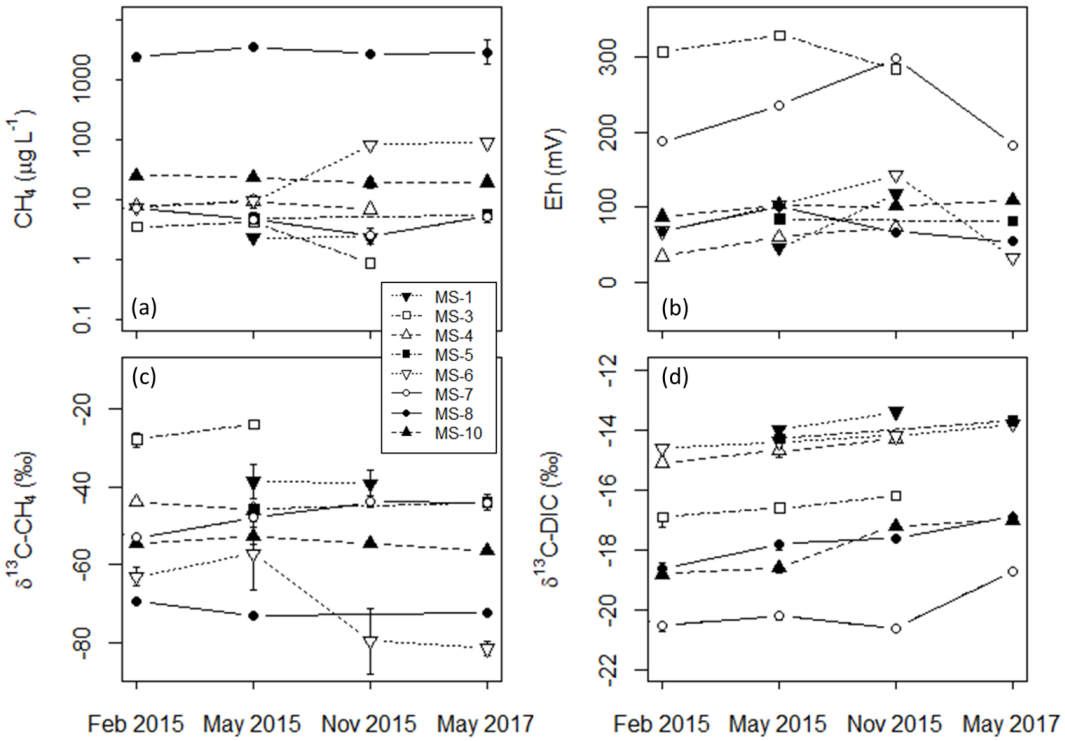

Figure 6.12 Temporal variation of select data for Middle Sands aquifer boreholes: (a) CH_4 concentration, (b) Eh, (c) $\delta^{13}C(CH_4)$ values, and (d) $\delta^{13}C(DIC)$ values. The majority of sites show little variation between site visits; however, variations are evident for MS-3, MS-6 and MS-7 for most parameters. Borehole MS-3 exhibited a slight decrease in CH_4 concentration and a corresponding increase in $\delta^{13}C(CH_4)$ values. For MS-6, there is a large difference between the first two and last two visits in which a 10-fold increase occurs in CH_4 concentration and a corresponding decrease in $\delta^{13}C(CH_4)$ values. For MS-7, for which there were an additional two visits prior to the start of general sampling (Table 5.2), there is a general decrease in CH_4 concentration with time, except for the final visit, where there is an increase. There is an initial decrease in $\delta^{13}C(CH_4)$ values during the first three visits and an increase over the next three visits.

ing ε_C and ε_H values determined from borehole MS-6 (59.5 ‰ and 311.8 ‰, respectively).

For the Sherwood Sandstone sites, due to the small range in $\delta^{13}C(CO_2)$ values, the same initial $\delta^{13}C(CH_4)$ value of -96.3 ‰ was used (borehole SS-3 was assumed to be the 'pristine' CH_4 value, i.e. the unaltered in situ value). This value was chosen as the lowest measured value, however it must be noted that it is not know if there have been post formation processes, such as transportation or oxidation that may have altered the original value; it is also not possible to defnitively assume the same CH_4 source, especially as there is no accompanying $\delta^2H(CH_4)$ value. The estimated F_{ox} ranged from 0.44 to 0.99 for mid-range closed system scenarios and for open system models values the fraction oxidized was ∼1.00, which can be interpreted broadly as a significantly large proportion of CH_4

removal via bacterial methanotrophy, taking into account the errors associated with assuming initial δ-values and fractionation factors (Table 6.4).

Table 6.4 Oxidation models for boreholes exhibiting evidence of methanotrophy.

Site	CH_4 at t_1 ($\mu g\ L^{-1}$)	CH_4 at t_2 ($\mu g\ L^{-1}$)	δA (‰)	δE (‰)	α_{ox}	α_{trans}	F_{ox} (closed)	F_{ox} (open)	1 - (CH_4 t2/CH_4 t_1)
SS-1	2.98	1.48	-35.5	-32.4	1.022	1	0.14	0.14	0.5
			-35.5	-32.4	1.01	1	0.27	0.31	
			-35.5	-32.4	1.04	1	0.08	0.08	
			-35.5	-32.4	1.022	1.014	-	0.39	
	2.98	0.22	-35.5	-29.7	1.022	1	0.24	0.26	0.93
			-35.5	-29.7	1.01	1	0.45	0.58	
			-35.5	-29.7	1.04	1	0.14	0.15	
			-35.5	-29.7	1.022	1.014	-	0.72	
	1.48	0.22	-32.4	-29.7	1.022	1	0.12	0.12	0.85
			-32.4	-29.7	1.01	1	0.24	0.27	
			-32.4	-29.7	1.04	1	0.07	0.07	
			-32.4	-29.7	1.022	1.014	-	0.34	
SS-4	1862	137	-73.1	-68.0	1.022	1	0.22	0.23	0.93
			-73.1	-68.0	1.01	1	0.42	0.51	
			-73.1	-68.0	1.04	1	0.13	0.13	
			-73.1	-68.0	1.022	1.014	-	0.64	
MS-2	68.7	1.8	-70.8	-46.0	1.022	1	0.7	1.13	0.97
			-70.8	-46.0	1.01	1	0.93	2.48	
			-70.8	-46.0	1.04	1	0.48	0.62	
			-70.8	-46.0	1.022	1.014	-	3.1	

δA = initial $\delta^{13}C(CH_4)$.
δE = final $\delta^{13}C(CH_4)$.
α_{ox} = fractionation factor for CH_4 oxidation.
α_{trans} = fractionation factor for CH_4 transport.
F_{ox} – fraction of CH_4 oxidised.

Table 6.5 Oxidation models for borehole sites sampled in 2017.

	^{13}C -CH_4						^{2}H -CH_4					
Site	δA (‰)	δE (‰)	α_{ox}		F_{ox} closed	F_{ox} open	δA (‰)	δE (‰)	α_{ox}		F_{ox} closed	F_{ox} open
SS-1	-96.3	-38	1.022	1	0.94	2.65						
			1.01	1	1	5.83						
			1.04	1	0.79	1.46						
			1.022	1.014	-	7.29						
SS-4	-96.3	-68	1.022	1	0.75	1.29						
			1.01	1	0.95	2.83						
			1.04	1	0.54	0.71						
			1.022	1.014	-	3.54						
SS-5	-96.3	-37.2	1.022	1	0.94	2.69						
			1.01	1	1	5.91						
			1.04	1	0.79	1.48						
			1.022	1.014	-	7.38						
MS-2	-83.6	-46	1.022	1	0.84	1.71						
			1.01	1	0.98	3.76						
			1.04	1	0.63	0.94						
			1.022	1.014	-	4.7						
MS-5	-81	-43.9	1.022	1	0.83	1.69	-354	52	1.1	1	0.99	4.06
			1.01	1	0.98	3.71			1.2	1	0.91	2.03
			1.04	1	0.63	0.93			1.3	1	0.8	1.35
			1.022	1.014	-	4.64			1.2	1.14	-	6.77
MS-6	-81.5	-81.5	1.022	1	0	0	-353	-353	1.1	1	0	0
			1.01	1	0	0			1.2	1	0	0
			1.04	1	0	0			1.3	1	0	0
			1.022	1.014	-	0			1.2	1.14	-	0
MS-7	-81.5	-44.2	1.022	1	0.84	1.7	-357	77	1.1	1	0.99	4.34
			1.01	1	0.98	3.73			1.2	1	0.92	2.17
			1.04	1	0.63	0.93			1.3	1	0.82	1.45
			1.022	1.014	-	4.66			1.2	1.14	-	7.24
MS-8	-83.8	-72.2	1.022	1	0.44	0.53	-352	-227	1.1	1	0.83	1.25
			1.01	1	0.72	1.16			1.2	1	0.58	0.62
			1.04	1	0.27	0.29			1.3	1	0.44	0.42
			1.022	1.014	-	1.45			1.2	1.14	-	2.08
MS-9	-81.1	-32.3	1.022	1	0.9	2.22	-354	248	1.1	1	1	6.02
			1.01	1	0.99	4.88			1.2	1	0.96	3.01
			1.04	1	0.73	1.22			1.3	1	0.89	2.01
			1.022	1.014	-	6.1			1.2	1.14	-	10.04
MS-10	-83.5	-56.4	1.022	1	0.73	1.23	-353	-202	1.1	1	0.88	1.51
			1.01	1	0.95	2.71			1.2	1	0.65	0.76
			1.04	1	0.52	0.68			1.3	1	0.5	0.5
			1.022	1.014	-	3.39			1.2	1.14	-	2.52

δA = initial $\delta^{13}C(CH_4)$.
δE = final $\delta^{13}C(CH_4)$.
α_{ox} = fractionation factor for CH_4 oxidation.
α_{trans} = fractionation factor for CH_4 transport.
F_{ox} – fraction of CH_4 oxidised.

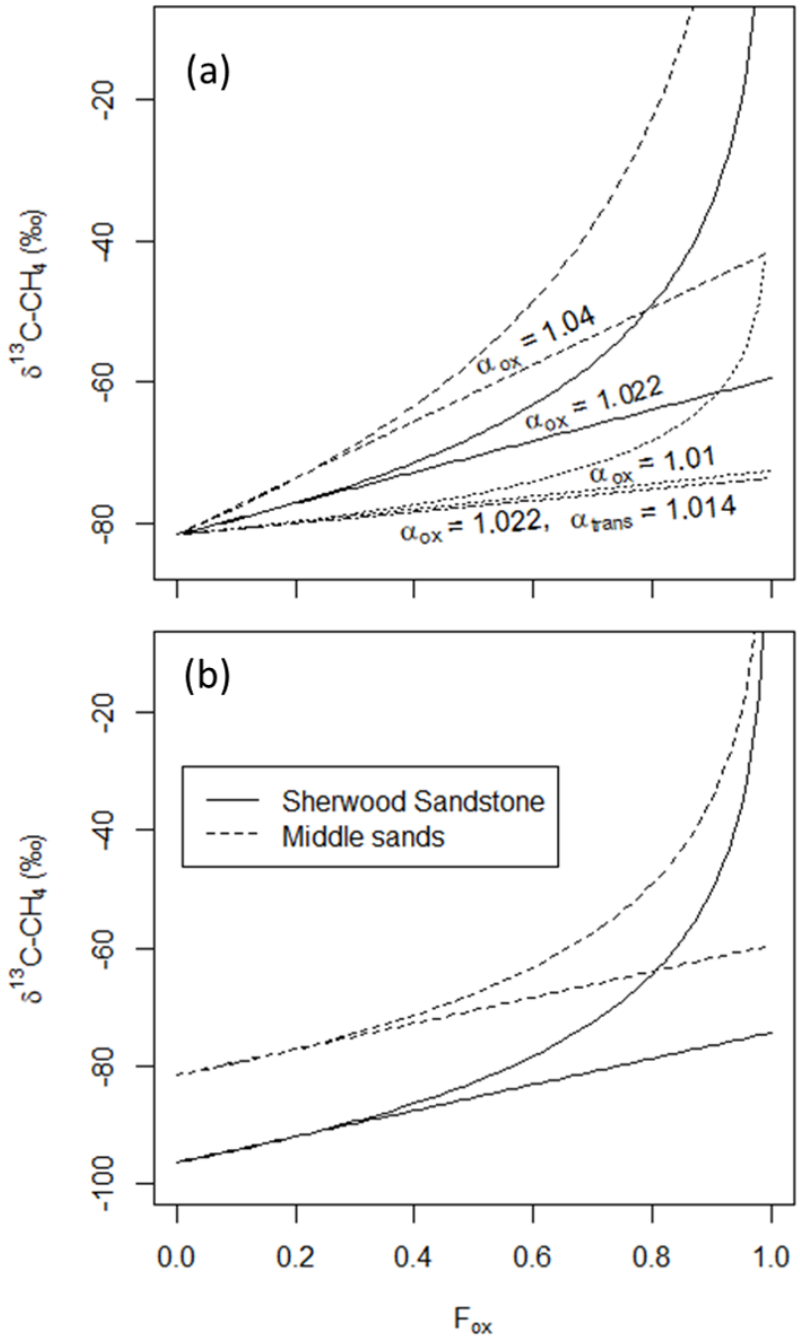

Figure 6.13 Oxidation model to account for variations in $\delta^{13}C(CH_4)$ values: (a) Middle Sands aquifer only, assuming initial $\delta^{13}C(CH_4)$ of -81.5 ‰, showing effect of changing fractionation factors, (b) models for Middle Sands aquifer and Sherwood Sandstone assumes initial $\delta^{13}C(CH_4)$ values of -81.5 ‰ and -96.3 ‰ respectively. Straight lines are open system models and exponential curves are closed system models. Higher fractionation factors cause a more rapid increase in $\delta^{13}C(CH_4)$ values, therefore large changes in $\delta^{13}C(CH_4)$ values would equate to less methane oxidation than for smaller fractionation factors. Initial $\delta^{13}C(CH_4)$ values for Middle Sands and Sherwood Sandstone aquifers were assumed to be different based on the most negative stable isotope values measured for each aquifer. The true initial $\delta^{13}C(CH_4)$ value is an unknown and may be the same for both aquifers.

6.4 Discussion

6.4.1 Effect of geology on geochemistry and mixing of waters

The trends of Eh, temperature, Na, Cl and δ^{13}C(DIC) values from east to west within the Middle Sands aquifer are likely due to mixing of oxidising waters to the west and reducing waters from the east of the area. The oxidising waters likely originate within the Middle Sands aquifer, a supposition which is supported by the slightly elevated concentrations of Na and Cl derived from the underlying Mercia Mudstone (Wilson and Evans, 1990). Alternatively, the higher Na and Cl content in the Middle Sands aquifer could originate from within the boulder clay hosted in the glacial deposits. Borehole MS-9 has a highly elevated NaCl content and it is possible that it might receive a more direct flow from the Mercia Mudstone, accounting for the much higher concentration of most ions and much increased SEC.

The E-W variation in groundwater solutes and geochemical conditions observed across the Middle Sands and to a lesser extent, the Sherwood Sandstone (Fig. 6.5), appears to be related to the NE-SW trending fault system, which depending on conditions, could act as either a conduit or a seal for groundwater. The more reducing and anoxic waters from the eastern part of the aquifer system may result from sealing along the fault and reduced water flow. Conditions in the most easterly borehole sites in the Middle Sands correspond closely to those of the Sherwood Sandstone in terms of temperature, Na and Cl concentrations, and δ^{13}C(DIC) values. Redox conditions (Eh) and DO concentration generally increase westward in the Middle Sands aquifer and eastward in the Sherwood Sandstone aquifer. From east to west, waters within the Middle Sands aquifer transition from reducing, low NaCl to more oxidising waters with slightly increased NaCl.

The concentration of CH_4 exhibits relatively little variation from E-W; however, if anomalously high CH_4 levels in borehole MS-7 are excluded then there is a minor increase of CH_4 closer to the fault. The amount of CH_4 is known to increase along fault zones (Boothroyd et al., 2017) and high levels of dissolved CH_4 have been linked to faults in other areas (e.g., Kreuzer et al., 2018; Nicot et al., 2017); however, in other cases there can be brine seepage along a fault, but not CH_4 even if CH_4 is known to exist at depth (Bordeleau et al., 2018). The absence of CH_4 along a fault zone may be due to the depth of the fault and a failure to intersect CH_4-bearing strata. The Woodsfold fault system in Lancashire is known to crosscut the CH_4-rich Bowland Shale (Arup-Cuadrilla, 2014) although

migration of CH_4 from such depths along the fault system has not been reported previously. Therefore any increase in CH_4 towards the fault could be due either to migration along the fault from depth or from increased anoxic conditions along the fault zone, due to sealing along the fault.

The $\delta^{13}C$(DIC) values within the Sherwood Sandstone cluster around a mean of -13 ‰, a value which is indicative of a portion of DIC being derived from dissolution of marine-derived carbonate (Clark and Fritz, 1997). The Middle Sands aquifer contains more variable $\delta^{13}C$(DIC) values ranging from $\sim$ -20 ‰ to -13 ‰, and generally becoming more negative in a westward direction. The lower values are consistent with DIC originating from CO_2 produced via plant or soil respiration or aerobic oxidation of organic matter within the aquifer (Clark and Fritz, 1997). The range of values likely results from a mixture of DIC derived from aerobic respiration (possibly CO_2 originating in soils above the Middle Sands aquifer) and DIC from carbonate dissolution at depth that has migrated in a westward direction; i.e. an open system re-equilibration between DIC and soil CO_2.

These factors collectively suggest that two geochemically distinct areas or sources of groundwater exist within the Middle Sands aquifer that need to be considered when attempting to establish baseline conditions with respect to CH_4. One area or source originates in the Middle Sands aquifer with potential for localised influence from the underlying Mercia mudstones. The second is derived from a deeper source or area characterised by more reducing conditions and which migrates upward through the Woodsfold fault system.

A range of geochemical conditions was observed within the Sherwood Sandstone aquifer; however, patterns with respect to local features such as the Woodsfold fault system are less clear. Again, it appears that the most reducing sites are closest to the fault, which may be due to upward migration of deeper waters or possibly confinement due to sealing along the fault and restriction of water movement, resulting in low oxygen conditions. The Sherwood Sandstone boreholes in the east of the area (i.e., SS-1, SS-2 and SS-5), farthest from the Woodsfold fault, generally contain water that is more oxidising and typical of an unconfined aquifer. The DO levels were variable at SS-2 (three different orders of magnitude during three separate visits), the CH_4 concentration consistent, and $\delta^{13}C(CH_4)$ values variable and generally decreasing in concert with DO. It appears that the sites farther from the fault system exhibit conditions typical of an unconfined aquifer whereas boreholes situated closer to the fault are more reducing, and therefore more typical of confined conditions.

6.4.2 Methane production and oxidation processes

Methane concentration generally increases with decreasing Eh (Fig. 6.6d), which is expected as CH_4 production increases under conditions that are more reducing and anoxic. The $\delta^{13}C(CH_4)$ and $\delta^2H(CH_4)$ values correlate more strongly with CH_4 ($r^2 = 0.29$ for log CH_4 versus Eh; $r^2 = 0.50$ for log CH_4 versus $\delta^{13}C(CH_4)$; $r^2 = 0.45$ for log CH_4 versus $\delta^2H(CH_4)$). The correlation of $\delta^{13}C(CH_4)$ and $\delta^2H(CH_4)$ values with CH_4 is expected because bacterial CH_4 oxidation preferentially removes and consumes $^{12}C^1H_4$, increasing $\delta^{13}C(CH_4)$ and $\delta^2H(CH_4)$ values.

Groundwater containing CH_4 with more positive $\delta^{13}C(CH_4)$ and $\delta^2H(CH_4)$ values generally also has high concentrations of DO (Fig. 6.7c and d), which promotes bacterial CH_4 oxidation. The exception of borehole MS-9, with its low DO, but high SO_4^{2-} concentration and the most positive $\delta^2H(CH_4)$ values, is likely due to DO consumption linked to CH_4 oxidation followed by a transition to anaerobic CH_4 oxidation using sulphate as an electron acceptor. The concentration of CH_4 is still relatively high and it is possible that CH_4 production may be ongoing concurrently because of the low DO conditions.

A correlation between $\delta^{13}C(CO_2)$ and $\delta^{13}C(CH_4)$ values, and $\delta^2H(H_2O)$ and $\delta^2H(CH_4)$ values, is expected in anaerobic environments where 'pristine' CH_4 exists that has been produced via CO_2/H_2 methanogenesis because both C and D enrichment factors are likely to be relatively constant in a spatially restricted production volume (Conrad et al., 2011). However, there is a lack correlation between these parameters and moreover, no correlation between C and H isotope fractionation and temperature. Values of $\alpha_{CO_2\text{-}CH_4}$ and ΔG exhibit large variation albeit plot close to the expected trend for hydrogenotrophic methanogenesis. Regardless, the strong correlation between $\delta^2H(CH_4)$ and $\delta^{13}C(CH_4)$ values ($r^2 = 0.85$ for all sites, $r^2 = 0.92$ for MS sites only and $r^2 = 0.80$ for SS sites only), provides compelling evidence that CH_4 within the aquifer is a residual of a common CH_4 source (or combination of well-mixed sources) that has been subjected to different degrees of methanotrophy (Fig. 8 c and d). For boreholes in the Middle Sands aquifer, $\delta^2H(CH_4)$ values increase 11.7 ‰ for every per mil increase in $\delta^{13}C(CH_4)$ values, which is comparable to relationships reported for bacterial CH_4 oxidation experiments (Coleman et al., 1981). Similar ranges of $\delta^{13}C(CH_4)$ and $\delta^2H(CH_4)$ values have been reported in freshwater environments (Cadieux et al., 2016; Sawakuchi et al., 2016) and attributed to CH_4 oxidation.

Groundwater CH_4 from one Middle Sands borehole site; MS-10 deviates from the $\delta^{13}C(CH_4)$ and $\delta^2H(CH_4)$ relationship in Fig 6.8 d and plot below the regression line. Groundwater from Middle Sands borehole MS-10 is likely influenced by effluent from a local landfill site and has twice the H_2 concentration of the next

highest Middle Sands site (labelled 'MS – landfill influenced' in Fig. 6.8d).

High H_2 concentrations impact the energetics of anaerobic systems, increasing availability of free energy and reducing the reversibility of the system, which results in smaller C fractionation (Hattori et al., 2012; Valentine et al., 2004). The $\delta^2H(CH_4)$ value also may be affected by elevated levels of H_2, though only under high growth rate conditions when H_2 consumption is as rapid as transmembrane H_2O transport, resulting in lower a $\delta^2H(CH_4)$ value, due to highly negative $\delta^2H(H_2)$ values affecting intracellular $\delta^2H(H_2O)$ values as a result of hydrogenase catalysed isotope exchange (Kawagucci et al., 2014; Okumura et al., 2016). Therefore, under higher energy conditions, the initial $\delta^{13}C$ value of CH_4 may be higher, and if the methanogenic growth rate is high, the initial $\delta^2H(CH_4)$ value may also be lower (Sugimoto and Fujita, 2006). If the ratio of C- and H-isotopic fractionation during subsequent methanotrophy remains the same as elsewhere in the aquifer system, the resulting $\delta^{13}C(CH_4)$ and $\delta^2H(CH_4)$ value will remain shifted to the right of the regression line (Fig. 6.8 d). It is also possible that the proportion of methane produced by an alternative pathway, such as acetoclastic methanogenesis, has increased.

The relationship between C and H isotopic compositions indicate that bacterial methanotrophy is the process that has the greatest impact on $\delta^2H(CH_4)$ and $\delta^{13}C(CH_4)$ values in the Lancashire groundwater system. Consequently, the poor fit of the relationship between $\alpha_{CO_2\text{-}CH_4}$ and ΔG (Fig. 6.10) can be explained by a spatial separation between methanogenesis and methanotrophy. Calculation of ΔG reflects conditions in parts of the aquifer that are likely dominated by methanotrophy or the net effects of CH_4 transport and methanotrophy. Aquifer conditions where CH_4 is produced are likely to be different, in particular, for the boreholes containing high levels of dissolved O_2 where methanogenesis is unlikely to occur. Moreover, given the extent of water transport in the system that likely occurs prior to abstraction at each borehole there is ample opportunity for CO_2/HCO_3^- to enter the system, which again is unrelated to conditions at the site of CH_4 production in the aquifer. Differences in H_2 concentrations and gradients would also affect the energetics. For example, if there is less H_2 in the CH_4 production microsites, the ΔG calculation shown in Fig. 6.10 would not represent the actual energetics of the system.

Finally, boreholes that exhibit the least evidence for bacterial CH_4 oxidation also correlate with relatively high ε_C and ε_H values (60 to 70 ‰ and 200 to 300 ‰, respectively). These ε values fall within the ranges of primary stable isotope fractionation for the hydrogenotrophic methanogenic pathway (Conrad, 2005; Whiticar et al., 1986).

6.4.3 Variations over time

Lateral spatial variations in solute content and geochemical conditions across the area can be explained by proximity to the Woodsfold fault system; however, the driver(s) of temporal variations in groundwater chemistry are less clear. Changes were observed in CH_4 concentration, $\delta^{13}C(CH_4)$ values and other parameters at some boreholes between sampling visits. At boreholes SS-1, SS-4 and MS-2 a decrease in CH_4 concentration was accompanied by an increase in $\delta^{13}C(CH_4)$ values, which is consistent with an increase in rates of CH_4 oxidation relative to CH_4 production or transport. Conversely, where an increase in CH_4 concentration occurred with time it was accompanied by a corresponding decrease in $\delta^{13}C(CH_4)$ values, reflecting input of newly produced CH_4 or an influx of exogenous CH_4 in excess of the capacity for methanotrophy in the aquifer. Large increases in CH_4 concentration and correspondingly large decreases in $\delta^{13}C(CH_4)$ values were measured at boreholes SS-3 and MS-6. At MS-6 there was an increase in DO, a decrease in pH and a concurrent increase in CO_2(aq) (from 47 to 128 mg L^{-1}) during the visit prior to the increase in CH_4 production. These changes indicate an influx of new water that is geochemically distinct, in particular, with respect to its O_2 and CO_2 content. The influx was accompanied by an increase in CH_4 concentration, which either must be derived from in situ production or the new water. If increased CH_4 production occurred, it coincided with decreases in Eh and DO to levels below conditions that existed prior to the influx of potentially OM-rich water. At borehole SS-3, there was no obvious change in site conditions prior to the increase in CH_4 concentration, which may have been short-lived and was not captured by sampling. An alternative explanation is that the influx of CH_4 was derived from deeper biogenic sources.

Conditions in borehole MS-7 also varied with time; however, unlike other borehole sites, the change in CH_4 concentration was not directly correlated to $\delta^{13}C(CH_4)$ values. The absence of a concurrent shift in stable isotope values suggests the process that decreased CH_4 levels was non-fractionating and may have been simple ingress of CH_4-poor water, which caused an apparent CH_4 concentration decrease due to dilution. The available data do not permit a rigorous examination of the cause; however, the observation is important because it suggests that processes other than methanogenesis and methanotrophy can influence the amount and stable isotope composition of CH_4 in the aquifer system on relatively short timeframes.

6.4.4 Oxidation models

In a closed system, any CH_4 lost would be via CH_4 oxidation, which would be reflected in the change in CH_4 concentration and stable C and H isotope compositions. In an open system, there can be influx and export of CH_4 in addition to methanotrophy and if a balance is achieved, the CH_4 concentration may not change perceptibly with time. The calculated F_{ox} for open system models often exceeds unity, which means that more CH_4 is oxidised that the amount that enters and/or is produced in the system, indicating that a fully open system model is inappropriate for these sites.

For sites SS-1 and SS-4, a fully closed model is unable to account for the decrease in CH_4 concentration with time even when using a large α_{ox}. When using a α_{ox} of 1.022, the decrease in CH_4 concentration is between 3.5 and 7 times greater than would be expected. With an α_{ox} of 1.01, the factor of change in CH_4 concentration can be reduced to 2 - 3 times greater than what would be expected, indicating that the system is at least partially open. Hence, it is likely that the situation in the Lancashire aquifer system falls somewhere between open and closed conditions whereby CH_4 can be lost via CH_4 oxidation and also via transport from the aquifer. The latter could include transport to the atmosphere and in a dissolved form within the aquifer. Both SS-1 and SS-4 boreholes are within the unconfined section of the Sherwood Sandstone aquifer and therefore transport within and out of the system is a reasonable expectation. Using the mid-range C-isotopic fractionation scenarios, the model suggests approximately 1/3 of CH_4 is lost via CH_4 oxidation and 2/3 is lost via transport.

In summary, it appears that CH_4 is lost from the Lancashire groundwater system via both oxidation and transport processes. The large range of $\delta^{13}C(CH_4)$ and $\delta^{2}H(CH_4)$ values indicates varying amounts of CH_4 oxidation with borehole sites exhibiting the most positive $\delta^{13}C(CH_4)$ and $\delta^{2}H(CH_4)$ values experiencing >99% removal of CH_4 via bacterial oxidation.

6.5 Conclusions

Local geology, in particular the Woodsfold fault system, appears to significantly impact geochemical conditions and groundwater chemistry in the Lancashire area. Highly reducing waters derived from deeper groundwater sources mixes with oxidising waters in the unconfined aquifers. The mixing is particularly evident in the Middle Sands aquifer, which covers the majority of the study area, and is accessible through the E-W transect of boreholes. Eh and DO increase in the western part of the area while H_2 concentration and $\delta^{13}C(DIC)$ values decrease, further

supporting the interpretation of mixing of geochemically distinct sources of water within the aquifer. The variable redox conditions across the aquifer results in varying amounts of CH_4 oxidation and thus, large ranges and co-variations in $\delta^{13}C(CH_4)$ and $\delta^{2}H(CH_4)$ values. Oxidation models indicate that CH_4 concentration may be controlled by both CH_4 oxidation rate and transport of CH_4 within, and potentially out, of the aquifer. This study demonstrates that the complexity of physical and geochemical conditions within the Lancashire groundwater system requires characterisation of solutes in the aquifer on temporal scales that will capture short-term impacts and spatial scales that take into account major geological features and formations. The aquifer also appears to host significant populations of methanotrophic bacteria that may be capable of remediating modest quantities of CH_4 released into the groundwater system as a result of shale gas development in the region.

Chapter 7

Assessment of the isotope biogeochemistry of CH_4 in major UK aquifers

Summary

The aim of assessing isotope biogeochemistry of CH_4 in UK aquifers, is to explore dominant geological and environmental controls on groundwater $\delta^{13}C(CH_4)$ and $\delta^2H(CH_4)$ values and to establish the degree of variability in the stable isotope composition of CH_4. There is a combination of CH_4 production and consumption processes that may occur within aquifers. These will depend on varying geochemistry and redox conditions. There may also be mixing of various sources of both microbial and thermogenic CH_4. This combination of processes and potential mixing of microbial and thermogenic CH_4 will contribute to variation in stable isotope composition within and across aquifers. The boreholes sampled for stable isotope analysis of CH_4 are a subset of sites investigated as part of the BGS CH_4 baseline survey. Sites were selected to encompass a variety of conditions across several aquifers, including the geographical breadth of each aquifer and a wide range of CH_4 concentrations (within analytical limits). A clear correlation of $\delta^{13}C(CH_4)$ of $\delta^2H(CH_4)$ was seen across aquifers, with the exception of sites with known thermogenic sources. Groundwater containing the highest CH_4 concentrations tended to have a higher proportion of thermogenic CH_4 and hence more positive $\delta^{13}C(CH_4)$ values. Correlation of $\delta^2H(H_2O)$ and $\delta^2H(CH_4)$ was observed for samples containing thermogenic sources of CH_4. In areas of little or no thermogenic source, the CH_4 isotope composition reflects varying degrees of methanotrophy, exhibited as a clear correlation of $\delta^{13}C(CH_4)$ and $\delta^2H(CH_4)$. Whereas, if there is a thermogenic source within an aquifer, isotope compositions reflect a degree of mixing with microbial sources within the aquifer and some post-formation H isotope exchange with water, establishing a correlation of $\delta^2H(H_2O)$ and $\delta^2H(CH_4)$.

7.1 Introduction

This study investigated the isotope biogeochemistry of a subset of groundwater sites (Fig. 7.1) from the UK-wide CH_4 baseline survey (Bell et al., 2017) to improve understanding of CH_4 production and alteration processes in UK aquifers.

Initially a subset of 30 sites were short-listed to acquire coverage of all major aquifers containing dissolved CH_4. Due to logistical issues, it was not possible to visit all the originally chosen sites and subsequently either a replacement site was selected or the site was abandoned. In total 22 of the 30 sites were sampled and with inclusion of data from six boreholes samples from previous campaigns, the final site total was 28 (Tables 7.1 and 7.2). All Oolitic limestone sites sampled by BGS contained CH_4 below the cut-off for stable isotope analysis, therefore they were excluded from the list.

Groundwater was analysed for CH_4 concentration, H_2 concentration, $\delta^{13}C(CH_4)$, $\delta^{2}H(CH_4)$, $\delta^{13}C(DIC)$, $\delta^{2}H(H_2O)$ and $\delta^{18}O(H_2O)$, and field measurements for pH, SEC, DO, ORP and total alkalinity were taken. Additional geochemical data were acquired from the BGS baseline survey from sampling conducted during 2012 to 2015. Details about sampling and analytical methods are presented in Chapter 3.

Analytical limitations required that a threshold of 3 µg CH_4 L^{-1} be used for stable isotope analysis of CH_4 when selecting sites; however, in some areas where CH_4 was present at lower concentrations it was possible to lower the cut-off concentration through longer sampling and processing times. Analysis of $\delta^{2}H(CH_4)$ values was possible for samples containing 2-3 µg CH_4 L^{-1}. Analysis of $\delta^{13}C(CH_4)$ values was possible for samples containing 0.5 to 1 µg L^{-1}.

Characterisation of CH_4 across UK aquifers was conducted to address project objectives O1, O2, O3 and O5, and the data will also contribute towards evaluation of objective O4. There is the opportunity to contribute to hypotheses H1, H2, H3, H4 and H5.

7.2 UK Aquifers

Water supply in the UK is derived from a combination of surface water and groundwater abstraction, the proportions of each varying across the country and depending on available water resource and public demand. Major UK aquifers are the Carboniferous Limestone, Sherwood Sandstone, Oolitic Limestone, Lower Greensand and Chalk (Allen et al., 1997). These aquifers all were investigated in this study with the exception of the Oolitic Limestone, which does not contain

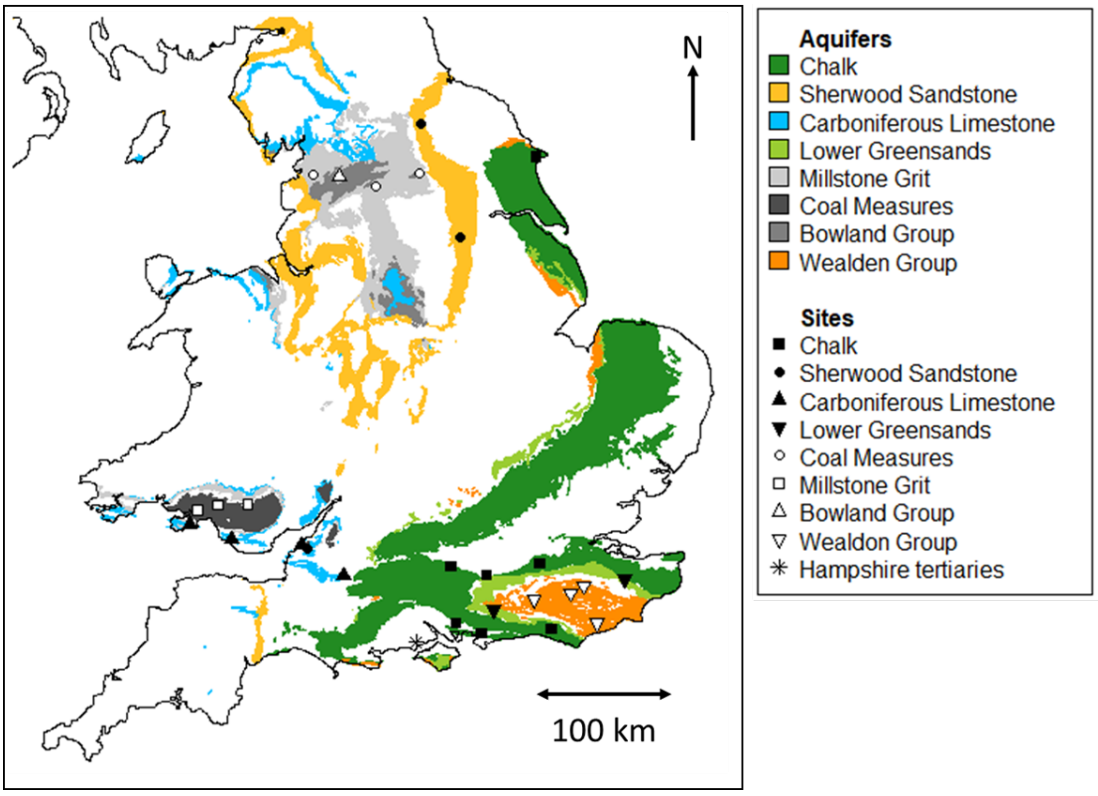

Figure 7.1 Bedrock geology of major UK aquifers and locations of borehole sites sampled in this study, shapefiles for geological formations obtained from British Geological Survey (2007)

CH_4 at levels sufficient for analysis. Additional borehole sites were situated within the Coal Measures, Millstone Grit, Bowland Group and Barton Group. Table 7.1 provides a summary of aquifers, borehole locations and other background details, including BGS baseline geochemical data for the sites investigated in this study and more details on each of the aquifers is provided below.

The Chalk was deposited during the Upper Cretaceous during a marine transgression over what is now southern England. It is formed from microscopic algae and shell fragments ('coccoliths') and is almost pure limestone, consisting of 98 % $CaCO_3$ (Hancock, 1975). The highly porous aquifer, which consists of the top 60 m of the Formation, has a low matrix permeability, with the majority of groundwater movement occurring through fracture flow. The majority of storage also is within fractures due to restrictive flow in the Chalk matrix (Allen et al., 1997). The median transmissivity is 540 m^2 d^{-1} and the greatest transmissivity values occur in the harder Chalk of Yorkshire and Lincolnshire (MacDonald and Allen, 2001). In the Thames basin, the mean hydraulic conductivity is 45.4 m d^{-1} (Allen et al., 1997). There is a relatively large seasonal variation in the water table level compared to other aquifers, which may result in surface flow as well as flow within the aquifer.

The Sherwood Sandstone was deposited in the late Permian to the early Triassic in a continental setting and consists largely of fluvial and aeolian deposits. Groundwater flow through the aquifer is both intergranular and via fracture flow, varying both laterally and vertically, and therefore predicting aquifer properties is complex. Allen et al. (1997) report hydraulic conductivities from 10^{-6} to 20 m d^{-1} (median = 0.56 m d^{-1}). Porosity ranges from 2 to 35 % (median 26 %) and median transmissivity is 206 m^2 d^{-1} (Allen et al., 1997).

The Lower Greensand Group was deposited in a mainly shallow marine and coastal environment during the Lower Cretaceous. Transmissivity of the Lower Greensand is 33 to 3400 m^2 d^{-1} (mean and median = 270 m^2 d^{-1}). Storage coefficient estimates are 10^{-5} to 0.08 (mean and median = $6x10^{-4}$) (Allen et al., 1997). Hydraulic conductivity is 10^{-4} to 10 m d^{-1} (mean 0.46 m d^{-1} and median = 0.53 m d^{-1}). Porosity is 6 to 41 % (median and mean = 29.5 % and 28 %, respectively) (Allen et al., 1997).

The Carboniferous Limestone was deposited during the Dinantian of the Lower Carboniferous. The permeability within the Carboniferous Limestone aquifer is almost entirely via fracture flow, and in karstic areas substantial flow occurs through large conduits, resulting in a highly variable transmissivity. Therefore, hydraulic properties are only useful locally. Pump tests in the Mendips have yielded an average transmissivity of 433 m^2 d^{-1} (Allen et al., 1997).

The Bowland Shale Group and the Millstone Grit Group were deposited in the Namurian (Upper Carboniferous) in deltaic, alluvial and deep marine environments. The Millstone Grit consists largely of sandstone units interbedded with argillaceous units. The underlying Bowland Shale Group consists of mudstones with varying proportions of fine-grained turbiditic limestones, sandstones and siltstones (Jones et al., 2000). Groundwater flow in both the Millstone Grit and Bowland Shale groups is mainly through joints and fractures, which are variable across the Groups.

The Coal Measures were deposited during the Westphalian (Upper Carboniferous) and rest unconformably on the Millstone Grit Group. The Lower and Middle Coal Measures are predominantly argillaceous with sandstone deposits rare and localised, but thick fluvial sandstone deposits are present in the Upper Coal Measures with subordinate argillaceous horizons and thicker coals (Jones et al., 2000). The sandstones are well-cemented and permeability is mostly via fracture flow.

The Barton Group within the Hampshire Basin was deposited in the late Eocene on a marine shelf environment. It consists of fossiliferous clay, fine-grained sand and sandy clay, and ranges in thickness from 20 to 70 m (Neumann et al.,

2004). Permeability is predominantly intergranular and median transmissivity across the basin, including other formations, is 72.5 m^2 d^{-1} (Jones et al., 2000).

7.3 Results

7.3.1 Sampling irregularities

At borehole sites WG-1 and CM-3, significant quantities of bubbles were observed in water outflow. The water level at WG-1 decreased with time and if the water level reached the depth of the pump, air bubbles in the flow would have resulted. For CM-3, the outflow pipe was cracked, which was sealed prior to sampling; however, it is possible that some level of air contamination may have occurred. For both sites, samples for CH_4 concentration were retrieved bubble-free in glass vials; however, samples for $\delta^{13}C(CH_4)$ and $\delta^{2}H(CH_4)$ analysis were collected in opaque polymer-coated foil bags and it is possible bubble or air entrainment occurred.

All sites in the Chalk and Sherwood Sandstone aquifer, and two of four sites in the Carboniferous limestone contained insufficient CH_4 (<0.5 µg L^{-1}) to enable analysis of $\delta^{13}C(CH_4)$ via polymer foil bags.

Table 7.1 Location details and partial baseline geochemistry[b] for groundwater study sites in the UK.

Area	Site	Aquifer	Easting	Northing	Depth (m)	Ca^{2+} (mg L^{-1})	Mg^{2+} (mg L^{-1})	Na^{+} (mg L^{-1})	K^{+} (mg L^{-1})	Cl^{-} (mg L^{-1})	SO_4^{2-} (mg L^{-1})	Mn (µg L^{-1})	Fe (µg L^{-1})
South	CHK-1	Chalk	538	109	-	95.7	2.43	15.9	1.17	29.9	15.6	2.5	47
	CHK-2	Chalk	528	159	135	128	2.43	11.4	1.4	24	11.3	1.2	2
	CHK-3	Chalk	486	149	-	-	-	-	-	-	-	-	-
	CHK-4	Chalk	483	105	30	113	3.69	13.3	1.4	28.1	19.5	1.2	10
	CHK-5	Chalk	463	112	95.4	114	4.56	10.8	1.7	23.3	16	0.6	4
	CHK-6	Chalk	459	155	152	-	-	-	-	-	-	-	-
	LGS-1	Lower Greensands	595	149	-	70.8	4.86	14.9	2	41.6	30.6	1.1	40
	LGS-2	Lower Greensands	493	122	-	91.8	2.23	12.6	1.75	23.5	31.7	3.6	80
	WG-1	Wealden group (TW[a])	563	142	-	10.3	3.10	80.0	1.42	24.6	38.1	240	2153
	WG-2	Wealden group (TW[a])	524	131	-	1.4	0.22	234	0.85	20.4	31.1	13.0	88
	WG-3	Wealden group (AB[a])	574	114	-	46	5.48	40.2	1.7	39.6	34.3	514	3846
	WG-4	Wealden group (AB[a])	553	137	-	17.7	4.95	28.0	1.43	24.2	22.3	1428	2881
	HT-1	Hampshire Tertiaries	432	97	-	69.5	13.6	13.6	7.67	24.6	66.5	20.8	383
	SS-1	Sherwood Sandstone	347	168	48.7	12.1	13.7	2.67	27.6	23.0	19.7	<1	<1
	CL-1	Carboniferous Limestone	376	148	9.3	9.34	9.8	1.96	17.2	24.3	28.5	1	1.0
	CL-2	Carboniferous Limestone	343	172	33.5	35.4	22.4	2.85	45.0	33.0	21.7	<1	<1
South	CM-1	Coal Measures	263	200	50	52.6	25.0	30.9	15.7	77.3	21.4	362	2823
Wales	CM-2	Coal Measures	278	203	183	6.9	1.32	45.8	0.89	12.8	3.14	4.6	243
	CM-3	Coal Measures	301	203	-	12.2	11.5	6.9	4.8	6.57	38.4	1017	5263
	CL-3	Carboniferous Limestone	257	189	50	103	25.8	30.5	1.33	63.1	21.9	1.1	4
	CL-4	Carboniferous Limestone	289	177	10	79.2	10.4	14.8	3.40	21.8	20.2	40.9	83
Lancashire	BG-1	Bowland Group	374	452	-	114	7.13	9.8	3.5	9.07	33.1	111	1855
	MG-1	Millstone Grit	355	454	-	71.1	9.74	11.2	1.5	17.9	14.9	83.9	164
	MG-2	Millstone Grit	400	445	-	49.6	8.93	46.0	5.67	19.5	0.445	37.0	188
East	MG-3	Millstone Grit	432	454	-	38.1	16.4	22.3	3.60	35.8	31.7	938	17219
Midlands	CHK-7	Chalk	517	469	57.7	107	4.17	15.9	1.2	32.7	25.9	<0.2	<1
	SS-2	Sherwood Sandstone	433	493	97.8	127	46.4	29.3	2.24	36.0	225	5.3	7
	SS-3	Sherwood Sandstone	463	406	162	54.1	22.4	14.8	2.45	39.1	69.8	0.5	<1

[a]TW – Tunbridge Wells Sand; AB – Ashdown Beds [b]Geochemistry data from BGS baseline survey 2012-2015 (BGS, unpublished data)

Table 7.2 Data summary for UK boreholes investigated in this study

Site	Sample date	T (°C)	pH	SEC (µS cm^{-1})	DO (mg L^{-1})	Eh (mV)	HCO_3^- (mg L^{-1})	H_2 (µg L^{-1})	CH_4 (µg L^{-1})	$\delta^{13}C$ (CH_4) (‰)	δ^2H (CH_4) (‰)	Range (‰)	$\delta^{13}C$ (DIC) (‰)	Range (‰)	δ^2H (H_2O) (‰)	$\delta^{18}O$ (H_2O) (‰)
CHK-1	21/10/2014	11.9	7.42	577	-	-	246	-	0.5 ±0.08	-	-	-	-14.1	-14.2 to -14.1	-40.3	-6.4
CHK-2	07/08/2017	12.3	7.01	647	-	332	313	1 ±0.2	0.07 ±0.09	-	-	-	-12.1	-	-47.9	-7.2
CHK-3	03/08/2017	12.1	7.05	686	1.35	372	336	1 ±0.2	bdl	-	-	-	-12.1	-12.2 to -12.1	-44.2	-6.8
CHK-4	17/07/2017	12.7	7.16	604	7.40	381	323	1 ±0.3	0.05 ±0.01	-	-	-	-13.1	-	-41.0	-6.4
CHK-5	17/07/2017	14.2	7.07	626	4.28	390	285	1 ±0.1	bdl	-	-	-	-10.1	-10.2 to -9.9	-42.6	-6.4
CHK-6	10/09/2017	11.4	7.12	634	7.09	334	295	1 ±0.1	0.04 ±0.03	-	-	-	-12.3	-12.5 to -12.0	-45.1	-6.9
LGS-1	11/08/2017	12.1	6.68	463	6.25	350	116	19 ±24.9	0.02 ±0.004	-	-	-	-15.1	-15.3 to -14.9	-45.9	-7.0
LGS-2	21/10/2014	11.5	7.36	540	-	-	202	-	0.42 ±0.13	-38.5 ±0.11	-	-	-14.1	-14.2 to -14.0	-41.1	-6.4
WG-1	25/09/2014	12.5	6.95	488	-	-	190	-	6.1 ±0.61	-64.4 ±2.84[a]	-	-	-15.8	-15.9 to -15.7	-	-
WG-1	24/08/2017	12.4	6.80	494	4.93	256	187	4 ±4.9	4.5 ±0.24	-75.2 ±1.52	-175	-177 to -174	-13.4	-13.5 to -13.4	-44.3	-6.9
WG-2	31/08/2017	14.3	8.86	988	0.20	44	507	23 ±9.9	39.6 ±1.56	-43.1 ±3.65	57	56 to 59	-11.7	-11.8 to -11.7	-50.6	-7.7
WG-3	25/08/2017	12.8	6.62	475	0.48	192	159	26 ±1.7	14.0 ±0.40	-56.3 ±2.77	-41	-42 to -39	-13.0	-	-39.9	-6.4
WG-4	25/09/2014	11.5	6.53	307	-	-	105	-	30.3 ±2.44	-58.8 ±1.26[a]	-	-	-18.5	-18.6 to -18.4	-	-
WG-4	24/08/2017	12.0	6.39	293	0.17	198	83	4 ±1.2	2.8 ±0.19	-55.9 ±0.45	-150	-	-15.9	-	-42.5	-6.6
HT-1	17/10/2014	14.7	7.82	535	-	-	191	-	12.7 ±3.03	-79.8 ±0.79	-	-	-13.4	-13.6 to -13.2	-	-
HT-1	21/07/2017	15.1	7.83	480	0.14	52	181	7 ±4.2	2.7 ±0.11	-78.0 ±2.19	-197	-198 to -197	-12.2	-	-45.5	-7.1
SS-1	10/09/2014	12.2	7.28	726	-	-	365	-	0.45 ±0.15	-	-	-	-16.2	-16.3 to -16.1	-	-
CL-1	10/09/2014	11.4	7.20	684	-	-	332	-	0.49 ±0.24	-36.9 ±0.08	-	-	-15.5	-15.5 to -15.4	-	-
CL-2	10/09/2014	13.6	7.30	851	-	-	386	-	0.54 ±0.17	-	-	-	-14.6	-14.8 to -14.7	-35.7	-5.6
CM-1	28/08/2014	-	-	-	-	-	214	-	50.4 ±8.23	-	-	-	-17.2	-17.6 to -17.0	-	-
CM-1	27/11/2014	11.1	6.82	677	-	-	212	-	86.8 ±5.44	-54.4 ±0.94[a]	-	-	-17.1	-17.1 to -17.0	-	-
CM-1	13/07/2017	11.6	6.69	658	0.09	37	200	13 ±9.3	90.5 ±12.0	-54.8 ±2.28	-121	-122 to -120	-14.4	-	-32.1	-5.0
CM-2	28/08/2014	-	-	-	-	-	246	-	649±8.1	-34.0 ±0.32[a]	-	-	-15.5	-15.8 to -15.7	-40.1	-6.1
CM-2	27/11/2014	12.1	7.14	328	-	-	192	-	136 ±84	-34.3 ±0.49[a]	-	-	-15.7	-15.9 to -15.7	-37.2	-5.9
CM-2	12/07/2017	12.7	7.19	410	0.65	164	199	6 ±1.4	1447 ±130	-38.3 ±2.18	-99	-99 to -98	-14.0	-14.0 to -13.9	-38.3	-6.0
CM-3	20/06/2017	14.2	5.97	217	8.53	286	569	4 ±0.3	1.2 ±0.04	-43.2 ±0.67	-189	-190 to -188	-14.1	-14.2 to -14.0	-43.6	-6.6
CL-3	27/11/2014	11.6	7.13	805	-	-	410	-	0.56 ±0.07	-36.1 ±0.01	-	-	-14.2	-14.3 to -14.2	-40.9	-6.3
CL-4	28/08/2014	-	-	-	-	-	232	-	0.60 ±0.09	-	-	-	-16.0	-16.1 to -15.9	-41.5	-6.3
BG-1	04/09/2017	13.7	7.11	584	0.36	120	324	5 ±1.0	10.6 ±0.69	-72.0 ±5.97	-196	-199 to -194	-13.8	-	-51.7	-7.7
MG-1	04/09/2017	12.5	6.87	446	0.56	374	241	6 ±1.8	0.22 ±0.02	-	-	-	-13.2	-13.4 to -13.1	-54.7	-8.1

Table 7.2 continued

Site	Sample date	T (°C)	pH	SEC (µS cm^{-1})	DO (mg L^{-1})	Eh (mV)	HCO_3^- (mg L^{-1})	H_2 (µg L^{-1})	CH_4 (µg L^{-1})	$\delta^{13}C$ (CH_4) (‰)	δ^2H (CH_4) (‰)	Range (‰)	$\delta^{13}C$ (DIC) (‰)	Range (‰)	δ^2H (H_2O) (‰)	$\delta^{18}O$ (H_2O) (‰)
MG-2	05/09/2017	12.6	7.60	556	0.39	105	315	4 ±1.5	1432 ±43	-78.0 ±0.48	-251	-252 to -249	-15.2	-	-56.1	-8.2
MG-3	05/09/2017	11.9	6.58	535	0.30	119	214	37 ±2.7	1368 ±69	-48.2 ±4.34	-132	-	-16.3	-	-43.2	-6.6
CHK-7	26/06/2017	10.8	7.24	635	8.60	422	171	12 ±5.1	0.05 ±0.03	-	-	-	-12.9	-	-48.2	-7.2
SS-2	27/06/2017	11.6	7.16	1105	2.70	297	329	9 ±3.2	0.15 ±0.07	-	-	-	-11.3	-11.3 to -11.2	-52.6	-7.6
SS-3	27/06/2017	11.0	7.83	574	9.22	393	107	8 ±1.6	0.06 ±0.04	-	-	-	-12.1	-12.2 to -12.1	-44.8	-7.0

[a]previously reported in Bell et al. (2017)

7.3.2 Geochemistry

Borehole sites within the Chalk, Lower Greensand and Hampshire Tertiaries (Fig. 7.2) host Ca-HCO_3 type waters. The Sherwood Sandstone, Carboniferous Limestone and Millstone Grit aquifers also contain mostly Ca-HCO_3 type waters but with greater ion exchange giving rise to Ca/Na-HCO_3 type waters. Aquifers in the Wealden Group and Coal Measures host higher maturity Na-HCO_3 type waters.

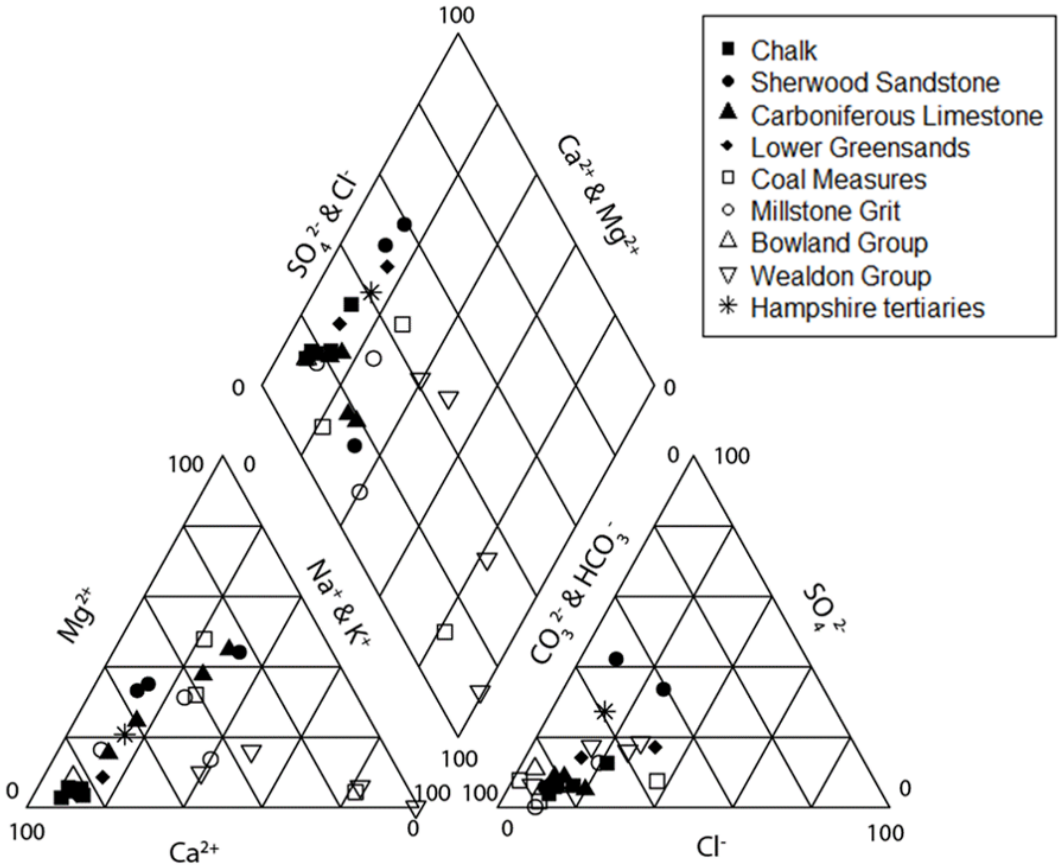

Figure 7.2 Piper diagram classification of groundwater geochemistry for aquifers investigated in this study. Water geochemistry range from fresher Ca-HCO_3 type common in shallow aquifers to mature Na-HCO_3 type where more extensive ion exchange has occurred.

7.3.3 CH_4 and redox conditions

The aquifers collectively exhibit a common trend of increasing Eh correlating with higher DO levels and a decrease in CH_4 concentration (Fig. 7.3). The concentration of H_2 does not correlate well with Eh but there is a positive correlation between H_2 and CH_4 and negative correlation between DO with CH_4 (Fig. 7.4). Boreholes containing CH_4 with more positive $\delta^{13}C$ and $\delta^{2}H$ values typically also

have relatively higher concentrations of DO, SO_4^{2-}, Mn and/or Fe (Figs. 7.5 and 7.6). The exceptions are sites within the Coal Measures, which appear to contain a significant component of thermogenic CH_4.

7.3.4 Isotope relationships

There is no strong relationship between $\delta^{13}C(CO_2)$ and $\delta^{13}C(CH_4)$ or $\delta^2H(CH_4)$ and $\delta^2H(H_2O)$ (Fig. 7.7), or C- or H- fractionation versus temperature (Fig. 7.8) in the UK-wide data. The lack of overarching relationships for these parameters probably reflects the complexity of factors within the different aquifers that contribute to controlling CH_4 production and alteration. There is a strong positive correlation between $\delta^2H(CH_4)$ and $\delta^{13}C(CH_4)$ values (Fig. 7.9) when boreholes within the Coal Measures are excluded (the latter generally have more positive $\delta^{13}C(CH_4)$ values). The relationship between apparent $\alpha_{CO_2\text{-}CH_4}$ values and ΔG (Fig. 7.10) also improves (i.e., fits better to the theoretical CO_2/H_2 methanogenesis curve from Penning et al., 2005) when borehole data from sites in the Coal Measures are excluded.

Stable isotope data for H_2O from all boreholes plot along the Global Meteoric Water Line (GMWL) (Craig, 1961) with little deviation (Fig. 7.11). The large range of $\delta^{18}O(H_2O)$ and $\delta^2H(H_2O)$ values results from temperature effects and Rayleigh fractionation associated with moisture bearing air masses moving SW to NE across the UK (Darling et al., 2003).

7.4 Discussion

7.4.1 Thermogenic vs microbial methane production

There are two main processes by which the CH_4 present in UK aquifers is produced: thermogenic methane production and microbial methane production (the latter of which can be produced via multiple biochemical pathways). Methane formed by thermal breakdown of organic matter is expected within the Coal Measures and potentially within the Millstone Grit (Abesser et al., 2005; Murphy et al., 2014). If thermogenic CH_4 occurs in an aquifer, it is expected to be present at a relatively high concentration, to be accompanied by higher (i.e., $C_{2\text{-}6}$ hydrocarbons; Bernard et al., 1976) and to have an isotopic signature that is distinct from microbial CH_4 (Whiticar et al., 1986).

Methane produced microbially is ^{13}C- and ^2H- poor (i.e. has more negative $\delta^{13}C$ and δ^2H values) relative to thermogenic CH_4. However, if post-formation CH_4 oxidation occurs, then both $\delta^{13}C(CH_4)$ and $\delta^2H(CH_4)$ values will increase.

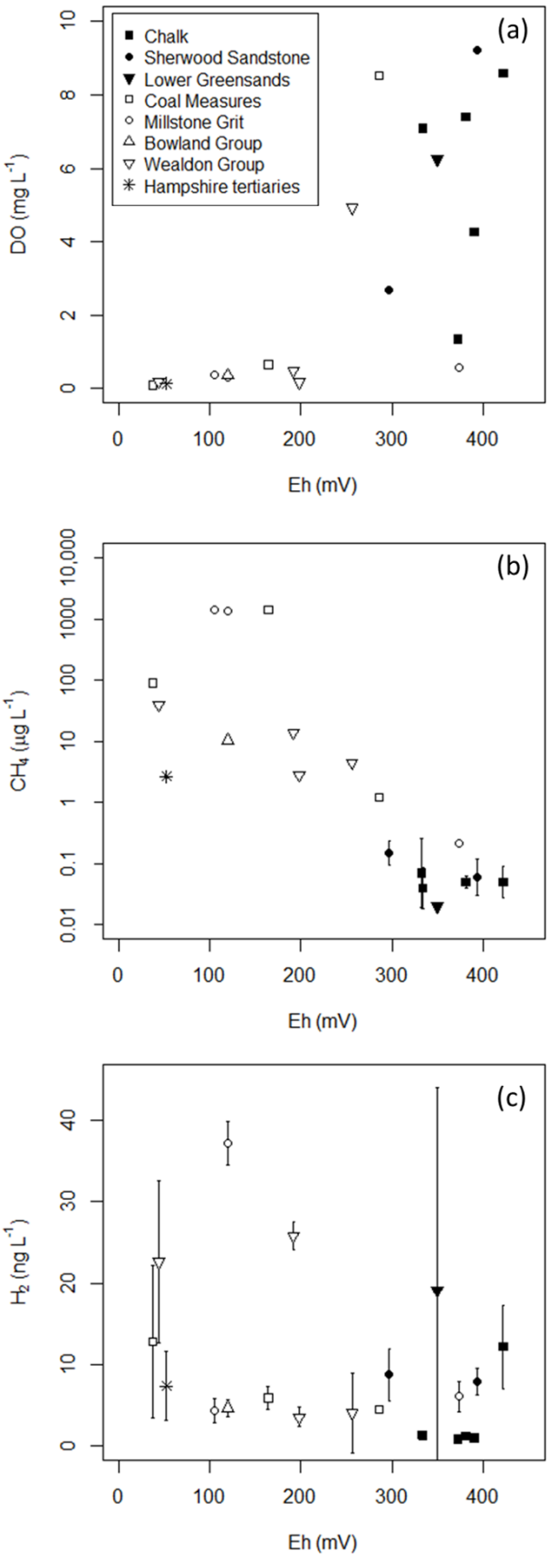

Figure 7.3 Redox relationships in studied aquifers: (a) DO versus Eh, (b) CH_4 concentration versus Eh, and (c) H_2 concentration versus Eh. As Eh decreases and waters become more reducing, CH_4 concentration increases and DO decreases. The concentration of H_2 generally is very low as expected in natural systems containing populations of hydrogenotrophic microorganisms. The concentration of H_2 in groundwater is more variable than CH_4 with higher concentrations more consistently at Eh <100 mV but occurrences of similarly high H_2 levels under more oxidizing conditions.

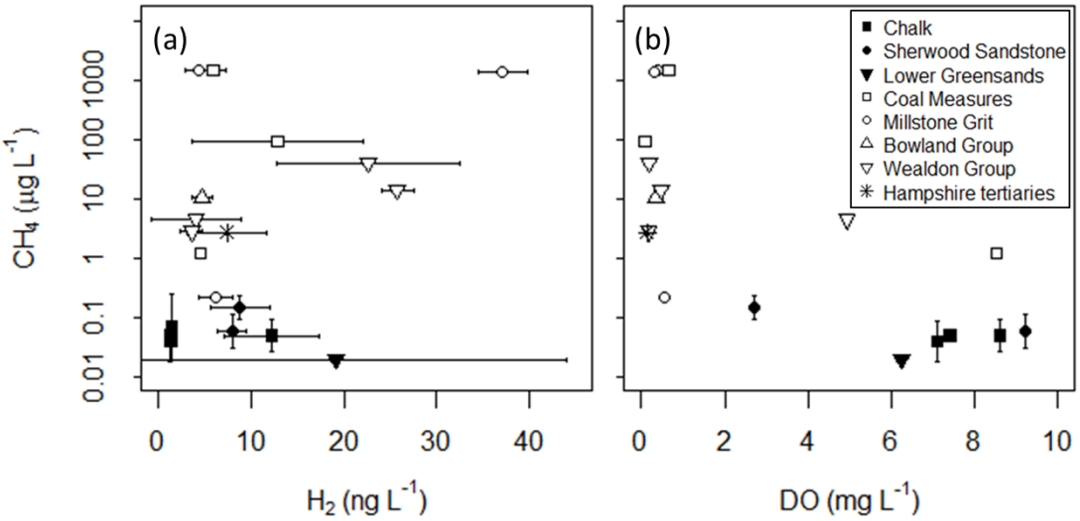

Figure 7.4 Relationships between CH_4 concentration and H_2 and DO concentrations: (a) CH_4 versus H_2 concentration, (b) CH_4 versus DO concentration. There is a positive correlation between CH_4 and H_2 concentrations and a negative correlation between CH_4 and DO concentrations. Aquifers that contain lower levels of O_2 tend to have higher steady state concentrations of H_2 and consequently, generate greater amounts of CH_4 .

The amount of increase will depend on the extent of fractionation but the ^{13}C and ^{2}H enrichment will be proportional (Coleman et al., 1981). It is expected that samples collected from a range of aquifers hosting different environmental conditions than a single aquifer will exhibit a weaker correlation between $\delta^{13}C(CH_4)$ and $\delta^{2}H(CH_4)$ values due to methanotrophy (Fig. 7.9). The correlation likely results from similarities in the stable isotope composition of CH_4 produced by CO_2/H_2 methanogenesis, regardless of location, and the consistency of fractionation for both C and H isotopes during bacterial CH_4 oxidation.

7.4.2 Coal Measures

Gas extracted from water collected at borehole sites within the Coal Measures contain higher concentrations of CH_4 compared to other aquifers. Higher hydrocarbons were not detected by gas chromatography analysis. The measured ranges of $\delta^{13}C(CH_4)$ and $\delta^{2}H(CH_4)$ values are -54.8 to -34.0 ‰ and -189 to -99 ‰, respectively. For $\delta^{13}C(CH_4)$, the most negative values agree with values measured previously from CH_4 plumes originating in South Wales coalfields (Zazzeri et al., 2016). There is a positive correlation between both CH_4 concentration and $\delta^{13}C(CH_4)$ values (Fig. 7.5c) and $\delta^{2}H(CH_4)$ values (Fig. 7.6c), suggesting possible mixing of a high CH_4 concentration thermogenic source and microbial CH_4; however, mixing between two sources should lead to a linear correlation of $\delta^{13}C(CH_4)$ and $\delta^{2}H(CH_4)$, which is absent (Fig. 7.12d). A negative correlation

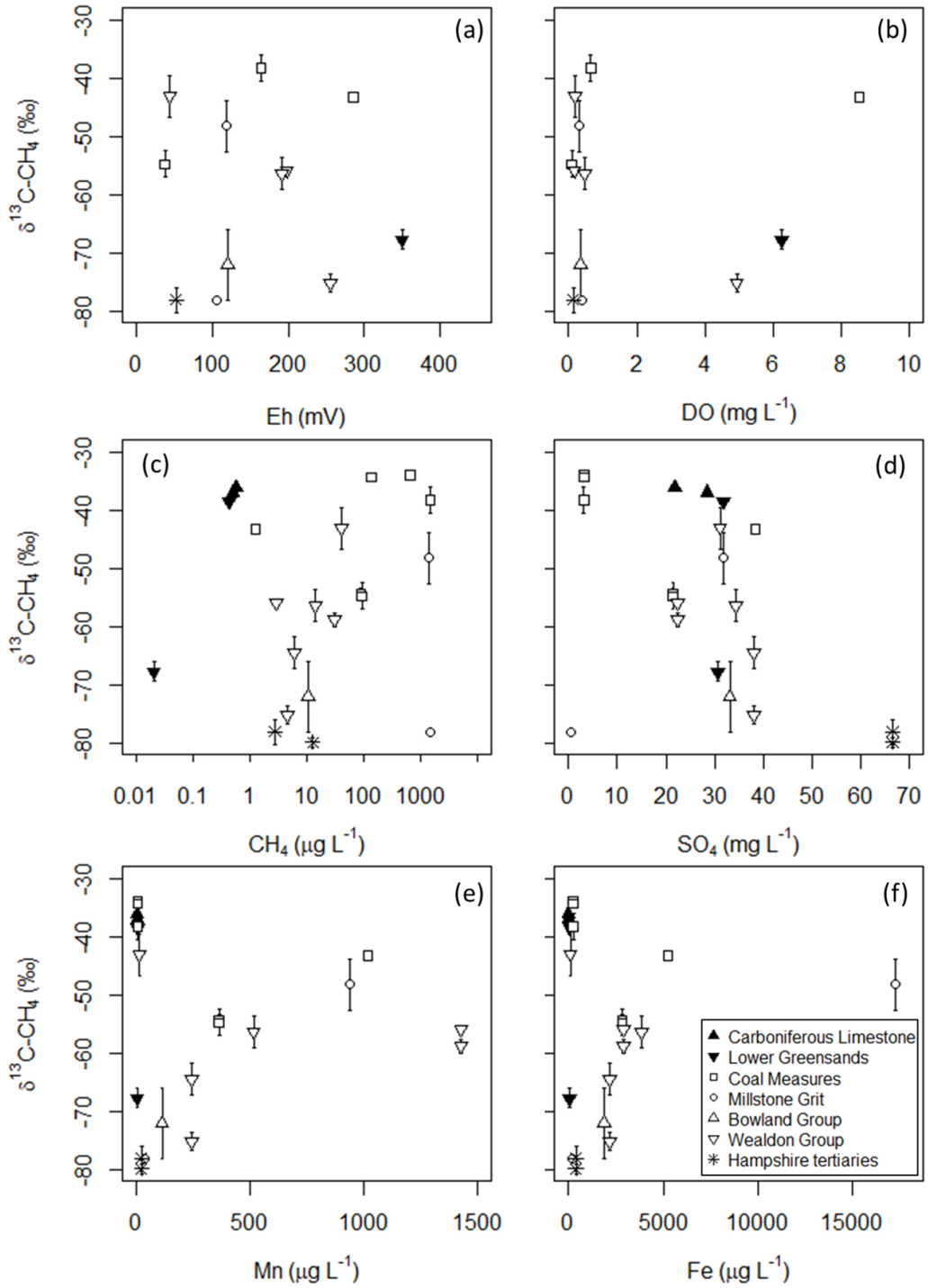

Figure 7.5 Relationships between $\delta^{13}C(CH_4)$ and geochemical parameters: (a) Eh, and concentrations of (b) DO, (c) CH_4, (d) SO_4^{2-}, (e) Mn, and (f) Fe. Boreholes situated in the Coal Measures contain a component of thermogenic gas and generally do not exhibit the same relationships as aquifers where CH_4 has a predominantly microbial origin. Aquifers dominated by microbial activity show a general increase (i.e., more positive) in $\delta^{13}C(CH_4)$ values with decreasing CH_4 concentration, and increasing DO, Mn and Fe concentrations. The $\delta^{13}C(CH_4)$ values are more negative at SO_4^{2-} concentrations. There is no discernible relationship between $\delta^{13}C(CH_4)$ values and Eh

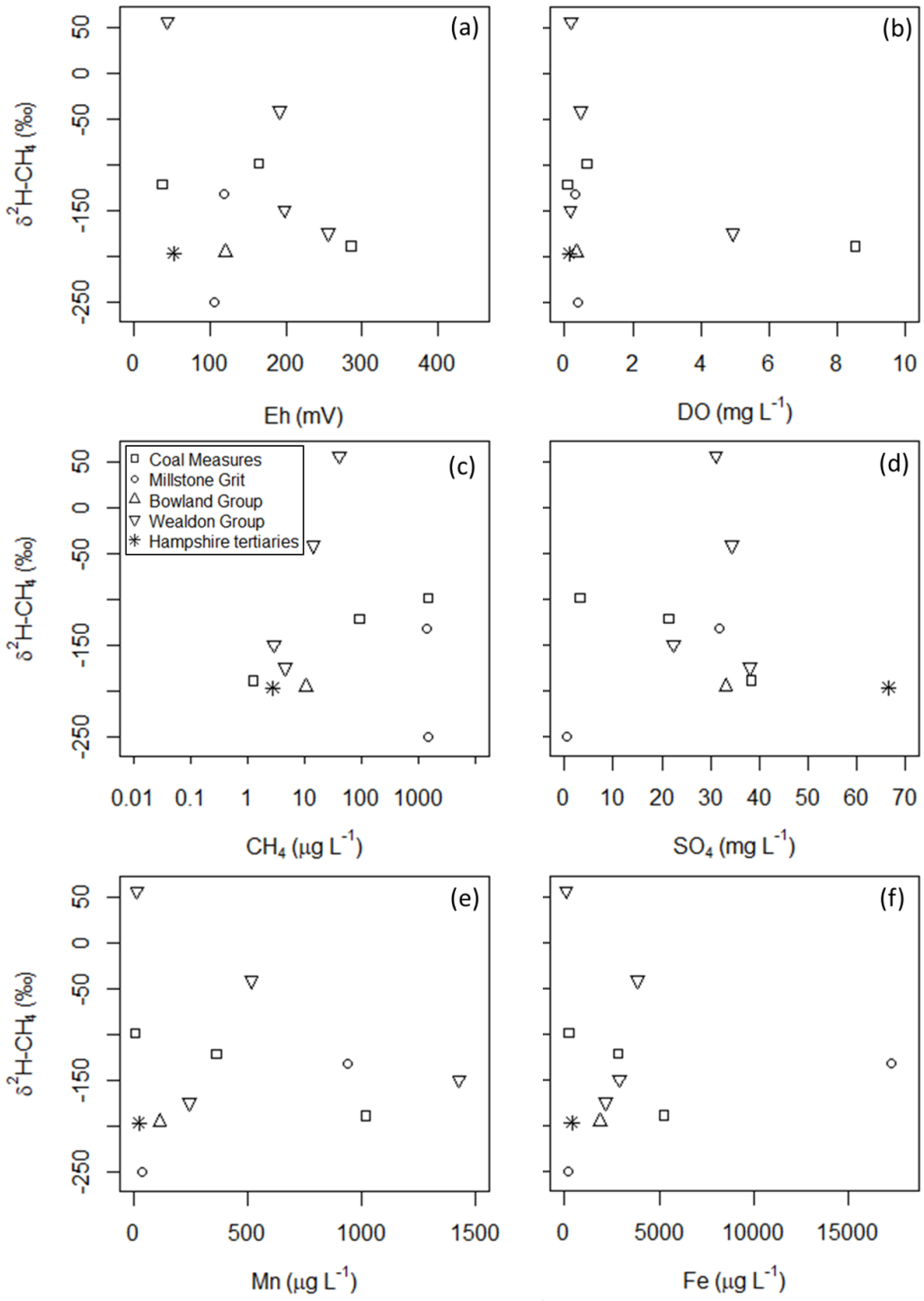

Figure 7.6 Relationships between $\delta^2H(CH_4)$ and geochemical parameters: (a) Eh, and concentrations of (b) DO, (c) CH_4, (d) SO_4^{2-}, (e) Mn, and (f) Fe. The pattern of correlations is similar to $\delta^{13}C(CH_4)$ values (Fig. 5); however, the relationships generally are less well defined, in part, because the data set of $\delta^2H(CH_4)$ values was much smaller. Boreholes within the Coal Measures show an increase in $\delta^2H(CH_4)$ values with increasing CH_4 concentration in contrast to a similar but weaker relationship for aquifers dominated by microbial CH_4 . Groundwater containing CH_4 having more positive δvalues generally also exhibit higher concentrations of DO, SO_4^{2-}, Mn and Fe.

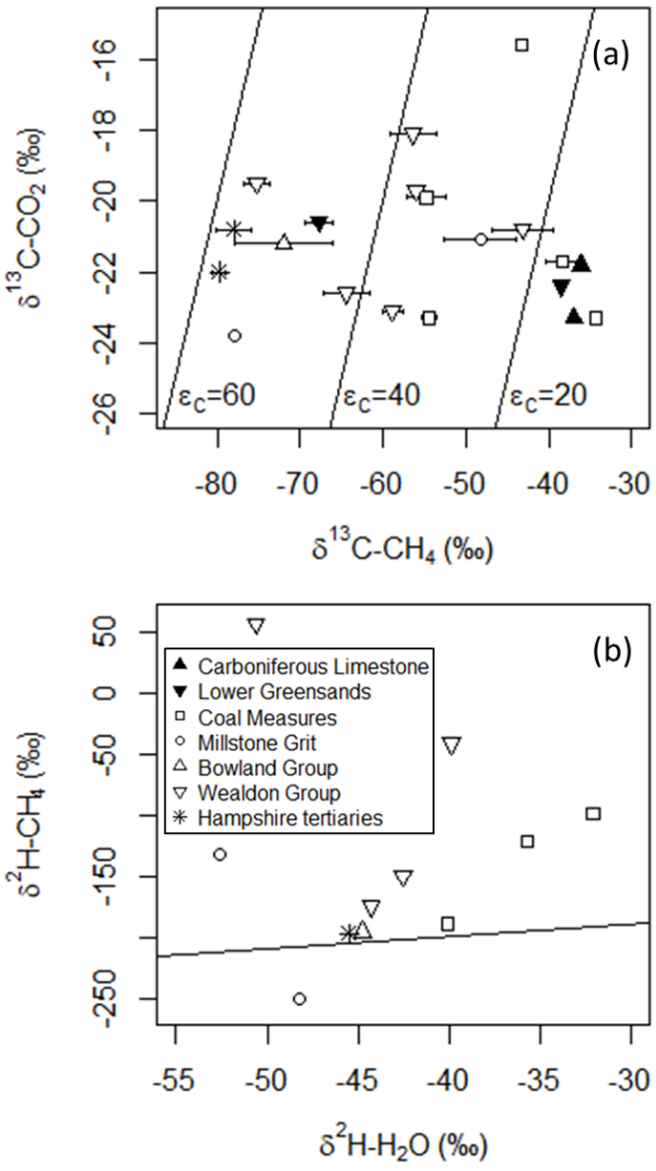

Figure 7.7 Stable carbon and hydrogen isotope data for: (a) $\delta^{13}C(CO_2)$ versus $\delta^{13}C(CH_4)$ values (solid lines represent constant fractionation separating field of thermogenic CH_4 and methanotrophy (ε_C 20 ‰), aceticlastic methanogenesis ((ε_C ~20 to 40 ‰), and CO_2 /H_2 methanogenesis (ε_C ~40 to 60 ‰) from Whiticar et al., (1986), and (b) $\delta^2H(CH_4)$ versus $\delta^2H(H_2O)$ values (solid line represents theoretical fractionation for CO_2/H_2 methanogenesis (ε_H -180 ± 20 ‰); Whiticar et al., 1986).

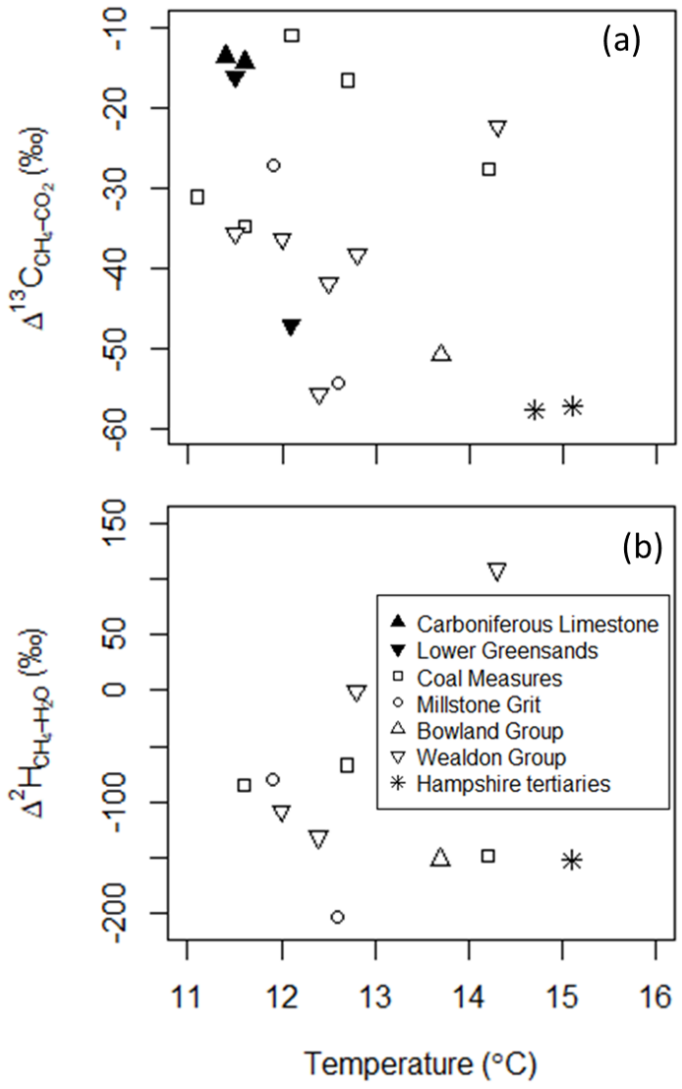

Figure 7.8 Relationships between stable C and H isotope fractionation and temperature: (a) $\Delta^{13}C_{CH_4\text{-}CO_2}$ versus temperature, (b) $\Delta^{2}H_{CH_4\text{-}H_2O}$ versus temperature. Stable isotope fractionation between CO_2 and CH_4 ($\Delta^{13}C_{CH_4\text{-}CO_2}$) and H_2O and CH_4 ($\Delta^{2}H_{CH_4\text{-}H_2O}$) does not exhibit a clear relationship with temperature, suggesting that primary formation of CH_4 may be spatially and/or temporally separated from current thermal conditions in the aquifers.

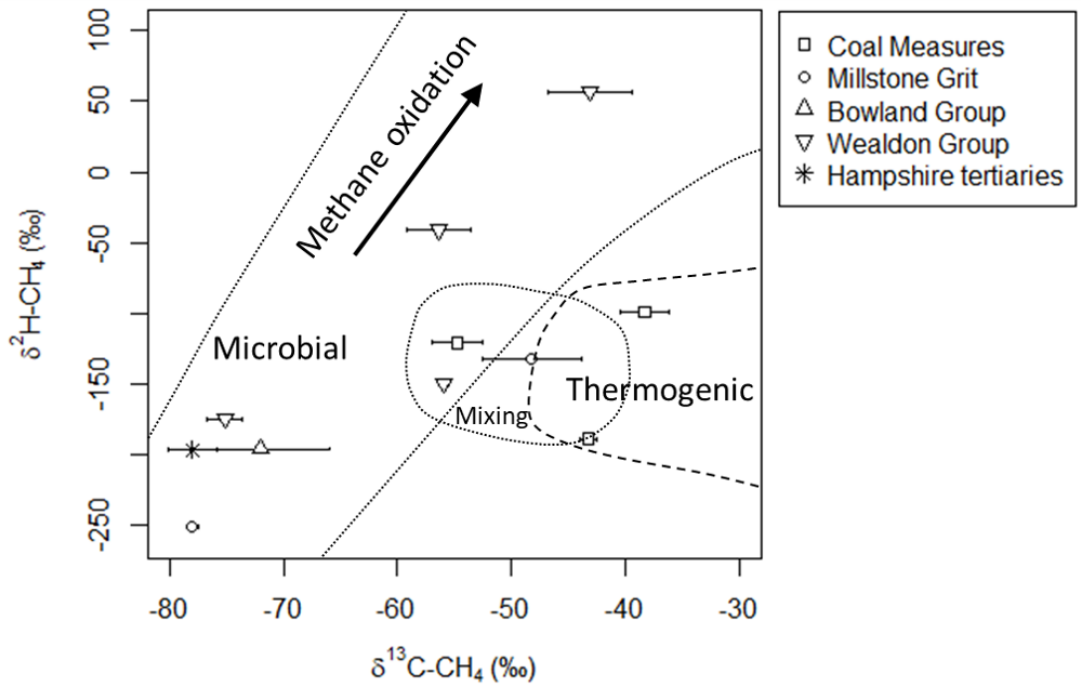

Figure 7.9 $\delta^2H(CH_4)$ versus $\delta^{13}C(CH_4)$ values exhibiting a positive correlation, which is indicative of bacterial CH_4 oxidation or potentially, mixing with a thermogenic source (Whiticar, 1999). Boreholes from the Coal Measures plot in a separate field from the predominantly microbial sources but appear also to contain a proportion of Archaeal CH_4. Groundwater CH_4 at all sites, regardless of origin, appears to have been subjected to some level of bacterial oxidation, which manifests as ^{13}C- and ^{2}H-enrichment in residual CH_4.

between Cl and $\delta^{13}C(CH_4)$ (Fig. 7.12a) also suggests mixing between two sources of water that contain different Cl concentrations and CH_4 but a similar relationship is not observed for Cl and $\delta^2H(CH_4)$ (Fig. 7.12b). A strong correlation does exist between $\delta^2H(CH_4)$ and $\delta^2H(H_2O)$ values (Fig. 7.12d), which indicates if Cl and $\delta^{13}C(CH_4)$ represent mixing between two sources, then $\delta^2H(CH_4)$ may have been influenced post-formation by $^2H/^1H$ in H_2O. Okumura et al. (2016) recently suggested that diagenetic H-isotope exchange takes place between CH_4 and H_2O catalysed by the reversible methanogenic pathway. Such an exchange was postulated to have occurred in older reservoirs, which exhibit less H-fractionation than younger reservoirs (e.g., Kimura et al., 2010; Stolper et al., 2015) because there has been time for equilibration to occur. The same reasoning could be applied to the Coal Measures if it is assumed that thermogenic CH_4 is an older source. It is acknowledged that the data set on which this conjecture is based contains only three data pairs and that additional measurements from boreholes situated in the Coal Measures are needed to explore this possibility further.

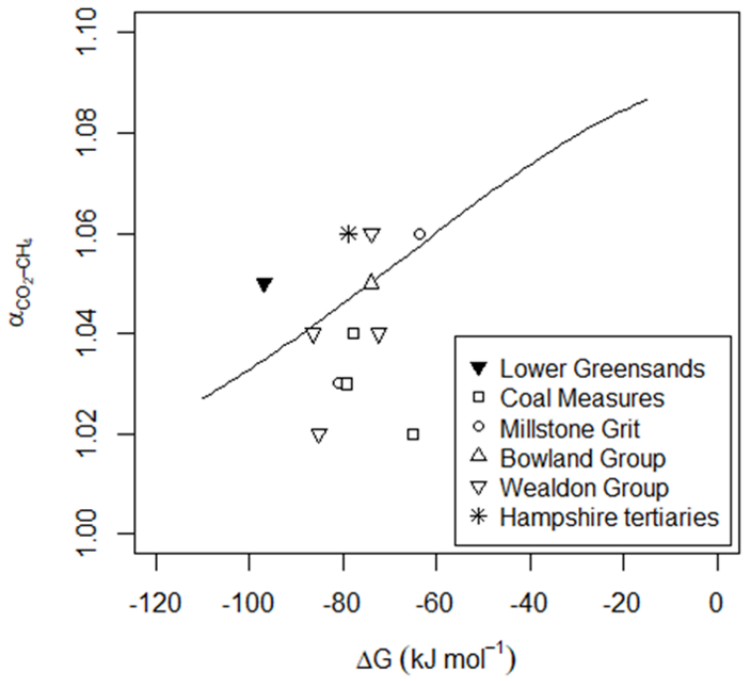

Figure 7.10 Apparent $\alpha_{CO_2\text{-}CH_4}$ and Gibbs free energy (ΔG). The solid line is the relationship between $\alpha_{CO_2\text{-}CH_4}$ and ΔG values for hydrogenotrophic methanogenesis reported by Penning et al. (2005). Groundwater CH_4 from the Coal Measures and Millstone Grit that contain thermogenic CH_4 are not expected to conform to this relationship. Borehole sites exhibiting evidence of post-formational CH_4 oxidation generally plot below the line from Penning et al. (2005).

7.4.3 Millstone Grit

Three boreholes were sampled in the Millstone Grit: MG-1 (very low CH_4 of 0.22 µg L^{-1}); MG-2 (high CH_4 of 1432 µg L^{-1}); and MG-3 (high CH_4 of 1368 µg L^{-1}). MG-2 and MG-3 contained CH_4 having $\delta^{13}C(CH_4)$ and $\delta^2H(CH_4)$ values, respectively, of -78 ‰ and -251 ‰, and -48.2 ‰ and -132 ‰. The relationship between $\delta^2H(CH_4)$ and $\delta^2H(H_2O)$ for borehole MG-3 also appear to correlate well with sites located in the Coal Measures (Fig. 7.7 b).

The very different values of $\delta^{13}C(CH_4)$ and $\delta^2H(CH_4)$ for sites MG-2 and MG-3 in conjunction with high CH_4 concentration suggests a different CH_4 source at each site (Fig. 7.9). MG-3 most likely has a thermogenic source and MG-2 a microbial source based upon on $\delta^{13}C(CH_4)$ and $\delta^2H(CH_4)$ values. The high CH_4 concentration suggests that the effect of methanotrophy has been minimal and would not account for the difference in isotopic compositions observed between boreholes MG-2 and MG-3. The Eh is much higher in MG-1, DO is slightly elevated, and SO_4^{2-} highly concentrated compared to MG-2, providing conditions unsuitable for CH_4 production and favourable for CH_4 oxidation. Thus, it appears that there are two sources of CH_4 within the Millstone Grit and that the spatial

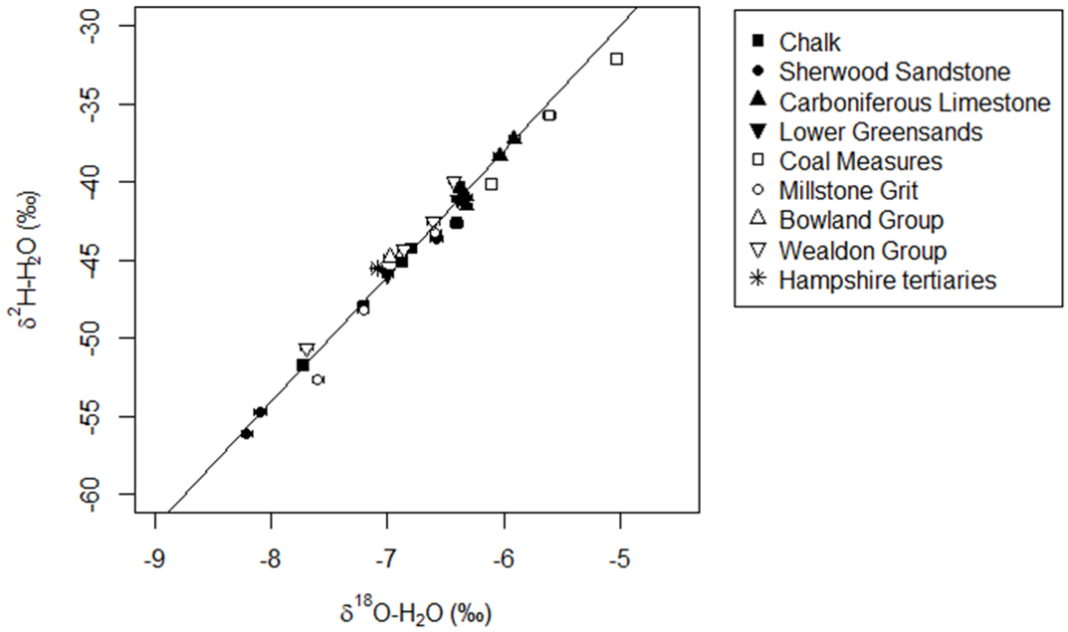

Figure 7.11 Values of $\delta^2H(H_2O)$ versus $\delta^{18}O(H_2O)$ from the aquifers studied, which largely plot along the Global Meteoric Water Line (GMWL; solid line; Craig, 1961) with the exception of one data pair from the Coal Measures.

distribution of CH_4 is highly variable. The latter may be due to the aquifer being geologically complex, consisting of multiple layers of shale that act as aquicludes or aquitards situated between sand layers (Jones et al., 2000). It is also possible that thermogenic CH_4 from neighbouring strata has entered the formation via faults or fractures and then been unable to migrate through consecutive layers. A similar scenario will apply to CH_4 produced in situ via microbial activity, the production of which will be governed by local redox conditions and availability of organic matter. However, only three sites were sampled in the Millstone Grit, which precludes at this time a detailed assessment of distribution patterns for CH_4 concentration or stable isotope composition within this aquifer.

7.4.4 Chalk, Sherwood Sandstone and Carboniferous Limestone

Seven boreholes were sampled in the Chalk aquifer, the majority of which were located in the south of England (Fig. 7.1). All sites had a concentration of CH_4 that was very low or below detection limits. The concentration of DO is consistently high and close to equilibrium with atmosphere (DO at atmospheric equilibrium $\sim$8 – 10 mg L^{-1}). The CH_4 concentration is significantly less than previously detected during BGS baseline sampling (Bell et al., 2017) where the

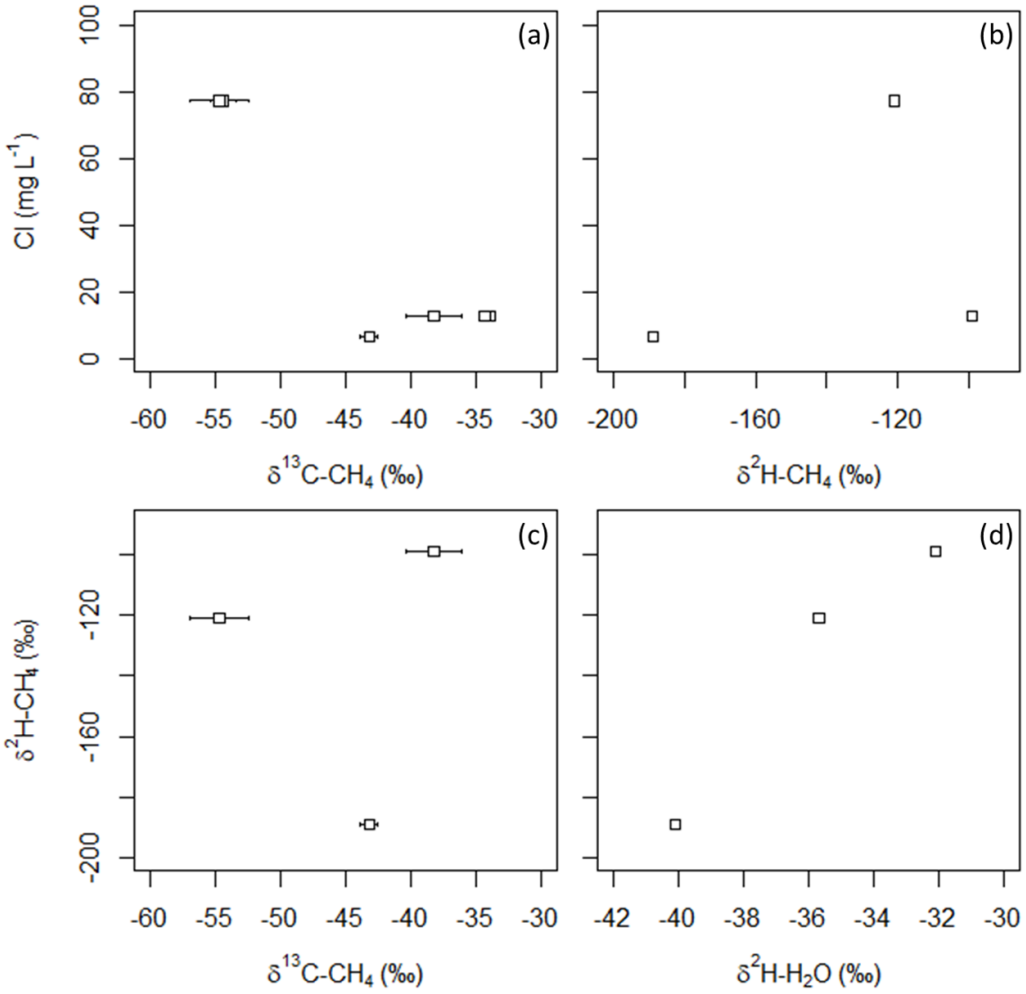

Figure 7.12 Attempt to identify mixing of groundwater and CH_4 sources in the Coal Measures via: (a) Cl versus $\delta^{13}C(CH_4)$ values, (b) Cl versus $\delta^{2}H(CH_4)$ values, (c) $\delta^{2}H(CH_4)$ versus $\delta^{13}C(CH_4)$ values, (d) $\delta^{2}H(CH_4)$ versus $\delta^{2}H(H_2O)$ values. A correlation between Cl and $\delta^{13}C(CH_4)$ values exists but not between Cl versus $\delta^{2}H(CH_4)$ values, which is consistent with the lack of relationship between $\delta^{2}H(CH_4)$ and $\delta^{13}C(CH_4)$ values. There lack of a $\delta^{2}H(CH_4)$ and $\delta^{13}C(CH_4)$ correlation appears to result from the dominant influence of $\delta^{2}H(H_2O)$ on $\delta^{2}H(CH_4)$ values (panel d). The best tracers for mixing are Cl and $\delta^{13}C(CH_4)$ values.

same boreholes sampled during this campaign contained ∼2 µg CH_4 L^{-1}. The presence of CH_4 in the Chalk aquifer has been evidenced by upwelling of dissolved CH_4 in Chalk streams partially sourced from groundwater (Trimmer et al., 2010). The absence of CH_4 in conjunction with high DO suggests extensive CH_4 oxidation has lowered the concentration of CH_4 below equilibrium with the atmosphere (∼0.05 µg L^{-1}) and speaks to the potential transient nature of CH_4 content in groundwater systems that are dominated by fracture flow and high transmissivity.

Minimal CH_4 also was detected in the three boreholes sampled in the Sherwood Sandstone and consequently, analysis of $\delta^{13}C(CH_4)$ and $\delta^{2}H(CH_4)$ was not

possible. The concentration of DO (where measured) was high with a maximum value of 9.22 mg L^{-1} in borehole SS-3. Sherwood Sandstone sites sampled during the Lancashire campaign (Chapter 6) exhibited significantly higher concentrations of CH_4; however, two of the five sites sampled were likely impacted by the proximity to the fault. The two located the farthest away contained significantly less CH_4 and exhibited increasing proportions of CH_4 oxidation with time.

Four boreholes were sampled in the Carboniferous Limestone aquifer during the BGS baseline campaign in 2014 and all contained <2 µg CH_4 L^{-1} at that time, though two, CL-1 and CL-3 contained >0.5 µg CH_4 L^{-1} and analysis of $\delta^{13}C(CH_4)$ was possible; values were -36.9 ‰ and -36.1 ‰ for CL-1 and CL-3, respectively. Borehole CL-3 could not be re-sampled during 2017 because of low water-levels. The other boreholes also were not re-sampled due to low concentrations of CH_4. DO and Eh were not measured and thus, redox status during sampling is unknown. However, low CH_4 concentration accompanied by high $\delta^{13}C(CH_4)$ indicates a high proportion of CH_4 oxidation. During initial sampling of Carboniferous Limestone in South Wales by BGS, relatively high CH_4 was recorded; however, on subsequent trips where a subset of sites were sampled the concentration of CH_4 reduced significantly (Bell et al., 2017) to values similar to those recorded during this study. This indicates a similar pattern to that observed at boreholes within the Chalk and Sherwood Sandstone aquifers whereby the amount of CH_4 is reduced over time due to significant bacterial CH_4 oxidation.

Though water-level data are not available for the sampled sites, there are several groundwater monitoring stations around the UK situated in major aquifers for which data are publicly available (BGS, 2018). Monitoring stations in the Chalk in SE England, where the majority of sites were sampled in this study, had high-water levels in 2014, which then decreased significantly in 2017. That trend is not consistent across all aquifers in the UK; however, it is a consistent pattern in many. A higher water-level due to infiltration into the aquifer could have increased the load of organic matter. Critically, it could have initiated the onset of anoxic conditions in the aquifer through sealing of pore spaces, which would enable increased CH_4 production. Over time, CH_4 oxidation would cause a decrease in CH_4 and ^{13}C and ^{2}H enrichment of residual CH_4. The change in water levels could explain the variability in CH_4 concentration from 2014 to 2017 and demonstrates that baseline CH_4 measurements are unlikely to remain constant with time. The concentration of CH_4 in the majority of boreholes appears to remain within the same order of magnitude over time, or a maximum change of one order of magnitude, according to data from revisited sites (Table 7.2).

In addition to the Chalk and Sherwood Sandstone sites that contained minimal CH_4 in 2017 (cf., 2 to 3 µg L^{-1} in 2014), boreholes in the Carboniferous Limestone in South Wales exhibited variation of three orders of magnitude in CH_4 concentration over that time period (Bell et al., 2017). Thus, it appears that CH_4 concentration in aquifer systems can change rapidly in response to lowering of water table levels or recharge bearing O_2 or substrates for methanogenesis.

7.4.5 Lower Greensand

The two boreholes sampled within the Lower Greensand were situated within the unconfined aquifer. The concentration of CH_4 was low (0.02 and 0.42 µg $L^{-1}$for LGS-1 and LGS-2, respectively), the amount of DO (where measured) was high (6.25 mg L^{-1}), and $\delta^{13}C(CH_4)$ values (where measured) were high (-38.5 ‰), indicating that bacterial CH_4 oxidation was an important process in the aquifer. These measurements agree well with data from the unconfined aquifer sampled during the LGS campaign (Chapter 5) where variable reducing conditions and variable amounts of CH_4 oxidation were observed.

7.4.6 Wealden Group

Four boreholes were sampled in the Wealden Group aquifer: two in the Tunbridge Wells Sands and two in the older Ashdown Beds. The concentration of CH_4 and $\delta^{13}C(CH_4)$ and $\delta^{2}H(CH_4)$ values were variable across these sites but exhibited a positive correlation between $\delta^{13}C(CH_4)$ and $\delta^{2}H(CH_4)$ (Fig. 7.9) but no clear relationship with redox conditions. Borehole WG-1 had the most negative $\delta^{13}C(CH_4)$ and $\delta^{2}H(CH_4)$ values and hence the closest to 'pristine' microbial CH_4 (i.e., early, in situ CH_4), but also has the highest DO concentration by an order of magnitude (7.93 mg L^{-1}, compared to <0.5 mg L^{-1}at the other three sites). The high levels of O_2 in WG-1 could be due to air contamination during sampling because of low water levels and entrainment of air bubbles in the water stream. The 'pristine' stable isotope composition of CH_4 would not be affected because the samples were kept cold and CH_4 is extracted soon after collection to ensure that methanotrophy does not cause alteration. Notably, there is also a positive correlation of both $\delta^{13}C(CH_4)$ and $\delta^{2}H(CH_4)$ values with CH_4 concentration (Fig. 7.5c and 7.6c); i.e., δ-values become more positive at higher CH_4 concentrations), which is the opposite trend of what would be expected if bacterial oxidation was a dominant process in the borehole.

The correlation of $\delta^{13}C(CH_4)$ and $\delta^{2}H(CH_4)$ values indicates a similar initial CH_4 isotope composition and varying proportions of CH_4 oxidation. However,

the lack of correlation of $\delta^{13}C(CH_4)$ and $\delta^{2}H(CH_4)$ values with redox conditions and the positive correlation of $\delta^{13}C(CH_4)$ and $\delta^{2}H(CH_4)$ with CH_4 concentration are unexpected. Possible explanations include: (i) there is mixing between two sources of CH_4, one with negative $\delta^{13}C(CH_4)$ and $\delta^{2}H(CH_4)$ values (microbial) and one with positive $\delta^{13}C(CH_4)$ and $\delta^{2}H(CH_4)$ values (thermogenic), the latter being more abundant; or (ii) the changes in $\delta^{13}C(CH_4)$ and $\delta^{2}H(CH_4)$ values are caused by differ rates of CH_4 production and oxidation that decoupled from the redox conditions measured at the time of sampling.

In scenario one, evidence of mixing of different waters would be expected, in particular, correlations with changes in Cl concentration; however, Cl levels are relatively constant in groundwater at all borehole sites. This observation does not necessarily mean that there is no mixing, as two different waters could have similar Cl concentrations; additionally elevated CH_4 and C_2H_6 has been reported previously within the Ashdown Beds of the Wealden Group at another location (Perry et al., 2013), which may represent a source of thermogenic CH_4. In scenario two, the rate of CH_4 production may be highly variable across the aquifer. If one site has a significantly higher CH_4 concentration, even if a higher proportion is oxidised, there may still be a higher CH_4 concentration in groundwater compared to other sites. Low DO across sites (with the exception of WG-1) coupled with high SO_4^{2-} concentration indicates that SO_4^{2-}-dependent anaerobic methane oxidation may be taking place. As anaerobic conditions are present, CH_4 production may also occur concurrently, and thus, the resulting values of $\delta^{13}C(CH_4)$ and $\delta^{2}H(CH_4)$ will be governed by both CH_4 oxidation and production rates.

7.4.7 General relationships across aquifers

Generalised relationships are challenging to infer because physical and geochemical conditions vary within and across aquifers. However, clear correlations exist between CH_4 concentrations and redox (Eh) conditions across aquifers as well as both H_2 and DO concentrations. These relationships are expected and observed across multiple aquifers under a range of geological conditions.

The relationships between $\delta^{13}C(CH_4)$ and $\delta^{2}H(CH_4)$ values and redox conditions are less clear although consistent patterns are observed in some aquifers (Figs. 7.5 and 7.6). Where a significant component of CH_4 has a thermogenic origin (CM-1, CM-2, CM-3 and MG-3), $\delta^{13}C(CH_4)$ and $\delta^{2}H(CH_4)$ values increase in concert with CH_4 concentration, indicating that some mixing has occurred with microbial CH_4 . This relationship is clearer at lower CH_4 concentrations because the thermogenic source does not dominate the isotopic compositions. For sites

where microbial CH_4 is predominant, there is no clear single pattern unless CH_4 oxidation has occurred, which manifests as increased values of $\delta^{13}C(CH_4)$ and $\delta^{2}H(CH_4)$ usually accompanied by high concentrations of DO, SO_4^{2-}, Mn, Fe or another electron acceptor. The majority of CH_4 oxidation appears to occur aerobically. The presence of the process in some cases can only be inferred because CH_4 concentration is below the threshold for $\delta^{13}C(CH_4)$ and $\delta^{2}H(CH_4)$ analysis.

7.5 Conclusions

The concentration of CH_4 and $\delta^{13}C(CH_4)$ and $\delta^{2}H(CH_4)$ values are variable across UK aquifers, including within an individual aquifer. Methanotrophy is the dominant control on $\delta^{13}C(CH_4)$ and $\delta^{2}H(CH_4)$ values for aquifers that contain CH_4 having a predominantly microbial origin. For sites containing a significant proportion of thermogenic CH_4, there is a much stronger relationship between $\delta^{2}H(H_2O)$ and $\delta^{2}H(CH_4)$ values and the dominant control on $\delta^{13}C(CH_4)$ values appears to be mixing with in situ archaeal CH_4. Groundwater containing the highest CH_4 concentrations tended to have a higher proportion of thermogenic CH_4 and hence more positive $\delta^{13}C(CH_4)$ values. That relationship is the opposite of sites dominated by microbial CH_4 subjected to methanotrophy, which resulted in more positive $\delta^{13}C(CH_4)$ and $\delta^{2}H(CH_4)$ values that correlate and much lower concentrations of CH_4.

Chapter 8

Synthesis and Conclusions

8.1 Aims, objectives and hypotheses

The aim of this project was to use stable isotope analysis to better understand CH_4 production and consumption processes in UK aquifers and how these processes relate to environmental conditions and geological context.

The study objectives were to (i) assess the range of stable isotope compositions of CH_4 within individual aquifers and across different UK aquifers in relation to geology and local conditions; (ii) extend the scope of characterisation of isotopic characterisation through refinement of a pre-concentration method to improve the detection limit for analysis of $\delta^{13}C(CH_4)$ and $\delta^{2}H(CH_4)$; (iii) evaluate the extent to which differences in CH_4 formation pathway and CH_4 oxidation contributes to stable isotope composition of CH_4 in groundwater; (iv) establish the degree to which stable isotope characterisation of CH_4 in UK groundwater can be used reliably to detect influx of exogenous CH_4 into an aquifer based on limits and precision of field and laboratory techniques for CH_4 extraction and stable isotope analysis; and (v) to assess the extent to which regional differences of $\delta^{2}H(H_2O)$ influence $\delta^{2}H(CH_4)$. Hypotheses explored in the study are that (i) CH_4 in the UK groundwater primarily has a microbial origin and is produced in-situ; (ii) there will be high degrees of variability of $\delta^{13}C(CH_4)$ and $\delta^{2}H(CH_4)$ values governed by a breadth of environmental conditions; (iii) a subset of aquifers will be impacted locally by allochthonous sources, such as coalfields or landfills; (iv) values of $\delta^{2}H(CH_4)$ will be linked to $\delta^{2}H(H_2O)$; and (v) the amount CH_4 will be impacted by bacterial oxidation, which will relate to the degree to which an aquifer is open, the Eh and pO_2 of the aquifer, and will be reflected in an increase and correlation between $\delta^{13}C(CH_4)$ and $\delta^{2}H(CH_4)$ values.

8.2 Synthesis

A large part of the study involved establishing a method by which low concentrations of dissolved CH_4 could be analysed for $\delta^{13}C(CH_4)$ and $\delta^{2}H(CH_4)$ values with larger quantities of CH_4 necessary for analysis of $\delta^{2}H(CH_4)$ as described in Chapter 4. An in-lab gas sparging method in conjunction with stable isotope ratio mass spectrometry was utilised for analysis of $\delta^{13}C(CH_4)$, which enabled analysis of samples containing as little as 0.5 – 1 µg CH_4 L^{-1}. An in-field sparging method was established for analysis of $\delta^{2}H(CH_4)$, whereby large quantities of water (75 to 300 litres) could be sparged and the resulting higher CH_4 concentration gas analysed. The final method enabled analysis of samples as low as 2 – 3 µg CH_4 L^{-1}.

A selection of boreholes covering the UK were chosen to include sites within multiple aquifers and variable conditions across each aquifer. The study was conducted in three parts: the first part whereby several sites within a syncline of a single aquifer (Lower Greensands) were investigated to understand how processes may vary across an aquifer as conditions change from confined to unconfined; the second area was selected due to its location in a shale gas development area, where exploitation is due to start in 2018; and the third covered a much broader area and several aquifers within the UK to explore dominant geological and environmental controls on groundwater $\delta^{13}C(CH_4)$ and $\delta^{2}H(CH_4)$ values and to establish the degree of variability in the stable isotope composition of CH_4.

Data from these sections have been combined and correlations observed between CH_4 and both Eh and DO (Fig. 8.1). Methane formation occurs only within reducing conditions and the amount of methanotrophy is dependent on the availability of O_2 or another electron acceptor, such as SO_4^{2-}. As CH_4 concentration decreases, both $\delta^{13}C(CH_4)$ and $\delta^{2}H(CH_4)$ values increase (Fig. 8.2). As the dominant process moves from methanogenesis to methanotrophy, CH_4 is consumed, with the lighter isotopes consumed preferentially, causing an increase in $\delta^{13}C(CH_4)$ and $\delta^{2}H(CH_4)$ values of the remaining CH_4. A clear correlation of $\delta^{13}C(CH_4)$ and $\delta^{2}H(CH_4)$ was observed across the majority of sites (Fig. 8.3a), which indicates methanotrophy is a dominant process across several sites. A relationship of $\delta^{2}H(CH_4)$ and $\delta^{2}H(H_2O)$ was observed across some sites, but not across others, again indicating that methanotrophy is a dominant process across sites.

The results highlight a wide variation of measurements across sites, indicating differing environmental conditions. When considered in detail within the separate chapters, it was observed how local geology and environmental conditions affect both CH_4 concentration and stable isotope composition. In the Lower Greensands, patterns of CH_4, $\delta^{13}C(CH_4)$ and $\delta^{2}H(CH_4)$ changed as the aquifer transitioned from confined to unconfined conditions. In the deeper, confined aquifer, a relationship between temperature and both $\delta^{13}C(CH_4)$ and $\delta^{2}H(CH_4)$ was observed, whereas for sites within the shallow unconfined aquifer, $\delta^{13}C(CH_4)$ and $\delta^{2}H(CH_4)$ appeared much more dependent on redox conditions, which were variable across the aquifer. For the sites in Lancashire, the influence of a major fault zone was observed, whereby reducing waters mixed with the more oxidising waters within the Middle Sands aquifer, resulting in variable amounts of methanotrophy and a very large range of both $\delta^{13}C(CH_4)$ and $\delta^{2}H(CH_4)$ values, with the range of $\delta^{2}H(CH_4)$ appearing particularly extreme.

For sites visited in Chapter 7, a large range of conditions were observed across

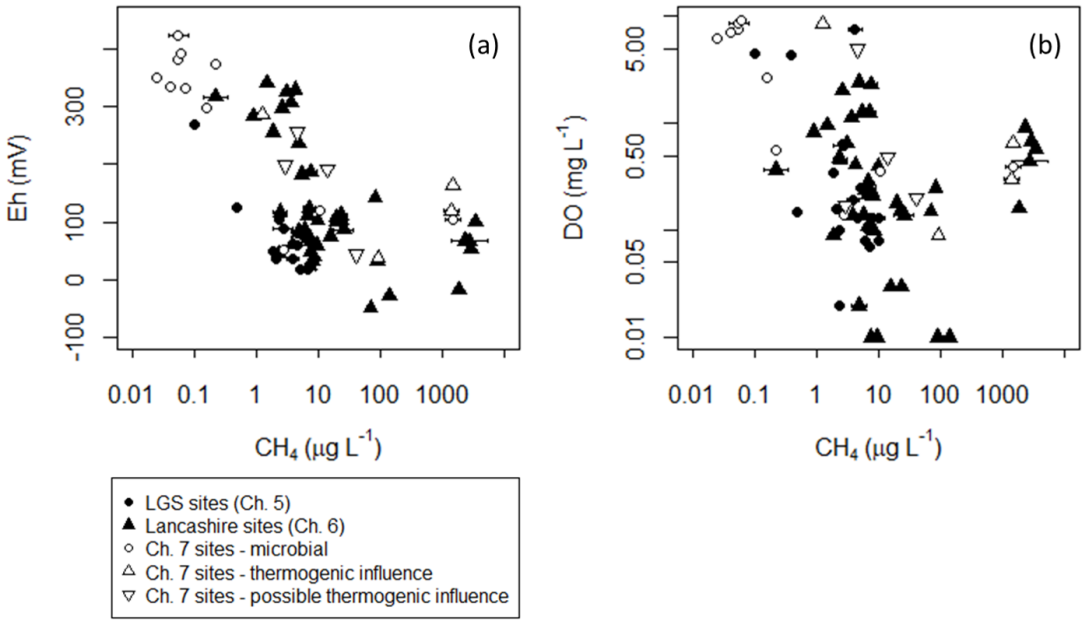

Figure 8.1 Relationship of CH_4 to redox conditions across all sites: (a) Eh versus CH_4, and (b) DO versus CH_4. The concentration of CH_4 increases with decreasing Eh and with decreasing DO. In (b), sites with a thermogenic influence and sites with very high concentrations of microbial CH_4 plot to the right of the trend for the majority of sites. For the microbial dominated sites the shift is likely due to the interplay between CH_4 production and oxidation rates.

different aquifers. This includes highly oxidising waters observed across all sites within the highly transmissive Chalk aquifer and correspondingly minimal or absent CH_4. In contrast, the Millstone Grit has low permeability shale layers that effectively compartmentalise the aquifer, giving rise to high concentrations of both thermogenic and microbial CH_4 in different parts of the aquifer.

Methane in aquifers can be identified as microbial, thermogenic or a combination through mixing, based on CH_4 concentration, redox conditions and the relationship to $\delta^{13}C(CH_4)$ and $\delta^{2}H(CH_4)$. Sites with a thermogenic influence, mostly exhibit high CH_4 concentrations in conjunction with relatively high values of $\delta^{13}C(CH_4)$ (Fig. 8.2b), though a similar correlation with $\delta^{2}H(CH_4)$ is not observed. Further information on production pathways for microbial CH_4 sites is difficult to establish, but where 'pristine' (i.e., early, in situ CH_4, whereby no post formation processes have taken place, such as oxidation or transportation) or 'close to pristine' methane was observed, corresponding $\delta^{13}C(CH_4)$ and $\delta^{2}H(CH_4)$ values expected for hydrogenotrophic methanogenesis (Whiticar et al., 1986) also were observed.

The majority of sites where microbially produced methane is present exhibit varying degrees of methane oxidation, leading to, in some cases unexpectedly

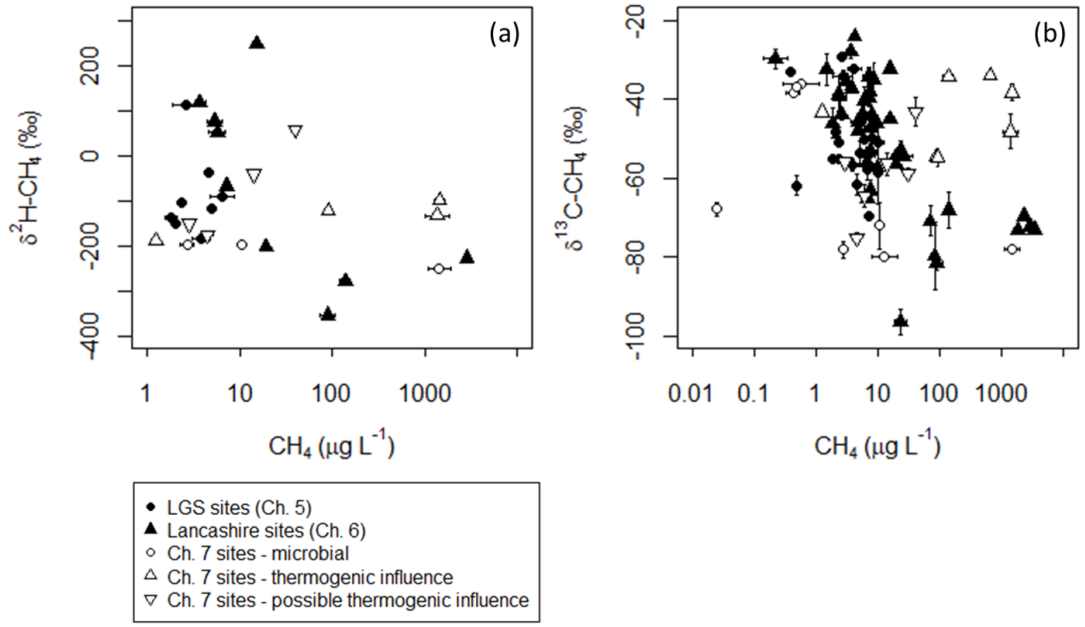

Figure 8.2 Relationship between CH_4 concentration and stable isotope compositions: (a) $\delta^2H(CH_4)$ versus CH_4; (b) $\delta^{13}C(CH_4)$ versus CH_4. As CH_4 concentration increases, there is a decrease in both $\delta^{13}C(CH_4)$ and $\delta^2H(CH_4)$ values. The relationship is more pronounced for $\delta^{13}C(CH_4)$ due to the increased number of sites. Sites with a thermogenic CH_4 influence plot to the right of the trend for the majority of sites.

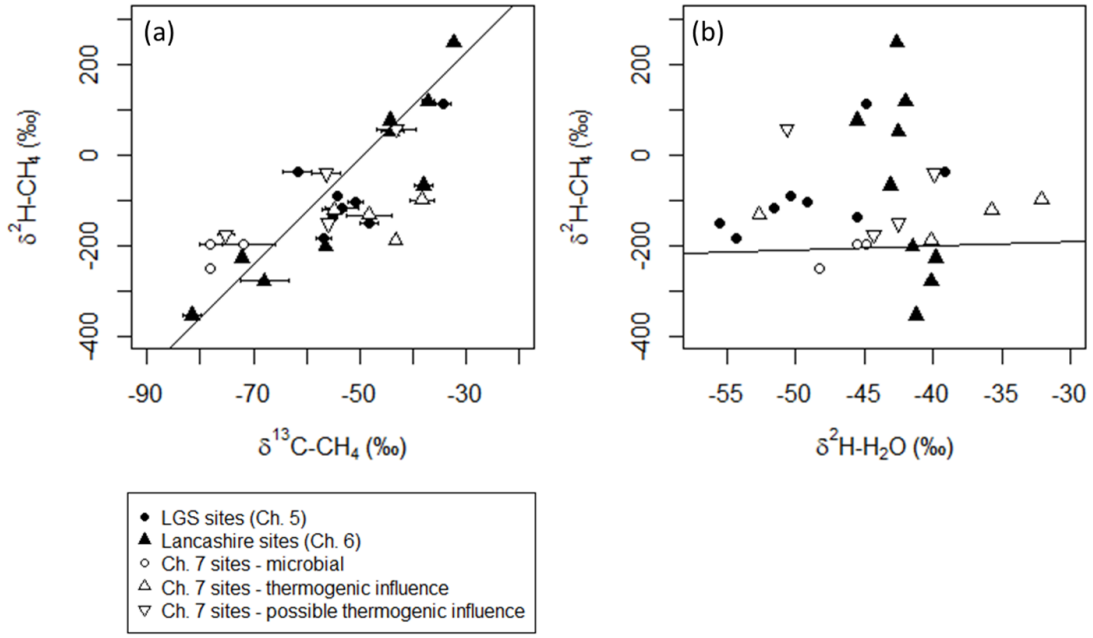

Figure 8.3 Relationships between $\delta^{13}C(CH_4)$, $\delta^2H(CH_4)$ and $\delta^2H(H_2O)$ values for all sites: (a) $\delta^{13}C(CH_4)$ versus $\delta^2H(CH_4)$; (b) $\delta^2H(CH_4)$ versus $\delta^2H(H_2O)$. In (a), the line is the relationship established in Chapter 6 for sites within the Middle Sands Formation in the Fylde, Lancashire. In (b) the line is an expected relationship between $\delta^2H(CH_4)$ and $\delta^2H(H_2O)$ values for CH_4 formed via hydrogenotrophic methanogenesis (Whiticar et al., 1986).

positive $\delta^{13}C(CH_4)$ and $\delta^{2}H(CH_4)$ values (Fig. 8.3 a), though similar values have been reported in other freshwater environments (Cadieux et al., 2016). In some aquifers, the concentration of CH_4 was too low for analysis, and at some sites it was below detection limits (<0.05 µg L^{-1}); however, high DO concentrations indicate significant amounts of CH_4 oxidation have taken place. As the extent of methanotrophy progresses, $\delta^{13}C(CH_4)$ and $\delta^{2}H(CH_4)$ values increase proportionally, with the increase in $\delta^{2}H(CH_4)$ always larger due to the mass change being proportionally greater for H than for C. For the Middle Sands aquifer, this factor was determined to be 11.7, which is within the range of experimental studies (Coleman et al., 1981; Whiticar, 1999). $\delta^{13}C(CH_4)$ and $\delta^{2}H(CH_4)$ values plotted for all sites where measurements were possible, generally follow a similar trend (Fig. 8.3a), though the spread is broader, likely due to a variation of initial 'pristine' $\delta^{13}C(CH_4)$ and $\delta^{2}H(CH_4)$ across sites.

It was possible to visit some boreholes more than once, the majority of which were in the Lancashire area (Chapter 6), but also a selection of the Lower Greensands sites (Chapter 5) and some of the sites reported in Chapter 7. The majority of sites changed very little with time, however, in a selection of sites in Lancashire, both increases and decreases in CH_4 concentration with time were recorded. For the sites with increases in CH_4, analysis of $\delta^{13}C(CH_4)$ and/or $\delta^{2}H(CH_4)$ indicated that the CH_4 was microbially produced and of expected isotopic composition (for the site with both $\delta^{13}C(CH_4)$ and $\delta^{2}H(CH_4)$), i.e., the same correlation of $\delta^{13}C(CH_4)$ and $\delta^{2}H(CH_4)$ was observed as for other sites within the aquifer. Variations of CH_4 with time were observed for some revisited sites and also when compared to previous site visits as part of the BGS baseline study (Bell et al., 2017). The majority of variation involved decreases in CH_4 concentration within the Chalk and Sherwood Sandstone aquifers, indicating that CH_4 concentration in aquifer systems can change rapidly in response to changes in environmental conditions.

The relationship of $\delta^{2}H(CH_4)$ and $\delta^{2}H(H_2O)$ was observed across multiple sites (Fig.8.3b), however, for a large proportion of sites, a large range of $\delta^{2}H(CH_4)$ were measured and no correlation of $\delta^{2}H(CH_4)$ and $\delta^{2}H(H_2O)$ was observed. The relationship between $\delta^{2}H(CH_4)$ and $\delta^{2}H(H_2O)$ values associated with microbial CH_4 formation has been well-established (e.g., Sugimoto and Wada, 1995; Valentine et al., 2004; Waldron et al., 1999; Whiticar et al., 1986), and though there are some variations in the expected relationship within these studies, they follow a similar broad trend. Therefore, such a relationship was expected across sites. For the studied sites where analysis was possible (Fig. 8.3b), several sites broadly follow an expected trend, whereas others do not. For sites with microbially pro-

duced CH_4, where there has been no or very limited methanotrophy, a general correlation was observed; however, for sites with microbially produced CH_4 that have undergone varying amount of methanotrophy, shifts away from the line were observed. This is due to effects of methanotrophy overprinting the initial isotopic signature. For sites with predominantly thermogenic CH_4, both $\delta^{13}C(CH_4)$ and $\delta^{2}H(CH_4)$ values are expected to be related to the initial organic matter from which the CH_4 was formed (Fuex, 1977), and not $\delta^{2}H(H_2O)$. However, isotopic equilibrium of CH_4 and H_2O via isotope exchange may be catalysed via the reversible hydrogenotrophic methanogenesis pathway utilised by methanogen populations (Okumura et al., 2016). Evidence for this was seen within the South Wales Coal Measures, where evidence of mixing was established using $\delta^{13}C(CH_4)$ and Cl, whereas $\delta^{2}H(CH_4)$ did not follow this pattern and instead correlated with $\delta^{2}H(H_2O)$.

8.3 Conclusions

The majority of CH_4 observed in UK aquifers appears to be of primarily microbial origin, likely produced in-situ, as indicated by stable isotope data in conjunction with redox measurements. The majority of microbial CH_4 has undergone varying degrees of methanotrophy, evidenced by a strong correlation as well as a wide range of $\delta^{13}C(CH_4)$ and $\delta^{2}H(CH_4)$ values, which have not been reported previously in groundwater, though similar values have been observed in surficial freshwater environments (Cadieux et al., 2016)

Values of $\delta^{13}C(CH_4)$ and $\delta^{2}H(CH_4)$ for sites within the same aquifer are more likely to correlate with each other, indicating either a single CH_4 source or CH_4 produced under similar conditions; therefore the majority of CH_4 is likely produced in-situ.

Evidence of allochthonous CH_4 was observed in a minority of sites and can be identified by differences in CH_4 stable isotope composition in comparison to other sites within the aquifer. The difficulty in detecting such gas can vary; for example, large quantities of thermogenic CH_4 observed in one site in the Millstone Grit, compared to significant quantities of microbial CH_4 in another, was easily established due to significant differences in $\delta^{13}C(CH_4)$ and $\delta^{2}H(CH_4)$ values. Another borehole potentially influenced by a landfill site in the Middle Sands aquifer showed a deviation from the correlation of $\delta^{13}C(CH_4)$ and $\delta^{2}H(CH_4)$ observed across remaining sites in the aquifer, which allowed inference of an allochthonous source; however, with a smaller deviation there is less certainty and it must be considered that such variation may be due to other variables

occurring within the aquifer.

Values of $\delta^2H(CH_4)$ can be linked to values of $\delta^2H(H_2O)$, but only under certain conditions. Microbial methane when produced will exhibit correlation of $\delta^2H(CH_4)$ and $\delta^2H(H_2O)$; however, stable isotope fractionation due to methane oxidation processes may rapidly cause an 'overprinting' of the initial stable isotope composition. Therefore only 'pristine' CH_4 will exhibit this correlation, and not the majority, which is likely to have undergone varying degrees of oxidation. For thermogenic CH_4 the correlation shows an opposite trend: hydrogen isotopic exchange of CH_4 and H_2O catalysed by hydrogenase (Okumura et al., 2016) may take place with time. Correlation of $\delta^2H(CH_4)$ and $\delta^2H(H_2O)$ values within the Coal Measures indicates that this process may have occurred previously and therefore may occur within other UK aquifers with an established thermogenic CH_4 source.

Understanding processes of methane production and consumption in aquifers is an essential part of monitoring groundwater in areas of shale gas exploration. For the majority of sites CH_4 concentration does not vary over time by more than an order of magnitude, however for a significant few this is not the case. By utilising the analysis of stable isotope composition of CH_4 in combination with an understanding of the local geology and geochemistry, it is possible to determine what processes are likely involved in methane formation and consequent post-formation consumption and transportation. This will also give an indiction of the likely impact of an influx of exogenous methane on an aquifer.

Appendices

Appendix A

Results for all sites

A.1 Site information and field data

Table A.1 Results from all sites - site information and field data

Area	Site	Aq	E	N	Elevation (m)	Depth (m)	Sampling date	Temp (°C)	pH	SEC (µS cm^{-1})	DO (mg L^{-1})	ORP (mv)	eh (mv)	TA (mg L^{-1})	HCO3 A (mg L^{-1})
LGS	OK	LGS	476	136	135	143	22/07/2014	13	8.05	260	0.07				
		LGS					21/08/2017	13	7.86	249	0.13	-152	59	99	121
	BN	LGS	484	146	109	134	22/07/2014	11.6	7.1	491	7.61				
		LGS					09/08/2017	11.8	7.38	484	0.61	-123	89	188	229
	TL	LGS	488	144	52	90	23/07/2014	11	7.52	324	0.1				
		LGS					09/08/2017	12.1	7.72	302	0.35	-162	50		
	TG	LGS	488	148	74	441	23/07/2014	20.4	7.87	464	0.1				
							05/10/2017	20.4	7.79	463	0.25	-185	19	112	137
	BH	LGS	486	149	72	468	24/07/2014	21.7	7.91	544	0.13				
							05/10/2017	22.3	7.91	543	0.25	-183	19	108	132
	TM	LGS	488	149	72	469	24/07/2014	22.4	7.87	451	0.13				
	SHP	LGS	495	182	34	349	25/07/2014	17.3	7.89	673	0.08				
		LGS	495	182		381	24/05/2017	17	7.92	738	0.19	-172	35	199	243
	HL	LGS	497	180	28	345	25/07/2014	17.7	7.82	549	0.08				
		LGS					25/07/2017	17.9	7.88	560	0.16	-169	37	190	232
	NM	LGS	508	148	77.8	83	14/10/2014	11.2	5.25	237	4.3				
		LGS	508	148	80	82.4	20/09/2017	11.1	6.77	343	4.53	57	270	107	130
	MH	LGS	494	142	73	86	22/10/2014	10.7	6.76	303	0.64				
	MP	LGS	515	237	56	52	17/07/2017	13.6	7.02	338	0.15	-86	124	145	177
	NS	LGS	521	242	51	54.5	17/07/2017	12.4	7.19	598	0.02	-107	105	229	279
Lancashire	SS-4	SS	347	435	22	30	02/02/2015	10.7	6.95	981	0.16	-230	-17		
		SS					09/05/2017	11.1	7.01	973	0.01	-240	-27	342	416
	SS-1	SS	350	441	23	100	03/02/2015	10.6	7.1	770	0.65	113	326	291	355
		SS					07/05/2015	10.7	7.07	749	0.97	128	341	279	339
		SS					17/11/2015	10.8	7.09	772	0.37	104	317	311	379
	MS-7	MS	330	432	10	15	27/10/2014	13.4	7.2	802				270	329
		MS					12/01/2015	13	7.11	870					
		MS					03/02/2015	12.4	7.09	959	2.31	-24.4	187	260	317
		MS					07/05/2015	12.8	7.09	893	2.43	25	236	260	316
		MS					17/11/2015	13.1	6.69	988	2.02	87	298	309	376

Table A.1 continued

Area	Site	Aq	E	N	Elevation (m)	Depth (m)	Sampling date	Temp (°C)	pH	SEC (µS cm^{-1})	DO (mg L^{-1})	ORP (mv)	eh (mv)	TA (mg L^{-1})	HCO3 A (mg L^{-1})
		MS					08/05/2017	13.4	7.12	823	1.26	-28	183		
	MS-4	MS	337	437	25	39.62	04/02/2015	10.6	7.38	1083	0.21	-179	34	315	383
		MS					06/05/2015	10.9	7.29	1072	0.01	-153	60	326	397
		MS					12/11/2015	10.9	7.42	1074	0.29	-140	73	337	411
	MS-6	MS	339	436	29	39.62	05/02/2015	9.8	7.22	799	0.23	-146	68	315	383
		MS					06/05/2015	10.5	6.81	794	0.4	-111	103	334	407
		MS					12/11/2015	11.1	7.4	782	0.25	-70	143	343	418
		MS					11/05/2017	11.4	7.33	779	0.01	-180	33	313	382
	MS-3	MS	334	437	20.5	30	06/02/2015	12.2	7.09	918	1.14	95.4	307	351	428
		MS					15/05/2015	11.9	7.12	906	0.41	117.2	329	366	446
		MS					10/11/2015	13.6	7.11	927	0.83	74	284	373	454
	MS-8	MS	334	428	25	5m (22 wells)	10/02/2015	9.8	7.17	756	0.91	-146	68	289	352
		MS					08/05/2015	7.8	7.2	722	0.58	-116	100	279	340
		MS					18/11/2015	13.3	7.21	633	0.44	-144	67		
		MS					09/05/2017	10.5	7.07	717	0.68	-160	54	219	266
	SS-3	SS	348	437	24	107	11/02/2015	9.3	7.26	692	0.11	-137.5	77	337	410
		SS					06/05/2015	11.1	7.24	690	0.22	-101	112	324	395
		SS					10/11/2015	11.6	7.29	699	0.15	-100	112	341	416
	MS-10	MS	347	429	4.7	5	11/02/2015	9.8	7.04	1180	0.14	-127	87	521	635
		MS					14/05/2015	10.2	7.01	1134	0.03	-111.3	103	518	631
		MS					11/11/2015	11.6	7.04	1109	0.18	-111	101	513	625
		MS					10/05/2017	11.8	6.99	1124	0	-103	109	371	452
	MS-1	MS	339	440	11	30	11/05/2015	9.8	7.21	843	0.48	-168	46	318	387
		MS					09/11/2015	11	7.14	841	0.46	-96	117	331	403
	MS-5	MS	338	437	17	15	13/05/2015	10.7	7.22	800	0.02	-129.2	84	310	378
		MS					11/05/2017	11.4	7.17	819	0.14	-132	81	160	195
	SS-2	SS	351	437	30	50	13/05/2015	10.7	7.31	723	0.1	-172	41	315	383
		SS					18/11/2015	10.8	7.29	725	1.27	-89	124		
		SS					10/05/2017	10.8	7.26	719	0.01	-164	49	250	305
	SS-5	SS	347	431	25	152	14/05/2015	11.4	7.19	765	0.11	-188.4	24	367	447
		SS					11/11/2015	11.9	7.24	765	0.24	-125	87	355	433

Table A.1 continued

Area	Site	Aq	E	N	Elevation (m)	Depth (m)	Sampling date	Temp (°C)	pH	SEC (µS cm^{-1})	DO (mg L^{-1})	ORP (mv)	eh (mv)	TA (mg L^{-1})	HCO3 A (mg L^{-1})
		SS					10/05/2017	11.7	7.2	747	0.14	-150	62	233	283
	MS-2	MS	339	439	14	20	09/11/2015	12.3	7.19	886	0.15	-260	-48	338	460
		MS					11/05/2017	10.9	7.16	883	0.09	43	256	232	282
	MS-9	MS	337	428	15	30	09/05/2017	10.7	7.23	2170	0.03	-137	76	249	303
BASELINE															
South	WG-1	TW	563	142	58	>100	25/09/2014	12.5	6.95	488				156	190
		TW					24/08/2017	12.4	6.8	494	4.93	44	256	154	187
	WG-4	AB	553	137	47		25/09/2014	11.5	6.53	307				86	105
	WG-4	AB	553	137	47		24/08/2017	12	6.39	293	0.17	-14	198	68	83
	HT-1	BG	432	97	6		17/10/2014	14.7	7.82	535				158	193
		BG					21/07/2017	15.1	7.83	480	0.14	-157	52	150	182
	CHK-1	CHK	538	109	36		21/10/2014	11.9	7.42	577				203	247
	LGS-2	LGS	493	122	42		21/10/2014	11.5	7.36	540				166	202
	CHK-3	CHK	486	149	72		03/08/2017	12.1	7.05	686	1.35	160	372	276	336
	CHK-4	CHK	483	105	5	30	17/07/2017	12.7	7.16	604	7.4	170	381	265	323
	CHK-5	CHK	463	112	36	95.4	17/07/2017	14.2	7.07	626	4.28	180	390	234	285
	CHK-2	CHK	528	159	96	135	07/08/2017	12.3	7.01	647	-	120	332	257	313
	CHK-6	CHK	459	155	159	152	10/09/2017	11.4	7.12	634	7.09	121	334	242	295
	LGS-1	LGS	595	149	89		11/08/2017	12.1	6.68	463	6.25	138	350	95	116
	WG-3	AB	574	114	37		25/08/2017	12.8	6.62	475	0.48	-19	192	131	159
	WG-2	TW	524	131	107	100	31/08/2017	14.3	8.86	988	0.2	-166	44	446	544
South Wales	CM-2	CM	278	203	100	183	28/08/2014							202	246
		CM					27/11/2014	12.1	7.14	328				158	192
		CM					12/07/2017	12.7	7.19	410	0.65	-47	164	163	199
	CM-1	CM	263	200	63	50	28/08/2014							176	214
		CM					27/11/2014	11.1	6.82	677				174	212
		CM					13/07/2017	11.6	6.69	658	0.09	-175	37	164	200
	CL-4	CL	289	177	20	10	28/08/2014							190	232
	CL-3	CL	257	189	72	50	27/11/2014	11.6	7.13	805				337	410

Table A.1 continued

Area	Site	Aq	E	N	Elevation (m)	Depth (m)	Sampling date	Temp (°C)	pH	SEC (µS cm^{-1})	DO (mg L^{-1})	ORP (mv)	eh (mv)	TA (mg L^{-1})	HCO3 A (mg L^{-1})
	CM-3	CM	301	203	169		20/06/2017	14.2	5.97	217	8.53	76	286	467	569
BB	CL-1	CL	376	148	80	9.3	10/09/2014	11.4	7.2	684				273	332
	CL-2	CL	343	172	17	33.5	10/09/2014	13.6	7.3	851				317	386
	SS-1	SS	347	168	18	48.7	10/09/2014	12.2	7.28	726				300	365
North	CHK-7	CHK	517	469	46.4	57.7	26/06/2017	10.8	7.24	635	8.6	209	422	140	171
	SS-3	SS	463	406	12	162	27/06/2017	11	7.83	574	9.22	180	393	89	108
	SS-2	SS	433	493	31.6	97.8	27/06/2017	11.6	7.16	1105	2.7	85	297	270	329
	MG-1	MG	355	454	136		04/09/2017	12.5	6.87	446	0.56	162	374	198	241
	BG-1	C-BG	374	452	223		04/09/2017	13.7	7.11	584	0.36	-90	120	266	324
	MG-2	MG	400	445	110		05/09/2017	12.6	7.6	556	0.39	-106	105	259	316
	MG-3	MG	432	454	98		05/09/2017	11.9	6.58	535	0.3	-93	119	176	214

A.2 dissolved gas concentration and isotope compositions

Table A.2 Results from all sites - dissolved gas concentration and isotopic compositions

Site	Sample date	CH_4 (µg L^{-1})	sd	H_2 (ng L^{-1})	sd	$\delta^{13}C(CH_4)$ (‰)	sd	$\delta^{2}H(CH_4)$ (‰)	min	max	$\delta^{13}C(DIC)$ (‰)	sd	min	max	$\delta^{2}H(H_2O)$ (‰)	$\delta^{18}O(H_2O)$ (‰)
OK	22/07/2014	6.85	0.21			-69.5	1.04				-16.3	0.06	-16.30	-16.17		
	21/08/2017	4.57	0.26	4.25	0.83	-61.7	2.69	-38	-39	-38	-15.3				-39.1	-6.0
BN	22/07/2014	4.10	0.73			-32.3	0.10				-12.6	0.22	-12.87	-12.36		
	09/08/2017	2.65	0.10	4.57	0.60	-34.3	1.54	114	109	121	-11.5		-11.51	-11.49	-44.9	-6.8
TL	23/07/2014	2.27	1.15			-55.2	0.09				-12.0	0.15	-12.24	-11.89		
	09/08/2017	1.80	0.16	7.97	2.32	-55.0	0.89	-136	-140	-130	-11.2		-11.18	-11.17	-45.5	-6.9
TG	23/07/2014	6.51	0.03			-57.6	0.72				-16.0	0.06	-16.09	-15.94		
	05/10/2017	5.01	0.22	3.23	0.79	-53.5	3.14	-118	-119	-117	-15.3		-15.28	-15.25	-51.6	-7.7

Table A.2 continued

Site	Sample date	CH_4 ($\mu g\ L^{-1}$)	sd	H_2 ($ng\ L^{-1}$)	sd	$\delta^{13}C(CH_4)$ (‰)	sd	$\delta^{2}H(CH_4)$ (‰)	min	max	$\delta^{13}C(DIC)$ (‰)	sd	min	max	$\delta^{2}H(H_2O)$ (‰)	$\delta^{18}O(H_2O)$ (‰)
BH	24/07/2014	7.85	0.41			-49.8	3.09				-16.0	0.14	-16.18	-15.87		
	05/10/2017	6.46	0.20	2.74	1.48	-54.3	0.45	-91	-94	-89	-15.5		-15.47	-15.44	-50.3	-7.5
TM	24/07/2014	10.04	1.06			-50.9	0.10				-16.2	0.24	-16.45	-15.70	-49.2	-7.4
SHP	25/07/2014	9.66	0.14			-58.4	0.54				-11.1	0.15	-11.32	-10.96		
	24/05/2017	3.77	0.29	4.85	2.57	-56.7	1.43	-183	-183	-182	-10.4		-10.45	-10.41	-54.3	-8.0
HL	25/07/2014	5.82	0.38		1.22	-50.0	0.52				-11.7	0.08	-11.76	-11.59		
	25/07/2017	2.00	0.19	4.88		-48.2	1.62	-150	-159	-145	-11.1		-11.17	-11.08	-55.5	-8.2
NM	14/10/2014	0.38	0.06			-33.0	0.54				-14.9	0.15	-15.06	-14.70		
	20/09/2017	0.10	0.01	1.26	0.12						-13.1		-13.15	-12.94	-46.2	-7.0
MH	22/10/2014	2.51	0.29			-29.3	0.16				-12.8	0.02	-12.85	-12.80	-46.4	-7.0
MP	17/07/2017	0.48	0.03	3.72	0.43	-61.8	2.38				-13.2		-13.29	-13.10	-49.4	-7.3
NS	17/07/2017	2.30	0.15	1.19	0.02	-50.8	1.39	-103	-103	-102	-12.2				-49.1	-7.3
													-12.31	-12.17		
SS-4	02/02/2015	1862.07	n/a			-73.1	0.87				-13.5	0.43	-13.96	-13.48		
	09/05/2017	136.78	15.71	154.22	49.34138527	-68.0	4.59	-278	-279	-277	-14.4		-14.42	-14.41	-40.1	-6.0
SS-1	03/02/2015	2.98	0.68			-35.5	2.15				-13.5	0.07	-13.57	-13.44		
	07/05/2015	1.48	0.56			-32.4	3.89				-13.2	0.14	-13.45	-13.15		
	17/11/2015	0.22	0.03			-29.7	2.49				-12.6				-42.6	-6.5
MS-7	27/10/2014	15.37	2.07			-45.0	0.41				-18.1	0.03	-18.12	-18.06		
	12/01/2015	7.63	0.46			-47.0	0.66				-19.6	0.09	-19.74	-19.54		
	03/02/2015	7.32	0.07			-53.0	0.77				-20.5	0.13	-20.72	-20.43		
	07/05/2015	4.69	1.31			-47.9	1.15				-20.2	0.08	-20.33	-20.17		
	17/11/2015	2.53	0.73			-43.9	1.46				-20.6		-20.66	-20.59		
	08/05/2017	5.29	1.07	27.53	8.10	-44.2	0.27	77	75	78	-18.7		-18.76	-18.70	-45.5	-6.6
MS-4	04/02/2015	7.94	0.07			-43.9	0.75				-15.1	0.08	-15.17	-15.00		
	06/05/2015	9.14	2.07			-45.9	0.59				-14.7	0.12	-14.90	-14.66		
	12/11/2015	6.79	0.39								-14.3		-14.35	-14.29	-42.0	-6.3
MS-6	05/02/2015	7.39	0.29			-63.0	2.49				-14.6	0.07	-14.70	-14.53		
	06/05/2015	9.58	1.31			-57.2	9.34				-14.4	0.06	-14.42	-14.31		
	12/11/2015	81.47	12.14			-79.6	8.50				-14.2		-14.17	-14.15		
	11/05/2017	89.66	10.47	65.32	20.87	-81.5	1.67	-353	-354	-351	-13.8		-13.87	-13.82	-41.2	-6.3

Table A.2 continued

Site	Sample date	CH_4 ($\mu g\ L^{-1}$)	sd	H_2 ($ng\ L^{-1}$)	sd	$\delta^{13}C(CH_4)$ (‰)	sd	$\delta^{2}H(CH_4)$ (‰)	min	max	$\delta^{13}C(DIC)$ (‰)	sd	min	max	$\delta^{2}H(H_2O)$ (‰)	$\delta^{18}O(H_2O)$ (‰)
MS-3	06/02/2015	3.53	0.13			-27.9	1.80				-16.9	0.05	-17.22	-16.85		
	15/05/2015	4.13	0.36			-24.1	0.65				-16.6	0.04	-16.62	-16.54	-41.9	-6.3
	10/11/2015	0.87	0.09								-16.2		-16.20	-16.09		
MS-8	10/02/2015	2319.72	321.18			-69.5	0.70				-18.6	0.13	-18.77	-18.45		
	08/05/2015	3448.83	156.03			-73.0	0.77				-17.8	0.12	-17.99	-17.72		
	18/11/2015	2709.94	126.07								-17.6		-17.63	-17.59		
	09/05/2017	2825.63	1273.40	26.32	1.91	-72.2	0.33	-227	-227	-226	-16.9		-16.92	-16.90	-39.8	-6.01
SS-3	11/02/2015	6.76	1.08			-56.1	4.22				-14.2	0.03	-14.26	-14.20		
	06/05/2015	6.59	1.88			-64.9	1.17				-14.3	0.09	-14.32	-14.15		
	10/11/2015	22.98	5.66			-96.3	3.21				-13.9		-13.87	-13.83	-45.3	-6.72
MS-10	11/02/2015	25.25	1.42			-54.5	0.44				-18.8	0.11	-18.95	-18.82		
	14/05/2015	23.36	3.13			-52.7	2.18				-18.6	0.12	-18.76	-18.51		
	11/11/2015	19.16	3.59			-54.6	0.25				-17.2		-17.25	-17.20		
	10/05/2017	19.31	2.79	168.71	32.80	-56.4	0.35	-202	-202	-201	-17.0		-17.05	-17.01	-41.5	-6.22
MS-1	11/05/2015	2.28	0.11			-38.67	4.33				-14.0	0.08	-14.15	-13.94		
	09/11/2015	2.35	0.17			-39.14	3.28				-13.4		-13.51	-13.30	-42.9	-6.43
MS-5	13/05/2015	4.78	0.23			-45.61	0.91				-14.3	0.05	-14.40	-14.29		
	11/05/2017	5.67	0.49	60.00	17.26	-43.91	2.12	52	50	54	-13.7		-13.80	-13.69	-42.5	-6.37
SS-2	13/05/2015	8.54	0.83			-34.94	4.14				-13.9	0.04	-13.98	-13.91		
	18/11/2015	7.07	1.24			-34.12	2.29				-13.6		-13.62	-13.60		
	10/05/2017	7.28	1.09	40.31	11.93	-37.96	1.74	-66	-67	-64	-13.6		-13.61	-13.52	-43.1	-6.6
SS-5	14/05/2015	7.15	0.59			-39.65	2.16				-13.6	0.11	-13.76	-13.52		
	11/11/2015	5.92	0.37			-40.17	3.19				-13.3		-13.34	-13.32		
	10/05/2017	3.70	0.15	41.53	0.46	-37.22	1.18	119	118	121	-13.3		-13.34	-13.32	-42	-6.27
MS-2	09/11/2015	68.73	n/a			-70.79	3.83				-17.4		-17.60	-17.23		
	11/05/2017	1.80	1.22	72.84	2.25	-46.02	3.91				-16.4		-16.49	-16.38	-41.7	-6.21
MS-9	09/05/2017	15.13	0.52	82.05	51.83	-32.27	0.41	248	247	249	-13.6		-13.64	-13.64	-42.6	-6.29
WG-1	25/09/2014	6.05	0.61			-64.41	2.84				-15.8	0.10	-15.94	-15.72		
	24/08/2017	4.49	0.24	4.04	4.89	-75.18	1.52	-175	-177	-174	-13.4		-13.46	-13.39	-44.3	-6.86

Table A.2 continued

Site	Sample date	CH_4 ($\mu g\ L^{-1}$)	sd	H_2 ($ng\ L^{-1}$)	sd	$\delta^{13}C(CH_4)$ (‰)	sd	$\delta^{2}H(CH_4)$ (‰)	min	max	$\delta^{13}C(DIC)$ (‰)	sd	min	max	$\delta^{2}H(H_2O)$ (‰)	$\delta^{18}O(H_2O)$ (‰)
WG-4	25/09/2014	30.33	2.44			-58.80	1.26				-18.5	0.09	-18.60	-18.39		
WG-4	24/08/2017	2.81	0.19	3.57	1.20	-55.94	0.45	-150	-150	-150	-15.9		-15.91	-15.91	-42.5	-6.61
HT-1	17/10/2014	12.66	3.03			-79.79	0.79				-13.4	0.16	-13.64	-13.25		
	21/07/2017	2.69	0.11	7.35	4.23	-78.03	2.19	-197	-198	-197	-12.2		-12.23	-12.19	-45.5	-7.09
CHK-1	21/10/2014	0.47	0.08								-14.1	0.08	-14.24	-14.05	-40.3	-6.39
LGS-2	21/10/2014	0.42	0.13			-38.47	0.11				-14.1	0.10	-14.23	-14.01	-41.1	-6.4
CHK-3	03/08/2017	bdl		0.90	0.19						-12.1		-12.17	-12.11	-44.2	-6.8
CHK-4	17/07/2017	0.05	0.01	1.29	0.27						-13.1		-13.15	-13.14	-41	-6.35
CHK-5	17/07/2017	bdl		1.00	0.10						-10.1		-10.20	-9.94	-42.6	-6.41
CHK-2	07/08/2017	0.07	0.09	1.41	0.21						-12.1		-12.07	-12.05	-47.9	-7.21
CHK-6	10/09/2017	0.04	0.03	1.30	0.10						-12.3		-12.53	-11.99	-45.1	-6.88
LGS-1	11/08/2017	0.02	0.00	19.12	24.91	-67.71	1.65				-15.1		-15.34	-14.89	-45.9	-7
WG-3	25/08/2017	14.00	0.40	25.80	1.70	-56.34	2.77	-41	-42	-39	-13.0		-13.04	-13.02	-39.9	-6.43
WG-2	31/08/2017	39.59	1.56	22.62	9.96	-43.11	3.65	57	56	59	-11.7		-11.75	-11.66	-50.6	-7.7
CM-2	28/08/2014	649.20	8.12			-33.99	0.32				-15.5	0.44	-15.79	-15.68		
	27/11/2014	135.89	83.83			-34.35	0.49				-15.7	0.11	-15.90	-15.66		
	12/07/2017	1446.95	129.99	5.90	1.40	-38.27	2.18	-99	-99	-98	-14.0		-14.02	-13.90	-32.1	-5.03
CM-1	28/08/2014	50.36	8.23								-17.2	0.20	-17.58	-17.04		
	27/11/2014	86.79	5.44			-54.41	0.94				-17.1	0.06	-17.15	-17.02		
	13/07/2017	90.48	12.03	12.83	9.32	-54.75	2.28	-121	-122	-120	-14.4		-14.42	-14.36	-35.7	-5.61
CL-4	28/08/2014	0.60	0.09								-16.0	0.09	-16.09	-15.88	-38.3	-6.04
CL-3	27/11/2014	0.56	0.07			-36.11	0.01				-14.2	0.06	-14.31	-14.19	-37.2	-5.91
CM-3	20/06/2017	1.24	0.04	4.49	0.31	-43.23	0.67	-189	-190	-188	-14.1		-14.20	-14.04	-40.1	-6.11
CL-1	10/09/2014	0.49	0.24			-36.89	0.08				-15.5	0.05	-15.52	-15.41	-40.9	-6.33
CL-2	10/09/2014	0.54	0.17								-14.6	0.32	-14.83	-14.70	-41.5	-6.32
SS-1	10/09/2014	0.45	0.15								-16.2	0.06	-16.26	-16.12	-43.6	-6.58
CHK-7	26/06/2017	0.05	0.03	12.20	5.10						-12.9		-12.93	-12.87	-51.7	-7.73
SS-3	27/06/2017	0.06	0.04	7.93	1.58						-12.1		-12.20	-12.06	-56.1	-8.21

Table A.2 continued

Site	Sample date	CH_4 ($\mu g\ L^{-1}$)	sd	H_2 ($ng\ L^{-1}$)	sd	$\delta^{13}C(CH_4)$ (‰)	sd	$\delta^{2}H(CH_4)$ (‰)	min	max	$\delta^{13}C(DIC)$ (‰)	sd	min	max	$\delta^{2}H(H_2O)$ (‰)	$\delta^{18}O(H_2O)$ (‰)
SS-2	27/06/2017	0.15	0.07	8.80	3.20						-11.3		-11.28	-11.23	-54.7	-8.1
MG-1	04/09/2017	0.22	0.02	6.08	1.82						-13.2		-13.38	-13.06	-43.2	-6.59
BG-1	04/09/2017	10.56	0.69	4.70	1.02	-71.99	5.97	-196	-199	-194	-13.8		-13.82	-13.80	-44.8	-6.98
MG-2	05/09/2017	1431.77	43.51	4.38	1.54	-78.03	0.48	-251	-252	-249	-15.2		-15.20	-15.16	-48.2	-7.21
MG-3	05/09/2017	1367.57	68.89	37.16	2.69	-48.20	4.34	-132	-132	-132	-16.3		-16.25	-16.25	-52.6	-7.6

Appendix B

Duplicates and data rejection

B.1 CH_4 concentration

Table B.1 Duplicates for CH_4 concentration analysis

Area	Site	Sample date	CH_4 (µg L^{-1})			
			1	2	3	4
l. greensands	OK	22/07/2014	6.77	6.81	7.16	6.67
		21/08/2017	4.88	4.46	4.66	4.27
	BN	22/07/2014	3.27	4.67	4.36	
		09/08/2017	2.51	2.71	2.72	2.68
	TL	23/07/2014	2.48	2.34	1.99	
		09/08/2017	1.73	2.00	1.68	1.65
	TG	23/07/2014	6.54	6.52	6.49	6.49
		05/10/2017	5.15	4.90	5.25	4.76
	BH	24/07/2014	7.61	8.40	7.48	7.89
		05/10/2017	6.50	6.17	6.63	6.53
	TM	24/07/2014	10.49	8.47	10.42	10.79
	SHP	25/07/2014	9.83	9.60	9.69	9.51
		24/05/2017	3.35	3.84	3.86	4.02
	HL	25/07/2014	5.52	5.60	5.80	6.36
		25/07/2017	2.11	2.16	2.00	1.73
	NM	14/10/2014	0.39	0.46	0.30	0.36
		20/09/2017	0.11	0.11	0.09	0.09
	MH	22/10/2014	2.12	2.81	2.61	2.49
	MP	17/07/2017	0.51	0.49	0.49	0.43
	NS	17/07/2017	2.23	2.23	2.54	2.22
Lancashire	SS-4	02/02/2015	1862.07			
		09/05/2017	132.26	159.98	129.33	125.55
	SS-1	03/02/2015	3.96	2.52	2.90	2.53
		07/05/2015	1.61	2.21	1.15	0.95
		17/11/2015	0.20	0.23	0.26	0.18
	MS-7	27/10/2014	13.23	13.99	16.89	17.39
		12/01/2015	7.54	7.21	8.13	
		03/02/2015	7.36	7.24	7.35	
		07/05/2015	6.12	5.48	3.55	3.61
		17/11/2015	2.18	2.33	3.61	2.00
		08/05/2017	5.90	3.70	5.74	5.83
	MS-4	04/02/2015	7.86	8.00	7.96	

Table B.1 continued

Area	Site	Sample date	CH_4 ($\mu g\ L^{-1}$)			
			1	2	3	4
		06/05/2015	7.48	11.47	8.48	
		12/11/2015	6.84	7.21	6.83	6.26
	MS-6	05/02/2015	7.04	7.29	7.67	7.58
		06/05/2015	10.44	9.43	10.66	7.78
		12/11/2015	90.06	72.88		
		11/05/2017	97.06	82.26		
	MS-3	06/02/2015	3.43	3.49	3.67	
		15/05/2015	4.51	4.20	4.16	3.64
		10/11/2015	0.93	0.90	0.75	0.91
	MS-8	10/02/2015	2546.83	2092.61		
		08/05/2015	3598.81	3374.59	3556.14	3265.76
		18/11/2015	2819.40	2528.24	2740.03	2752.10
		09/05/2017	1532.81	4578.49	2682.00	2509.23
	SS-3	11/02/2015	8.25	6.54	6.60	5.66
		06/05/2015	7.31	8.26	6.88	3.91
		10/11/2015	15.82	24.32	22.29	29.50
	MS-10	11/02/2015	25.51	27.10	24.59	23.79
		14/05/2015	24.49	21.95	19.89	27.10
		11/11/2015	21.00	21.73	20.02	13.88
		10/05/2017	17.34	21.28		
	MS-1	11/05/2015	2.12	2.34	2.37	2.30
		09/11/2015	2.26	2.51	2.15	2.46
	MS-5	13/05/2015	5.06	4.79	4.49	4.76
		11/05/2017	5.47	6.22	5.31	
	SS-2	13/05/2015	8.05	9.03	9.44	7.65
		18/11/2015	7.12	7.85	8.00	5.29
		10/05/2017	6.46	8.58	6.30	7.77
	SS-5	14/05/2015	7.74	6.56	7.15	
		11/11/2015	5.46	5.88	6.35	5.99
		10/05/2017	3.67	3.86	3.56	
	MS-2	09/11/2015	1099.73			
		11/05/2017	1.04	3.61	1.16	1.38
	MS-9	09/05/2017	15.73	14.89	14.77	
BASELINE						
South	WG-1	25/09/2014	5.38	5.70	6.67	6.46
		24/08/2017	4.66	4.56	4.13	4.59
	WG-4	25/09/2014	27.60	31.08	32.31	
	WG-4	24/08/2017	2.70	3.06	2.84	2.65
	HT-1	17/10/2014	9.53	15.50	15.00	10.59
		21/07/2017	2.69	2.77	2.53	2.77
	CHK-1	21/10/2014	0.37	0.45	0.50	0.57
	LGS-2	21/10/2014	0.61	0.32	0.35	0.39
	CHK-3	03/08/2017	bdl	bdl	bdl	bdl
	CHK-4	17/07/2017	0.07	0.05	0.05	0.05
	CHK-5	17/07/2017	bdl	bdl	bdl	bdl
	CHK-2	07/08/2017	0.20	0.04	0.01	0.02
	CHK-6	10/09/2017	0.05	0.01	0.08	0.02
	LGS-1	11/08/2017	0.03	0.03	0.02	0.02
	WG-3	25/08/2017	14.46	13.84	13.71	
	WG-2	31/08/2017	38.91	41.30	40.38	37.78
South Wales	CM-2	28/08/2014	654.94	643.46		
		27/11/2014	225.78	59.86	122.03	

Table B.1 continued

Area	Site	Sample date	CH_4	(µg L^{-1})		
			1	2	3	4
		12/07/2017	1294.00	1374.41	1355.04	1538.87
	CM-1	28/08/2014	53.87	38.67	57.69	51.23
		27/11/2014	83.43	93.07	83.88	
		13/07/2017	80.49	103.84	87.11	
	CL-4	28/08/2014	0.59	0.69	0.50	
	CL-3	27/11/2014	0.61	0.49	0.50	0.62
	CM-3	20/06/2017	1.19	1.26	1.26	
Bristol and Bath	CL-1	10/09/2014	0.56	0.76	0.20	0.42
	CL-2	10/09/2014	0.50	0.34	0.55	0.77
	SS-1	10/09/2014	0.34	0.31	0.59	0.58
North	CHK-7	26/06/2017	0.10	0.03	0.06	0.03
	SS-3	27/06/2017	0.04	0.02	0.11	0.07
	SS-2	27/06/2017	0.20	0.08	0.09	0.23
	MG-1	04/09/2017	0.24	0.22	0.20	0.21
	BG-1	04/09/2017	11.31	10.98	9.89	10.07
	MG-2	05/09/2017	1376.21	1431.58	1436.85	1482.44
	MG-3	05/09/2017	1463.31	1370.55	1308.51	1327.90

B.2 H_2 concentration

Table B.2 Duplicates for H_2 concentration analysis

Area	Site	Sample date	H_2	(µg L^{-1})		
			1	2	3	4
l. greensands	OK	21/08/2017	0.003076625	0.00414976	0.002625529	0.003263928
	BN	09/08/2017	0.003936803	0.003019848	0.003621342	
	TL	09/08/2017	0.008786446	0.005743509	0.005176753	0.004901336
	TG	05/10/2017	0.003183669	0.001831688	0.002154885	0.002805633
	BH	05/10/2017	0.001550292	0.001841386	0.003790748	0.001271979
	SHP	24/05/2017	0.006278578	0.003217381	0.00395853	0.001502217
	HL	25/07/2017	0.002611842	0.003418954	0.004708836	0.004319095
	NM	20/09/2017	0.000967628	0.000946756	0.000882092	0.001103106
	MP	17/07/2017	0.003285208	0.002534762	0.002982907	0.002694521
	NS	17/07/2017	0.00090477	0.000920028	0.00093149	
Lancashire	SS-4	09/05/2017	0.17267602	0.113635681	0.106672935	0.083107611
	MS-7	08/05/2017	0.026705352	0.06332541	0.014430732	0.022597629
	MS-6	11/05/2017	0.03199847	0.071132011	0.051174489	0.047327838
	MS-8	09/05/2017	0.020878849	0.018641258	0.000973365	0.02141601
	MS-10	10/05/2017	0.121007755	0.158832577	0.110768838	
	MS-5	11/05/2017	0.056427259	0.055077223	0.046193158	0.027519262
	SS-2	10/05/2017	0.041544831	0.103408129	0.02411277	0.027678566
	SS-5	10/05/2017	0.032302065	0.102907984	0.031804505	
	MS-2	11/05/2017	0.057987251	0.054523614	0.02343508	0.056122245
	MS-9	09/05/2017	0.075154259	0.036026659	0.027495915	0.114619211
BASELINE						
South	WG-1	24/08/2017	0.008628158	0.00232498	0.001295771	0.00021672
	WG-4	24/08/2017	0.00221091	0.003820252	0.002231682	
	HT-1	21/07/2017	0.001244941	0.007696483	0.008520496	0.005235114
	CHK-3	03/08/2017	0.000612643	0.000912843	0.000596806	0.000641536

Table B.2 continued

Area	Site	Sample date	H_2 ($\mu g\ L^{-1}$)			
			1	2	3	4
	CHK-4	17/07/2017	0.000974864	0.001271208	0.000960936	0.000775339
	CHK-5	17/07/2017	0.002668228	0.000889602	0.000784469	0.00066677
	CHK-2	07/08/2017	0.021077262	0.001072948	0.001255461	0.000926052
	CHK-6	10/09/2017	0.000953745	0.001952209	0.000936383	0.001067657
	LGS-1	11/08/2017	0.00112947	0.042470924	0.002442837	0.012987031
	WG-3	25/08/2017	0.008628158	0.00232498	0.001295771	0.00021672
	WG-2	31/08/2017	0.011356657	0.010801186	0.021151362	0.026506989
South Wales	CM-2	12/07/2017	0.005149241	0.005168867	0.003350008	0.018249606
	CM-1	13/07/2017	0.004980103	0.019579689	0.011140202	0.003910631
	CM-3	20/06/2017	0.003276362	0.00368146	0.003240839	0.003667883
North	CHK-7	26/06/2017	0.013387535	0.005558674	0.009354871	0.063837735
	SS-3	27/06/2017	0.007295012	0.004614797	0.00567049	0.00690226
	SS-2	27/06/2017	0.001187092	0.007714006	0.004037711	0.008716529
	MG-1	04/09/2017	0.003595455	0.005846459	0.003352719	0.005963004
	BG-1	04/09/2017	0.003736402	0.003203815	0.00288936	0.004687523
	MG-2	05/09/2017	0.00477058	0.002223506	0.002587383	0.003946544
	MG-3	05/09/2017	0.030084426	0.029215006	0.029810809	0.025608636

B.3 $\delta^{13}C(CH_4)$ analysis

Table B.3 Duplicates for analysis of $\delta^{13}C(CH_4)$ and rejected data

Area	Site	Sample date	d1	v1	d2	v2	d3	v3	d4	v4	Reject[a]
LGS	OK	22/07/2014	-69.62	7.91	-70.25	9.22	-70.07	14.83	-68.06	17.08	
									-68.19	12.90	
		21/08/2017	-58.47	5.95	-60.60	6.60	-60.47	8.01	-61.56	8.42	
			-61.54	8.66	-61.28	6.93	-67.79	8.37	-61.89	10.32	
	BN	22/07/2014	-32.29	6.45	-32.47	6.92	-32.29	5.28	-32.24	9.19	
		09/08/2017	-65.29	11.17	-61.66	10.71	-36.33	1.77	-34.17	4.65	A
			-66.01	10.68	-53.16	4.33	-33.95	1.71	-32.62	3.55	
	TL	23/07/2014	-55.13	3.89	-55.30	5.59	-55.18	5.52			
	TG	09/08/2017	-67.10	15.64	-55.39	5.90	-65.94	10.77	-50.58	4.75	B
			-67.77	14.38	-55.09	4.82	-63.86	10.68	-50.41	4.55	
	BH	21/08/2017	-55.82	5.50	-54.21	4.53					
			-55.66	5.08	-54.20	4.53					
	TM	23/07/2014	-57.39	8.22	-57.93	12.91	-58.41	13.00	-56.74	16.99	
		05/10/2017	-76.41	15.11	-56.14	6.13	-55.81	3.93	-54.79	5.15	A
			-76.76	20.38	-53.85	4.50	-52.51	3.34	-47.64	2.84	
	BH	24/07/2014	-50.77	10.84	-51.27	16.51	-51.53	12.63	-45.45	3.77	
									-45.69	3.89	
		05/10/2017	-45.57	3.90	-54.54	12.59	-53.85	16.01	-54.78	16.14	D
			-51.64	4.71	-54.48	12.39	-54.55	16.96	-53.65	12.98	
	TM	24/07/2014	-50.85	12.75	-50.99	17.26					
	SHP	25/07/2014	-58.68	13.32	-58.74	13.11	-57.79	16.71			
							-57.76	18.18			
		24/05/2017	-53.38	4.78	-57.10	14.52	-56.72	12.41	-57.54	15.88	

Table B.3 continued

Area	Site	Sample date	d1	v1	d2	v2	d3	v3	d4	v4	Reject[a]
			-56.15	8.48	-57.25	9.34	-57.45	12.82	-57.81	10.16	
	HL	25/07/2014	-50.41	9.28	-50.55	10.94	-49.75	10.18	-49.50	7.63	
									-49.44	6.83	
		25/07/2017	-49.45	7.75	-48.70	9.73	-46.22	4.30	-45.13	3.95	
			-49.21	4.12	-49.44	10.21	-48.39	6.30	-48.99	9.81	
	NM	14/10/2014	-33.40	1.05							
			-32.63	0.70							
		20/09/2017	-63.64	22.71	-68.31	20.47					A
			-60.65	15.84	-58.94	6.93					
	MH	22/10/2014	-29.40	7.03	-29.46	6.43	-29.27	5.68	-29.05	7.25	
			-29.22	5.09	-29.30	6.39	-29.57	4.52	-29.33	6.54	
	MP	17/07/2017	-62.39	5.43	-59.68	5.68	-65.27	9.97	-64.27	8.51	
			-63.44	6.39	-58.79	4.96	-61.02	7.25	-59.74	6.05	
	NS	17/07/2017	-51.05	10.74	-47.76	13.75	-52.75	11.50	-51.23	11.08	
			-50.82	11.10	-51.08	9.99	-51.22	12.04	-50.88	9.93	
LANCS	SS-4	02/02/2015	-72.81	0.39	-74.22	0.11	-72.50	0.40			
			-72.78	0.22			-71.84	0.20			
		09/05/2017	-57.56	13.91	-69.75	33.47	-69.98	27.77	-68.73	23.70	
			-70.32	28.00	-69.27	21.55	-69.65	19.54			
	SS-1	03/02/2015	-35.72	1.99	-39.25	1.87	-34.24	1.72			
			-35.08	2.13	-35.99	1.98	-32.86	1.79			
		07/05/2015	-31.65	3.96	-32.26	2.34	-29.91	3.52	-31.61	4.73	
			-34.72	4.44	-39.89	2.74	-27.70	3.77	-47.17	14.37	C
		17/11/2015	-29.82	2.22	-32.95	2.16	-26.41	1.61	-44.98	4.52	C
			-30.77	2.37	-27.24	1.64	-31.29	2.30			
	MS-7	27/10/2014	-44.42	11.20	-45.01	12.06	-45.25	9.45	-45.40	10.33	
			-44.36	12.33	-45.14	12.55	-45.22	9.69	-45.34	10.68	
		12/01/2015	-47.31	6.56	-47.59	6.23	-46.46	2.87			
					-47.48	4.68	-46.13	4.31			
		03/02/2015	-48.43	3.14	-52.34	3.36	-53.87	4.35	-46.90	1.07	C
			-52.61	11.35	-52.62	2.87	-53.95	5.34			
		07/05/2015	-47.10	2.18	-47.30	13.07	-47.09	7.47	-46.65	0.91	
					-47.66	14.00	-47.17	7.25	-50.03	3.29	
		17/11/2015	-42.51	7.08	-43.39	4.80	-44.37	7.55	-45.44	3.07	
			-42.38	7.55	-46.35	2.47	-43.99	6.60	-42.57	6.06	
		08/05/2017			-44.53	16.18			-44.23	7.59	
					-43.88	11.92			-44.21	6.15	
	MS-4	04/02/2015	-44.22	2.84	-43.23	3.86	-43.44	5.25	-44.54	2.36	
			-43.13	4.58	-44.75	2.34	-42.96	5.24	-44.68	2.76	
		06/05/2015	-44.90	3.51	-46.18	7.00	-46.05	6.10	-46.69	1.15	
					-45.92	7.64			-46.19	1.06	
		12/11/2015	-43.11	3.78	-65.13	13.64	-43.68	3.50	-61.90	12.52	A
			-43.17	5.59	-63.85	8.19	-44.34	1.23	-62.17	10.94	
	MS-6	05/02/2015	-61.63	4.05	-66.80	16.22	-62.61	3.09	-61.09	3.57	
			-61.51	4.34	-67.08	16.55	-62.66	3.93	-60.93	3.45	
		06/05/2015			-61.40	7.25	-59.05	4.94	-61.68	6.60	
					-61.01	7.20	-61.72	7.26	-38.23	1.54	
		12/11/2015	-83.44	12.73	-83.88	10.29	-81.41	3.75	-58.79	3.71	C
			-83.50	12.28	-83.62	12.73	-81.35	3.78	-80.77	10.66	
		11/05/2017	-82.64	26.76	-81.81	22.21					
			-82.37	16.12	-79.00	14.02					
	MS-3	06/02/2015	-30.06	4.54	-26.75	7.30	-44.83	3.29	-27.53	5.64	C
			-30.21	6.62	-25.98	5.10	-40.66	5.97	-26.93	6.04	
		15/05/2015	-23.62	8.39	-24.37	8.76	-44.33	2.79	-41.46	13.49	A,C

Table B.3 continued

Area	Site	Sample date	d1	v1	d2	v2	d3	v3	d4	v4	Reject[a]
			-40.01	4.07	-23.29	9.69	-24.70	8.21	-41.54	13.28	
		10/11/2015	-39.34	2.59	-45.62	3.30			-47.97	2.26	B
			-24.48	2.32	-53.76	2.59			-22.68	2.41	
	MS-8	10/02/2015	-69.30	0.64	-68.92	0.70	-69.96	1.67	-70.13	1.41	
					-69.69	0.41	-70.16	1.28	-68.29	1.01	
		08/05/2015	-73.61	8.77	-74.03	9.18	-71.85	6.06			
			-73.12	5.44	-72.55	3.30	-73.01	3.91			
		18/11/2015	-58.64	2.12	-74.72	7.78	-52.23	1.23	-61.74	3.69	B
			-74.36	5.95	-59.79	3.44	-57.46	0.64	-66.27	4.61	
		09/05/2017	-71.81	5.39	-72.32	7.85	-72.01	5.68	-72.36	8.20	
			-71.71	6.67	-72.19	16.51	-72.66	21.37			
	SS-3	11/02/2015	-50.94	2.55	-58.93	6.68	-63.15	3.20	-58.76	4.81	D
			-50.47	3.48	-59.70	6.06	-46.90	1.45	-57.78	4.71	
		06/05/2015	-64.75	7.45	-63.85	9.28	-65.66	8.26	-63.86	4.10	
			-63.64	7.70	-64.73	9.04	-67.02	8.96	-65.68	6.70	
		10/11/2015	-95.27	5.69	-99.60	3.35	-96.41	6.25			
			-90.63	2.43	-97.30	2.32	-98.82	13.49			
	MS-10	11/02/2015	-54.32	7.68	-54.76	6.63	-55.16	9.31			
			-54.21	9.33	-54.80	9.33	-53.99	9.23			
		14/05/2015	-54.60	12.51	-52.84	10.92			-51.46	3.14	
			-54.33	12.40	-49.00	8.08			-54.23	8.90	
		11/11/2015	-54.48	6.62					-54.83	7.14	
			-54.34	5.75					-42.44	2.71	C
		10/05/2017	-57.05	14.93	-56.57	21.77			-56.26	16.23	
			-56.06	11.07	-56.26	19.47			-56.42	17.16	
	MS-10	11/05/2015	-59.93	16.35	-42.92	7.57	-34.02	4.66	-41.11	5.57	D
			-55.02	9.17	-42.14	8.26	-32.67	5.50	-39.17	3.13	
		09/11/2015			-66.08	9.78	-42.48	7.88	-40.32	1.97	A
					-65.67	9.92	-39.06	3.71	-34.70	1.92	
	MS-5	13/05/2015	-44.99	6.58	-45.16	7.10	-45.42	6.24	-47.01	6.91	
			-45.31	6.98	-44.94	7.30	-44.96	5.72	-47.11	6.52	
		11/05/2017	-42.69	5.28	-42.62	8.90	-42.87	7.60			
			-43.49	4.64	-43.64	9.20	-48.15	3.40			
	SS-2	13/05/2015	-37.38	4.82	-50.92	14.53	-35.99	11.89	-36.59	8.86	A
			-36.71	4.12	-50.19	10.11	-36.41	11.36	-26.53	5.45	
		18/11/2015	-33.92	7.66	-35.45	6.38	-35.98	9.77	-29.84	10.08	
			-35.71	6.65	-35.97	8.76	-36.22	7.22			
		10/05/2017	-40.85	5.53			-39.33	14.55	-36.44	13.99	
			-37.09	4.70			-36.80	8.99	-37.26	14.98	
	SS-5	14/05/2015	-39.53	7.05	-38.6	4.742	-39.35	3.23	-38.82	5.881	
			-44.75	8.10	-38.99	6.353	-39.55	3.85	-37.57	5.796	
		11/11/2015			-46.22	1.38	-38.04	8.03	-41.25	5.50	C
					-38.88	9.58	-38.60	5.54	-38.05	6.94	
		10/05/2017	-38.72	9.24	-36.87	8.85	-38.08	7.11	-35.63	7.67	
			-38.83	6.65	-36.63	7.17	-36.20	7.21	-36.77	9.32	
	MS-2	09/11/2015	-71.37	4.10	-73.03	7.98	-58.58	1.91			C
			-65.72	3.87			-56.47	0.93			
		11/05/2017	-48.59	3.56	-49.54	5.53	-39.90	3.67			
			-49.11	3.93	-46.22	4.10	-42.78	4.59			
	MS-9	09/05/2017			-31.67	6.55	-32.52	17.21			
					-32.50	7.36	-32.40	9.86			
South	WG-1	25/09/2014	-66.42	0.50	-62.40	2.22					
			-66.42	1.01	-73.03	0.87					

Table B.3 continued

Area	Site	Sample date	d1	v1	d2	v2	d3	v3	d4	v4	Reject[a]
		24/08/2017	-74.83	17.39	-75.58	10.72	-76.54	13.69	-75.90	12.74	
			-71.68	6.18	-74.98	9.37	-75.86	10.53	-76.08	11.12	
	WG-4	25/09/2014	-58.27	12.02	-60.49	16.62	-57.94	2.54			
			-57.95	12.35	-60.34	16.53	-57.83	4.02			
		24/08/2017	-56.12	8.86	-56.40	11.36	-55.28	9.69	-56.14	13.15	
			-55.68	8.40	-56.49	11.79	-55.37	9.04	-56.07	13.29	
	HT-1	17/10/2014	-79.63	9.04	-78.83	8.64	-79.38	8.73	-80.27	7.64	
			-80.43	10.27	-80.83	8.57	-78.66	7.86	-80.27	7.64	
		21/07/2017	-80.10	17.64	-78.23	12.28	-70.14	5.11	-75.05	9.26	C, D
			-80.55	22.23	-79.21	10.00	-56.12	2.91			
	CHK-1	21/10/2014	-39.71	0.25	-39.43	0.40					
			-37.90	0.22	-39.72	0.42					
	LGS-2	21/10/2014	-38.54	2.42	-39.58	0.83					
			-38.39	1.84	-41.04	0.51					
	LGS-1	11/08/2017	-68.87	10.33							A
			-66.54	12.34							
	WG-3	25/08/2017	-56.00	12.47	-59.04	15.83	-58.81	15.29	-54.77	3.99	
			-57.11	11.75	-51.45	15.50	-58.76	14.67			
	WG-2	31/08/2017	-39.53	7.83	-27.52	4.84	-16.62	1.59	-29.33	0.75	C
			-41.16	14.71	-41.22	17.11	-47.77	19.50	-14.23	1.71	
South Wales	CM-2	28/08/2014	-35.98	0.05	-34.38	0.41	-34.35	0.37			
			-33.63	0.40	-33.88	0.33	-34.11	0.27			
		27/11/2014	-34.64	0.40	-34.29	0.48	-33.51	0.27	-34.58	0.41	
					-34.76	0.43	-41.67	0.01	-34.85	0.32	
		12/07/2017	-38.81	6.21	-34.04	0.18	-39.64	7.45	-35.64	5.01	
			-39.19	15.03	-39.62	6.85	-39.47	8.80	-39.77	12.52	
	CM-1	28/08/2014	-39.10	3.34	-56.37	4.35	-30.61	3.21	-56.85	4.90	B
			-39.14	2.90	-55.64	3.98	-30.67	2.55	-56.79	3.02	
		27/11/2014	-54.64	5.28	-54.69	2.94	-54.83	5.72	-54.84	4.26	
			-52.41	3.79					-54.34	5.22	
		13/07/2017	-55.42	8.98	-26.70	2.65	-52.68	7.56	-51.37	8.05	D
			-56.08	18.51	-43.13	10.01	-58.00	30.46	-56.14	9.70	
	CL-4	28/08/2014	-63.50	2.81	-43.17	1.04					
			-51.90	1.09	-43.27	0.23					
	CL-3	27/11/2014	-40.51	0.42	-36.11	3.75	-41.49	0.60			
			-41.35	0.41	-36.10	3.93	-42.31	0.57			
	CM-3	20/06/2017	-42.91	5.61	-44.00	8526.00	-43.51	5766.00			
			-42.05	4.76	-43.50	6909.00	-43.40	4667.00			
Bristol and Bath	CL-1	10/09/2014	-39.07	0.79	-39.26	0.87	-36.83	1.43	-40.63	0.52	
			-38.80	0.74	-38.53	0.84	-36.95	1.25	-39.96	0.31	
	CL-2	10/09/2014	-37.55	0.89	-37.78	0.26					
			-37.64	0.59	-36.83	0.26					
	SS-1	10/09/2014	-43.92	0.57							
			-43.36	0.44							
North	CHK-7	26/06/2017									
	SS-3	27/06/2017									
	SS-2	27/06/2017									
	MG-1	04/09/2017	-70.30	21.07	-46.63	7.51					B
			-70.43	20.39	-46.32	7.04					

Table B.3 continued

Area	Site	Sample date	d1	v1	d2	v2	d3	v3	d4	v4	Reject[a]
	BG-1	04/09/2017	-75.27	7.71	-76.38	13.02	-66.06	7.19			
			-75.58	8.68	-62.76	6.14	-75.88	11.01			
	MG-2	05/09/2017	-77.91	6.34	-78.02	5.61	-77.95	7.21	-78.52	9.45	
			-77.99	6.99	-77.11	5.59	-78.72	1.13	-78.01	11.17	
	MG-3	05/09/2017	-41.72	6.53	-51.30	7.53	-51.46	7.89	-50.98	7.02	
			-40.90	11.74	-50.60	9.21	-48.98	9.81	-49.62	11.23	

All data with voltage below acceptable level (1 v) - rejected [a] other reasons for data rejection: A: not consistent with GC concentration - ignore - well artifact B: whole day reject due to inconsistency C: voltage not consistent with concentration - processing error D: 2 vials from same bag completely different - processing collection error

B.4 $\delta^2H(CH_4)$ analysis

Table B.4 Duplicates for analysis of $\delta^2H(CH_4)$ analysis by UoO[a]

Area	Site	Sample date	$\delta^2H(CH_4)$ (‰)		
			1	2	3
l. greensands	OK	21/08/2017	-39	-38	
	BN	09/08/2017	109	113	121
	TL	09/08/2017	-138	-140	
	TG	05/10/2017	-119	-117	
	BH	05/10/2017	-90	-89	
	SHP	24/05/2017	-183	-182	
	HL	25/07/2017	-159	-146	-145
	NS	17/07/2017	-102	-103	
Lancashire	SS-4	09/05/2017	-279	-279	
	MS-7	08/05/2017	78	75	
	MS-6	11/05/2017	-351	-354	
	MS-8	09/05/2017	-227	-226	
	MS-10	10/05/2017	-202	-201	
	MS-5	11/05/2017	50	54	
	SS-2	10/05/2017	-67	-64	
	SS-5	10/05/2017	118	121	
	MS-9	09/05/2017	247	249	
BASELINE					
South	WG-1	24/08/2017	-177	-174	
	WG-4	24/08/2017	-150	-150	
	HT-1	21/07/2017	-197	-198	
	WG-3	25/08/2017	-39	-42	
	WG-2	31/08/2017	56	59	
South Wales	CM-2	12/07/2017	-99	-98	
	CM-1	13/07/2017	-120	-122	
	CM-3	20/06/2017	-188	-190	
North	BG-1	04/09/2017	-199	-194	
	MG-2	05/09/2017	-251	-249	

Table B.4 continued

Area	Site	Sample date	$\delta^2H(CH_4)$ (‰)		
			1	2	3
	MG-3	05/09/2017	-132	-132	

[a] Analyses by GGHatch Stable Isotope Laboratories, University of Ottawa; 2 isotubes sent per site + duplicates for BN, HL and NS

B.5 $\delta^{13}C$(DIC) analysis

Table B.5 Duplicates for analysis of $\delta^{13}C(DIC)$ [a]

Area	Site	Sample date	d1	v1	d2	v2	d3	v3	d4	v4	d13C - Isoanalytical	
l. greensands	OK	22/07/2014	-16.27	21.29	-16.17	19.09	-16.30	22.19	-16.28	21.93		
		21/08/2017										
	BN	22/07/2014	-12.87	29.58	-12.49	35.25	-12.58	35.21	-12.36	36.06		
		09/08/2017									-11.51	-11.49
	TL	23/07/2014	-12.03	26.01	-12.24	24.83	-11.96	25.12	-11.89	25.63		
		09/08/2017									-11.18	-11.17
	TG	23/07/2014	-15.94	26.77	-16.06	25.65	-16.09	25.24	-16.03	26.14		
		05/10/2017									-15.28	-15.25
	BH	24/07/2014	-15.87	24.50	-15.94	24.70	-16.05	24.50	-16.18	24.88		
		05/10/2017									-15.47	-15.44
	TM	24/07/2014	-16.22	24.51	-16.21	20.28	-16.17	24.43	-16.27	23.98		
		repeat					-15.91	11.11	-16.32	18.21		
		repeat					-15.70	5.92	-16.45	14.00		
	SHP	25/07/2014	-10.90	33.13	-11.24	32.23	-11.09	32.99	-10.96	32.96		
		repeat	-10.92	28.22								
		repeat	-11.07	19.74								
		repeat	-11.23	15.48								
		repeat	-11.21	12.21								
		repeat	-11.29	8.95								
		repeat	-11.24	7.06								
		repeat	-11.24	5.18								
		repeat	-11.32	3.94								
		24/05/2017									-10.45	-10.41
	HL	25/07/2014	-11.76	33.57	-11.67	34.26	-11.59	34.66	-11.62	34.64		
		25/07/2017									-11.17	-11.08
	NM	14/10/2014	-15.06	7.77	-14.70	7.81	-14.81	7.44	-14.85	7.93		
		20/09/2017									-13.15	-12.94
	MH	22/10/2014	-12.85	9.82	-12.80	10.56	-12.84	10.58	-12.83	10.93		
	MP	17/07/2017									-13.29	-13.10
	NS	17/07/2017									-12.31	-12.17
Lancashire	SS-4	02/02/2015	-13.85	36.70	-13.00	36.77	-13.04	37.41	-13.08	37.14	-13.96	-13.48

Table B.5 continued

Area	Site	Sample date	d1	v1	d2	v2	d3	v3	d4	v4	d13C - Isoanalytical	
		rep	-14.20	29.30	-13.48	29.27	-13.65	29.70	-13.67	29.05		
		rep	-13.96	8.44								
		09/05/2017									-14.42	-14.41
	SS-1	03/02/2015	-13.44	24.34	-13.46	18.04	-13.57	22.98	-13.57	23.02		
		07/05/2015	-13.15	22.73	-13.45	25.21	-13.23	23.70	-13.17	23.39		
		17/11/2015										
	MS-7	27/10/2014	-18.06	21.63	-18.06	21.63	-18.12	22.10	-18.12	23.66		
		rep					-18.12	22.37				
		12/01/2015	-19.60	21.73	-19.74	22.02	-12.94	0.29	-19.54	22.10		
							-19.68	19.60				
		03/02/2015	-20.52	20.32	-20.47	21.70	-20.43	21.56	-20.72	21.59		
		07/05/2015	-20.33	15.46	-20.18	23.27	-20.20	23.18	-20.17	22.78		
		17/11/2015									-20.66	-20.59
		08/05/2017									-18.76	-18.70
	MS-4	04/02/2015	-15.14	23.80	-15.00	24.25	-15.05	23.77	-14.41	0.36		
		rep							-50.99	47.72		
		rep							-15.17	18.57		
		06/05/2015	-14.90	23.13	-14.67	24.80	-14.66	25.07	-14.67	25.45		
		12/11/2015									-14.35	-14.29
	MS-6	05/02/2015	-14.70	24.66	-14.65	25.18	-14.62	24.76	-14.53	23.56		
		06/05/2015	-14.42	25.53	-14.31	25.72	-14.40	25.39	-14.31	27.28		
		12/11/2015									-14.17	-14.15
		11/05/2017									-13.87	-13.82
	MS-3	06/02/2015	-11.31	0.24	-16.85	28.09	-16.94	27.29	-16.87	28.39		
		rep	-80.76	49.99								
		rep	-17.22	21.64								
		15/05/2015	-16.62	27.82	-16.54	28.48	-16.60	26.67	-16.59	27.75		
		10/11/2015									-16.20	-16.09
	MS-8	10/02/2015	-18.45	23.44	-11.76	0.35	-18.65	23.96	-18.56	24.60		
					-18.77	22.41						
		08/05/2015	-17.99	23.16	-17.79	23.84	-17.76	19.21	-17.72	23.76		
		18/11/2015									-17.63	-17.59

Table B.5 continued

Area	Site	Sample date	d1	v1	d2	v2	d3	v3	d4	v4	d13C - Isoanalytical	
		09/05/2017									-16.92	-16.90
	SS-3	11/02/2015	-11.89	0.20	-14.26	25.12	-14.20	26.38	-14.20	25.29		
		rep	-14.25	25.14								
		06/05/2015	-14.32	26.28	-14.15	16.86	-14.28	21.19				
		10/11/2015									-13.87	-13.83
	MS-10	11/02/2015	-18.12	36.51	-18.82	21.05	-18.64	26.69	-18.83	21.82		
		rep	-18.95	16.77			-18.88	20.06				
		14/05/2015	-18.58	18.44	-18.51	21.79	-18.72	19.82	-18.76	15.59		
		11/11/2015									-17.25	-17.20
		10/05/2017									-17.05	-17.01
	MS-1	11/05/2015	-14.15	24.43	-13.94	25.03	-14.02	25.23	-14.05	24.95		
		09/11/2015									-13.51	-13.30
	MS-5	13/05/2015	-14.33	24.00	-14.29	24.32	-14.30	24.27	-14.40	24.21		
		11/05/2017									-13.80	-13.69
	SS-2	13/05/2015	-14.30	87.06	-13.98	23.73	-13.92	24.60	-13.91	24.14		
		18/11/2015									-13.62	-13.60
		10/05/2017									-13.61	-13.52
	SS-5	14/05/2015	-13.76	28.01	-13.58	28.79	-13.52	28.55	-13.26	0.81		
									-13.56	28.13		
		11/11/2015									-13.34	-13.32
		10/05/2017									-13.34	-13.32
	MS-2	09/11/2015									-17.60	-17.23
		11/05/2017									-16.49	-16.38
	MS-9	09/05/2017									-13.64	-13.64
BASELINE												
South	WG-1	25/09/2014	-15.94	15.80	-15.72	15.91	-15.78	16.07	-15.76	10.78		
		24/08/2017									-13.46	-13.39
	WG-4	25/09/2014	-18.60	14.87	-18.39	15.22	-18.43	14.78	-18.49	15.10		
		24/08/2017									-15.91	-15.91
	HT-1	17/10/2014	-14.45	0.14	-13.28	13.27	-13.25	11.30	-13.34	13.43		
		rep	-13.45	29.23								

Table B.5 continued

Area	Site	Sample date	d1	v1	d2	v2	d3	v3	d4	v4	d13C - Isoanalytical	
		rep	-13.64	21.22								
		21/07/2017									-12.23	-12.19
	CHK-1	21/10/2014	-14.24	17.37	-14.13	17.61	-14.07	17.69	-14.05	16.60		
	LGS-2	21/10/2014	-14.01	12.65	-14.10	15.20	-14.23	15.42	-14.21	15.59		
	CHK-3	03/08/2017									-12.17	-12.11
	CHK-4	17/07/2017									-13.15	-13.14
	CHK-5	17/07/2017									-10.20	-9.94
	CHK-2	07/08/2017									-12.07	-12.05
	CHK-6	10/09/2017									-12.53	-11.99
	LGS-1	11/08/2017									-15.34	-14.89
	WG-3	25/08/2017									-13.04	-13.02
	WG-2	31/08/2017									-11.75	-11.66
South Wales	CM-2	28/08/2014	-16.21	39.87	-14.84	38.70	-15.25	39.19	-14.96	38.88		
		repeat	-15.67	28.97	-15.71	29.16	-15.68	29.03	-15.79	29.06		
		repeat	-15.77	22.71								
		27/11/2014	-15.90	16.53	-15.66	17.01	-15.71	16.44	-15.69	16.70		
		12/07/2017									-14.02	-13.90
	CM-1	28/08/2014	-19.26	41.07	-17.09	19.53	-17.10	20.30	-17.04	19.03		
		repeat	-17.27	30.92	-17.35	29.51						
		repeat	-16.84	1.62								
		repeat	-17.58	18.15								
		27/11/2014	-17.02	19.89	-17.12	19.82	-17.11	19.07	-17.15	19.18		
		13/07/2017									-14.42	-14.36
	CL-4	28/08/2014	-16.09	17.41	-15.88	16.76	-16.02	17.63	-16.03	17.04		
	CL-3	27/11/2014	-14.31	27.25	-10.91	0.26	-14.19	26.19	-14.19	26.81		
		repeat			-14.21	26.46						
	CM-3	20/06/2017									-14.20	-14.04
Bristol and Bath	CL-1	10/09/2014	-15.46	22.91	-15.52	23.61	-15.41	23.27	-15.52	22.60		
	CL-2	10/09/2014	-14.71	23.82	-14.74	22.94	-13.93	0.66	-14.70	24.78		
		repeat					-14.03	34.79				

Table B.5 continued

Area	Site	Sample date	d1	v1	d2	v2	d3	v3	d4	v4	d13C - Isoanalytical	
		repeat					-14.83	13.05				
	SS-1	10/09/2014	-16.26	23.83	-16.16	24.06	-16.12	22.78	-16.21	23.77		
North	CHK-7	26/06/2017									-12.93	-12.87
	SS-3	27/06/2017									-12.20	-12.06
	SS-2	27/06/2017									-11.28	-11.23
	MG-1	04/09/2017									-13.38	-13.06
	BG-1	04/09/2017									-13.82	-13.80
	MG-2	05/09/2017									-15.20	-15.16
	MG-3	05/09/2017									-16.25	-16.25

[a]Samples collected 2014 - May 2015 - Analysed in Biogeochemistry Laboratory, Bristol - 4 samples per site; Samples collected Nov 2015 - 2017 - Analysed by IsoAnalytical - 2 samples per site Reasons for data rejection: voltage below or above acceptable level; acceptable range 1 - 35 V; if outside range, analysis repeated

Appendix C

Errors and uncertainties

Reported errors given within data analysis are dependent on methodology and number of duplicates taken. Full details of methodologies and number of samples and duplicates taken are given in Chapter 3 and duplicates for each site are given in Appendix B.

For each site, four samples for each of CH_4, and $\delta^{13}C(CH_4)$ are taken for analysis in the Bristol Biogeochemistry laboratories. An average and standard deviation of each set of four analyses are used in the data analysis. Occasionally less than four samples are available and these details are given in Appendix B, where all duplicates are listed.

For each site, four samples for analysis of $\delta^{13}C(DIC)$ were also taken. The earlier samples were all analysed in the Bristol Biogeochemistry laboratories, however, due to equipment issues, later samples were analysed by Iso Analytical Laboratories. Two samples per site visit were sent for analysis to Iso Analytical. Ranges of min and max values were used during data analysis for all sites, for consistency.

At each site where samples were taken for the analysis of $\delta^{2}H(CH_4)$, one gas bag of sample was collected during the field sparging process. Two duplicates were taken from each gas bag and tranfered into Isotubes for analysis by G.G Hatch Stable Isotope Laboratories. Ranges of min and max values were used during data analysis.

For analysis of $\delta^{18}O(H_2O)$ and $\delta^{2}H(H_2O)$, one sample for each site vist (plus a duplicate for every 10th sample) was send to the BGS NERC Isotope Geoscience Laboratory (NIGL). Errors used in data analysis, were the analytical errors given by NIGL, which were ± 0.05 ‰and ± 1.0 ‰ for $\delta^{18}O(H_2O)$ and $\delta^{2}H(H_2O)$ repectively. All duplicates were well within these errors.

References

Abesser, C., Shand, P., Ingram, J., 2005. Baseline report series. 18, the Millstone Grit of Northern England. Environment Agency, 30pp. (CR/05/015N)

Abril, G., Commarieu, M.-V., Guérin, F., 2007. Enhanced methane oxidation in an estuarine turbidity maximum. Limnology and Oceanography *52*, 470–475.

Aitkenhead, N., Williams, G.M., 1986. Geological evidence to the Public Inquiry into the gas explosion at Loscoe. British Geological Survey Report (FP/87/8/83AS).

Allen, D.J., Brewerton, L.J., Coleby, L.M., Gibbs, B.R., Lewis, M.A., MacDonald, A.M., Wagstaff, S.J., Williams, A.T., 1997. The physical properties of major aquifers in England and Wales. British Geological Survey Technical Report (WD/97/34).

Alter, M.D., Steiof, M., 2005. Optimized method for dissolved hydrogen sampling in groundwater. Journal of Contaminant Hydrology *78*, 71–86.

Ambrose, K., Hough, E., Smith, N.J.P., Warrington, G., 2014. Lithostratigraphy of the Sherwood Sandstone Group of England, Wales and south-west Scotland. British Geological Survey, 50pp. (RR/14/001)

Amos, R.T., Bekins, B.A., Cozzarelli, I.M., Voytek, M.A., Kirshtein, J.D., Jones, E.J.P., Blowes, D.W., 2012. Evidence for iron-mediated anaerobic methane oxidation in a crude oil-contaminated aquifer. Geobiology *10*, 506–517.

Andrews, I.J., 2013. The Carboniferous Bowland Shale gas study: geology and resource estimation. British Geological Survey for Department of Energy and Climate Change, London, UK.

Anthony, C., 1982. Biochemistry of methylotrophs. Academic Press, London.

Appleton, J.D., Hooker, P.J., Smith, N.J.P., 1995. Methane, carbon dioxide and oil seeps from natural sources and mining area: characteristics, extent and relevance to planning and development in Great Britain. British Geological Survey Technical Report (WP/95/1).

Aravena, R., Harrison, S.M., Barker, J.F., Abercrombie, H., Rudolph, D., 2003. Origin of methane in the Elk Valley coalfield, southeastern British Columbia, Canada. Chemical Geology, Isotopic records of microbially mediated processes *195*, 219–227.

Aravena, R., Wassenaar, L.I., Plummer, L.N., 1995. Estimating C-14 groundwater ages in a methanogenic aquifer. Water Resources Research *31*, 2307–2317.

Arup-Cuadrilla, 2014. Environmental statement; temporary shale gas exploration - Roseacre Wood, Lancashire. https://cuadrillaresources.com/wp-content/uploads/2015/02/Roseacre-Wood-ES.pdf

Aselmann, I., Crutzen, P.J., 1989. Global distribution of natural freshwater wetlands and rice paddies, their net primary productivity, seasonality and possible methane emissions. Journal of Atmospheric Chemistry *8*, 307–358.

Avery, G.B., Shannon, R.D., White, J.R., Martens, C.S., Alperin, M.J., 1999. Effect of seasonal changes in the pathways of methanogenesis on the $\delta^{13}C$ values of pore water methane in a Michigan peatland. Global Biogeochemical Cycles *13*, 475–484.

Avrahamov, N., Gelman, F., Yechieli, Y., Aizenshtat, Z., Nissenbaum, A., Sivan, O., 2015. Proposed sources of methane along the Dead Sea Transform. Chemical Geology 395, 165–175.

Baker, K.M., Bottrell, S.H., Thornton, S.F., Peel, K.E., Spence, M.J., 2012. Effect of contaminant concentration on in situ bacterial sulfate reduction and methanogenesis in phenol-contaminated groundwater. Applied Geochemistry *27*, 2010–2018.

Balabane, M., Galimov, E., Hermann, M., Létolle, R., 1987. Hydrogen and carbon isotope fractionation during experimental production of bacterial methane. Organic Geochemistry 11, 115–119.

Baldassare, F.J., McCaffrey, M.A., Harper, J.A., 2014. A geochemical context for stray gas investigations in the northern Appalachian Basin: Implications of analyses of natural gases from Neogene-through Devonian-age strata. AAPG Bulletin *98*, 341–372.

Banning, N., Brock, F., Fry, J.C., Parkes, R.J., Hornibrook, E.R.C., Weightman, A.J., 2005. Investigation

of the methanogen population structure and activity in a brackish lake sediment. Environmental Microbiology *7*, 947–960.
Barker, J.F., Fritz, P., 1981. The occurrence and origin of methane in some groundwater flow systems. Can. J. Earth Sci. *18*, 1802–1816.
Barnes, R.O., Goldberg, E.D., 1976. Methane production and consumption in anoxic marine sediments. Geology *4*, 297–300.
Barth, J.A.., Cronin, A.., Dunlop, J., Kalin, R.., 2003. Influence of carbonates on the riverine carbon cycle in an anthropogenically dominated catchment basin: evidence from major elements and stable carbon isotopes in the Lagan River (N. Ireland). Chemical Geology 200, 203–216.
Bartlett, K.B., Harriss, R.C., 1993. Review and assessment of methane emissions from wetlands. Chemosphere *26*, 261–320.
Bath, A.H., Darling, W.G., Hitchman, S.P., Andrews, J.N., Cave, M.R., Green, K.A., Reeder, S., 1988. Chemical and Stable Isotopic Analyses of Dissolved Gases and Groundwater Seepages Collected from Wyresdale Tunnel, November 1987. British Geological Survey Technical Report (WE/88/1C).
BBC, 2018. Fracking protesters guilty of road block. BBC News. http://www.bbc.co.uk/news/uk-england-york-north-yorkshire-43388891
BBC, 2017a. Anti-fracking protest blocks busy road. BBC News. http://www.bbc.co.uk/news/uk-england-lancashire-39779068
BBC, 2017b. Scottish government backs fracking ban. BBC News. http://www.bbc.co.uk/news/uk-scotland-scotland-politics-41484153
Beal, E.J., House, C.H., Orphan, V.J., 2009. Manganese- and iron-dependent marine methane oxidation. Science *325*, 184–187.
Beckmann, M., Sheppard, S.K., Lloyd, D., 2004. Mass spectrometric monitoring of gas dynamics in peat monoliths: effects of temperature and diurnal cycles on emissions. Atmospheric Environment *38*, 6907–6913.
Beeskow, B., Treloar, P.J., Rankin, A.H., Vennemann, T.W., Spangenberg, J., 2006. A reassessment of models for hydrocarbon generation in the Khibiny nepheline syenite complex, Kola Peninsula, Russia. Lithos, Peralkaline Rocks *91*, 1–18.
Begos, K., 2014. 4 states confirm water pollution from drilling. USA Today. http://www.usatoday.com/story/money/business/2014/01/05/some-states-confirm-water-pollution-from-drilling/4328859/
Bell, R.A., Darling, W.G., Manamsa, K., O Dochartaigh, B.E.O., 2016. The baseline concentrations of methane in Great British groundwater: the National Methane Baseline Survey. British Geological Survey, 46pp (OR/15/071).
Bell, R.A., Darling, W.G., Ward, R.S., Basava-Reddi, L., Halwa, L., Manamsa, K., Ó Dochartaigh, B.E., 2017. A baseline survey of dissolved methane in aquifers of Great Britain. Science of The Total Environment *601–602*, 1803–1813.
Belyaev, S.S., Wolkin, R., Kenealy, W.R., DeNiro, M.J., Epstein, S., Zeikus, J.G., 1983. Methanogenic bacteria from the Bondyuzhskoe Oil Field: General characterization and analysis of stable-carbon isotopic fractionation. Appl. Environ. Microbiol. *45*, 691–697.
Bergamaschi, P., 1997. Seasonal variations of stable hydrogen and carbon isotope ratios in methane from a Chinese rice paddy. Journal of Geophysical Research-Atmospheres *102*, 25383–25393.
Bergamaschi, P., Lubina, C., Konigstedt, R., Fischer, H., Veltkamp, A.C., Zwaagstra, O., 1998. Stable isotopic signatures (delta C-13, delta D) of methane from European landfill sites. Journal of Geophysical Research-Atmospheres *103*, 8251–8265.
Bergman, I., Svensson, B.H., Nilsson, M., 1998. Regulation of methane production in a Swedish acid mire by pH, temperature and substrate. Soil Biology and Biochemistry *30*, 729–741.
Bernard, B.B., Brooks, J.M., Sackett, W.M., 1976. Natural gas seepage in the Gulf of Mexico. Earth and Planetary Science Letters *31*, 48–54.
Bertram, S., Blumenberg, M., Michaelis, W., Siegert, M., Krueger, M., Seifert, R., 2013. Methanogenic

capabilities of ANME-archaea deduced from C-13-labelling approaches. Environ. Microbiol. *15*, 2384–2393.
BGS, 2018a. Groundwater level information. British Geological Survey. http://www.bgs.ac.uk/research/groundwater/datainfo/levels/home.html.
BGS, 2018b. Groundwater monitoring in Lancashire. http://www.bgs.ac.uk/research/groundwater/shaleGas/monitoring/waterQualityLancashire.html.
Bhattacharjee, A.S., Motlagh, A.M., Jetten, M.S.M., Goel, R., 2016. Methane dependent denitrification-from ecosystem to laboratory-scale enrichment for engineering applications. Water Research *99*, 244–252.
Billett, M.F., Harvey, F.H., 2013. Measurements of CO_2 and CH_4 evasion from UK peatland headwater streams. Biogeochemistry *114*, 165–181.
Bishop, P.K., Lloyd, J.W., 1990. Chemical and isotopic evidence for hydrogeochemical processes occurring in the Lincolnshire Limestone. Journal of Hydrology *121*, 293–320.
Bock, M., Schmitt, J., Beck, J., Schneider, R., Fischer, H., 2014. Improving accuracy and precision of ice core $\delta D(CH_4)$ analyses using methane pre-pyrolysis and hydrogen post-pyrolysis trapping and subsequent chromatographic separation. Atmos. Meas. Tech. *7*, 1999–2012.
Bogner, J.E., Sweeney, R.E., Coleman, D., Huitric, R., Ririe, G.T., 1996. Using isotopic and molecular data to model landfill gas processes. Waste Management & Research *14*, 367–376.
Bonnett, S.A.F., Ostle, N., Freeman, C., 2006. Seasonal variations in decomposition processes in a valley-bottom riparian peatland. Science of the Total Environment *370*, 561–573.
Boothroyd, I.M., Almond, S., Qassim, S.M., Worrall, F., Davies, R.J., 2016. Fugitive emissions of methane from abandoned, decommissioned oil and gas wells. Science of the Total Environment *547*, 461–469.
Boothroyd, I.M., Almond, S., Worrall, F., Davies, R.J., 2017. Assessing the fugitive emission of CH_4 via migration along fault zones – Comparing potential shale gas basins to non-shale basins in the UK. Science of The Total Environment *580*, 412–424.
Bordeleau, G., Rivard, C., Lavoie, D., Lefebvre, R., Malet, X., Ladevèze, P., 2018. Geochemistry of groundwater in the Saint-Édouard area, Quebec, Canada, and its influence on the distribution of methane in shallow aquifers. Applied Geochemistry *89*, 92–108.
Bordeleau, G., Rivard, C., Lavoie, D., Mort, A., Ahad, J., Malet, X., Xu, X., 2015. Identifying the source of methane in groundwater in a "virgin" area with regards to shale gas exploitation: a multi-isotope approach, in: Millot, R., Negrel, P. (Eds.), 11th Applied Isotope Geochemistry Conference Aig-11. Elsevier Science Bv, Amsterdam, pp. 219–222.
Borowski, W.S., 2004. A review of methane and gas hydrates in the dynamic, stratified system of the Blake Ridge region, offshore southeastern North America. Chemical Geology, Geomicrobiology and Biogeochemistry of Gas Hydrates and Hydrocarbon Seeps *205*, 311–346.
Boschetti, T., Etiope, G., Toscani, L., 2013. Abiotic methane in the hyperalkaline springs of Genova, Italy. Procedia Earth and Planetary Science, Proceedings of the Fourteenth International Symposium on Water-Rock Interaction, WRI 14 *7*, 248–251.
Botz, R., Pokojski, H.-D., Schmitt, M., Thomm, M., 1996. Carbon isotope fractionation during bacterial methanogenesis by CO_2 reduction. Organic Geochemistry *25*, 255–262.
Bowes, H.L., Hornibrook, E.R.C., 2006. Emission of highly ^{13}C-depleted methane from an upland blanket mire. Geophysical Research Letters *33*, L04401
Brass, M., Röckmann, T., 2010. Continuous-flow isotope ratio mass spectrometry method for carbon and hydrogen isotope measurements on atmospheric methane. Atmospheric Measurement Techniques *3*, 1707.
Bristow, C., 1995. Facies analysis in the Lower Greensand using ground-penetrating radar. Journal of the Geological Society *152*, 591–598.
British Geological Survey, 2010. DiGMapGB-625 [ESRI Shapefile geospatial data], Scale 1:625000, Updated: July 2013, 5.17, British Geological Survey (BGS), UK, Using: EDINA Geology Digimap Service, http://digimap.edina.ac.uk/, Downloaded: June 2016

Browne, B.A., 2004. Pumping-induced ebullition: A unified and simplified method for measuring multiple dissolved gases. Environmental science & technology *38*, 5729–5736.
Bryant, M.P., 1979. Microbial methane production - theoretical aspects. Journal of Animal Science *48*, 193–201.
Burke, R.A., 1993. Possible influence of hydrogen concentration on microbial methane stable hydrogen isotopic composition. Chemosphere *26*, 55–67.
Cadieux, S.B., White, J.R., Sauer, P.E., Peng, Y., Goldman, A.E., Pratt, L.M., 2016. Large fractionations of C and H isotopes related to methane oxidation in Arctic lakes. Geochimica et Cosmochimica Acta *187*, 141–155.
Çağatay, M.N., Borowski, W.S., Ternois, Y.G., 2001. Factors affecting the diagenesis of Quaternary sediments at ODP Leg 172 sites in western North Atlantic: evidence from pore water and sediment geochemistry. Chemical Geology *175*, 467–484.
Carr, S.A., Schubotz, F., Dunbar, R.B., Mills, C.T., Dias, R., Summons, R.E., Mandernack, K.W., 2018. Acetoclastic Methanosaeta are dominant methanogens in organic-rich Antarctic marine sediments. The ISME Journal *12*, 330–342.
Case, D.H., Ijiri, A., Morono, Y., Tavormina, P., Orphan, V.J., Inagaki, F., 2017. Aerobic and anaerobic methanotrophic communities associated with methane hydrates exposed on the seafloor: A High-Pressure sampling and stable isotope-incubation experiment. Front. Microbiol. *8*, 2569.
Casey, R., 1961. The stratigraphical palaeontology of the Lower Greensand. Palaeontology 3, 487–621.
Chanton, J.P., Bauer, J.E., Glaser, P.A., Siegel, D.I., Kelley, C.A., Tyler, S.C., Romanowicz, E.H., Lazrus, A., 1995. Radiocarbon evidence for the substrates supporting methane formation within northern Minnesota peatlands. Geochimica et Cosmochimica Acta *59*, 3663–3668.
Chanton, J.P., Powelson, D.K., Abichou, T., Fields, D., Green, R., 2008. Effect of temperature and oxidation rate on carbon-isotope fractionation during methane oxidation by landfill cover materials. Environmental Science & Technology *42*, 7818–7823.
Chapelle, F.H., Vroblesky, D.A., Woodward, J.C., Lovley, D.R., 1997. Practical considerations for measuring hydrogen concentrations in groundwater. Environmental science & technology *31*, 2873–2877.
Charman, D.J., Aravena, R., Bryant, C.L., Harkness, D.D., 1999. Carbon isotopes in peat, DOC, CO_2, and CH_4 in a holocene peatland on Dartmoor, southwest England. Geology *27*, 539–542.
Cheung, K., Klassen, P., Mayer, B., Goodarzi, F., Aravena, R., 2010. Major ion and isotope geochemistry of fluids and gases from coalbed methane and shallow groundwater wells in Alberta, Canada. Applied Geochemistry *25*, 1307–1329.
Chidthaisong, A., Chin, K.-J., Valentine, D.L., Tyler, S.C., 2002. A comparison of isotope fractionation of carbon and hydrogen from paddy field rice roots and soil bacterial enrichments during CO_2/H_2 methanogenesis. Geochimica et Cosmochimica Acta *66*, 983–995.
Christian, K.M., Lautz, L.K., Hoke, G.D., Siegel, D.I., Lu, Z., Kessler, J., 2016. Methane occurrence is associated with sodium-rich valley waters in domestic wells overlying the Marcellus shale in New York State: Water Resources Research *52*, 206–226.
Clark, I., Fritz, P., 1997. Environmental isotopes in hydrology. Lewis Publishers, Boca Raton, Florida.
Clymo, R.S., Bryant, C.L., 2008. Diffusion and mass flow of dissolved carbon dioxide, methane, and dissolved organic carbon in a 7-m deep raised peat bog. Geochimica Et Cosmochimica Acta *72*, 2048–2066.
Coleman, D.D., Liu, C.L., Riley, K.M., 1988. Microbial methane in the shallow Palaeozoic sediments and glacial deposits of Illinois, USA. Chemical Geology *71*, 23–40.
Coleman, D.D., Risatti, J.B., Schoell, M., 1981. Fractionation of carbon and hydrogen isotopes by methane-oxidizing bacteria. Geochimica Et Cosmochimica Acta *45*, 1033–1037.
Coleman, M.L., Shepherd, T.J., Durham, J.J., Rouse, J.E., Moore, G.R., 1982. Reduction of water with zinc for hydrogen isotope analysis. Analytical chemistry *54*, 993–995.
Comas, X., Kettridge, N., Binley, A., Slater, L., Parsekian, Baird, A.J., Strack, M., Waddington, J.M., 2013. The effect of peat structure on the spatial distribution of biogenic gases within bogs.

Hydrological Processes *28*, 5483–5494.
Conrad, R., 2005. Quantification of methanogenic pathways using stable carbon isotopic signatures: a review and a proposal. Organic Geochemistry, Stable isotope applications in methane cycle studies *36*, 739–752.
Conrad, R., 1999. Contribution of hydrogen to methane production and control of hydrogen concentrations in methanogenic soils and sediments. FEMS Microbiol Ecol *28*, 193–202.
Conrad, R., Claus, P., 2005. Contribution of methanol to the production of methane and its ^{13}C-isotopic signature in anoxic rice field soil. Biogeochemistry *73*, 381–393.
Conrad, R., Claus, P., Casper, P., 2009. Characterization of stable isotope fractionation during methane production in the sediment of a eutrophic lake, Lake Dagow, Germany. Limnology and Oceanography *54*, 457–471.
Conrad, R., Klose, M., Claus, P., 2002. Pathway of CH_4 formation in anoxic rice field soil and rice roots determined by ^{13}C-stable isotope fractionation. Chemosphere *47*, 797–806.
Conrad, R., Klose, M., Lu, Y., Chidthaisong, A., 2012. Methanogenic pathway and archaeal communities in three different anoxic soils amended with rice straw and maize straw. Front. Microbiol. *3*.
Conrad, R., Noll, M., Claus, P., Klose, M., Bastos, W.R., Enrich-Prast, A., 2011. Stable carbon isotope discrimination and microbiology of methane formation in tropical anoxic lake sediments. Biogeosciences *8*, 795–814.
Cooper, M.D.A., Evans, C.D., Zielinski, P., Levy, P.E., Gray, A., Peacock, M., Norris, D., Fenner, N., Freeman, C., 2014. Infilled ditches are hotspots of landscape methane flux following peatland re-wetting. Ecosystems *17*, 1227–1241.
Coplen, T.B., 2011. Guidelines and recommended terms for expression of stable-isotope-ratio and gas-ratio measurement results. Rapid Communications in Mass Spectrometry *25*, 2538–2560.
Craig, H., 1961. Isotopic Variations in Meteoric Waters. Science *133*, 1702–1703.
Crowe, S.A., Katsev, S., Leslie, K., Sturm, A., Magen, C., Nomosatryo, S., Pack, M.A., Kessler, J.D., Reeburgh, W.S., Roberts, J.A., González, L., Haffner, G.D., Mucci, A., Sundby, B., Fowle, D.A., 2011. The methane cycle in ferruginous Lake Matano. Geobiology *9*, 61–78.
Cuadrilla, 2018. Lancashire, https://cuadrillaresources.com/our-sites/lancashire/
Dai, J., Xia, X., Qin, S., Zhao, J., 2004. Origins of partially reversed alkane $\delta^{13}C$ values for biogenic gases in China. Organic Geochemistry, Conference on Emerging Concepts in Organic Petrology and Geochemistry *35*, 405–411.
Daniels, L., Fulton, G., Spencer, R.W., Orme-Johnson, W.H., 1980. Origin of hydrogen in methane produced by Methanobacterium thermoautotrophicum. J. Bacteriol. *141*, 694–698.
Darling, W.G., Bath, A.H., Talbot, J.C., 2003. The O and H stable isotope composition of freshwaters in the British Isles. 2, surface waters and groundwater. Hydrology and Earth System Sciences *7*, 183–195.
Darling, W.G., Edmunds, W.M., Smedley, P.L., 1997. Isotopic evidence for palaeowaters in the British Isles. Applied Geochemistry *12*, 813–829.
Darling, W.G., Gooddy, D.C., 2006. The hydrogeochemistry of methane: Evidence from English groundwaters. Chemical Geology *229*, 293–312.
Datta, S., Do, L.V., Young, T.M., 2004. A simplified method for sampling and analysis of high volume surface water for organic contaminants using XAD-2. Journal of Environmental Science and Health, Part B *39*, 225–234.
Daulat, W.E., Clymo, R.S., 1998. Effects of temperature and water table on the efflux of methane from peatland surface cores. Atmospheric Environment *32*, 3207–3218.
Dawson, J.J.C., Billett, M.F., Hope, D., Palmer, S.M., Deacon, C.M., 2004. Sources and sinks of aquatic carbon in a peatland stream continuum. Biogeochemistry *70*, 71–92.
Dawson, J.J.C., Billett, M.F., Neal, C., Hill, S., 2002. A comparison of particulate, dissolved and gaseous carbon in two contrasting upland streams in the UK. Journal of Hydrology *257*, 226–246.
de Angelis, M.A., Scranton, M.I., 1993. Fate of methane in the Hudson River and Estuary. Global Biogeochemical Cycles *7*, 509–523.

de Graaf, W., Wellsbury, P., Parkes, R.J., Cappenberg, T.E., 1996. Comparison of acetate turnover in methanogenic and sulfate-reducing sediments by radiolabeling and stable isotope labeling and by use of specific inhibitors: evidence for isotopic exchange. Applied and Environmental Microbiology *62*, 772–777.

De Visscher, De Pourcq Ingrid, Jeffrey, C., 2004. Isotope fractionation effects by diffusion and methane oxidation in landfill cover soils. Journal of Geophysical Research: Atmospheres *109*.

Dean, J.F., Billett, M.F., Murray, C., Garnett, M.H., 2017. Ancient dissolved methane in inland waters revealed by a new collection method at low field concentrations for radiocarbon (^{14}C) analysis. Water Research *115*, 236–244.

DECC, 2015. Onshore oil and gas exploration in the UK: regulation and best practice. https://www.gov.uk/government/publications/regulatory-roadmap-onshore-oil-and-gas-exploration-in-the-uk-regulation-and-best-practice

DECC, 2012. The Unconventional Hydrocarbon Resources of Britain's Onshore Basins - Shale Gas. Department of Energy and Climate Change. https://www.ogauthority.co.uk/media/1693/shalegas_uk.pdf

DEFRA, 2014. Indicator DD1: Methane emissions. Department for Environment, Food & Rural Affairs. https://www.gov.uk/government/statistical-data-sets/agri-environment-indicators

DEFRA, 2013. Water abstraction from non-tidal surface water and groundwater, ENV15 - Water abstraction tables. Department for Environment, Food & Rural Affairs. https://www.gov.uk/government/statistical-data-sets/env15-water-abstraction-tables

DEFRA, 2017. Pollutant information (CH_4), UK. http://naei.beis.gov.uk/overview/pollutants?pollutant_id=3

Deines, P., Grey, J., 2006. Site-specific methane production and subsequent midge mediation within Esthwaite Water, UK. Archiv für Hydrobiologie *167*, 317–334.

Deines, P., Wooller, M.J., Grey, J., 2009. Unravelling complexities in benthic food webs using a dual stable isotope (hydrogen and carbon) approach. Freshwater Biology *54*, 2243–2251.

Ding, J., Ding, Z.-W., Fu, L., Lu, Y.-Z., Cheng, S.H., Zeng, R.J., 2015. New primers for detecting and quantifying denitrifying anaerobic methane oxidation archaea in different ecological niches. Appl Microbiol Biotechnol *99*, 9805–9812.

Dinsmore, K.J., Billett, M.F., Dyson, K.E., 2013. Temperature and precipitation drive temporal variability in aquatic carbon and GHG concentrations and fluxes in a peatland catchment. Global Change Biology *19*, 2133–2148.

Dinsmore, K.J., Billett, M.F., Skiba, U.M., Rees, R.M., Drewer, J., Helfter, C., 2010. Role of the aquatic pathway in the carbon and greenhouse gas budgets of a peatland catchment. Global Change Biology *16*, 2750–2762.

Down, A., Schreglmann, K., Plata, D.L., Elsner, M., Warner, N.R., Vengosh, A., Moore, K., Coleman, D., Jackson, R.B., 2015. Pre-drilling background groundwater quality in the Deep River Triassic Basin of central North Carolina, USA. Appl. Geochem. *60*, 3–13.

Drewer, J., Anderson, M., Levy, P.E., Scholtes, B., Helfter, C., Parker, J., Rees, R.M., Skiba, U.M., 2017. The impact of ploughing intensively managed temperate grasslands on N_2O, CH_4 and CO_2 fluxes. Plant Soil *411*, 193–208.

Drimmie, R., Aravena, R., Wassenaar, L., Fritz, P., Hendry, M., Hut, G., 1991. Radiocarbon and stable isotopes in water and dissolved constituents, Milk River aquifer, Alberta, Canada. Appl. Geochem. *6*, 381–392.

Duddleston, K.N., Kinney, M.A., Kiene, R.P., Hines, M.E., 2002. Anaerobic microbial biogeochemistry in a northern bog: Acetate as a dominant metabolic end product. Global Biogeochemical Cycles *16*, 11-1-11–9.

Dzyuban, A.N., 2011. Methane and its transformation processes in water of some tributaries of the Rybinsk Reservoir. Water Resources *38*, 615.

Egerton, R.H.L., 1994. Recharge of the Lower Greensand aquifer at Slough, England. Quarterly Journal of Engineering Geology and Hydrogeology *27*, S57-S71.

Egger, M., Jilbert, T., Behrends, T., Rivard, C., Slomp, C.P., 2015. Vivianite is a major sink for phosphorus in methanogenic coastal surface sediments. Geochimica et Cosmochimica Acta *169*, 217–235.
Eiler, J.M., Clog, M., Magyar, P., Piasecki, A., Sessions, A., Stolper, D., Deerberg, M., Schlueter, H.-J., Schwieters, J., 2013. A high-resolution gas-source isotope ratio mass spectrometer. International Journal of Mass Spectrometry *335*, 45–56.
Environment Agency, 2015. Historical and current landfill in England and Wales. http://apps.environment-agency.gov.uk/wiyby/37823.aspx
Environment Agency, 1997. Fylde Aquifer/Wyre catchment water resources study, Final Report. Environment Agency. www.environmentdata.org/archive/ealit:920/OBJ/19001203.pdf
Etiope, G., Judas, J., Whiticar, M.J., 2015. Occurrence of abiotic methane in the eastern United Arab Emirates ophiolite aquifer. Arab. J. Geosci. *8*, 11345–11348.
Etiope, G., Lollar, B.S., 2013. Abiotic methane on Earth. Rev Geophys *51*, 276–299.
Etiope, G., Tsikouras, B., Kordella, S., Ifandi, E., Christodoulou, D., Papatheodorou, G., 2013. Methane flux and origin in the Othrys ophiolite hyperalkaline springs, Greece. Chem. Geol. *347*, 161–174.
Etiope, G., Vadillo, I., Whiticar, M.J., Marques, J.M., Carreira, P.M., Tiago, I., Benavente, J., Jimenez, P., Urresti, B., 2016. Abiotic methane seepage in the Ronda peridotite massif, southern Spain. Appl. Geochem. *66*, 101–113.
Ettwig, K.F., Zhu, B., Speth, D., Keltjens, J.T., Jetten, M.S.M., Kartal, B., 2016. Archaea catalyze iron-dependent anaerobic oxidation of methane. PNAS *113*, 12792–12796.
Eymold, W.K., Swana, K., Moore, M.T., Whyte, C.J., Harkness, J.S., Talma, S., Murray, R., Moortgat, J.B., Miller, J., Vengosh, A., Darrah, T.H., 2018. Hydrocarbon-rich groundwater above shale-gas formations: A Karoo Basin case study. Groundwater *56*, 204–224.
Feisthauer, S., Seidel, M., Bombach, P., Traube, S., Knoeller, K., Wange, M., Fachmann, S., Richnow, H.H., 2012. Characterization of the relationship between microbial degradation processes at a hydrocarbon contaminated site using isotopic methods. Journal of Contaminant Hydrology *133*, 17–29.
Fernández-Fuentes, M.A., Ortega Morente, E., Abriouel, H., Pérez Pulido, R., Gálvez, A., 2012. Isolation and identification of bacteria from organic foods: Sensitivity to biocides and antibiotics. Food Control *26*, 73–78.
Fey, A., Claus, P., Conrad, R., 2004. Temporal change of ^{13}C-isotope signatures and methanogenic pathways in rice field soil incubated anoxically at different temperatures. Geochimica et Cosmochimica Acta *68*, 293–306.
Fisher, R., Lowry, D., Wilkin, O., Sriskantharajah, S., Nisbet, E.G., 2006. High-precision, automated stable isotope analysis of atmospheric methane and carbon dioxide using continuous-flow isotope-ratio mass spectrometry. Rapid Communications in Mass Spectrometry *20*, 200–208.
Flint, R., 2017. Fracking ban: What is Wales' situation? BBC News. http://www.bbc.co.uk/news/uk-wales-politics-41489253
Freeman, C., Nevison, G.B., Kang, H., Hughes, S., Reynolds, B., Hudson, J.A., 2002. Contrasted effects of simulated drought on the production and oxidation of methane in a mid-Wales wetland. Soil Biology & Biochemistry *34*, 61–67.
Frenzel, P., Bosse, U., 1996. Methyl fluoride, an inhibitor of methane oxidation and methane production. FEMS Microbiol Ecol *21*, 25–36.
Fu, L., Li, S.-W., Ding, Z.-W., Ding, J., Lu, Y.-Z., Zeng, R.J., 2016. Iron reduction in the DAMO/Shewanella oneidensis MR-1 coculture system and the fate of Fe(II). Water Res. *88*, 808–815.
Fuchs, G., Thauer, R., Ziegler, H., Stichler, W., 1979. Carbon isotope fractionation by Methanobacterium thermoautotrophicum. Arch. Microbiol. *120*, 135–139.
Fuex, A.N., 1977. The use of stable carbon isotopes in hydrocarbon exploration. Journal of Geochemical Exploration *7*, 155–188.
Gallagher, M.W., Choularton, T.W., Bower, K.N., Stromberg, I.M., Beswick, K.M., Fowler, D.,

Hargreaves, K.J., 1994. Measurements of methane fluxes on the landscape scale from a wetland area in north Scotland. Atmospheric Environment *28*, 2421–2430.
Games, L.M., Hayes, R., J.M., Gunsalus, P., 1978. Methane-producing bacteria: natural fractionations of the stable carbon isotopes. Geochimica et Cosmochimica Acta *42*, 1295–1297.
Garnett, M.H., Hardie, S.M.L., Murray, C., 2011. Radiocarbon and stable carbon analysis of dissolved methane and carbon dioxide from the profile of a raised peat bog. Radiocarbon *53*, 71–83.
Garnett, M.H., Hardie, S.M.L., Murray, C., Billett, M.F., 2013. Radiocarbon dating of methane and carbon dioxide evaded from a temperate peatland stream. Biogeochemistry *114*, 213–223.
Gehring, T., Klang, J., Niedermayr, A., Berzio, S., Immenhauser, A., Klocke, M., Wichern, M., Lübken, M., 2015. Determination of methanogenic pathways through carbon isotope ($\delta^{13}C$) analysis for the two-stage anaerobic digestion of high-solids substrates. Environ. Sci. Technol. *49*, 4705–4714.
Gelwicks, J.T., Risatti, J.B., Hayes, J.M., 1994. Carbon isotope effects associated with aceticlastic methanogenesis. Appl. Environ. Microbiol. *60*, 467–472.
Giggenbach, W.F., 1997. Relative importance of thermodynamic and kinetic processes in governing the chemical and isotopic composition of carbon gases in high-heatflow sedimentary basins. Geochimica et Cosmochimica Acta *61*, 3763–3785.
Goevert, D., Conrad, R., 2009. Effect of substrate concentration on carbon isotope fractionation during acetoclastic methanogenesis by Methanosarcina barkeri and M. acetivorans in rice field soil. Appl. Environ. Microbiol. *75*, 2605–2612.
Golding, S.D., Boreham, C.J., Esterle, J.S., 2013. Stable isotope geochemistry of coal bed and shale gas and related production waters: A review. International Journal of Coal Geology *120*, 24–40.
Gooddy, D C, and Darling, W G. 2005. The Potential for Methane Emissions from Groundwaters of the UK. Science of the Total Environment Vol. 339, 117-126.
Gooddy, D.C., Clay, J.W., Bottrell, S.H., 2002. Redox-driven changes in porewater chemistry in the unsaturated zone of the chalk aquifer beneath unlined cattle slurry lagoons. Applied Geochemistry *17*, 903–921.
Gooddy, D.C., Hughes, A.G., Williams, A.T., Armstrong, A.C., Nicholson, R.J., Williams, J.R., 2001. Field and modelling studies to assess the risk to UK groundwater from earth-based stores for livestock manure. Soil Use and Management *17*, 128–137.
Gooddy, D.C.; Hughes, A.G., Armstrong, A.C., Williams, A.T., Griffiths, K.J., Nicholson, R.A., Williams, J.W.; Jones, H.K.; Chilton, P.J. 2000 Impact of farm waste stores on groundwater quality. Final report. British Geological Survey, 92pp. (WD/00/009)
Grasby, S.E., Ferguson, G., Brady, A., Sharp, C., Dunfield, P., McMechan, M., 2016. Deep groundwater circulation and associated methane leakage in the northern Canadian Rocky Mountains. Applied Geochemistry *68*, 10–18.
Gray, A., Levy, P.E., Cooper, M.D.A., Jones, T., Gaiawyn, J., Leeson, S.R., Ward, S.E., Dinsmore, K.J., Drewer, J., Sheppard, L.J., Ostle, N.J., Evans, C.D., Burden, A., Zielinski, P., 2013. Methane indicator values for peatlands: a comparison of species and functional groups. Global Change Biology *19*, 1141–1150.
Green, C., Styles, P., Baptie, B., 2012. Preese Hall shale gas fracturing review and recommendations for induced seismic mitigation. DECC. https://www.gov.uk/government/publications/preese-hall-shale-gas-fracturing-review-and-recommendations-for-induced-seismic-mitigation
Green, S.M., Baird, A.J., 2013. The importance of episodic ebullition methane losses from three peatland microhabitats: a controlled-environment study. European Journal of Soil Science *64*, 27–36.
Green, S.M., Baird, A.J., Evans, C.D., Peacock, M., Holden, J., Chapman, P.J., Smart, R.P., 2018. Methane and carbon dioxide fluxes from open and blocked ditches in a blanket bog. Plant Soil *424*, 619-938.
Grey, J., Jones, R.I., Sleep, D., 2001. Seasonal changes in the importance of the source of organic matter to the diet of zooplankton in Loch Ness, as indicated by stable isotope analysis. Limnology and

Oceanography *46*, 505–513.
Grossman, E.L., Coffman, B.K., Fritz, S.J., Wada, H., 1989. Bacterial production of methane and its influence on groundwater chemistry in east-central Texas aquifers. Geology *17*, 495–499.
Györe, D., McKavney, R., Gilfillan, S.M.V., Stuart, F.M., 2018. Fingerprinting coal-derived gases from the UK. Chemical Geology, The noble gases as geochemical tracers – in celebration of Pete Burnard *480*, 75–85.
Hammond, P.A., 2016. The relationship between methane migration and shale-gas well operations near Dimock, Pennsylvania, USA. Hydrogeol J *24*, 503–519.
Hancock, J.M., 1975. The petrology of the Chalk. Proceedings of the Geologists' Association *86*, 499–535.
Hansen, L.K., Jakobsen, R., Postma, D., 2001. Methanogenesis in a shallow sandy aquifer, Rømø, Denmark. Geochimica et Cosmochimica Acta *65*, 2925–2935.
Hanson, R.S., Hanson, T.E., 1996. Methanotrophic bacteria. Microbiol. Rev. *60*, 439–471.
Happell, J.D., Chanton, J.P., Showers, W.S., 1994. The influence of methane oxidation on the stable isotopic composition of methane emitted from Florida swamp forests. Geochimica Et Cosmochimica Acta *58*, 4377–4388.
Hargreaves, K.J., Fowler, D., 1998. Quantifying the effects of water table and soil temperature on the emission of methane from peat wetland at the field scale. Atmospheric Environment *32*, 3275–3282.
Harley, J.F., Carvalho, L., Dudley, B., Heal, K.V., Rees, R.M., Skiba, U., 2015. Spatial and seasonal fluxes of the greenhouse gases N_2O, CO_2 and CH_4 in a UK macrotidal estuary. Estuarine, Coastal and Shelf Science *153*, 62–73.
Harrison, S.M., Gentzis, T., Labute, G., Seifert, S., Payne, M., 2006. Preliminary hydrogeological assessment of Late Cretaceous-Tertiary Ardley coals in part of the Alberta Basin, Alberta, Canada. Int. J. Coal Geol. *65*, 59–78.
Hattori, S., Nashimoto, H., Kimura, H., Koba, K., Yamada, K., Shimizu, M., Watanabe, H., Yoh, M., Yoshida, N., 2012. Hydrogen and carbon isotope fractionation by thermophilic hydrogenotrophic methanogens from a deep aquifer under coculture with fermenters. Geochem. J. *46*, 193–200.
Hays, J., Finkel, M.L., Depledge, M., Law, A., Shonkoff, S.B.C., 2015. Considerations for the development of shale gas in the United Kingdom. Science of The Total Environment *512–513*, 36–42.
He, Z., Geng, S., Cai, C., Liu, S., Liu, Y., Pan, Y., Lou, L., Zheng, P., Xu, X., Hu, B., 2015. Anaerobic oxidation of methane coupled to nitrite reduction by halophilic marine NC10 Bacteria. Appl. Environ. Microbiol. *81*, 5538–5545.
He, Z., Zhang, Q., Feng, Y., Luo, H., Pan, X., Gadd, G.M., 2018. Microbiological and environmental significance of metal-dependent anaerobic oxidation of methane. Sci. Total Environ. *610*, 759–768.
Hedderich, R., Whitman, W.B., 2013. Physiology and biochemistry of the methane-producing archaea, in: The Prokaryotes. Springer, Berlin, Heidelberg, pp. 635–662.
Heimann, A., Marczinek, S., Kloosb, K., Peiffer, S., 2003. Optimization of the sampling technique for the determination of dissolved hydrogen in groundwater. CLEAN–Soil, Air, Water *31*, 491–500.
Hershey, A.E., Northington, R.M., Whalen, S.C., 2014. Substrate limitation of sediment methane flux, methane oxidation and use of stable isotopes for assessing methanogenesis pathways in a small arctic lake. Biogeochemistry *117*, 325–336.
Hines, M.E., Duddleston, K.N., Kiene, R.P., 2001. Carbon flow to acetate and C1 compounds in northern wetlands. Geophysical Research Letters *28*, 4251–4254.
Hines, M.E., Duddleston, K.N., Rooney-Varga, J.N., Fields, D., Chanton, J.P., 2008. Uncoupling of acetate degradation from methane formation in Alaskan wetlands: Connections to vegetation distribution. Global Biogeochemical Cycles *22*, GB2017.
Hitchman, S.P., Darling, W.G., Williams, G.M., 1989. Stable isotope ratios in methane containing gases in the United Kingdom. British Geological Survey, 23pp. (WE/89/030)

Hoehler, T.M., Alperin, M.J., Albert, D.B., Martens, C.S., 1994. Field and laboratory studies of methane oxidation in an anoxic marine sediment: Evidence for a methanogen-sulfate reducer consortium. Global Biogeochemical Cycles *8*, 451–463.
Holmes, M.E., Chanton, J.P., Bae, H.-S., Ogram, A., 2014. Effect of nutrient enrichment on $\delta^{13}CH_4$ and the methane production pathway in the Florida Everglades. Journal of Geophysical Research: Biogeosciences 119, 1267–1280.
Holt, B.D., Sturchio, N.C., Arehart, G.B., Bakel, A.J., 1995. Ultrasonic vacuum extraction of gases from water for chemical and isotopic analysis. Chemical geology *122*, 275–284.
Hope, D., Palmer, S.M., Billett, M.F., Dawson, J.J.C., 2004. Variations in dissolved CO_2 and CH_4 in a first-order stream and catchment: an investigation of soil-stream linkages. Hydrological Processes *18*, 3255–3275.
Hope, D., Palmer, S.M., Billett, M.F., Dawson, J.J.C., 2001. Carbon dioxide and methane evasion from a temperate peatland stream. Limnology and Oceanography *46*, 847–857.
Hopson, P., Wilkinson, I., Woods, M., 2008. A stratigraphical framework for the Lower Cretaceous of England. British Geological Survey. British Geological Survey Research Report (RR/08/03).
Hornibrook, E.R.C., Bowes, H.L., 2007. Trophic status impacts both the magnitude and stable carbon isotope composition of methane flux from peatlands. Geophysical Research Letters *34*, L21401.
Hornibrook, E.R.C., Bowes, H.L., Culbert, A., Gallego-Sala, A.V., 2009. Methanotrophy potential versus methane supply by pore water diffusion in peatlands. Biogeosciences *6*, 1490–1504.
Hornibrook, E.R.C., Longstaffe, F.J., Fyfe, W.S., 2000. Evolution of stable carbon isotope compositions for methane and carbon dioxide in freshwater wetlands and other anaerobic environments. Geochimica Et Cosmochimica Acta *64*, 1013–1027.
Hornibrook, E.R.C., Longstaffe, F.J., Fyfe, W.S., 1997. Spatial distribution of microbial methane production pathways in temperate zone wetland soils: Stable carbon and hydrogen isotope evidence. Geochimica et Cosmochimica Acta *61*, 745–753.
Huang, T., Pang, Z., Tian, J., Li, Y., Yang, S., Luo, L., 2017. Methane content and isotopic composition of shallow groundwater: implications for environmental monitoring related to shale gas exploitation. J Radioanal Nucl Chem *312*, 577–585.
Hughes, S., Dowrick, D.J., Freeman, C., Hudson, J.A., Reynolds, B., 1999. Methane emissions from a gully mire in mid-Wales, UK under consecutive summer water table drawdown. Environmental Science & Technology *33*, 362–365.
Humez, P., Mayer, B., Ing, J., Nightingale, M., Becker, V., Kingston, A., Akbilgic, O., Taylor, S., 2016a. Occurrence and origin of methane in groundwater in Alberta (Canada): Gas geochemical and isotopic approaches. Science of The Total Environment *541*, 1253–1268.
Humez, P., Mayer, B., Nightingale, M., Becker, V., Kingston, A., Taylor, S., Bayegnak, G., Millot, R., Kloppmann, W., 2016b. Redox controls on methane formation, migration and fate in shallow aquifers. Hydrol. Earth Syst. Sci. *20*, 2759–2777.
Humphrey, H.B., 1960. Historical Summary of Coal-Mine Explosions in the United States, 1810-1958. https://digital.library.unt.edu/ark:/67531/metadc12740/
Jacinthe, P.-A., Groffman, P.M., 2001. Silicone rubber sampler to measure dissolved gases in saturated soils and waters. Soil Biology and Biochemistry *33*, 907–912.
Jackson, D.I., 1995. The geology of the Irish Sea. Balogh Scientific Books.
Jackson, R.B., Vengosh, A., Darrah, T.H., Warner, N.R., Down, A., Poreda, R.J., Osborn, S.G., Zhao, K., Karr, J.D., 2013. Increased stray gas abundance in a subset of drinking water wells near Marcellus shale gas extraction. Proceedings of the National Academy of Sciences of the United States of America *110*, 11250–11255.
Jahangir, M.M., Johnston, P., Khalil, M.I., Grant, J., Somers, C., Richards, K.G., 2012. Evaluation of headspace equilibration methods for quantifying greenhouse gases in groundwater. Journal of environmental management *111*, 208–212.
Jahangir, M.M.R., Johnston, P., Khalil, M.I., Hennessy, D., Humphreys, J., Fenton, O., Richards, K.G., 2012. Groundwater: A pathway for terrestrial C and N losses and indirect greenhouse gas

emissions. Agriculture Ecosystems & Environment *159*, 40–48.
Janssen, P.H., Frenzel, P., 1997. Inhibition of methanogenesis by methyl fluoride: studies of pure and defined mixed cultures of anaerobic bacteria and archaea. Appl. Environ. Microbiol. *63*, 4552–4557.
Jedrysek, M.O., 2005. S–O–C isotopic picture of sulphate–methane–carbonate system in freshwater lakes from Poland. A review. Environ Chem Lett *3*, 100–112.
Johnson, V., Graham, D., Reidel, S., 1993. Methane in Columbia River Basalt aquifers - Isotopic and geohydrologic evidence for a deep coal-bed gas-source in the Columbia Basin, Washington. AAPG Bull.-Am. Assoc. Petr. Geol. *77*, 1192–1207.
Jones, H.K., Morris, B.L., Cheney, C.S., Brewerton, L.J., Merrin, P.D., Lewis, M.A., MacDonald, A.M., Coleby, L.M., Talbot, J.C., Mckenzie, A.A., Bird, M.J., Cunningham, J.E., Robinson, V., 2000. The physical properties of minor aquifers in England and Wales. http://nora.nerc.ac.uk/id/eprint/12663/
Jones, N. S., Holloway, S., Creedy, D. P., Garner, K., 2005. Can UK coal resources contribute to a gas renaissance? Geological Society, London, Petroleum Geology Conference series, 6, 715-722.
Jones, R. I. and Grey, J. (2011), Biogenic methane in freshwater food webs. Freshwater Biology, 56: 213-229.
Kawagucci, S., Kobayashi, M., Hattori, S., Yamada, K., Ueno, Y., Takai, K., Yoshida, N., 2014. Hydrogen isotope systematics among H_2-H_2O-CH_4 during the growth of the hydrogenotrophic methanogen Methanothermobacter thermautotrophicus strain Delta H. Geochim. Cosmochim. Acta *142*, 601–614.
Kelly, A., Jones, R.I., Grey, J., 2004. Stable isotope analysis provides fresh insights into dietary separation between Chironomus anthracinus and C. plumosus. Journal of the North American Benthological Society *23*, 287–296.
Kennedy, G.W., Drage, J., 2015. Assessing patterns of dissolved methane in shallow aquifers related to carboniferous and Triassic sedimentary basins, Nova Scotia, Canada. Geol *51*, 233–241.
Kietäväinen, R., Purkamo, L., 2015. The origin, source, and cycling of methane in deep crystalline rock biosphere. Front. Microbiol. *6*, 275.
Kimura, H., Nashimoto, H., Shimizu, M., Hattori, S., Yamada, K., Koba, K., Yoshida, N., Kato, K., 2010. Microbial methane production in deep aquifer associated with the accretionary prism in Southwest Japan. The ISME Journal *4*, 531–541.
King, G.M., 1990. Dynamics and controls of methane oxidation in a Danish wetland sediment. FEMS Microbiology Letters *74*, 309–323.
Kinnaman, F.S., Valentine, D.L., Tyler, S.C., 2007. Carbon and hydrogen isotope fractionation associated with the aerobic microbial oxidation of methane, ethane, propane and butane. Geochimica et Cosmochimica Acta *71*, 271–283.
Kirk, M.F., Martini, A.M., Breecker, D.O., Colman, D.R., Takacs-Vesbach, C., Petsch, S.T., 2012. Impact of commercial natural gas production on geochemistry and microbiology in a shale-gas reservoir. Chemical Geology *332–333*, 15–25.
Kjeldsen, P., Barlaz, M.A., Rooker, A.P., Baun, A., Ledin, A., Christensen, T.H., 2002. Present and Long-Term Composition of MSW Landfill Leachate: A Review. Critical Reviews in Environmental Science and Technology *32*, 297–336.
Konn, C., Charlou, J. l., Holm, N. g., Mousis, O., 2015. The production of methane, hydrogen, and organic compounds in ultramafic-hosted hydrothermal vents of the Mid-Atlantic Ridge. Astrobiology *15*, 381–399.
Kotelnikova, S., 2002. Microbial production and oxidation of methane in deep subsurface. Earth-Science Reviews *58*, 367–395.
Kreuzer, R.L., Darrah, T.H., Grove, B.S., Moore, M.T., Warner, N.R., Eymold, W.K., Whyte, C.J., Mitra, G., Jackson, R.B., Vengosh, A., Poreda, R.J., 2018. Structural and hydrogeological controls on hydrocarbon and brine migration into drinking water aquifers in southern New York. Groundwater *56*, 225–244.

Krzycki, J.A., Kenealy, W.R., DeNiro, M.J., Zeikus, J.G., 1987. Stable carbon isotope fractionation by Methanosarcina barkeri during methanogenesis from acetate, methanol, or carbon dioxide-hydrogen. Appl. Environ. Microbiol. *53*, 2597–2599.

Lansdown, J.M., Quay, P.D., King, S.L., 1992. CH_4 production via CO_2 reduction in a temperate bog: A source of ^{13}C-depIeted CH_4. Geochimica et Cosmochimica Acta *56*, 3493–3503.

Lavoie, D., Pinet, N., Bordeleau, G., Ardakani, O.H., Ladevèze, P., Duchesne, M.J., Rivard, C., Mort, A., Brake, V., Sanei, H., Malet, X., 2016. The Upper Ordovician black shales of southern Quebec (Canada) and their significance for naturally occurring hydrocarbons in shallow groundwater. International Journal of Coal Geology *158*, 44–64.

LeDoux, S.T.M., Szynkiewicz, A., Faiia, A.M., Mayes, M.A., McKinney, M.L., Dean, W.G., 2016. Chemical and isotope compositions of shallow groundwater in areas impacted by hydraulic fracturing and surface mining in the Central Appalachian Basin, Eastern United States. Applied Geochemistry *71*, 73–85.

Legere, L., 2013. Sunday Times review of DEP drilling records reveals water damage, murky testing methods. The Times-Tribune. http://thetimes-tribune.com/news/sunday-times-review-of-dep-drilling-records-reveals-water-damage-murky-testing-methods-1.1491547

Levy, P.E., Burden, A., Cooper, M.D.A., Dinsmore, K.J., Drewer, J., Evans, C., Fowler, D., Gaiawyn, J., Gray, A., Jones, S.K., Jones, T., McNamara, N.P., Mills, R., Ostle, N., Sheppard, L.J., Skiba, U., Sowerby, A., Ward, S.E., Zielinski, P., 2012. Methane emissions from soils: synthesis and analysis of a large UK data set. Global Change Biology *18*, 1657–1669.

Li, H., Carlson, K. H., 2014, Distribution and Origin of Groundwater Methane in the Wattenberg Oil and Gas Field of Northern Colorado. Environmental Science & Technology *48* (3), 1484-1491

Li, Z., You, C., Gonzales, M., Wendt, A.K., Wu, F., Brantley, S.L., 2016. Searching for anomalous methane in shallow groundwater near shale gas wells. Journal of Contaminant Hydrology *195*, 23–30.

Liptay, K., Chanton, J., Czepiel, P., Mosher, B., 1998. Use of stable isotopes to determine methane oxidation in landfill cover soils. Journal of Geophysical Research-Atmospheres *103*, 8243–8250.

Liu, T.-K., Chen, K.-Y., Yang, T.F., Chen, Y.-G., Chen, W.-F., Kang, S.-C., Lee, C.-P., 2009. Origin of methane in high-arsenic groundwater of Taiwan – Evidence from stable isotope analyses and radiocarbon dating. Journal of Asian Earth Sciences *36*, 364–370.

Liu, Y., Whitman, W.B., 2008. Metabolic, phylogenetic, and ecological diversity of the methanogenic archaea. Annals of the New York Academy of Sciences *1125*, 171–189.

Lokhurst, A., 1998. Northwest European gas atlas - composition and isotope ratio of natural gases. NITG-TNO, Haarlem.

Lollar, B.S., Lacrampe-Couloume, G., Slater, G.F., Ward, J., Moser, D.P., Gihring, T.M., Lin, L.H., Onstott, T.C., 2006. Unravelling abiogenic and biogenic sources of methane in the Earth's deep subsurface. Chemical Geology *226*, 328–339.

Londry, K.L., Dawson, K.G., Grover, H.D., Summons, R.E., Bradley, A.S., 2008. Stable carbon isotope fractionation between substrates and products of Methanosarcina barkeri. Organic Geochemistry, Compound Specific Isotope Analysis *39*, 608–621.

Long, Y., Liu, C., Lin, H., Li, N., Guo, Q., Xie, S., 2017. Vertical and horizontal distribution of sediment nitrite-dependent methane-oxidizing organisms in a mesotrophic freshwater reservoir. Can. J. Microbiol. *63*, 525–534.

Lovley, D.R., Chapelle, F.H., Woodward, J.C., 1994. Use of dissolved H_2 concentrations to determine distribution of microbially catalyzed redox reactions in anoxic groundwater. Environ. Sci. Technol. *28*, 1205–1210.

Lowry, D., Holmes, C.W., Rata, N.D., O'Brien, P., Nisbet, E.G., 2001. London methane emissions: Use of diurnal changes in concentration and delta C-13 to identify urban sources and verify inventories. Journal of Geophysical Research-Atmospheres 106, 7427–7448.

Lu, Y.-Z., Fu, L., Ding, J., Ding, Z.-W., Li, N., Zeng, R.J., 2016. Cr(VI) reduction coupled with anaerobic

oxidation of methane in a laboratory reactor. Water Res. *102*, 445–452.
MacDonald, A.M., Allen, D.J., 2001. Aquifer properties of the Chalk of England. Quarterly Journal of Engineering Geology and Hydrogeology *34*, 371–384.
Mahieu, K., De Visscher, A., Vanrolleghem, P.A., Van Cleemput, O., 2006. Carbon and hydrogen isotope fractionation by microbial methane oxidation: Improved determination. Waste Management *26*, 389–398.
Martini, A.M., Walter, L.M., Budai, J.M., Ku, T.C.W., Kaiser, C.J., Schoell, M., 1998. Genetic and temporal relations between formation waters and biogenic methane: Upper Devonian Antrim Shale, Michigan Basin, USA. Geochimica Et Cosmochimica Acta *62*, 1699–1720.
Mather, J.D., Gray, D.A., Allen, R.A., Smith, D.B., 1973. Groundwater recharge in the Lower Greensand of the London Basin—results of tritium and carbon-14 determinations. Quarterly Journal of Engineering Geology and Hydrogeology *6*, 141–152.
Mayer, B., Humez, P., Becker, V., Nightingale, M., Ing, J., Kingston, A., Clarkson, C., Cahill, A., Parker, E., Cherry, J., Millot, R., Kloppmann, W., Osadetz, K., Lawton, D., 2015. Prospects and limitations of chemical and isotopic groundwater monitoring to assess the potential environmental impacts of unconventional oil and gas development. Procedia Earth and Planetary Science, 11th Applied Isotope Geochemistery Conference AIG-11 *13*, 320–323.
McInnes, D.M., Kampbell, D., 2000. The Bubble stripping method for determining dissolved hydrogen (H_2) in well water. Field Analytical Chemistry & Technology *4*, 283–296.
McIntosh, J.C., Grasby, S.E., Hamilton, S.M., Osborn, S.G., 2014. Origin, distribution and hydrogeochemical controls on methane occurrences in shallow aquifers, southwestern Ontario, Canada. Appl. Geochem. *50*, 37–52.
McMahon, P.B., Caldwell, R.R., Galloway, J.M., Valder, J.F., Hunt, A.G., 2015. Quality and age of shallow groundwater in the Bakken Formation production area, Williston Basin, Montana and North Dakota. Groundwater *53*, 81–94.
McMahon, P.B., Thomas, J.C., Hunt, A.G., 2013. Groundwater ages and mixing in the Piceance Basin natural gas province, Colorado. Environ. Sci. Technol. *47*, 13250–13257.
McNamara, N.P., Plant, T., Oakley, S., Ward, S., Wood, C., Ostle, N., 2008. Gully hotspot contribution to landscape methane (CH_4) and carbon dioxide (CO_2) fluxes in a northern peatland. Science of the Total Environment *404*, 354–360.
McNamara, N. P., Chamberlain, P. M., Piearce, T.G., Sleep, D. S., Black, H. I. J., Reay, D. S., Ineson, P. (2006) Impact of water table depth on forest soil methane turnover in laboratory soil cores deduced from natural abundance and tracer ^{13}C stable isotope experiments, Isotopes in Environmental and Health Studies, 42:4, 379-390
McPhillips, L.E., Creamer, A.E., Rahm, B.G., Walter, M.T., 2014. Assessing dissolved methane patterns in central New York groundwater. Journal of Hydrology: Regional Studies *1*, 57–73.
Meulepas, R.J.W., Jagersma, C.G., Khadem, A.F., Stams, A.J.M., Lens, P.N.L., 2010. Effect of methanogenic substrates on anaerobic oxidation of methane and sulfate reduction by an anaerobic methanotrophic enrichment. Appl Microbiol Biotechnol *87*, 1499–1506.
Middelburg, J.J., Nieuwenhuize, J., Iversen, N., Høgh, N., Wilde, H. de, Helder, W., Seifert, R., Christof, O., 2002. Methane distribution in European tidal estuaries. Biogeochemistry *59*, 95–119.
Middlemiss, F.A., 1975. Studies in the sedimentation of the Lower Greensand of the Weald, 1875–1975: a review and commentary. Proceedings of the Geologists' Association *86*, 457–473.
Milucka, J., Ferdelman, T.G., Polerecky, L., Franzke, D., Wegener, G., Schmid, M., Lieberwirth, I., Wagner, M., Widdel, F., Kuypers, M.M.M., 2012. Zero-valent sulphur is a key intermediate in marine methane oxidation. Nature *491*, 541–546.
Mitchell, J.K., Seed, R.B., Seed, H.B., 1990. Kettleman Hills waste landfill slope failure. I: Liner-system properties. Journal of Geotechnical Engineering *116*, 647–668.
Molofsky, L.J., Connor, J.A., McHugh, T.E., Richardson, S.D., Woroszylo, C., Alvarez, P.J., 2016. Environmental factors associated with natural methane occurrence in the Appalachian Basin. Groundwater *54*, 656–668.

Molofsky, L.J., Connor, J.A., Wylie, A.S., Wagner, T., Farhat, S.K., 2013. Evaluation of methane sources in groundwater in northeastern Pennsylvania. Ground Water *51*, 333–349.
Monaghan, A.A., 2014. The Carboniferous shales of the Midland Valley of Scotland: geology and resource estimation. British Geological Survey for Department of Energy and Climate Change, London, UK. https://www.ogauthority.co.uk/exploration-production/onshore/reports-bgs-midland-valley-of-scotland-shale/
Mook, W.G., Bommerson, J.C., Staverman, W.H., 1974. Carbon isotope fractionation between dissolved bicarbonate and gaseous carbon dioxide. Earth and Planetary Science Letters *22*, 169–176.
Moran, J.J., Beal, E.J., Vrentas, J.M., Orphan, V.J., Freeman, K.H., House, C.H., 2008. Methyl sulfides as intermediates in the anaerobic oxidation of methane. Environmental Microbiology *10*, 162–173.
Morgan-Jones, M., 1985. The hydrogeochemistry of the Lower Greensand aquifers south of London, England. Quarterly Journal of Engineering Geology and Hydrogeology *18*, 443–458.
Moritz, A., Hélie, J.-F., Pinti, D.L., Larocque, M., Barnetche, D., Retailleau, S., Lefebvre, R., Gélinas, Y., 2015. Methane baseline concentrations and sources in shallow aquifers from the shale gas-prone region of the St. Lawrence Lowlands (Quebec, Canada). Environ. Sci. Technol. *49*, 4765–4771.
Murase, J., Sakai, Y., Sugimoto, A., Okubo, K., Sakamoto, M., 2003. Sources of dissolved methane in Lake Biwa. Limnology *4*, 91–99.
Murphy, P.J., Bottrell, S.H., Parker, K., 2014. Sulphur springs of the Craven Basin, NW England: indicators of natural methane leakage? Quarterly Journal of Engineering Geology and Hydrogeology *47*, 81–88.
Nakagawa, F., Yoshida, N., Nojiri, Y., Makarov, V., 2002. Production of methane from alasses in eastern Siberia: Implications from its ^{14}C and stable isotopic compositions. Global Biogeochemical Cycles *16*, 14–1.
Nazaries, L., Pan, Y., Bodrossy, L., Baggs, E.M., Millard, P., Murrell, J.C., Singh, B.K., 2013. Evidence of Microbial Regulation of Biogeochemical Cycles from a Study on Methane Flux and Land Use Change. Appl. Environ. Microbiol. *79*, 4031–4040.
Neumann, I., Cobbing, J., Tooth, A.F., Shand, P., 2004. Baseline Report Series 15: The Palaeogene of the Wessex Basin. British Geological Survey Commissioned Report (CR/04/254N).
Nicot, J.-P., Larson, T., Darvari, R., Mickler, P., Slotten, M., Aldridge, J., Uhlman, K., Costley, R., 2017a. Controls on methane occurrences in shallow aquifers overlying the Haynesville Shale gas field, east Texas. Groundwater *55*, 443–454.
Nicot, J.-P., Mickler, P., Larson, T., Clara Castro, M., Darvari, R., Uhlman, K., Costley, R., 2017b. Methane occurrences in aquifers overlying the Barnett Shale play with a focus on Parker County, Texas. Groundwater *55*, 469–481.
Nihous, G.C., 2010. Notes on the temperature dependence of carbon isotope fractionation by aerobic CH_4-oxidising bacteria. Isotopes in Environmental and Health Studies 46, 133–140.
Northern Ireland Environment Agency, 2016. NIEA – Authorised landfill sites - Open Data NI. https://www.opendatani.gov.uk/dataset/niea-authorised-landfill-sites.
Nwachukwu, A.N., Anonye, D., 2013. The effect of atmospheric pressure on CH_4 and CO_2 emission from a closed landfill site in Manchester, UK. Environ Monit Assess *185*, 5729–5735.
O'Dochartaigh, B.E.; Smedley, P.L.; MacDonald, A.M.; Darling, W.G.; Homoncik, S., 2011. Baseline Scotland: groundwater chemistry of the Carboniferous sedimentary aquifers of the Midland Valley. British Geological Survey, 91pp. (OR/11/021)
OGA, 2016. Onshore Licensing Rounds, https://www.ogauthority.co.uk/licensing-consents/licensing-rounds/onshore-licensing-rounds/.
O'Hara, S., Humphrey, M., Andersson-Hudson, J., Knight, W., 2016. Public perceptions of shale gas in the UK: From positive to negative. University of Nottingham (2016)
O'Hara, S., Humphrey, M., Jaspal, R., Nerlich, B., Poberezhskaya, M., 2013. Public perception of shale gas extraction in the UK: How people's views are changing. University of Nottingham (2013)
Okumura, T., Kawagucci, S., Saito, Y., Matsui, Y., Takai, K., Imachi, H., 2016. Hydrogen and carbon

isotope systematics in hydrogenotrophic methanogenesis under H_2-limited and H_2-enriched conditions: implications for the origin of methane and its isotopic diagnosis. Prog. in Earth and Planet. Sci. *3*, 14.

Ono, S., Wang, D.T., Gruen, D.S., Sherwood Lollar, B., Zahniser, M.S., McManus, B.J., Nelson, D.D., 2014. Measurement of a doubly substituted methane isotopologue, $^{13}CH_3D$, by tunable infrared laser direct absorption spectroscopy. Anal. Chem. *86*, 6487–6494.

Oremland, R.S., Marsh, L., DesMarais, D.J., 1982. Methanogenesis in Big Soda Lake, Nevada: an alkaline, moderately hypersaline desert lake. Appl. Environ. Microbiol. *43*, 462–468.

Osborn, S.G., McIntosh, J.C., 2010. Chemical and isotopic tracers of the contribution of microbial gas in Devonian organic-rich shales and reservoir sandstones, northern Appalachian Basin. Applied Geochemistry *25*, 456–471.

Osborn, S.G., Vengosh, A., Warner, N.R., Jackson, R.B., 2011. Methane contamination of drinking water accompanying gas-well drilling and hydraulic fracturing. Proceedings of the National Academy of Sciences of the United States of America *108*, 8172–8176.

Owen, D.D.R., Shouakar-Stash, O., Morgenstern, U., Aravena, R., 2016. Thermodynamic and hydrochemical controls on CH_4 in a coal seam gas and overlying alluvial aquifer: new insights into CH_4 origins. Scientific Reports *6*, 32407.

Pangala S. R., Hornibrook E. R.C., Gowing D. J., Gauci V., 2015. The contribution of trees to ecosystem methane emissions in a temperate forested wetland. Global Change Biology *21*, 2642–2654.

Parkin, G., Birkinshaw, S.J., Younger, P.L., Rao, Z., Kirk, S., 2007. A numerical modelling and neural network approach to estimate the impact of groundwater abstractions on river flows. Journal of Hydrology *339*, 15–28.

Penger, J., Conrad, R., Blaser, M., 2012. Stable carbon isotope fractionation by methylotrophic methanogenic archaea. Appl. Environ. Microbiol. *78*, 7596–7602.

Penning, H., Claus, P., Casper, P., Conrad, R., 2006. Carbon isotope fractionation during acetoclastic methanogenesis by Methanosaeta Concilii in culture and a lake sediment. Appl. Environ. Microbiol. *72*, 5648–5652.

Penning, H., Plugge, C.M., Galand, P.E., Conrad, R., 2005. Variation of carbon isotope fractionation in hydrogenotrophic methanogenic microbial cultures and environmental samples at different energy status. Global Change Biology *11*, 2103–2113.

Perry, W., Dyer, J., Naylor, J., 2013. Drill-phase environmental monitoring report: Balcombe site, Sussex. Ground-Gas Solutions Ltd Report (GG2222-06 DPr01). https://cuadrillaresources.com/site/balcombe/

Potter, J., Longstaffe, F. J., 2007. A gas-chromatograph, continuous flow-isotope ratio mass-spectrometry method for $\delta^{13}C$ and δD measurement of complex fluid inclusion volatiles: Examples from the Khibina alkaline igneous complex, northwest Russia and the south Wales coalfields. Chemical Geology *244*, 186-201.

Potter, J., Konnerup-Madsen, J., 2003. A review of the occurrence and origin of abiogenic hydrocarbons in igneous rocks. Geological Society, London, Special Publications *214*, 151–173.

Quay, P., Stutsman, J., Wilbur, D., Snover, A., Dlugokencky, E., Brown, T., 1999. The isotopic composition of atmospheric methane. Global Biogeochem. Cycles *13*, 445–461.

Raghoebarsing, A.A., Pol, A., Pas-Schoonen, K.T. van de, Smolders, A.J.P., Ettwig, K.F., Rijpstra, W.I.C., Schouten, S., Damsté, J.S.S., Camp, H.J.M.O. den, Jetten, M.S.M., Strous, M., 2006. A microbial consortium couples anaerobic methane oxidation to denitrification. Nature *440*, 918–921.

Rasigraf, O., Vogt, C., Richnow, H.-H., Jetten, M.S.M., Ettwig, K.F., 2012. Carbon and hydrogen isotope fractionation during nitrite-dependent anaerobic methane oxidation by Methylomirabilis oxyfera. Geochimica Et Cosmochimica Acta *89*, 256–264

Reeburgh, W.S., 1976. Methane consumption in Cariaco Trench waters and sediments. Earth and Planetary Science Letters *28*, 337–344.

Revesz, K., Coplen, T.B., Baedecker, M.J., Glynn, P.D., Hult, M., 1995. Methane production and

consumption monitored by stable H and C isotope ratios at a crude oil spill site, Bemidji, Minnesota. Applied Geochemistry *10*, 505–516.
Revesz, K.M., Breen, K.J., Baldassare, A.J., Burruss, R.C., 2010. Carbon and hydrogen isotopic evidence for the origin of combustible gases in water-supply wells in north-central Pennsylvania. Applied Geochemistry *25*, 1845–1859.
Rhodes, A.L., Horton, N.J., 2015. Establishing baseline water quality for household wells within the Marcellus Shale gas region, Susquehanna County, Pennsylvania, U.S.A. Applied Geochemistry, Geochemistry of Unconventional Shale Gas from Formation to Extraction: Petrogenesis, Hydraulic Fracturing, and Environmental Impacts *60*, 14–28.
Riddick, S.N., Hancock, B.R., Robinson, A.D., Connors, S., Davies, S., Allen, G., Pitt, J., Harris, N.R.P., 2018. Development of a low-maintenance measurement approach to continuously estimate methane emissions: A case study. Waste Management *73*, 210–219.
Robinson, H., 1987. Design and Operation of Leachate Control Measures at Compton Bassett Landfill Site, Wiltshire UK. Waste Management & Research *5*, 107–122.
Robinson, H.D., Grantham, G., 1988. The Treatment of Landfill Leachates in on-site Aerated Lagoon Plants - Experience in Britain and Ireland. Water Research *22*, 733–747.
Rosenfeld, W.D., Silverman, S.R., 1959. Carbon isotope fractionation in bacterial production of methane. Science *130*, 1658–1659.
Sage, R.C., Lloyd, J.W., 1978. Drift deposit influences on the Triassic Sandstone aquifer of NW Lancashire as inferred by hydrochemistry. Quarterly Journal of Engineering Geology and Hydrogeology *11*, 209–218.
Samad, M.S., Bertilsson, S., 2017. Seasonal variation in abundance and diversity of bacterial methanotrophs in five temperate lakes. Front. Microbiol. *8*, 1-12.
Sanders, I.A., Heppell, C.M., Cotton, J.A., Wharton, G., Hildrew, A.G., Flowers, E.J., Trimmer, M., 2007. Emission of methane from chalk streams has potential implications for agricultural practices. Freshwater Biology *52*, 1176–1186.
Sawakuchi, H.O., Bastviken, D., Sawakuchi, A.O., Ward, N.D., Borges, C.D., Tsai, S.M., Richey, J.E., Ballester, M.V.R., Krusche, A.V., 2016. Oxidative mitigation of aquatic methane emissions in large Amazonian rivers. Global Change Biology *22*, 1075–1085.
Scheller, S., Yu, H., Chadwick, G.L., McGlynn, S.E., Orphan, V.J., 2016. Artificial electron acceptors decouple archaeal methane oxidation from sulfate reduction. Science *351*, 703–707.
Schimel J.P., Holland E.A., Valentine D., 1993. Controls on methane flux from terrestrial ecosystems. In: Harper L.A., Mosier A.R., Duxbury J.M., Rolston D.E. (Eds). Agricultural Ecosystem Effects on Trace Gases and Global Climate Change (pp 167–182). American Society of Agronomy, Madison, USA.
Schloemer, S., Elbracht, J., Blumenberg, M., Illing, C.J., 2016. Distribution and origin of dissolved methane, ethane and propane in shallow groundwater of Lower Saxony, Germany. Appl. Geochem. *67*, 118–132.
Schloemer, S., Krooss, B.M., 2004. Molecular transport of methane, ethane and nitrogen and the influence of diffusion on the chemical and isotopic composition of natural gas accumulations. Geofluids *4*, 81–108.
Schoell, M., 1988. Multiple origins of methane in the Earth. Chemical Geology *71*, 1–10.
Segers, R., 1998. Methane production and methane consumption: a review of processes underlying wetland methane fluxes. Biogeochemistry *41*, 23–51.
Semrau, J.D., DiSpirito, A.A., Murrell, J.C., 2008. Life in the extreme: thermoacidophilic methanotrophy. Trends in Microbiology *16*, 190–193.
SEPA, 2015. Location and details of landfill sites in Scotland https://www.sepa.org.uk/environment/waste/waste-data/waste-data-reporting/waste-site-information/waste-sites-and-capacity-excel/
Sgouridis F., Ullah S., 2017. Soil Greenhouse Gas Fluxes, Environmental Controls, and the Partitioning of N_2O Sources in UK Natural and Seminatural Land Use Types. Journal of Geophysical

Research: Biogeosciences *122*, 2617–2633.
Shand, P., Cobbing, J., Tyler-Whittle, R., Tooth, A.F., Lancaster, A., 2003. Baseline report series. 9, the Lower Greensand of southern England. British Geological Survey. Commissioned Report (CR/03/273N).
Shand, P., Edmunds, W.M., Lawrence, A.R., Smedley, P., Burke, S., 2007. The natural (baseline) quality of groundwater in England and Wales. British Geological Survey Research Report (RR/07/06).
Sharma, S., Mulder, M.L., Sack, A., Schroeder, K., Hammack, R., 2013. Isotope Approach to Assess Hydrologic Connections During Marcellus Shale Drilling. Groundwater *52*, 424-433.
Shelley, F., Grey, J., Trimmer, M., 2014. Widespread methanotrophic primary production in lowland chalk rivers. Proc Biol Sci *281*, 20132854.
Shen, L., Huang, Q., He, Z., Lian, X., Liu, S., He, Y., Lou, L., Xu, X., Zheng, P., Hu, B., 2015a. Vertical distribution of nitrite-dependent anaerobic methane-oxidising bacteria in natural freshwater wetland soils. Appl Microbiol Biotechnol *99*, 349–357.
Shen, L., Wu, H., Gao, Z., 2015b. Distribution and environmental significance of nitrite-dependent anaerobic methane-oxidising bacteria in natural ecosystems. Appl Microbiol Biotechnol *99*, 133–142.
Sherwood, O.A., Rogers, J.D., Lackey, G., Burke, T.L., Osborn, S.G., Ryan, J.N., 2016. Groundwater methane in relation to oil and gas development and shallow coal seams in the Denver-Julesburg Basin of Colorado. Proc Natl Acad Sci USA *113*, 8391.
Shuai, Y., Zhang, S., Grasby, S.E., Chen, Z., Ma, D., Wang, L., Li, Z., Wei, C., 2013. Controls on biogenic gas formation in the Qaidam Basin, northwestern China. Chemical Geology *335*, 36–47.
Siegel, D.I., Azzolina, N.A., Smith, B.J., Perry, A.E., Bothun, R.L., 2015. Methane concentrations in water wells unrelated to proximity to existing oil and gas wells in northeastern Pennsylvania. Environ. Sci. Technol. *49*, 4106–4112.
Simpkins, W., Parkin, T., 1993. Hydrogeology and Redox Geochemistry of CH_4 in a Late Wisconsinan Till and Loess Sequence in Central Iowa. Water Resour. Res. *29*, 3643–3657.
Slater, G.F., Lippmann-Pipke, J., Moser, D.P., Reddy, C.M., Onstott, T.C., Lacrampe-Couloume, G., Lollar, B.S., 2006. ^{14}C in methane and DIC in the deep terrestrial subsurface: Implications for microbial methanogenesis. Geomicrobiology Journal *23*, 453–462.
Smith, P., Martino, D., Cai, Z., Gwary, D., Janzen, H., Kumar, P., McCarl, B., Ogle, S., O'Mara, F., Rice, C., Scholes, B., Sirotenko, O., 2007. Agriculture., in: Metz, B., Davidson, O.R., Bosch, P.R., Dave, R., Meyer, L.A. (Eds.), Climate Change 2007: Mitigation. Contribution of Working Group III to the Fourth Assessment Report of the Intergovernmental Panel on Climate Change. Cambridge University Press, Cambridge, United Kingdom and New York, NY, USA.
Sparrow, K.J., Kessler, J.D., 2017. Efficient collection and preparation of methane from low concentration waters for natural abundance radiocarbon analysis: Measuring ^{14}C-CH_4 in background waters. Limnology and Oceanography: Methods *15*, 601–617.
Spooner, N., Rieley, G., Collister, J.W., Lander, M., Cranwell, P.A., Maxwell, J.R., 1994. Stable carbon isotopic correlation of individual biolipids in aquatic organisms and a lake bottom sediment. Organic Geochemistry, Compound-Specific Isotope Analysis in Biogeochemistry and Petroleum Research *21*, 823–827.
Stanley, E.H., Casson, N.J., Christel, S.T., Crawford, J.T., Loken, L.C., Oliver, S.K., 2016. The ecology of methane in streams and rivers: patterns, controls, and global significance. Ecological Monographs *86*, 146–171.
Stolper, D.A., Lawson, M., Davis, C.L., Ferreira, A.A., Neto, E.V.S., Ellis, G.S., Lewan, M.D., Martini, A.M., Tang, Y., Schoell, M., Sessions, A.L., Eiler, J.M., 2014a. Formation temperatures of thermogenic and biogenic methane. Science *344*, 1500–1503.
Stolper, D.A., Martini, A.M., Clog, M., Douglas, P.M., Shusta, S.S., Valentine, D.L., Sessions, A.L., Eiler, J.M., 2015. Distinguishing and understanding thermogenic and biogenic sources of methane using multiply substituted isotopologues. Geochimica et Cosmochimica Acta *161*, 219–247.

Stolper, D.A., Sessions, A.L., Ferreira, A.A., Santos Neto, E.V., Schimmelmann, A., Shusta, S.S., Valentine, D.L., Eiler, J.M., 2014b. Combined ^{13}C–D and D–D clumping in methane: Methods and preliminary results. Geochimica et Cosmochimica Acta *126*, 169–191.

Sugimoto, A., Fujita, N., 2006. Hydrogen Concentration and Stable Isotopic Composition of Methane in Bubble Gas Observed in a Natural Wetland. Biogeochemistry *81*, 33–44.

Sugimoto, A., Wada, E., 1995. Hydrogen isotopic composition of bacterial methane: CO_2/H_2 reduction and acetate fermentation. Geochimica et Cosmochimica Acta *59*, 1329–1337.

Sugimoto, A., Wada, E., 1993. Carbon isotopic composition of bacterial methane in a soil incubation experiment: Contributions of acetate and CO_2/H_2. Geochimica et Cosmochimica Acta *57*, 4015–4027.

Suzuki, Y., Suko, T., Yoshioka, H., Takahashi, M., Nanba, K., Tsunogai, U., Takeno, N., Ito, K., 2009. Biogeochemical profiles in deep sedimentary rocks in an inland fore-arc basin, Central Japan. Chemical Geology *259*, 107–119.

Swackhamer, D.L., Pearson, R.F., Schottler, S.P., 1998. Toxaphene in the great lakes. Chemosphere *37*, 2545–2561.

Task Force on Shale Gas, 2015. Final Conclusions and Recommendations. https://www.taskforceonshalegas.uk/reports

Teh, Y.A., Silver, W.L., Conrad, M.E., Borglin, S.E., Carlson, C.M., 2006. Carbon isotope fractionation by methane-oxidizing bacteria in tropical rain forest soils. Journal of Geophysical Research: Biogeosciences *111*, G02001.

The Royal Society, 2012. Shale gas extraction in the UK: a review of hydraulic fracturing. https://royalsociety.org/topics-policy/projects/shale-gas-extraction/report/

Third Energy, 2018. KM8 Portal, Third Energy. https://www.third-energy.com/km8-portal.

Thornton, S.F., Bright, M.I., Lerner, D.N., Tellam, J.H., 2000. Attenuation of landfill leachate by UK Triassic sandstone aquifer materials 2. Sorption and degradation of organic pollutants in laboratory columns. Journal of Contaminant Hydrology *43*, 355–383.

Thornton, S.F., Lerner, D.N., Banwart, S.A., 2001. Assessing the natural attenuation of organic contaminants in aquifers using plume-scale electron and carbon balances: model development with analysis of uncertainty and parameter sensitivity. Journal of Contaminant Hydrology *53*, 199–232.

Tranvik Lars J., Downing John A., Cotner James B., Loiselle Steven A., Striegl Robert G., Ballatore Thomas J., Dillon Peter, Finlay Kerri, Fortino Kenneth, Knoll Lesley B., Kortelainen Pirkko L., Kutser Tiit, Larsen Soren., Laurion Isabelle, Leech Dina M., McCallister S. Leigh, McKnight Diane M., Melack John M., Overholt Erin, Porter Jason A., Prairie Yves, Renwick William H., Roland Fabio, Sherman Bradford S., Schindler David W., Sobek Sebastian, Tremblay Alain, Vanni Michael J., Verschoor Antonie M., von Wachenfeldt Eddie, Weyhenmeyer Gesa A., 2009. Lakes and reservoirs as regulators of carbon cycling and climate. Limnology and Oceanography *54*, 2298–2314.

Trimmer, M., Hildrew, A.G., Jackson, M.C., Pretty, J.L., Grey, J., 2009. Evidence for the role of methane-derived carbon in a free-flowing, lowland river food web. Limnology and Oceanography *54*, 1541–1547.

Trimmer, M., Maanoja, S., Hildrew, A.G., Pretty, J.L., Grey, J., 2010. Potential carbon fixation via methane oxidation in well-oxygenated riverbed gravels. Limnology and Oceanography *55*, 560–568.

Trimmer, M., Shelley, F. C., Purdy, K. J., Maanoja, S. T., Chronopoulou, P.-M., Grey, J., 2015. Riverbed methanotrophy sustained by high carbon conversion efficiency. The ISME Journal *9*, 2304-2314.

Tyler, S.C., Bilek, R.S., Sass, R.L., Fisher, F.M., 1997. Methane oxidation and pathways of production in a Texas paddy field deduced from measurements of flux, delta C-13, and delta D of CH_4. Global Biogeochemical Cycles *11*, 323–348.

Tyler, S.C., Crill, P.M., Brailsford, G.W., 1994. $^{13}C/^{12}C$ fractionation of methane during oxidation in a temperate forested soil. Geochimica et Cosmochimica Acta *58*, 1625–1633.

Upstill-Goddard, R.C., Barnes, J., 2016. Methane emissions from UK estuaries: Re-evaluating the estuarine source of tropospheric methane from Europe. Marine Chemistry *180*, 14–23.
Upstill-Goddard, R.C., Barnes, J., Frost, T., Punshon, S., Owens, N.J.P., 2000. Methane in the southern North Sea: Low-salinity inputs, estuarine removal, and atmospheric flux. Global Biogeochemical Cycles *14*, 1205–1217.
Valentine, D.L., Chidthaisong, A., Rice, A., Reeburgh, W.S., Tyler, S.C., 2004. Carbon and hydrogen isotope fractionation by moderately thermophilic methanogens. Geochimica et Cosmochimica Acta *68*, 1571–1590.
van Breukelen, B.M., Röling, W.F.M., Groen, J., Griffioen, J., van Verseveld, H.W., 2003. Biogeochemistry and isotope geochemistry of a landfill leachate plume. Journal of Contaminant Hydrology *65*, 245–268.
van Winden, J.F., Reichart, G.-J., McNamara, N.P., Benthien, A., Damste, J.S.S., 2012. Temperature-Induced Increase in Methane Release from Peat Bogs: A Mesocosm Experiment. PLoS ONE *7*(6): e39614.
Vaughan, A., 2015. Government will step in if councils don't fast-track fracking applications. The Guardian. http://www.theguardian.com/environment/2015/aug/13/government-will-step-in-if-councils-dont-fast-track-fracking-applications
Viggi, C.C., Matturro, B., Frascadore, E., Insogna, S., Mezzi, A., Kaciulis, S., Sherry, A., Mejeha, O.K., Head, I.M., Vaiopoulou, E., Rabaey, K., Rossetti, S., Aulenta, F., 2017. Bridging spatially segregated redox zones with a microbial electrochemical snorkel triggers biogeochemical cycles in oil-contaminated River Tyne (UK) sediments. Water Research *127*, 11–21.
Vogel, J.C., Grootes, P.M., Mook, W.G., 1970. Isotopic fractionation between gaseous and dissolved carbon dioxide. Zeitschrift für Physik A Hadrons and nuclei *230*, 225–238.
Waldron, S., Lansdown, J.M., Scott, E.M., Fallick, A.E., Hall, A.J., 1999. The global influence of the hydrogen isotope composition of water on that of bacteriogenic methane from shallow freshwater environments. Geochimica Et Cosmochimica Acta *63*, 2237–2245.
Waldron, S., Hall, A. J., Fallick A. E., 1999b. Enigmatic stable isotope dynamics of deep peat methane, Global Biogeochem. Cycles, *13* (1), 93–100
Waldron, S., Watson-Craik, I.A., Hall, A.J., Fallick, A.E., 1998. The carbon and hydrogen stable isotope composition of bacteriogenic methane: a laboratory study using a landfill inoculum. Geomicrobiology Journal *15*, 157–169.
Walsh, K.P., McLaughlan, R.G., 1999. Bubble extraction of dissolved gases from groundwater samples. Water Air Soil Pollut. *115*, 525–534.
Wankel, S.D., Adams, M.M., Johnston, D.T., Hansel, C.M., Joye, S.B., Girguis, P.R., 2012. Anaerobic methane oxidation in metalliferous hydrothermal sediments: influence on carbon flux and decoupling from sulfate reduction. Environmental Microbiology *14*, 2726–2740.
Ward, R.S., Williams, G.M., Hills, C.C., 1996. Changes in major and trace components of landfill gas during subsurface migration. Waste Management & Research *14*, 243–261.
Watt, N., 2014. Fracking in the UK: "We're going all out for shale," admits Cameron. The Guardian. http://www.theguardian.com/environment/2014/jan/13/shale-gas-fracking-cameron-all-out
Whalen, S.C., Reeburgh, W.S., Sandbeck, K.A., 1990. Rapid methane oxidation in a landfill cover Soil. Appl. Environ. Microbiol. *56*, 3405–3411.
Whiticar, M.J., 1999. Carbon and hydrogen isotope systematics of bacterial formation and oxidation of methane. Chemical Geology *161*, 291–314.
Whiticar, M.J., Faber, E., Schoell, M., 1986. Biogenic methane formation in marine and fresh-water environments CO_2 reduction vs acetate fermentation Isotope evidence. Geochimica Et Cosmochimica Acta *50*, 693–709.
Wilhelm, E., Battino, R., Wilcock, R.J., 1977. Low-pressure solubility of gases in liquid water. Chemical reviews 77, 219–262.
Williams, G.M., Ward, R.S., Noy, D.J., 1999. Dynamics of landfill gas migration in unconsolidated

sands. Waste Management & Research *17*, 327–342.
Williams, H.G., Bialowiec, A., Slater, F., Randerson, P.F., 2010. Spatial variation of dissolved gas concentrations in a willow vegetation filter treating landfill leachate. Ecological Engineering *36*, 1774–1778.
Wilson, A.A., Evans, W.B., 1990. Geology of the country around Blackpool. Stationery Office Books.
Worrall, F., Rowson, J.G., Evans, M.G., Pawson, R., Daniels, S., Bonn, A., 2011. Carbon fluxes from eroding peatlands - the carbon benefit of revegetation following wildfire. Earth Surface Processes and Landforms *36*, 1487–1498.
Worthington, P.F., 1977. Permeation properties of the Bunter Sandstone of northwest Lancashire, England. Journal of Hydrology *32*, 295–303.
Yoshioka, H., Sakata, S., Kamagata, Y., 2008. Hydrogen isotope fractionation by Methanothermobacter thermoautotrophicus in coculture and pure culture conditions. Geochimica et Cosmochimica Acta *72*, 2687–2694.
Zazzeri, G., Lowry, D., Fisher, R.E., France, J.L., Lanoisellé, M., Kelly, B.F.J., Necki, J.M., Iverach, C.P., Ginty, E., Zimnoch, M., Jasek, A., Nisbet, E.G., 2016. Carbon isotopic signature of coal-derived methane emissions to the atmosphere: from coalification to alteration. Atmos. Chem. Phys. *16*, 13669–13680.
Zazzeri, G., Lowry, D., Fisher, R.E., France, J.L., Lanoisellé, M., Nisbet, E. G., 2015. Plume mapping and isotopic characterisation of anthropogenic methane sources. Atmospheric Environment *110*, 151-162.
Zhang, T.W., Krooss, B.M., 2001. Experimental investigation on the carbon isotope fractionation of methane during gas migration by diffusion through sedimentary rocks at elevated temperature and pressure. Geochimica Et Cosmochimica Acta *65*, 2723–2742.